

STUDIES OF COUNTERCURRENT
GAS-LIQUID FLOW IN PACKED BEDS

by

Tsuyoshi FUKUTAKE

A thesis presented for the degree of
Master of Philosophy in the University
of London

September 1977

John Percy Research Group,
Department of Metallurgy and
Materials Science,
Imperial College of Science
and Technology,
London SW7

ABSTRACT

Studies of Countercurrent Gas-Liquid Flow in Packed Beds

by

Tsuyoshi FUKUTAKE

The total hold-up, liquid distribution, gas pressure drop and flooding velocities were measured at low superficial velocities of liquid for various degrees of wetting between liquids and packings. The packed beds consisted of spheres and coke particles. The ranges of experimental variables, chosen to cover the prevailing flow conditions in iron blast furnaces, were: particle size (8~13mm); contact angle ($0\sim 114^\circ$); liquid density ($807\sim 1920\text{ kg/m}^3$), viscosity ($0.0009\sim 0.064\text{ Ns/m}^2$) and velocity ($0.02\sim 1.0\text{ mm/s}$).

The total hold-up was significantly lower with non-wetting flows than with wetting flows. Correlations for both static and dynamic hold-up were obtained and shown as mathematical formulae which are in dimensionless form and are valid for non-wetting as well as wetting flows.

Mersmann's flooding diagram, which correlated the measured data better than Sherwood diagram, was modified to incorporate the effect of the degree of wetting on the flooding velocities.

The gas flow influenced the liquid distribution in the column. The changes in the liquid distribution with gas flow for non-wetting flows were significantly larger than for the wetting flows.

Instability of the bed, in which a transition from a stable to a fluidized bed occurred, was observed before the onset of flooding in some of the experiments in which a heavy liquid ($\rho_l=1920\text{ kg/m}^3$) was used. A diagram was developed to identify the operating state of the bed in relation to the flow conditions. This diagram indicated that in blast furnaces the fluidization of the coke bed is likely to start before the onset of flooding by the slag.

CONTENTS

	<u>page</u>
TITLE PAGE	1
ABSTRACT	2
CONTENTS	3
LIST OF FIGURES	7
LIST OF PLATES	9
LIST OF TABLES	10
CHAPTER 1 INTRODUCTION	11
CHAPTER 2 LITERATURE SURVEY	14
2.1 Formation of the Melting zone and Flow Conditions below it	14
2.2 Previous Work on Irrigated Packed Columns	18
2.2.1 Hold-up	18
2.2.1.1 Experimental data on hold-up	19
2.2.1.2 Generalized correlation for operational hold-up in the absence of gas flow	21
2.2.1.3 Static hold-up	24
2.2.2 Influence of gas flow on hold-up and gas pressure drop	27
2.2.2.1 Hold-up correlation	27
2.2.2.2 Pressure drop of gas in dry column	29
2.2.2.3 Pressure drop of gas in irrigated column	30
2.2.2.4 Influence of gas flow on liquid flow distribution	31
2.2.3 Flooding	31
2.3 Application to the Blast Furnace Process	35
2.4 Summary	36

	<u>page</u>	
CHAPTER 3	DESIGN OF EXPERIMENTAL SYSTEM	38
CHAPTER 4	EXPERIMENTAL WORK	46
4.1	Apparatus	46
4.1.1	Column	51
4.1.2	Control and measurement of liquid flow rate	51
4.1.3	Gas flow control	57
4.1.4	Recording of the data	64
4.2	Liquids and Packings	64
4.3	Experimental procedures	70
4.3.1	Experimental procedure for first series of experiments	70
4.3.2	Experimental procedure for experiments with gas flow (second series)	71
4.4	Data Processing	72
4.4.1	Calibration curves	72
4.4.2	Correction for the influence of gas pressure on column weight	73
4.4.3	Calculation of liquid flow	73
CHAPTER 5	EXPERIMENTAL RESULTS	75
5.1	Experimental Data	75
5.2	Experiments in the Absence of Gas Flow	78
5.3	Experiments with Gas Flow	82
5.3.1	Change of the flow pattern of the liquid with gas velocity	82
5.3.2	Reproducibility of the measurements	87
CHAPTER 6	DISCUSSION	89
6.1	Hold-up in the Absence of Gas Flow	89
6.1.1.	Calculation of dynamic and static hold-up	89

	<u>page</u>
CHAPTER 6	DISCUSSION (continued)
6.1.2	Correlation for static hold-up 93
6.1.3	Correlation for dynamic hold-up 101
6.1.4	Correlation for the total hold-up 104
6.1.5	Comparison of estimated hold-up with published experimental data 105
6.2	Gas Pressure Drop 109
6.2.1	Gas pressure drop through dry column 109
6.2.2	Pressure drop through irrigated column 111
6.3	Flooding 119
6.4	Instability of the Bed 125
6.5	Liquid Distribution 129
6.6	Possibility of the Occurrence of the Flooding in the Blast Furnace 132
CHAPTER 7	CONCLUSIONS 135
APPENDIX I	METHOD FOR COMPUTING LIQUID FLOW RATES 138
I.1	Introduction 138
I.2	Principle of the method 138
I.3	Program and Calculated Results 139
APPENDIX II	GENERALIZED CURVE-FITTING 143
II.1	Introduction 143
II.2	Parametric Interpolation 143
II.3	Conditional Least-Square Method 144
II.4	Mathematical Formulation 145
II.5	Computer Program 147
APPENDIX III	ITERATIVE METHOD FOR LEAST SQUARES 153
III.1	Introduction 153
III.2	Mathematical Formulation 153

	<u>page</u>
APPENDIX III (continued)	
III.3 Computer Program	155
APPENDIX IV EXPERIMENTAL DATA	157
ACKNOWLEDGEMENTS	187
LIST OF SYMBOLS	188
REFERENCES	192

LIST OF FIGURES

<u>Fig. No.</u>		<u>Page</u>
2.1	State of burden in a blast furnace	15
2.2	Operational ranges of superficial velocities of slag and metal in commercial blast furnaces	15
2.3	Relationship between residual saturation, S_r , and capillary number, N_{cap} , after Dombrowski and Brownell(49).	26
2.4	Typical examples of the changes in total hold-up and pressure drop with gas velocity at a constant liquid velocity	28
2.5	Flooding diagrams showing the limiting condition for flooding	33
4.1	Schematic drawing of experimental apparatus in the main section	50
4.2	Design of the liquid distributor	53
4.3	Four arrangements of supply points of distributor used in experiments	54
4.4	Liquid collector/gas distributor and position of the column	56
4.5	Liquid flow meter	59
4.6	Schematic drawing of gas flow control section	61
4.7	Dew point meter	63
4.8	Calibration curve for micromanometer	65
4.9	Calibration curve for the effect of the gas pressure on the column weight for Run 340.	74
5.1	Graphical representation of experimental results for Run 17	79
5.2	Influence of the distributor arrangement on liquid flow distribution and total hold-up.	80

<u>Fig. No</u>		<u>Page</u>
5.3	Relationship between total hold-up and liquid velocity for different columns of PL13/WATR system.	81
5.4	Variation of total hold-up, pressure drop and relative liquid flux to outer annulus with gas velocity, Run 13183 (AL13/WATR)	83
5.5	Variation of total hold-up, pressure drop and relative liquid flux to outer annulus with gas velocity, Run 19171 (PL13/WATR)	84
5.6	Variation of total hold-up pressure drop and relative liquid flux to outer annulus with gas velocity, Run 30361 (W13/GLY)	85
5.7	Examples of variation of total hold-up with gas velocity for PL13/WATR and W13/WATR systems	88
6.1	Examples of variation of total hold-up with liquid velocity	94
6.2	Plot of experimental data for wetting flows on Dombrowski's diagram	95
6.3	Relationship between static hold-up h_s^* , and modified capillary number, C_{pm}	100
6.4	Comparison between measured and estimated dynamic hold-up	102
6.5	Comparison between measured and estimated total hold-up	103
6.6	Relationship between the static hold-up, h_s and the modified capillary number for published data	107
6.7	Schematic drawing of three different ways in which liquid is held by a tube	108
6.8	Relationship between friction factor, f_k , and Reynolds number, Re_g , for dry columns	112
6.9	Relationship between the total hold-up and the ratio of the pressure drop through irrigated column to that through dry column	113
6.10	Relationship between the total hold-up and the ratio of the pressure drop through irrigated column to that through dry column	114
6.11	Variation of friction factor, f_k , with gas Reynold's number Re_g for dry and irrigated columns.	116

<u>Fig. No.</u>		<u>Page</u>
6.12	Variation of friction factor f_k with gas Reynolds number Re_g for dry and irrigated columns.	117
6.13	Schematic drawing of the variation of f_k with Re_g .	118
6.14	Plots of flooding data on Sherwood diagram	121
6.15	Plots of flooding data on Mersmann's diagram	122
6.16	Flooding diagram based on modified dimensionless irrigation density	124
6.17	Variations of total hold-up and gas pressure with gas velocity for Run 430 (PL9/ZNCL)	126
6.18	Diagram showing the regions of bed instability	128
6.19	Variation of relative liquid flux to outer annulus with dimensionless gas pressure drop, ΔP_w^* .	131
A1-1	Variation of the weight of the container with time in two typical cases	142
A2-1	Physical model of generalized curve fitting.	149

LIST OF PLATES

Plate 1	General view of the apparatus	48
Plate 2	Detailed view of some parts of the apparatus (a) Column (b) Liquid collector and flow meter (c) Gas humidification column	52
Plate 3	Appearance of particles in dry and wet states	66

LIST OF TABLES

		<u>Page</u>
Table 2.1	Typical conditions of liquid flow in blast furnaces	17
Table 2.2	Experimental conditions of hold-up measurements by previous authors	20
Table 2.3	Published correlations for operational hold-up	22
Table 2.4	Comparison between observed and calculated hold-up	23
Table 3.1	Data on packings used in experiments	42
Table 3.2	Physical properties of liquids used in experiments	43
Table 3.3	Comparison of the values of dimensionless numbers for the blast furnace with those of experiments for different liquids	44
Table 5.1	Summary of experimental runs	76
Table 6.1	Static part of the hold-up, h_S^* , obtained by least-squares fit	91
Table 6.2	Results of the least-squares fit by Equation (6.1)	92
Table 6.3	Comparison of various correlations for static hold-up	98
Table 6.4	Published data on static hold-up	106
Table 6.5	Comparison of measured dynamic and operational hold-ups, %, with values estimated using various correlations	110
Table 6.6	Flooding velocities and dimensionless parameters for the flooding diagrams	120
Table A1-1	Listing of computer program for the calculation of liquid flow rate	140
Table A2-1	Calling form of subroutine SMR	148
Table A2-2	Calling form of subroutine YQ	149
Table A2-3	Listing of computer program for generalized curve fitting	150
Table A3-1	Listing of computer program for iterative method of least squares	156

CHAPTER I

INTRODUCTION

The blast furnace is basically a counter-current packed bed reactor. The hot air, blown into the furnace through tuyères, forms a raceway in which the coke burns to produce a highly reducing gas. The gas then flows upwards through beds of coke and ore. The consumption of coke by combustion or chemical reaction and of ore by melting cause the bed of coke and ore to descend.

The ascending stream of hot gas supplies almost all the energy that is needed to produce pig iron from the ore. The productivity of the blast furnace, therefore, depends primarily on the amount of the gas it can take and on the efficiency of energy utilization which in turn is influenced by the radial distribution of the gas and burden and the rate of energy transfer.

It is clear that investigations on the flows of gas, solid and liquid are of basic importance in understanding the prevailing mechanisms of heat, mass and momentum transfer in blast furnaces and this has led to an upsurge of interest in this field in recent years⁽¹⁾.

The furnace can be divided into two parts: the upper part where only solid phase exists other than gas and the lower part where liquid metal and slag flow counter-current to the rising gas stream through a bed of coke.

In the upper part, the gas flows through beds of ore and coke stacked layer by layer. Since the burden descends by its own weight and the excess pressure drop of the gas disturbs its smooth descent, much of the earlier work was concerned with the application of existing correlations from the chemical engineering literature to estimate the

influence of various factors on the pressure drop of the gas in the furnace^(2,3).

The lower part of the furnace is apparently similar to a packed absorption tower commonly used by chemical engineers though, in the latter, the bed is usually stationary. Elliott et al.⁽⁴⁾ were the first workers who suggested that flooding could be one of the factors which limit the amount of gas that the furnace can take. Although, as we will see later, the coke-slag and coke-metal systems in the furnace differ in several aspects from those commonly used in chemical engineering, the phenomenon of flooding, particularly of the slag, has been considered by many authors as one of the factors which limit the furnace productivity^(5,6,7,8).

In recent years, helped by the rapid development in computer technology, mathematical simulation models of the blast furnace have been developed^(9,10,11). The earlier one-dimensional models led to predictions of the profiles of variables such as temperatures and chemical compositions of both solid and gas along the furnace axis as well as the effect of operational variables on coke rate. However, when a model attempts to cover the transport phenomena between liquid and solid, it needs at least the data on liquid hold-up and effective interfacial area between solid and liquid. Because of the lack of reliable data, authors of mathematical models for this region of the furnace have often resorted to semi-empirical analyses which rely on comparison between observed furnace performance and predictions from their models. For example, Flieman⁽¹²⁾ derived a model in which he had to assume arbitrarily that the ratio of the velocities of the liquid and coke is equal to unity until the ore melts after which it increases linearly with temperature.

In view of the importance of the radial distribution of burden and gas, two dimensional models for the region between the top of the furnace and the melting zone have been proposed⁽¹³⁾. It is clear, however, that one needs more detailed information

on the nature of the liquid and gas flows to extend the model to cover the entire furnace and to incorporate liquid flow re-distribution under the influence of the gas flow.

The present work is intended to give an insight into the nature of flow of slag and metal over the bed of coke counter-current to the rising gas stream. In view of the difficulties in carrying out meaningful high temperature experiments, this investigation deals with a room-temperature model of the system. The experimental conditions for the present studies were chosen to establish liquid flow patterns as close to those in the blast furnace as possible; dimensionless numbers characterizing these flow systems were used as criteria for modelling. Special attention was paid to obtain high contact angles since non-wetting flow characterizes the blast furnace system together with low superficial liquid velocity.

Flooding velocities, liquid hold-up, gas pressure drop and liquid flow distribution at the bottom of the column were measured. The influences of the velocities of liquid and gas; of density, viscosity, and surface tension of liquid; of the degree of wetting between solid and liquid (contact angle); and of size and shape of the packings were investigated.

CHAPTER 2

LITERATURE SURVEY

The formation of a melting zone and the conditions of flow of molten slag and metal below the melting zone in the blast furnace will be discussed first in Section 2.1. Previous work on hold-up, gas pressure drop and flooding in irrigated packed columns will be discussed in Section 2.2 and the application of the results of these studies to the blast furnace process will be discussed briefly in Section 2.3.

2.1 Formation of the Melting Zone and Flow Conditions below it

Recent investigations on blown-out blast furnaces^(14,15,16) have provided valuable information on the melting process in the furnace. Fig. 2.1 shows that the layered structure of ore and coke persists down to the level where melting begins. Although the position of the melting zone as well as its shape differed from one furnace to another depending on the operating conditions, the existence of the melting zone was clearly observed in all these furnaces.

Below the melting zone, there is a bed of coke through which molten slag and metal flow downward. Recent observations with a probe introduced into the high temperature region of an experimental furnace^(19,20) have confirmed that the molten slag and metal flow as slugs over coke particles. This is because, on the one hand, the surface tension and contact angle of slag and metal on coke are high and on the other, the velocities of slag and metal averaged over the hearth area is very low. Fig. 2.2 shows histograms of the velocities of slag and of metal (mm/s) derived from operational data for 34 blast furnaces^(21,22). The scatter in the histogram

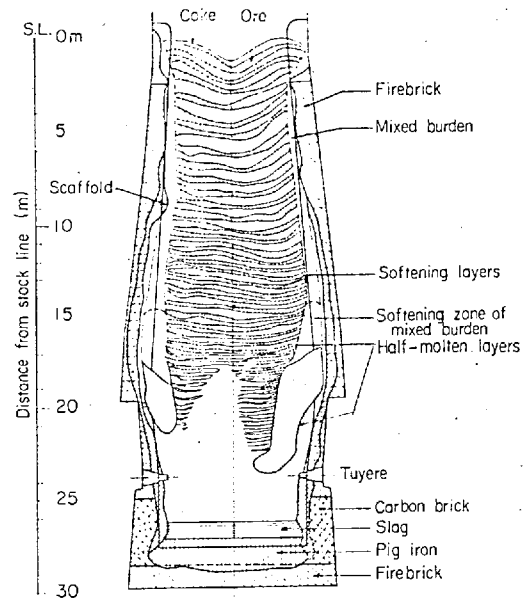


Fig. 2.1 State of burden in a blast furnace(14)

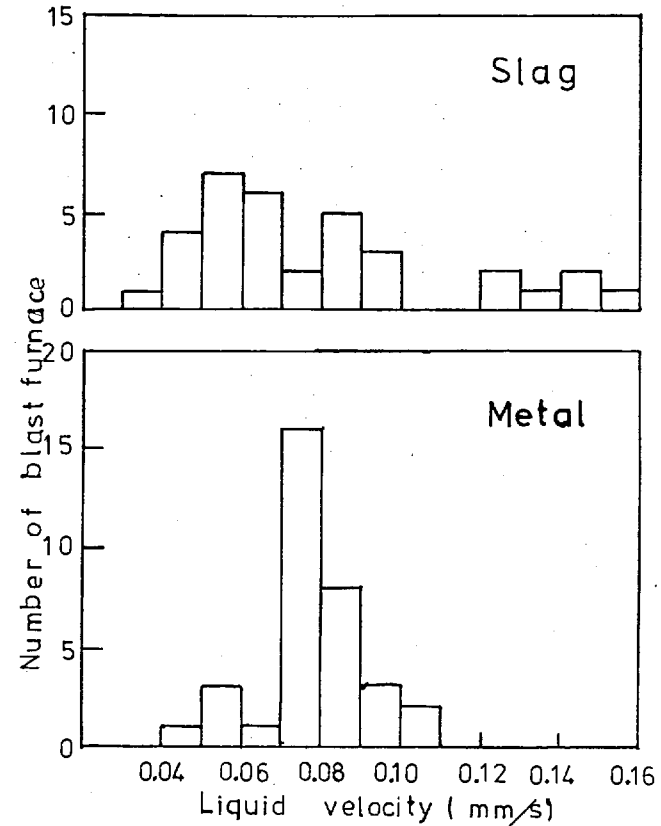


Fig 2.2 Operational ranges of superficial velocities of slag and metal in commercial blast furnaces

based on slag velocity is greater than that based on metal because of the wider range of slag volumes encountered.

The gas velocity calculated over the hearth area at NTP is within a range of 0.65 - 1.0 m/s which is narrower than the range of metal and slag velocities. It must be noted that, because the hot air is blown horizontally into the furnace, the velocity and direction of gas flow change greatly in the vicinity of the raceway. In the case of an isothermal, uniform column without irrigation, uniform vertical flow of the gas is achieved at a height approximately equal to the radius of the column from the horizontal gas inlet^(17,18).

Table 2.1 shows the mean physical properties of liquid slag and pig iron. In view of the considerable scatter in the reported results, the range of variation for each property is also shown in the Table. The values are based on the chemical composition of tapped slag and pig iron. It should be noted that the slag and iron flowing through the bed of coke in the lower part of the blast furnace may be different in both composition and temperature. For example, Elliott et al⁽⁴⁾ noted that small changes in temperature and composition could change the viscosity of slags from 0.2 to 7.8 Ns/m².

Data on the contact angle between graphite or coke and slag or pig iron are scarce. Humenik et al⁽²³⁾ have reported 128° as the contact angle of iron containing 5% carbon on graphite at just above the melting temperature. The contact angle decreased with the decrease in carbon content and they reported a value of 60° when no carbon was present in the iron.

Keveryan and Taylor⁽²⁴⁾ measured the surface tension and contact angle on graphite carbon of carbon saturated iron at 1200°C. They reported a contact angle of 121° for carbon-saturated iron. With the addition of sulphur, the surface tension decreased while the contact angle increased

	Density [†] (Kg/m ³)	Viscosity [†] (Ns/m ²)	Surface [†] tension (N/m)	Contact angle with carbon (Degree)	Superficial velocity (10 ⁻³ m/s)	Coke Size (m)
Pig iron	6600	0.005	1.1	125*	0.08	
(range)	(6300-6900)	(0.004-0.006)	(0.9-1.3)		(0.04-0.11)	0.024 (0.02-0.03)
Slag	2600	0.3	0.47	105-160*	0.08	
(range)	(2500-2700)	(0.25-0.6)	(0.45-0.5)		(0.03-0.16)	

* See text for explanation

† (26)

Table 2.1 Typical conditions of liquid flow in blast furnaces

to 129, 132, 155° for 0.01, 0.019, 0.07, %S respectively. The addition of 1% silicon did not change the surface tension or contact angle significantly.

Towers⁽²⁵⁾ has reported that the angle between graphite and a synthetic blast-furnace slag was a function of the time of contact and decreased from 160° at the start to 105° after one hour and to 30° after five hours. The author suggested that this decrease was caused by a reaction between SiO₂ in the slag and carbon yielding SiC or SiO. In the blast furnace, the time of contact of the coke with slag depends on the residence time of the coke below the melting zone and the effective contact area between the coke and slag. The average residence time of ore and coke in modern blast furnaces is about eight hours. The volume of the coke bed between the melting zone and tuyère level can be estimated from the reported profile of the melting zone. Among four furnaces reported^(14,16), the maximum volume is about two ninths of the effective inner volume of the furnace. All the surface of the coke is not always in contact with the slag and a contact area of 50% would be too high an estimate. Therefore, it is unlikely that the coke is in contact with the slag for more than an hour and the contact angle between slag and coke in the furnace is likely to be more than 105°.

2.2 Previous Work on Irrigated Packed Columns

2.2.1 Hold-up

Shulman et al⁽²⁷⁾ defined three different types of liquid hold-up:

- (1) the total hold-up, h_t , which is the total liquid in the packing under operating conditions,
- (2) The static hold-up, h_s , which is the amount of liquid that does not drain from a column when the liquid supply to the column is discontinued.

- (3) the operating hold-up, h_o , which is the difference between the total and static hold-ups.

The hold-up is usually expressed as the volume of liquid per unit volume of the packed bed and is dimensionless. The relation between the three hold-ups is given by:

$$h_t = h_s + h_o \quad (2.1)$$

Shulman et al. measured h_t and h_s from which h_o was calculated.

Gardner⁽²⁸⁾ has suggested that the total hold-up consists of another component, h_f , caused by a superimposed slow liquid flow which persists after stopping the liquid supply. In this case

$$h_t = h_s + h_f + h_d \quad (2.2)$$

where h_d is the dynamic part of the hold-up which is zero at zero liquid flow rate. The operational hold-up, h_o , also referred to by some authors as dynamic hold-up, is assumed to be zero at zero liquid flow rate. This assumption contradicts Gardner's analysis, though, at high liquid flow rates the operational hold-up makes such a large contribution to the total hold-up that the difference between h_o and h_d is negligible.

2.2.1.1 Experimental data on hold-up

Table 2.2 summarises the experimental conditions of liquid hold up measurement by various investigators. It will be noted that these studies cover a wide range of liquid viscosity (0.00059 - 0.185 Ns/m²) but the density of liquid is changed only within the narrow range of 800-1320 Kg/m³. Excepting the data of Gardner, the liquid velocities are higher than those existing in blast furnaces (Fig. 2.2). The majority of investigators have used rings

Ref.	Author	Column d x h (m)	Packing Material	size (mm)		u (mm/s)	Liquid ρ (kg/m ³)	μ (Ns/m ²)	σ (N/m)	Measurement method	remarks
29)	Elgin & Weiss	0.073 x 1.5	CL-BS POR-BS CL-RR CL-SP	13 6.3 16 13	Water	1.01- 56.8	1000	0.001	0.072	DR	G,FL
30) 31)	Uchida & Fujita	0.36 x 1.5 0.26 x 1.5,3.3	POR-RR Crushed Lime	15,26,35 16,25,35	Water	0.55- 55.5	1000	0.001	0.072	DR	G,FL
32)	Piret et al	0.762 x 1.83	Gravel	42.7	Water	0.065- 3.05	1000	0.001	0.072	DR	
33)	Jesser & Elgin	0.152 x 1.28	GL-SP BS C-RR	13,19,25 6.3,13,25 13	Water Water, aq.sol.of NaCl, SA, Sugar	0.72- 48.5	1000- 1206	0.001- 0.01	0.029- 0.081	DR	
27)	Shulman et al	0.254 x 0.91	POR-RR POR-BS C-RR	13,25,38 13,25 25	Water	0.69- 13.9	1000	0.001	0.072	WEI	G,HS
34)	Shulman et al	0.254 x 0.91	POR-RR POR-BS C-RR	25 25 25	Aq.sol.of sorbitol. CaCl ₂ , SA Methanol Benzene	1.39- 13.9	800- 1320	0.00059- 0.185	0.0226- 0.086	WEI	HS
35)	Larkins et al	0.05 x 0.1 x	RR SP CYL	9.5 3,9,5 3	Aq.sol. & Org.sol.	0.14- 265	800- 1200	0.00033- 0.041	--	DR	Co-curr. gas flow
36)	Ross	0.05 x 0.01 1.9	Catalyst cylinder	4.8x4.8	Water	0.68- 16.9	1000	0.001	0.072	DR TR	
37)	Mohunta Laddha	0.076 x 0.6	RR LR SP	6.3,9,13 6.3,9 13	Water Aq.sol.of C.M.C.	0.60- 32	800- 1320	0.0006- 0.162	0.226- 0.086	DR	
38)	Broz & Kolar	0.19 x 1.0	GL-SP	10.2	Water Aq.sol.of glycerol, methanol	0.22- 19.9	843- 1212	0.0089- 0.057	0.028- 0.073	WEI	G,HS
39)	Tichy	- x 1.0	GL-SP	10,15,20	Water Aq.sol.of glycerol, butanol, K ₂ CO ₃	0.765- 5.23	993- 1430	0.001- 0.02	0.0405- 0.073	--	G
Non-wetting experiments											
28)	Gardner	rectang. .19x.22 x .61	Coke coated with silicone	6.3-13 13-19 19-25	Water	0.068- 1.013	1000	0.001	0.072	h _s :TR h _o :DR	G,HS
40)	Warner	0.047 x 0.53	ST-RR	6.3	Mercury	0.54- 7.35	13600	0.0015	0.47	h _s :WEI h _o :DR	
41) 42)	Standish	0.44 x -	ST-RR POR-RR C-RR POR-BS	6.3	Mercury Cerro- bend water	1.07- 10.7	1000- 13600	0.001- 0.0023	0.072- 0.47	WEI	HS
44)	Andriew	0.15 x --	POR-RR silicone coated	10	Water	3.15- 6.30	1000	0.001	0.072	--	G,FL,HS

Abbreviations

CL = clay, POR = porcelain, GL = glass, C = carbon, ST = steel, BS = berl saddles,
RR = raschig rings, SP = spheres, LS = lessig rings
SA = surface active agent, C.M.C. = carboxy-methyl-cellulose
DR = draining, WEI weighing, TR = tracer method
G = with gas flow, FL = flooding velocities measurement also, HS = static hold-up measurement also.

Table 2.2 Experimental conditions of hold-up measurements by various authors

and berl saddles as packing materials. These materials are common in the field of chemical engineering. However, only a few studies have been reported with spheres and granular solids which are more relevant to the blast furnace process.

Measurements under the non-wetting condition are scarce. Warner⁽⁴⁰⁾ and Standish^(41,42) studied non-wetting systems with raschig rings or berl saddles as the packing and, moreover, their range of liquid velocities is outside of that of blast furnaces. The only experiments which are particularly relevant are those of Gardner⁽²⁸⁾.

Of those who studied non-wetting systems, Standish compared operational⁽⁴¹⁾ and static hold-up⁽⁴²⁾ between wetting and non-wetting systems. He concluded that there was no significant difference in operational hold-up between wetting and non-wetting systems. For static hold-up, his measured results showed values which were much smaller for non-wetting system compared with those for wetting systems. Andrieu⁽⁴³⁾ showed that the static hold-up was 2.3% with silicone-coated raschig rings and 5.4% with uncoated ones. The dynamic hold-up with the coated packing was about 10% smaller than with the uncoated one.

2.2.1.2 Generalized correlation for operational hold-up in the absence of gas flow

Table 2.3 shows generalized correlations for operational hold-up given by various authors. Although these correlations are in the dimensionless form, those of Buchanan⁽⁴⁶⁾ and of Gelbe⁽⁴⁷⁾ are applicable only to ring packings. Davidson⁽⁴⁴⁾ combined a theoretical analysis with results from liquid flow experiments on a string of spheres⁽⁴⁸⁾ to develop a correlation which is claimed to be valid for low liquid flow rates where the liquid flows as a laminar film over the surface of the packing. Under these conditions, the operational hold-up was proportional to the one-third power of

No.	Author	Correlation	Ref
1	Otake and Okada	$h_o = 1.295 \left(\frac{d_p u \rho_l}{\mu_l} \right)^{0.676} \left(\frac{g d_p^3 \rho_l^2}{\mu_l^2} \right)^{-0.44} (a_t d_p)$	45
2	Davidson	$h_o = 1.217 \left(\frac{2\pi u \rho_l}{a_t \mu_l} \right)^{1/3} \left(\frac{g d_p^3 \rho_l^2}{\mu_l^2} \right)^{-1/3} (a_t d_p)$	44
3	Mohuntha and Laddah	$h_o = 16.13 \left(\frac{\mu_l u^3 N}{g^2 \rho_l} \right)^{1/4} (N d_{pe}^3)^{-1/2}$	37
4	Buchanan [†]	$h_o = 8.1 \left(\frac{\mu_l u}{\rho_l g d_p^2} \right)^{1/3} + 1.8 \left(\frac{u^2}{g d_p} \right)^{1/2}$	46
5	Gelbe [†]	$h_o^* = 1.59 \left(\frac{d_i}{d_p} \right)^{-5/9} \left(\frac{\rho_l g}{\sigma} d_h^2 \right)^{-1/7} \left(\frac{g d_h \rho_l^2}{\mu_l^2 a_t^2} \right)^{-0.3} \left(\frac{u \rho_l}{a_t \mu_l} \right)^n$	47
		$n = 1/3 \text{ for } \rho_l u / a_t \mu_l < 1; \quad n = 5/11 \text{ for } \rho_l u / a_t \mu_l \geq 1$	

† Valid only for raschig ring packings

Table 2.3 Published correlations for operational hold-up

Worker System	Warner ⁽⁴⁰⁾ Mercury-steel raschig ring		Gardner ⁽²⁸⁾ Water-coke coated with silicone fluid				Blast furnace	
							Metal	Slag
d_p (m)	0.00635		0.0155		0.022		0.024	
a_t (l/m)	635.8		349.8		244.5		229.2	
N (l/m ³)	3108000		276000		96500		87300	
d_{pe} (m)	0.00727		0.0155		0.022		0.024	
ϵ (-)	0.72		0.456		0.462		0.45	
ρ_l (kg/m ³)	13600		1000				6600	2600
μ_l (Ns/m ²)	0.00155		0.0009				0.005	0.3
u (m/s)	0.00571	0.00141	0.000067	0.00101	0.000068	0.00068	0.00008	0.00008
Measured h_o	0.074	0.023	0.0080	0.0263	0.0050	0.0127	--	--
data h_s	0.136	0.119	0.0213		0.0168		--	--
Calculated 2	0.0685	0.043	0.0205	0.0505	0.0161	0.0348	0.0154	0.0824
h_o 1	0.0597	0.0232	0.0033	0.0208	0.0026	0.0125	0.0028	0.0077
by Cor.* 3	0.0755	0.0265	0.0027	0.0203	0.00206	0.0116	0.0022	0.0076

* Table 2.3

Table 2.4 Comparison between observed and calculated operational hold-up

the liquid flow rate. At higher flow rates, the exponent was larger because of the onset of turbulence. The variation in the exponent of the superficial velocity from 1/3 at low flow rate to greater than 1/3 at high flow rate is also reflected in the correlations of Buchanan and of Gelbe in which the exponent changes with liquid flow rate.

Apart from the use of different symbols and correction factors for the shape of packings, the first three correlations use basically the same dimensionless numbers, i.e. Reynolds number $Re(=\rho_l u D/\mu_l)$ and Galileo number $Ga(Re^2/Fr)$, where Fr is Froude number; $= u^2/gD$). The fifth correlation uses an additional dimensionless number We/Fr , where We is Weber number given by

$$We = \rho_l u^2 D / \sigma$$

The first three correlations are tested against the measured data of Warner⁽⁴⁰⁾ and of Gardner⁽²⁸⁾, which are for non-wetting conditions, in Table 2.4. Calculated results for assumed blast furnace conditions are also shown in the Table. Davidson's correlation predicts very high operational hold-up at low flow rates, although the agreement is reasonable at high flow rates. The other two correlations predict better values, however even in these cases, the calculated values for Gardner's data at low flow rates are less than half of the measured values.

Although Gardner⁽²⁸⁾ and Standish⁽⁴¹⁾ showed the correlations for operational hold-up for the non-wetting systems, none of them are in generalized form applicable to the blast furnace process.

2.2.1.3 Static hold-up

The measured static hold-up is also shown in Table 2.4. It will be noted that the static hold-up is significantly larger than the operational hold-up at low flow rates.

Since the residence time of the liquid is related to the total hold-up, it is important to estimate the static hold-up as well as operational hold-up.

Dombrowski and Brownell⁽⁴⁹⁾ have shown a diagram which relates the residual saturation to the capillary number (Fig. 2.3). Turner and Hewitt⁽⁵⁰⁾ defined the capillary number in the absence of external forces other than gravity as follows:

$$N_{\text{cap}} = \frac{\epsilon^3}{5 a_t^2} \frac{g \rho_l}{\sigma \cos \theta} \quad (2.3)$$

or for the sphere packing

$$N_{\text{cap}} = \frac{\epsilon^3}{180 (1-\epsilon)^2} \frac{d_p^2 g \rho_l}{\sigma \cos \theta} \quad (2.4)$$

The static hold-up, h_s , is related to the residual saturation S_r as follows:

$$h_s = S_r \cdot \epsilon \quad (2.5)$$

From Eq. (2.3) it is clear that the capillary number tends to infinity as θ approaches 90° . This would imply that the residual saturation becomes zero since the residual saturation decreases as the capillary number increases. However, a finite static hold-up was observed by Gardner (Table 2.4) when the contact angle, θ , was about 90° . Therefore, Eq. (2.3) or (2.4) cannot be applied under non-wetting conditions where the liquid seems to be held on the surface of packings as shown by Turner and Hewitt⁽⁵⁰⁾ (See also Plate 3 in Sec. 4.2).

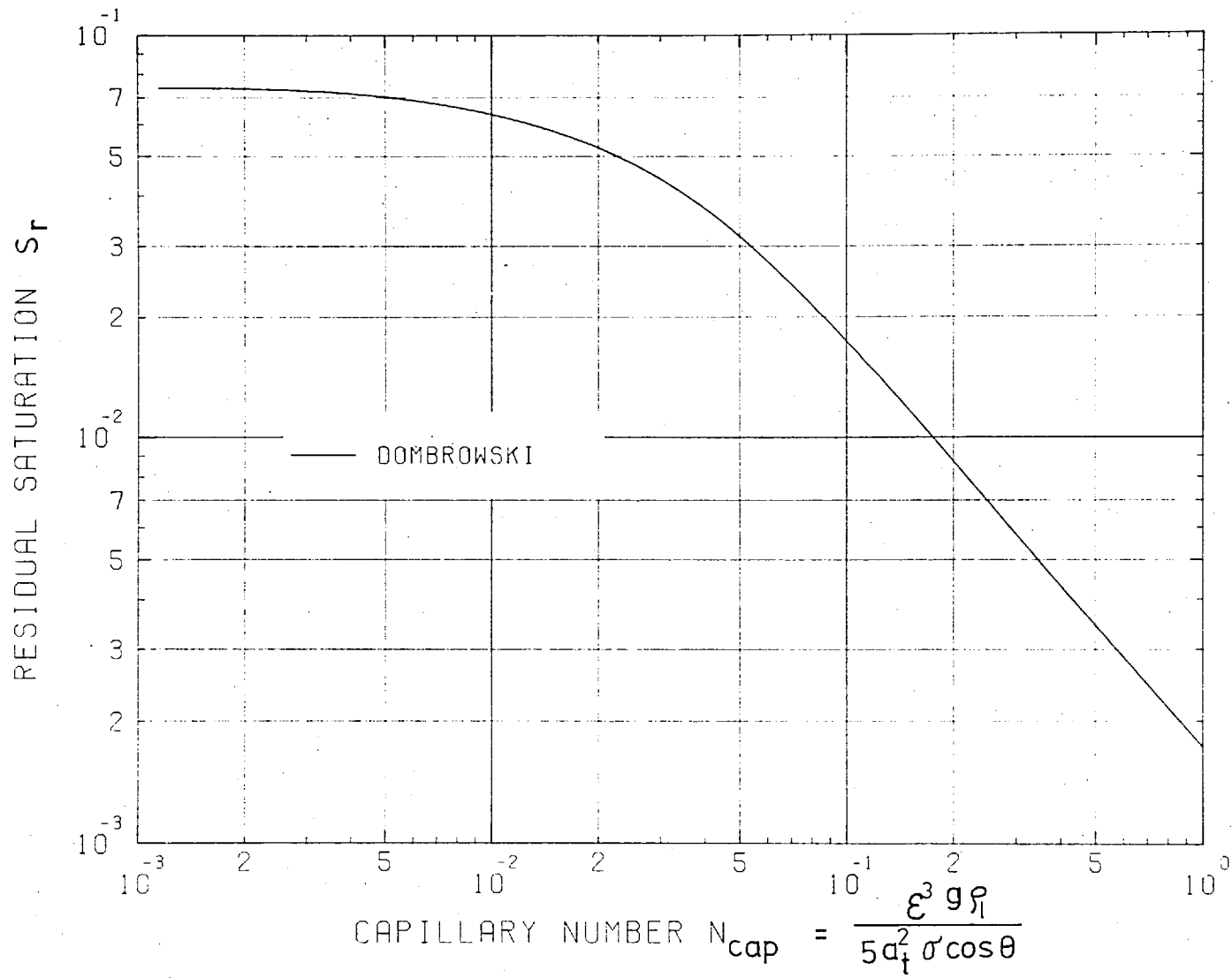


Fig. 2.3 Relationship between residual saturation, S_r , and capillary number, N_{cap} , after Dombrowski and Brownell(49)

2.2.2 Influence of gas flow on hold-up and gas pressure drop

In Fig. 2.4 typical example of the variations in gas pressure drop and total hold-up with gas velocity are shown for a constant liquid velocity. At low gas velocity, the hold-up increases, if at all, very slowly and approximately linearly with gas velocity. Above a certain gas velocity the hold-up increases sharply at an increasing rate until the hold-up curve becomes almost vertical.

As shown in the upper half of Fig. 2.4, the region in which hold-up begins to increase significantly corresponds closely to that in which the slope of the pressure drop line on a plot of $\log(\text{pressure drop})$ vs. $\log(\text{gas velocity})$ increases. This region, or more specifically this point is called the loading point and above this point the column is said to be loaded⁽⁴⁶⁾.

At the point where the hold-up curve becomes almost vertical, the pressure drop curve also becomes almost vertical. Under these conditions the liquid cannot flow through the column at the rate it is supplied at the top of the column and rapid accumulation of liquid destroys the normal operation of the column. This point is called flooding point and the column is said to be flooded.

2.2.2.1 Hold-up correlation

Below the loading point, the hold-up is regarded the same as that without gas flow since the change of hold-up with gas velocity is very small⁽⁴⁶⁾.

Only a few authors have tried to correlate the hold-up above the loading point to flow conditions. Uchida and Fujita^(30,31,51) and Mersmann⁽⁵²⁾ gave the correlation in the form of a diagram. Neither of these diagrams covers the low liquid velocity region which is important to the blast furnace system. The correlation given by Gardner⁽²⁸⁾ covers the desired low liquid velocity region, though,

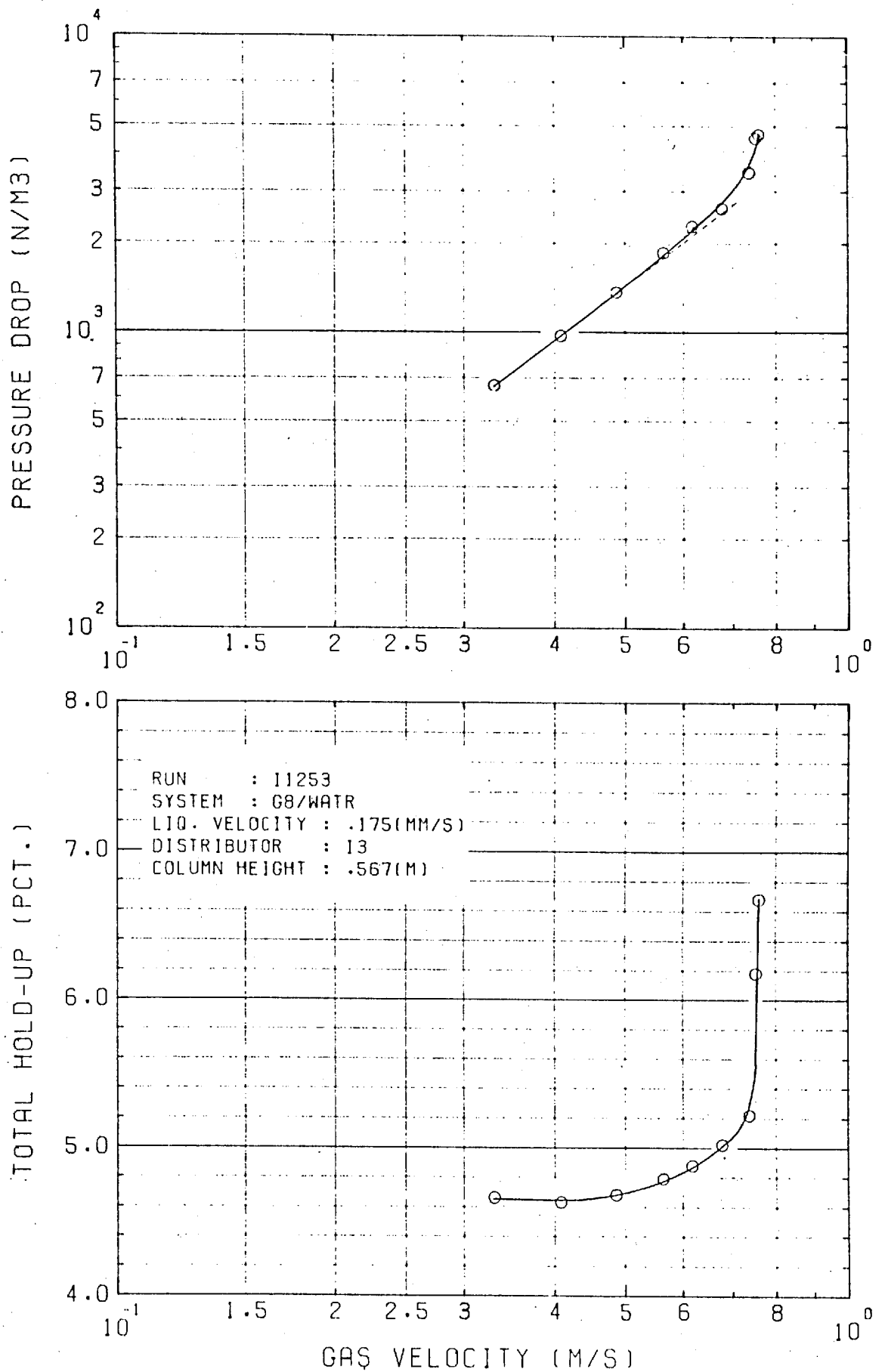


Fig. 2.4 Typical example of the changes in total hold-up and pressure drop with gas velocity at a constant liquid velocity

its applicability to systems other than his own (silicone coated coke/water/air) has not been tested.

2.2.2.2 Pressure drop of gas in dry column

Ergun⁽⁵³⁾, using pressure drop data in columns of granular materials, correlated the friction factor f_k with gas Reynolds number Re_g where

$$f_k = \frac{\Delta P \cdot d_p \cdot \phi}{L \cdot \rho_g \cdot V^2} \cdot \frac{\epsilon^3}{1-\epsilon} \quad (2.6)$$

and
$$Re_g = \rho \cdot V \cdot d_p \cdot \phi / \mu_g \quad (2.7)$$

He gave the following formula to relate f_k with Re_g :

$$f_k = 1.75 + 150 \cdot (1 - \epsilon) / Re_g \quad (2.8)$$

In an earlier study Carman⁽⁵⁴⁾, using a similar plot, arrived at the following expression:

$$f_k = 2.87 \left(\frac{1-\epsilon}{Re_g} \right)^{0.1} + 180 \cdot (1-\epsilon) / Re_g \quad (2.9)$$

It is worth noting that the specific surface area of the packing, a_t , is given by

$$a_t = \frac{6}{d_p} \frac{(1-\epsilon)}{\phi} \quad (2.10)$$

Comparing Eqs. (2.6), (2.7), and (2.10) one can see that the effect of packing on the pressure drop can be represented physically by a_t and ϵ .

2.2.2.3 Pressure drop of gas in irrigated column

Correlations for gas pressure drop in irrigated packed column fall largely into two categories:

those shown in forms of diagrams and those expressed as mathematical formulae.

Leva⁽⁵⁵⁾ incorporated pressure drop data in the flooding diagram which he obtained after a small modification of the Sherwood diagram⁽⁶⁰⁾ while Mersmann⁽⁵²⁾ used his own flooding diagram for the pressure drop correlation (see section 2.2.3 for flooding diagram). Neither of these diagrams shows the pressure drop in the low liquid velocity region.

The various mathematical formulae for the pressure drop require the knowledge of total hold-up. To be consistent with the pressure drop in the dry column, these formulae take the form:

$$\Delta P_w = \Delta P_d F \quad (2.11)$$

where the function $F=1$ when total hold-up, h_f , equals to zero. Different authors have proposed different forms for the function F as shown below:

Uehida and Fujita⁽⁵¹⁾

$$F = e^{-k h_t} \quad (2.12)$$

$k = 15$ for raschig ring and $k = 20$ for crushed lime

Brauer⁽⁵⁶⁾ :

$$F = [1 + h_t / (1 - \epsilon)] / (1 - h_t / \epsilon)^3 \quad (2.13)$$

Morton⁽⁵⁷⁾ :

$$F = 1 / (1 - h_t / \epsilon)^3 \quad (2.14)$$

Buchanan⁽⁵⁸⁾ :

$$F = [1 - 2.0(h_t - 0.01)]^{-5} \quad (2.15)$$

Warner⁽⁴⁰⁾ :

$$F = 1 + 23.9 h_t^2 \quad (2.16)$$

Jeschar et al⁽⁸⁾ :

$$F = \left[\frac{1+h_t/(1-\epsilon)}{1-h_t/\epsilon} \right]^{1.2} \left[1.5 \frac{u \epsilon}{V h_t} + \frac{\epsilon}{\epsilon-h_t} \right]^{1.8} \quad (2.17)$$

It is clear from the above expressions that there is no general agreement on how the function should be expressed.

2.2.2.4 Influence of gas flow on liquid flow distribution

Dutkai and Ruchenstein⁽⁵⁹⁾ measured the liquid distribution for a wetting system (rings and saddles/water/air) and reported that the liquid distribution did not change until the gas velocity reached 70% of that at flooding. Above that velocity they observed a decrease in the flow rate in the region near the column wall, though the overall liquid distribution did not change very much.

It would appear that no systematic studies on the influence of gas flow on liquid distribution have been reported for non-wetting systems.

2.2.3 Flooding

Since flooding limits the maximum allowable liquid and gas flow rates in packed columns, many investigators have studied this phenomenon. Sherwood et al.⁽⁶⁰⁾ have correlated the flooding velocities by the two parameters:

$$\text{Flooding factor} \quad \frac{V^2 a_t \rho_g}{g \epsilon^3 \rho_l} \eta^{0.2} \quad (2.18)$$

$$\text{Fluid ratio} \quad \frac{u}{V} \sqrt{\frac{\rho_l}{\rho_g}} \quad (2.19)$$

Later, Lobo et al.⁽⁶¹⁾ measured the value, a_t/ϵ^3 , for different packing materials and correlated the reported experimental data on flooding. Fig. 2.5a shows the correlation of flooding velocities as a relationship between Flooding factor and Fluid ratio. This type of diagram is often referred to as the Sherwood diagram. The solid line in the diagram is after Lobo et al.⁽⁶¹⁾ and the source of the plots in the diagram will be mentioned later.

Mersmann⁽⁵²⁾, criticising that the Flooding factor is not dimensionless, proposed a different flooding diagram (Fig. 2.5b) in which he showed the flooding velocities as the relationship between the following two dimensionless numbers:

$$\text{Dimensionless pressure drop} = \frac{\Delta P_d/L}{g \rho_l} \quad (2.20)$$

$$= f_k \frac{1-\epsilon}{\epsilon^3} \frac{v^2 \rho_g}{d_p g \rho_l} \quad (2.21)$$

Dimensionless irrigation density

$$= \left(\frac{\mu_l}{\rho_l g^2} \right)^{1/3} \frac{u(1-\epsilon)}{d_p \epsilon} \quad (2.22)$$

Although neither Sherwood nor Mersmann considered the effects of the surface tension of the liquid, Newton⁽⁶²⁾ showed that the effect of surface tension can be accounted for by multiplying the Fluid ratio (Eq. 2.19) on the abscissa of the Sherwood diagram, by the term $(\sigma_w/\sigma)^3$. Standish and Drinkwater⁽⁶³⁾ found the exponent of (σ_w/σ) to be 2.5. Since in these two investigations a surface active agent was used to change the surface tension of the liquid, the validity of their correlations for other liquids is not clear.

Leva⁽⁵⁵⁾ proposed that the Flooding factor (Eq. 2.17) on the ordinate of the Sherwood diagram should be multiplied

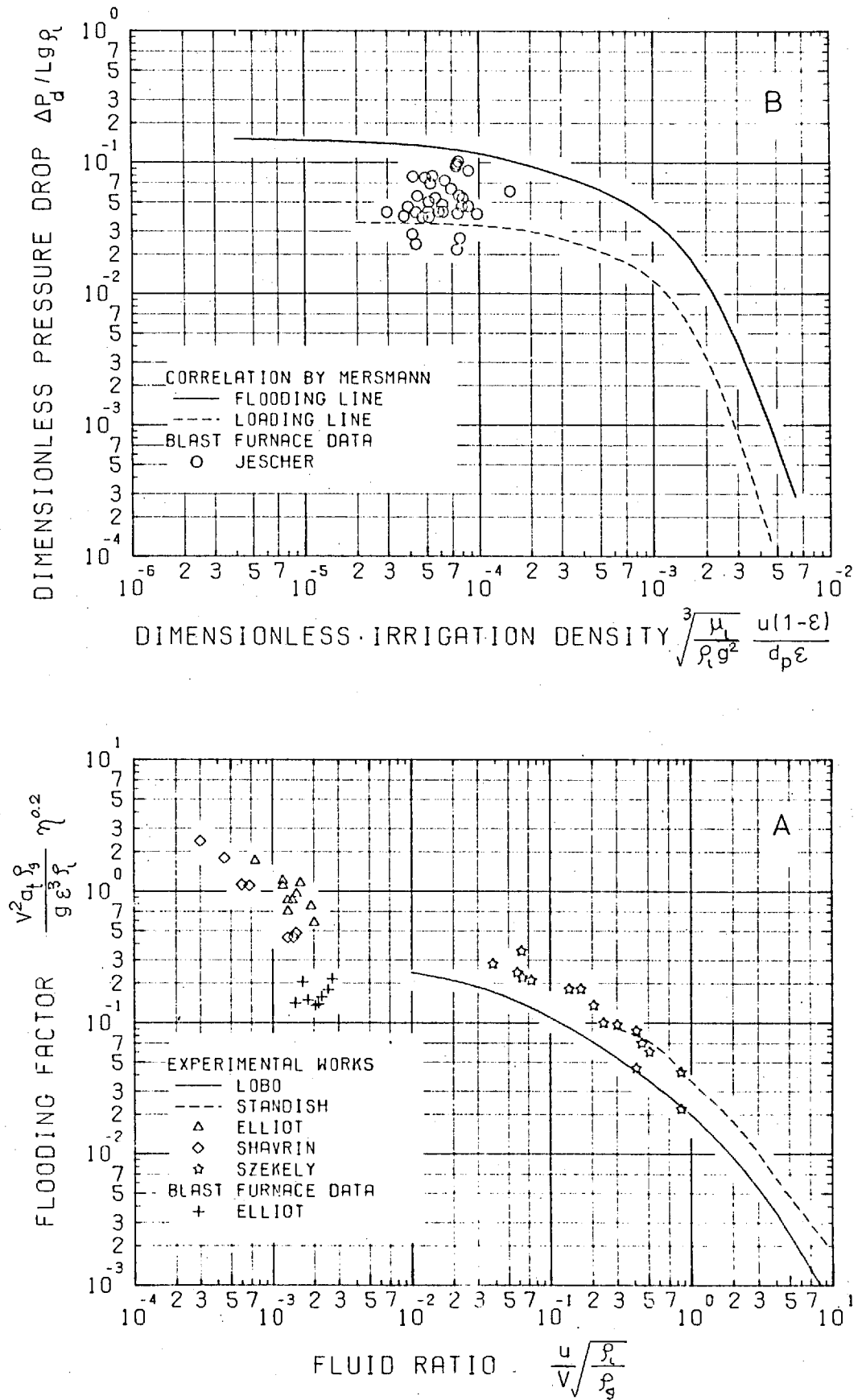


Fig. 2.5 Flooding diagrams showing the limiting condition for flooding. The bottom left region corresponds to non-flooding operation.

A: after Sherwood⁽⁶⁰⁾, B: after Mersmann⁽⁵²⁾

by the term $(\rho_w/\rho_\ell)^2$ where ρ_w is density of water. Later, Szekely and Mendrykowski⁽⁶⁴⁾ found that their data on flooding of mercury in columns packed with spherical particles were in better agreement with the original Sherwood correlation rather than with that proposed by Leva.

Experimental work on flooding which is particularly related to the blast furnace system has not been done extensively.

Elliott et al.⁽⁴⁾ have extended the range of the Sherwood diagram to the lower values of the Fluid ratio by adding their experimental results on 5mm glass bead/wax/heated air system in a 5cm glass column. Their range of Fluid ratio is from 0.0007 to 0.002; the range in the blast furnace shown by the same authors is from 0.001 to 0.003 whereas the range of the diagram given by Lobo et al.⁽⁶¹⁾ is from 0.01 to 10.

Sharvin et al.⁽⁶⁵⁾ made experiments with a carbon/slag (32% CaO, 46.9% SiO₂, 5.7% MgO, 15.4% Al₂O₃)/N₂ system and their data are in good agreement with the results of Elliott et al. as shown in Fig. 2.5. However, the reliability of data on the coke-slag system is questionable since their column diameter, 3 cm, is very small compared with packing diameter of 1.1 cm.

Szekely and Mendrykowski⁽⁶⁴⁾ measured flooding velocities using mercury as the liquid. Glass beads of 3.175 and 6.35mm, 6.35mm ceramic cylinders and "interlock" saddles were used as packings. Standish and Drinkwater⁽⁶³⁾ showed the effect of non-wetting conditions on the flooding velocities using waxed particles. The magnitudes of the fluid ratio for both experiments are considerably higher than that for the blast furnace. Both results, shown in Fig. 2.5 show that the Flooding factor is about twice as much as that predicted by Lobo's correlation. It is

interesting to note that Standish and Drinkwater used water as an irrigating liquid while szekely and Mendrykowski used mercury; the physical properties of these two liquids differ significantly.

Rikhter and Potevnya⁽⁶⁶⁾, using alcohol-castor oil solution of zinc chloride, glycerol at 60°C and aqueous solution of sugar, managed to change the surface tension of the liquid (0.029, 0.050, 0.0845 N/m respectively) while maintaining the density (1210 Kg/m³) and viscosity (0.0124 Ns/m²) constant. Using 25-50mm sized coke coated by an organic silicone lacquer, on which the above liquids showed contact angles of 15, 60, and 100° respectively they measured flooding velocities. From the plot of their results on Mersmann's diagram, they found that the flooding limit increased with the contact angle. To correct the effect of contact angle, they multiplied the dimensionless irrigation density (Eq. 2.22) by the factor of $\cos^6\left(\frac{\theta}{2}\right)$ where θ is the contact angle.

2.3 Application to the Blast Furnace Process

The flooding phenomenon has been one of the major subjects for those who investigate the factors which limit the blast furnace production rate^(5,6,7,8). This is understandable when one recognises⁽⁴⁾ the remarkable agreement between the factors affecting flooding and the factors commonly supposed⁵ to influence the tendency for hanging in the furnace. In spite of this agreement, opinions differ as to whether or not flooding actually takes place in the furnace. As shown in Fig. 2.5 plots of blast furnace data mostly fall just below the flooding line indicating that the conditions in the blast furnace are between the loading and flooding points. Attempts to initiate flooding in an experimental furnace were made by Nakane et al⁽⁶⁷⁾. Granulated blast furnace slag and pig iron were added to the charged material to get a liquid flow rate as high as 0.4 Kg/m²s. They, nonetheless, failed to obtain a clear occurrence of flooding. Instead, they observed channelling

in the stack followed by fluidization.

In a recent study Standish and Colquhoun⁽⁶⁸⁾ observed the effect on the flooding limit of the direction of the inlet gas flow at the bottom of a column in which water was flowed through packings of 6mm glass spheres and rings and 8~16mm coke particles. They found the flooding factor for horizontal gas entry was approximately four times as large as that for vertical gas entry.

Warner⁽⁶⁹⁾, noting a larger non-uniformity of gas flow across the furnace at the level near the raceway, proposed a hypothetical model in which the slag is held locally above the raceway.

The above three papers^(67,68,69) indicate clearly the limitations of the one-dimensional flow model and the need for further investigation on the flows of liquid and gas in this region.

2.4 Summary

The flow system in the lower part of the blast furnace where molten slag and metal flow counter-current to rising gas stream through a bed of coke is apparently similar to that in packed absorption columns commonly used in the chemical engineering field. However, there are substantial differences between these two systems in that:

- (a) the slag and metal do not wet the coke while wetting flow is common in the latter,
- (b) the liquid velocities in the former are substantially lower than that in the latter,
- (c) crushed coke particles form the packing in the former while hollow packings such as rings, saddles etc. are more common in the latter.

The available information on the hold-up and flooding at low liquid velocities or for non-wetting flows is very limited. No generalized correlations have been proposed for operational and static hold-ups for non-wetting flow.

Although several papers on flooding are available in either low liquid velocity or non-wetting flow, more data seems to be needed to assess the influence of degree of wetting.

CHAPTER 3

DESIGN OF EXPERIMENTAL SYSTEM

As shown in the preceding Chapter, non-wetting flow and low superficial velocity of liquid distinguish the slag/metal/coke system in the blast furnace from those common in chemical engineering field. No systematic studies have been published on the influence of the degree of wetting between the packing and liquid on hold-up and flooding at low liquid velocities.

It is appreciated that in operating furnaces the gas flow, introduced horizontally through the tuyères, changes direction as it ascends through the bed of coke. Consequently, the flow pattern in the lower region of the furnace will be quite complex. However, a complete understanding of the flow process in this region cannot be attempted before adequate theoretical and experimental information on the simpler, "one-dimensional" model in which the gas flow is introduced vertically at the bottom of a column is available. Therefore, it was decided that the present study would deal with the "one-dimensional" flow situation.

Since it would be extremely difficult to carry out accurate experiments on the high temperature slag/coke/metal system, it was decided to use a room temperature model. The idea of using a $\text{SnCl}_2\text{-KCl}$ slag/carbon system at about 200°C was also abandoned because the measured values of the contact angle between the slag and carbon were too low (less than 90°).

For the systems of the same geometry, dynamic similarity between the flows in the room temperature model and in the high temperature system can be checked by comparing the ranges of dimensionless numbers for both systems. These

numbers are derived from the combinations of forces which influence the flow.

The gas flows through two packed beds will be similar if the Reynolds numbers for the gas flow, Re_g (Eq. 2.7), are the same.

The forces which would affect the liquid flow are:

- 1) gravitational force

$$f_g = \rho g D^3 \quad (3.1)$$

- 2) inertial force,

$$f_i = \rho u^2 D^2 \quad (3.2)$$

- 3) viscous force,

$$f_v = \mu u D \quad (3.3)$$

- 4) surface force,

$$f_s = \sigma D \quad (3.4)$$

- 5) solid-liquid interfacial force,

$$f_{si} = \sigma D(1+\cos\theta) \quad (3.5)$$

- 6) the force exerted by the gas flowing through the bed

$$f_p = \left(\frac{\Delta P}{L}\right) D^3 \quad (3.6)$$

where D is the characteristic length of the system.

It would be necessary to add a proportionality constant to the right hand side of each of the above equations if the absolute values of the forces were required. In the present case, however, each proportionality constant is the same for assumed geometrically similar systems and since we are only interested in the relative magnitudes of the forces, the constants do not appear in the above equations.

Eq. (3.5) and (3.6) require some explanation. Eq. (3.5) is based on equilibrium conditions in which the reversible work per unit area, W_a , of adhesion of the liquid to the solid when coated with an adsorbed film of the saturated vapour is given by⁽⁷⁰⁾

$$W_a = \sigma(1 + \cos\theta) \quad (3.7)$$

Noting that the energy E is related to the force f by $E = f D$ and since in this case $E \propto W_a D^2$, one can obtain Eq. (3.5) from Eq. (3.7). The force acting on the liquid is assumed to be proportional to the gas pressure drop. The proportionality constant can be assumed to be the same for similar flow systems and hence it does not appear in Eq. (3.6).

For the characteristic length D , the packing diameter d_p is commonly used for packed columns. Although the combination of the forces to yield various dimensionless numbers is arbitrary, the following numbers, are chosen in order to maintain consistency with those used by previous authors:

$$\text{Reynolds number} \quad \text{Re} = f_i / f_v = \rho_\ell u d_p / \mu_\ell \quad (3.8)$$

$$\text{Galileo number} \quad \text{Ga} = f_i f_g / f_v^2 = d_p^3 \rho_\ell^2 g / \mu_\ell^2 \quad (3.9)$$

Capillary number $C_p = f_g/f_s = \rho_l g d_p^2 / \sigma$ (3.10)

Dimensionless interfacial force

$$N_c = f_{si}/f_s = 1 + \cos\theta$$
 (3.11)

Dimensionless pressure drop

$$\Delta P^* = f_p/f_g = \Delta P/L \rho g$$
 (3.12)

It will be noted that Re , Ga , C_p are used in Table 2.3 in the correlations for operational hold-up. Furthermore one can see that C_p is essentially the same as the capillary number N_{cap} (Eq. 2.4) defined by Turner and Hewitt⁽⁵⁰⁾.

Tables 3.1 and 3.2 show the physical properties of the packing materials and of the liquids respectively. Table 3.3 shows a comparison of the values of the dimensionless numbers for the blast furnace with those obtained in the present work. The dimensionless pressure drop is not given in the Table since its value for the blast furnace is not available. It will be noted that except for the Galileo number of the metal, and the dimensionless interfacial force, N_c , the values for the blast furnace are well within the range of the experiments. The relatively small size of the packing used in the experiments is the main reason for the difference of the values of the Galileo number.

Three different materials were used for the same size packing (W13, PL13, AL13) to obtain different contact angles. Paraffin wax was chosen as one of the materials as it probably gives the largest contact angle among the commonly available materials.^(70,71) The choice of $CaCl_2$ solution made it possible to increase the contact angle further, though, it still fell slightly short of those estimated for the blast furnace conditions.

Table 3.1 Data on packings used in experiments

Packing	Diameter mean (mm)	Standard deviation (mm)	Apparent density (kg/m ³)	Symbol
Polythene spheres	13.2	0.10	921	PL13
	9.0	0.08		PL9
	10.6	--		PLM**
Alumina spheres	13.1	0.34	3465	AL13
Wax-coated polythene spheres	13.3	0.10	921	W13
Glass spheres	8.1	0.15	2500	G8
Wax-coated coke	11.0	9.5~12.7*	1210	C11

* size range (openings of sieves)

** 50-50% mixture of PL13 and PL9

Liquid	Concentration (wt. %)	Density (Kg/m ³)	Viscosity* (Ns/m ²)	Surface tension (N/m)	Contact angle on polythene wax (Degree)		Symbol
Water	--	1000	0.0010	0.0732	92.6	105.6	WATR
Aq. sol. of ethanol	96**	807	0.0016	0.0240	0	--	ETOH
Aq. sol. of glycerol	80	1210	0.064	0.0652	88.1	96.6	GLY
Aq. sol. of CaCl ₂	35	1350	0.0059	0.0888	108.9	114.1	CACL
Aq. sol. of ZnCl ₂	75	1920	0.034	0.0809	84.5	97.9	ZNCL

* Nominal value,

** Azeotrope

Table 3.2 Physical properties of liquids used in experiments

System	Liquid	Re	Ga ($\times 10^4$)	C_p	N_c
Blast furnace	Metal slag	2.5 0.017	23600 1.0	34 31	0.43 0.06 ~ 0.74
Experiment	WATR	0.07 ~ 22	610 ~ 2600	8.6 ~ 23	0.73 ~ 2.0
	ETOH	0.05 ~ 7	83 ~ 3500	25 ~ 63	2.0
	GLY	0.005 ~ 0.11	0.18 ~ 0.74	12 ~ 30	0.88 ~ 2.0
	CACL	0.02 ~ 4.5	26 ~ 110	9.5 ~ 25	0.59 ~ 0.68
	ZNCL	0.01 ~ 0.6	1.6 ~ 6.9	15 ~ 40	0.86 ~ 1.1

Table 3.3 Comparison of the values of dimensionless numbers for the blast furnace with those for experiments with different liquids.

The use of high-density liquid, ZnCl_2 solution, is primarily intended to test the effect of the ratio of liquid to solid densities on the stability of the bed. This factor has not been studied previously although it is easy to imagine that fluidisation of the column would start before the column floods if one uses a heavy liquid with a light packing. With a density ratio of about 2.5 estimated for the slag/coke system the instability of the bed is possible at or near flooding. It must be noted that the apparent absence of flooding in the experimental blast furnace⁽⁶⁷⁾ mentioned earlier could be explained by the instability of the bed.

CHAPTER 4

EXPERIMENTAL WORK

4.1 Apparatus

Plate 1 shows general arrangement of the apparatus which consists of two parts: the main section in the centre and the gas flow control section on the left of the plate.

Fig. 4.1 shows a schematic diagram of the apparatus in the main section. The column, 12, was suspended from one end of a steel beam, 2, with a T-shaped cross-section. The weight of the dry column was balanced by adjusting the counter balancing weight, 4. The weight change of the column was measured and transformed into an electronic signal by a load cell, the actuator of which rested on a small steel ball partially embedded in the beam, 2. The zero point of the load^{cell} was shifted electrically to read zero when the load was 100g. This ensured that the actuator of the load cell and the steel ball were in good contact. The range of output of the load cell could be varied by appropriate changes in the balancing weight, 3. The weight change of the column due to the pressure loss of the gas flowing through the column was compensated by introducing the pressure at the gas inlet to a chamber with a thin film diaphragm, 5, on which the counter weight, 4, rested.

The sensitivity of the balance was better than 0.2 g. A continuous recording of the weight of the dry bed for more than 200 hours showed that the zero drift of the balance was less than ± 0.5 g. The balance was calibrated before each experiment and together with the zero drift mentioned above, the accuracy of the balance was within $\pm 0.5\%$ of reading ± 0.5 g.

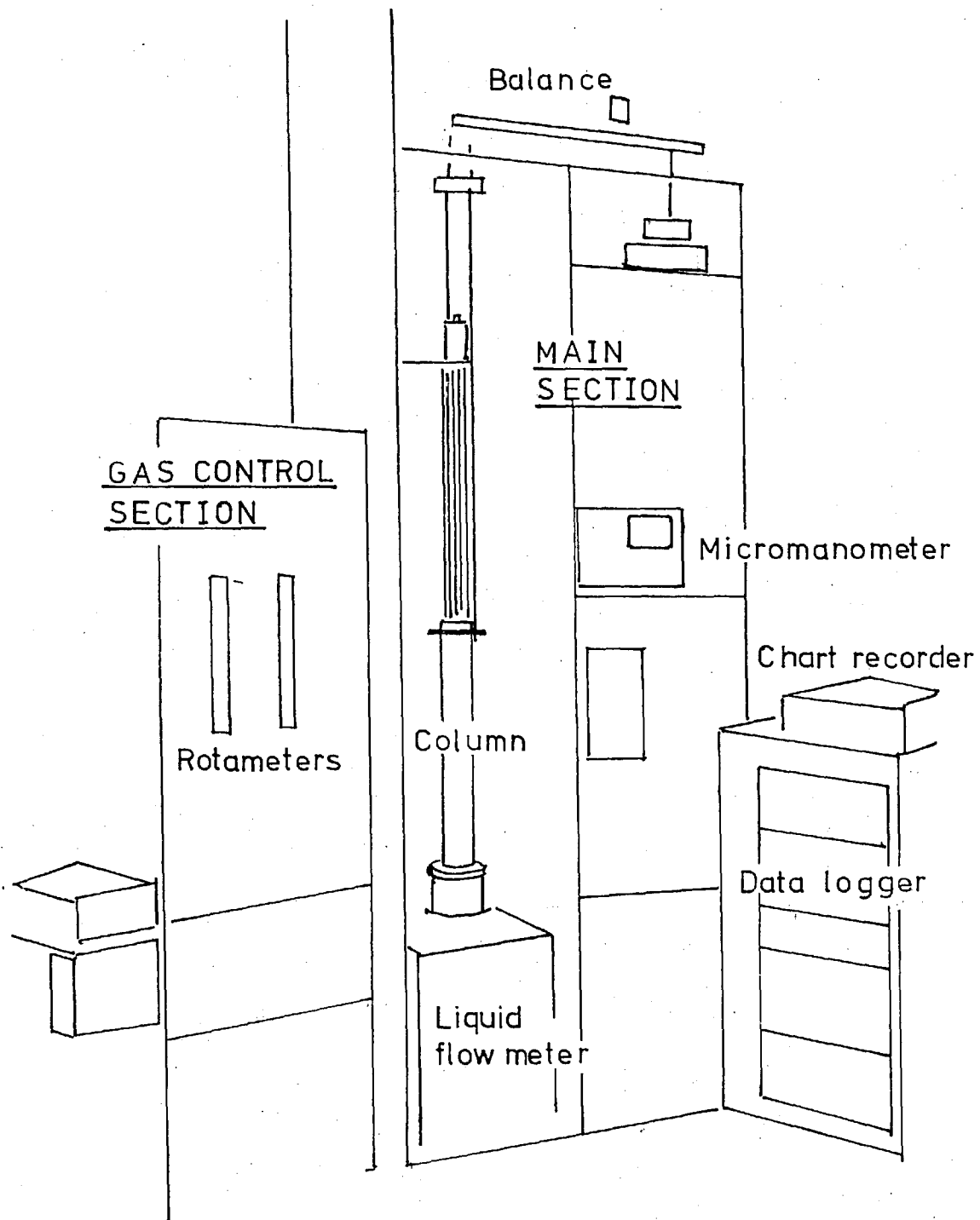
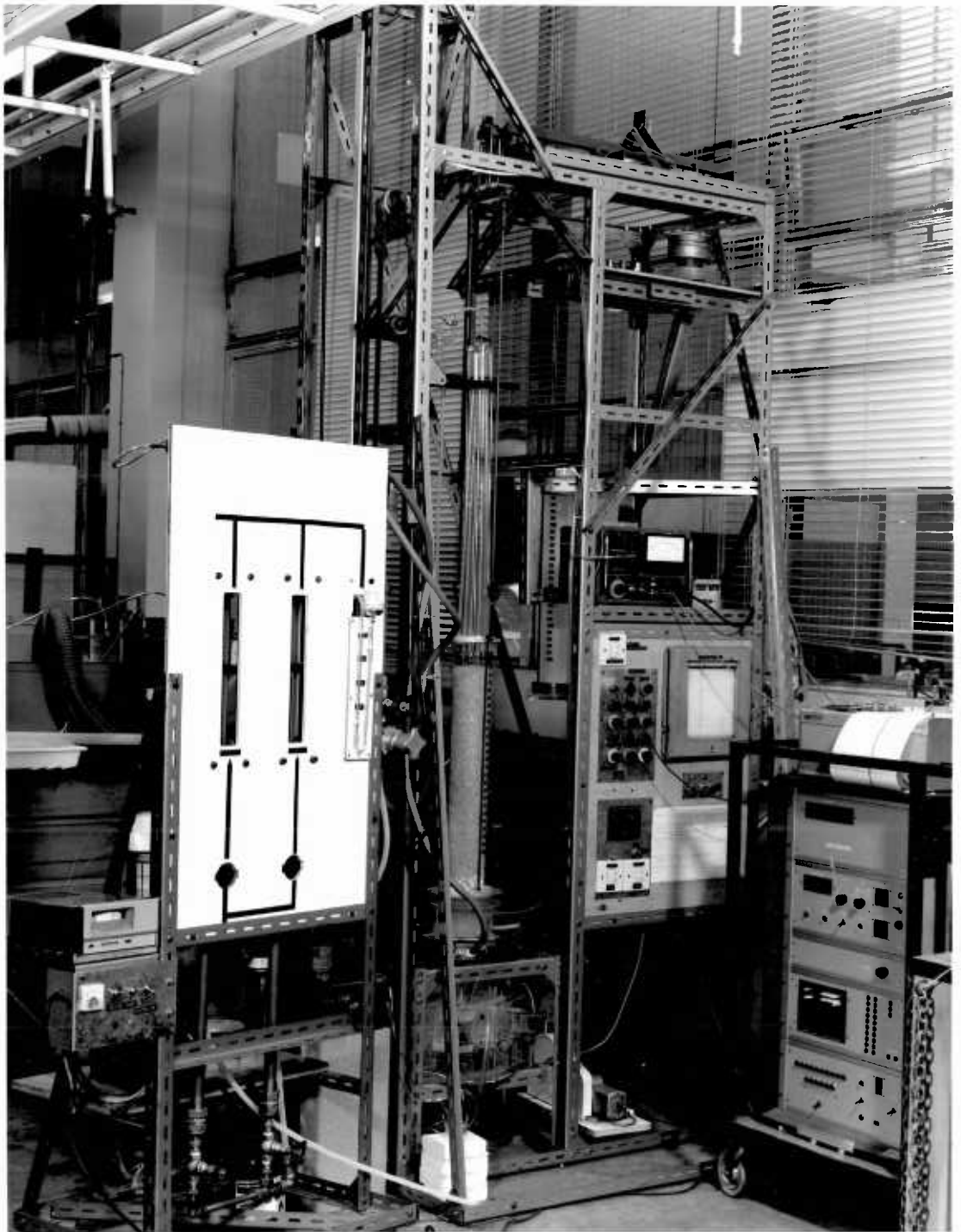


Plate 1 General view of the apparatus



KEY TO FIG. 4.1

- 1 Load cell (900g full load)
- 2 Beam of the balance (T-shaped)
- 3 Balancing weight
- 4 Counter balancing weight
- 5 Diaphragm (to compensate the effect of gas pressure on the balance)
- 6 Constant head tank
- 7 Three-way cock
- 8 Reservoir for distributor
- 9 Capillaries
- 10 Silicone rubber tubing
- 11 Distributor head
- 12 Glass column (95mm x 650mm)
- 13 Pressure transducer
- 14 Sintered glass filter
- 15 Liquid collector/gas distributor, details in Fig. 4.4
- 16 Gas supply main
- 17 Vessel to remove pulsation in the liquid flow
- 18 Thermometer
- 19 Liquid flow meter, details in Fig. 4.5
- 20 Electric motor with speed control
- 21 Peristaltic pump
- 22 Liquid reservoir tank
- 23 Dew point monitor, details in Fig. 4.7b.

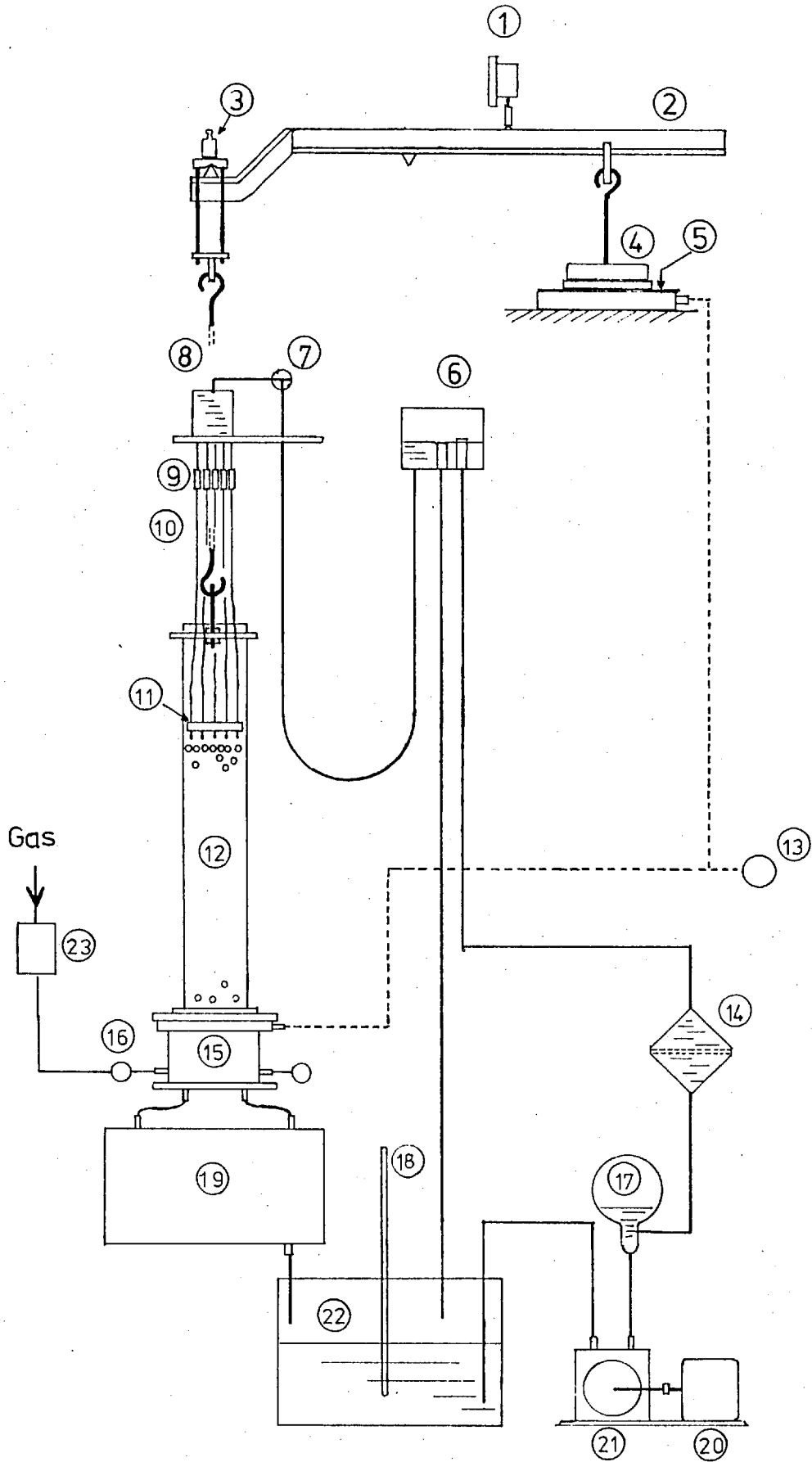


Fig. 4.1 Schematic drawing of experimental apparatus' in the main section

4.1.1 Column

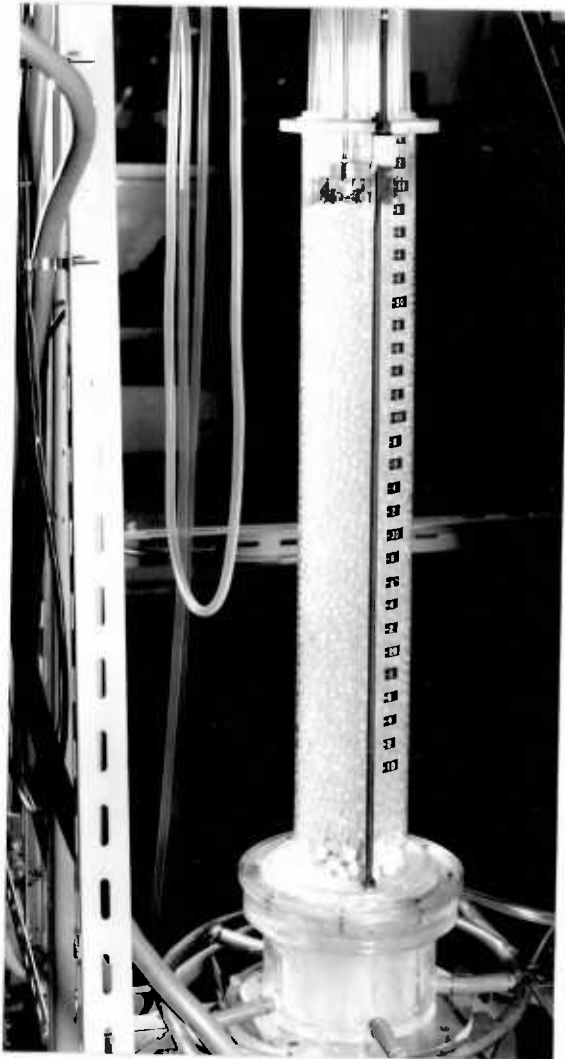
Two different columns of the same size, 95mm id., 650mm length, were used. Both were made of glass tubing; one was coated with PTFE-spray for experiments in the non-wetting conditions while the other was used for experiments in the wetting conditions.

The grid for the non-wetting column was made of 13mm polythene balls which were fused to one another at the points of contact. The grid for the wetting column was made of 13mm alumina balls stuck with silicone rubber at the points of contact. These grids, being almost the same structure as the beds above them, gave as little influence as possible to the results of experiments, especially in the liquid distribution measurement. The depth of the grid was about 35mm in both columns.

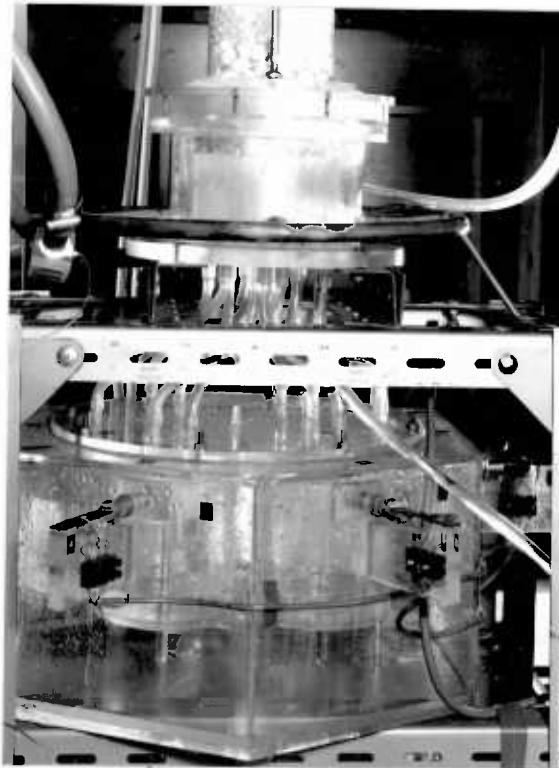
Plate 2a shows the wetting column being used for 8mm glass ball packing.

4.1.2 Control and measurement of liquid flow rate

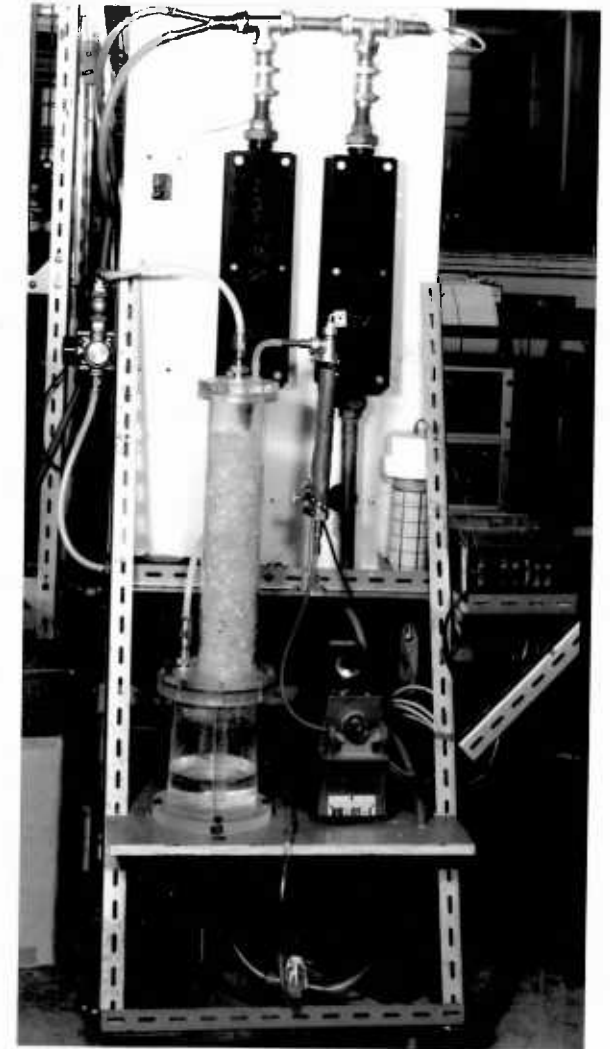
The liquid was stored in a reserve tank, 22. A peristaltic pump, 21, driven by an electric motor with speed control, 20, was used to circulate the liquid. The liquid flow rate was adjusted by either changing the height of the constant head tank, 6, or by changing the size of capillaries, 9. The liquid supply to the column, 12, was controlled by stop cock, 7. The distributor head, 11, had 19 supply points according to the arrangement shown in Fig. 4.2 through which the liquid flowed as droplets. The distribution of the liquid flow at the top of the column was changed by stopping the liquid supply to some of the 19 supply points. Four different arrangements of the supply points, shown in Fig. 4.3 were used in the experiments. The arrangement "19" gave the evenest while "71" gave the most centralized liquid flow distribution at the top of the column.



(a) column



(b) liquid collector and flow meter



(c) Gas humidification column

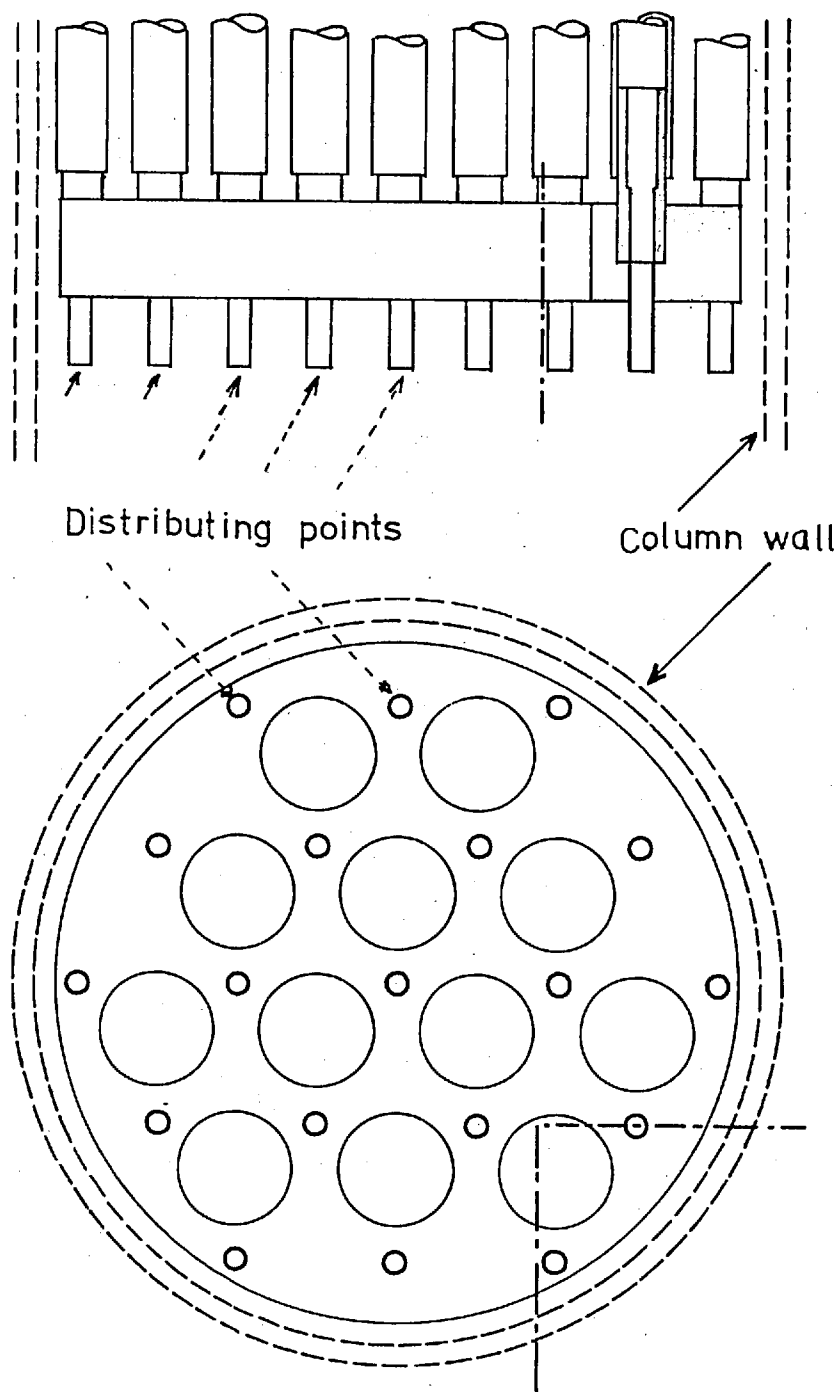
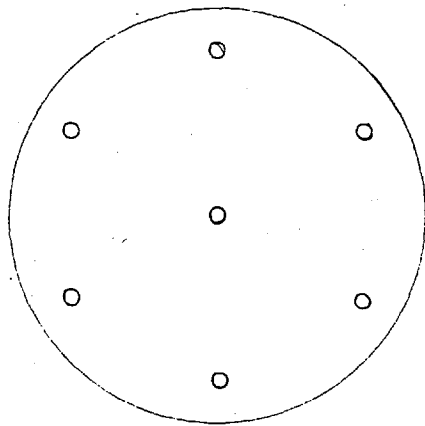
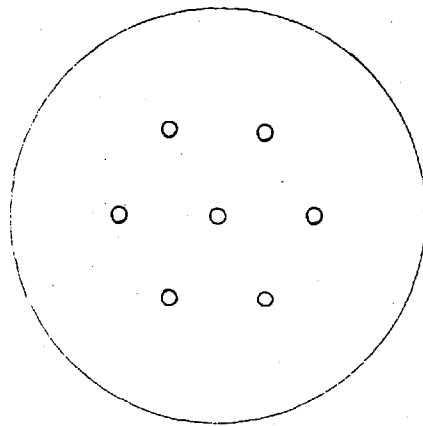


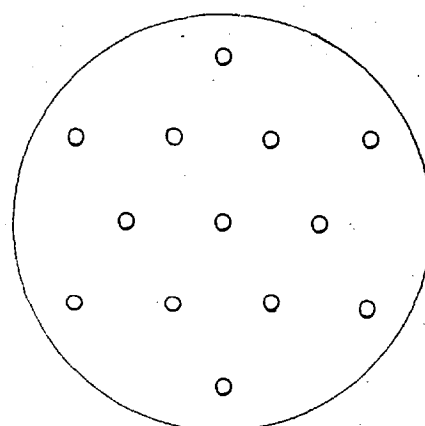
Fig. 4.2 Design of the liquid distributor (Scale 1:1)



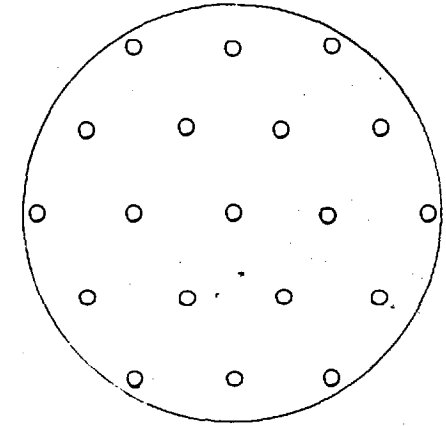
Symbol : 7M



7I



13

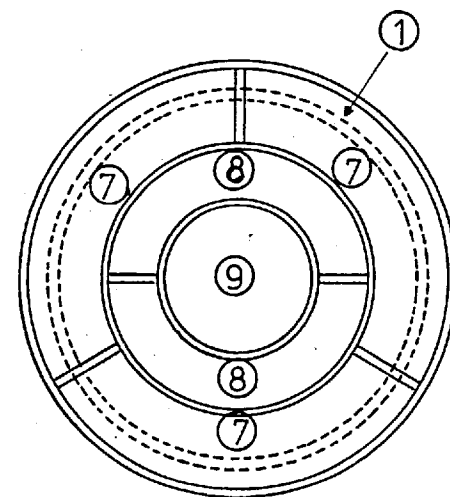
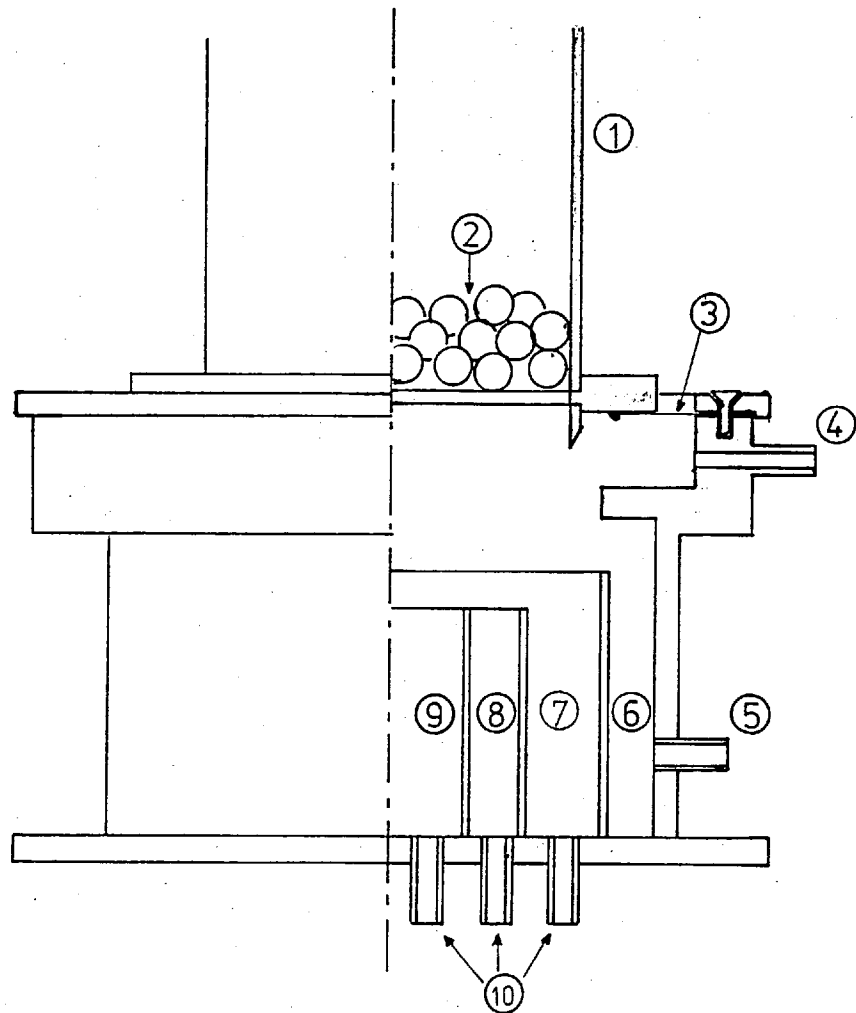


19

Fig. 4.3 Arrangement of supply points of distributor used in experiments (enclosing circle shows the cross section of the column).

KEY TO FIG 4.4

- 1 Glass column
- 2 Grid: made of 13mm plastic balls for experiments on non-wetting flows
made of 13mm alumina balls for experiments on wetting flows
- 3 Diaphragm, made of thin plastic sheet
- 4 Gas pressure tap
- 5 Gas nozzle (5 in total)
- 6 Gas distributing port
- 7 Outer liquid collector (3 in total)
- 8 Middle liquid collector (2 in total)
- 9 Inner liquid collector
- 10 Outlets of liquid



Cross-section of the liquid collector

Fig. 4.4 Liquid collector/gas distributor and position of the column (Scale 1:2)

The liquid flowed out of the column into the collector 15, which had six separate compartments (Fig. 4.4). Each compartment collected the liquid from almost the same cross-sectional area of the column. The liquid flow rate to each compartment was measured by specially designed liquid flow meters. As shown in Fig. 4.5 the measuring mechanism consisted of a container, 6, with siphon, 7, for self-draining of the liquid and a spring beam, 4, on which a pair of strain gauges was fixed. An increase in the weight of the container, 6, increased the bending of the beam which led to an increase in the output of the strain gauges. When the liquid level rose to the top of the siphon, 7, it started to drain automatically. Special attention was paid to the design and construction of the siphon to make the draining process reliable. The measuring containers were kept inside a gas-tight vessel, 8, so that the liquid flow rate could be measured continuously even in the presence of gas flow. Plate 2b shows the arrangement of liquid collector and liquid flow meters.

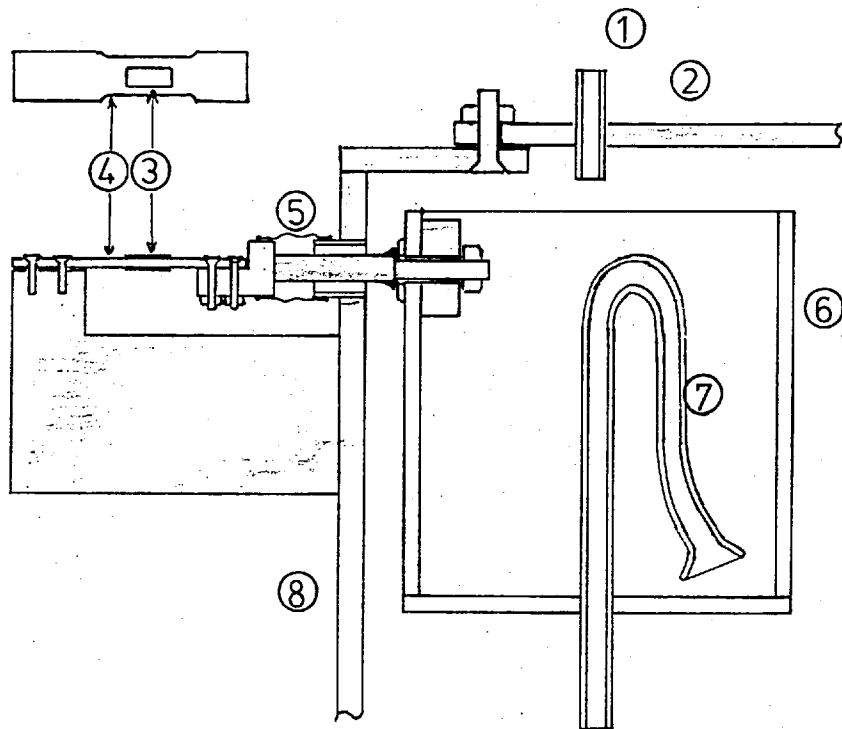
The zero drift of the liquid flow meter was as high as $\pm 5\%$ over a period of 24 hours mainly due to temperature changes. Since the data used for the flow rate calculation were always for a period of four to eight minutes, the accuracy of the calculated flow rate was not affected by the zero drift and depended mainly on the accuracy of the calibration and was better than 1% of the reading.

4.1.3 Gas flow control

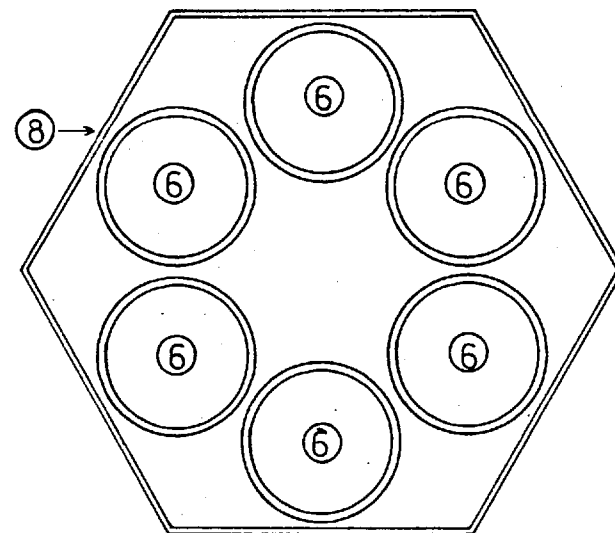
Fig. 4.6 shows a schematic diagram of the gas flow control section and Plate 2c shows the arrangements of the gas humidification column. Compressed air (7 atm) from the supply line was first passed through a filter, 1, (MARTONAIR, type S/F164) which removed traces of oil as well as dirt. The flow rate of the cleaned air was adjusted to the desired value by the valve 3. The pressure regulator, 2, minimized fluctuations in the gas flow rate due to any changes in the pressure of the air supply.

KEY TO FIG. 4.5

- 1 Liquid inlet
- 2 Lid of gas-tight vessel
- 3 Strain gauges
- 4 Beam spring
- 5 Thin-wall rubber tubing
- 6 Liquid measuring container
- 7 Siphon
- 8 Wall of gas-tight hexagonal vessel



(Scale 1:2)



Arrangement of the six containers
in the gas-tight vessel (Scale 1:5)

Fig. 4.5 Liquid flow meter

KEY TO FIG. 4.6

- 1 Filter
- 2 Pressure regulator
- 3 Flow control valve
- 4 Gas inlet to humidifier
- 5 Liquid distributors (6 points)
- 6 Packed column of 9mm glass raschig rings,
column id: 90mm, height: 370mm
- 7 Liquid reservoir
- 8 Chromel-alumel thermocouple
- 9 Heater for liquid
- 10 Heating element
- 11 Liquid circulating pump (peristaltic)
- 12 Temperature controller
- 13 Three-way cock
- 14 Tank for distilled water
- 15 Rotameters for gas flow measurement
- 16 Hg manometer

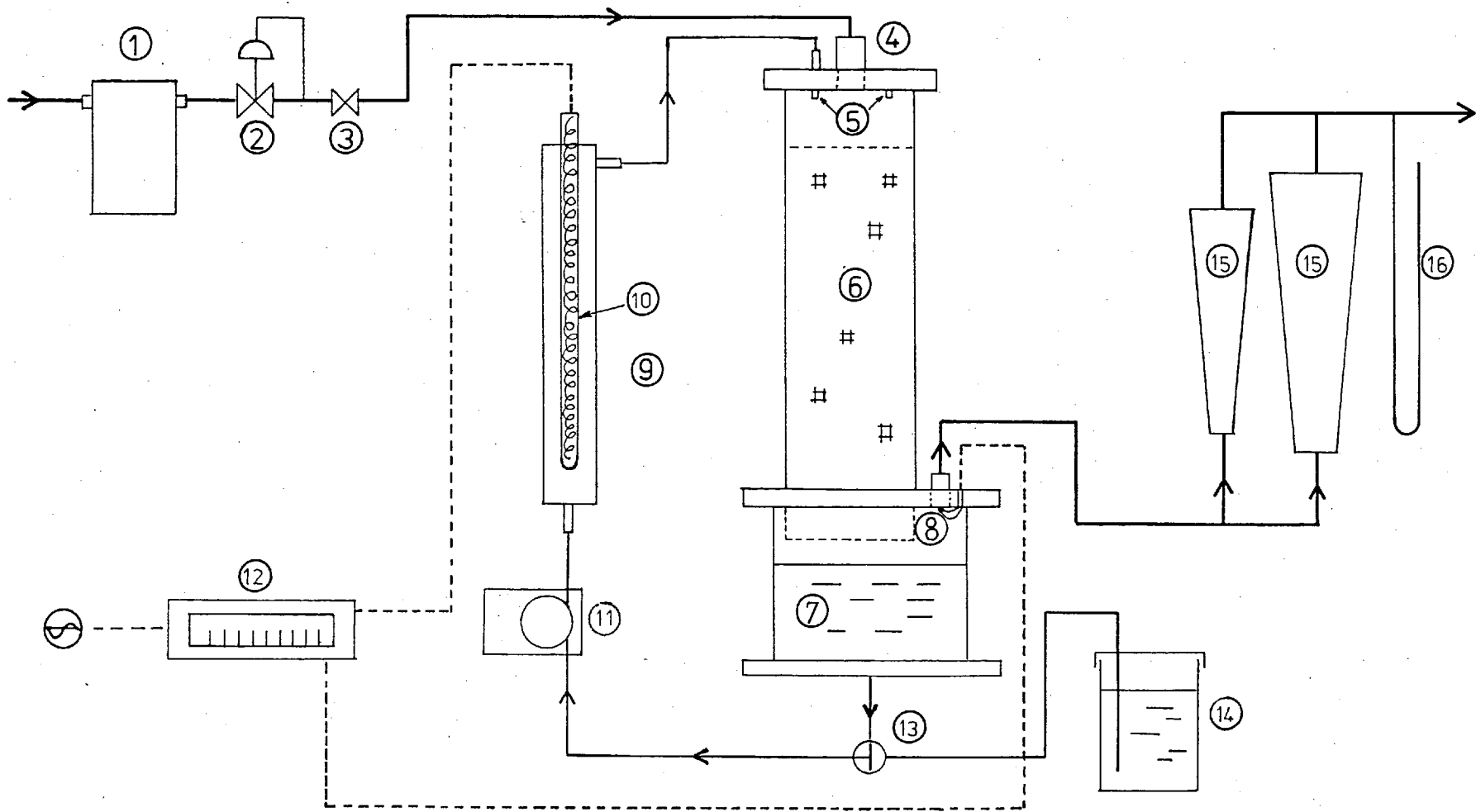
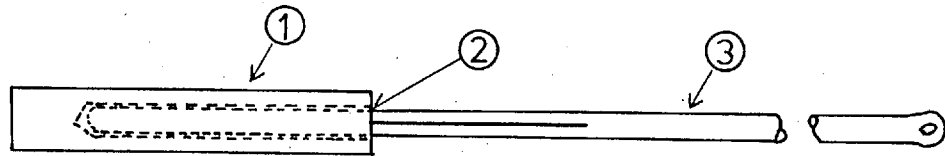


Fig. 4.6 Schematic drawing of gas flow control section

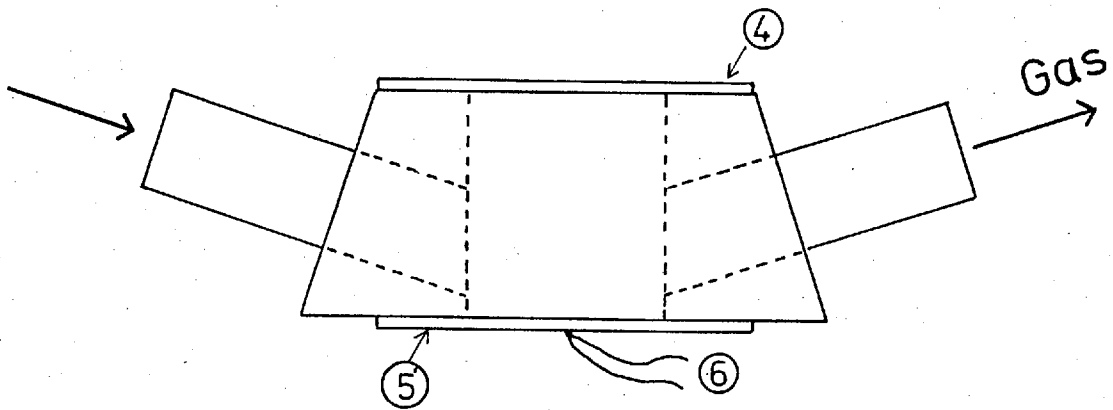
The air was then passed through a humidifier column 6, co-current with the liquid which was circulated by the pump, 11. The humidity of the air was controlled by adjusting the power input to the heating element, 10, in such a way that the gas temperature measured by the thermocouple, 8, was constant. The control temperature was set relative to room temperature, i.e., an increase in room temperature caused an increase in the gas temperature. This method of control proved satisfactory though the response was somewhat slow. By careful setting of the control temperature, it was possible to control the dew point of the gas at the outlet of the humidifier column within $\pm 0.2^{\circ}\text{C}$ of the room temperature.

In preliminary tests it was observed that the dew point at the inlet of the gas supply main (16, Fig. 4.1) measured with a dewpoint meter (Fig. 4.7), decreased with the increase in the pressure drop of the gas between the humidifier column and the inlet of the gas supply main. This decrease in the dew point with the increase in gas flow was compensated for either by increasing the control temperature (when water was the irrigating liquid) or by diluting the circulating liquid with water (when glycerol - or CaCl_2 solution was the irrigating liquid). This humidifier and its control were proved successful except for a few runs with water as an irrigating liquid at the lowest flow rates. The humidifier was not used when the ZnCl_2 solution was the irrigating liquid. The air was found humid enough to dilute the solution whose density decreased from 1940 to 1910 (Kg/m^3) during the whole series of experiments.

After the humidification, the gas flow rate was measured by two rotameters, 15, corrected for the pressure measured by the mercury manometer, 16. No correction was made for the temperature or for the humidity of the gas. The accuracy of the rotameter is better than $\pm 3\%$ of the measured flow rates.



(a) For use in open atmosphere



(b) On-line monitor

Fig. 4.7 Dew point meter

- | | |
|---------------------------------|------------------|
| (1) Copper block (8 x 8 x 60mm) | (4) Glass window |
| (2) Silicone grease | (5) Copper plate |
| (3) Thermometer | (6) Thermocouple |

The copper block (1) or plate (5) is cooled down to the temperature where dew just starts to form on the polished surface of the copper block or plate and the temperature (dew point) is measured by the thermometer (3) or by a thermocouple (6).

Gas distributor

The gas was fed into the column through the gas supply main (16, in Fig. 4.1) , via. five gas nozzles (5, Fig. 4.4) to the gas distributing port (6, in Fig. 4.4). The maximum velocity of the gas leaving the port was 2.5 m/s. At this velocity, the dynamic pressure of the gas, 4 N/m^2 was approximately equivalent to the pressure drop through 1mm thickness of the bed of 13mm spheres. Therefore it is unlikely that maldistribution of the gas was caused by this arrangement.

Measurement of gas pressure drop

The static pressure was measured at the gas pressure tap, 4, in Fig. 4.4, with a pressure transducer (micromanometer, manufactured by Furnace Control Limited). The micromanometer was calibrated using a simple water manometer. The calibration curve is given in Fig. 4.8.

4.1.4 Recording of the data

The outputs of the load cell and the micromanometer were recorded on paper tape by a data logger together with the output of strain gauges for each container of the liquid flow meter. A set of 15 to 20 data were measured at either 15 or 30 seconds interval. The outputs of the load cell and the micromanometer were also recorded continuously on a two-pen chart recorder.

4.2 Liquids and Packings

The physical properties of the liquids and packings used in the experiments are given in Tables 3.1 and 3.2. Plate 3 shows the appearance of the particles of the packings in both dry and wet states.

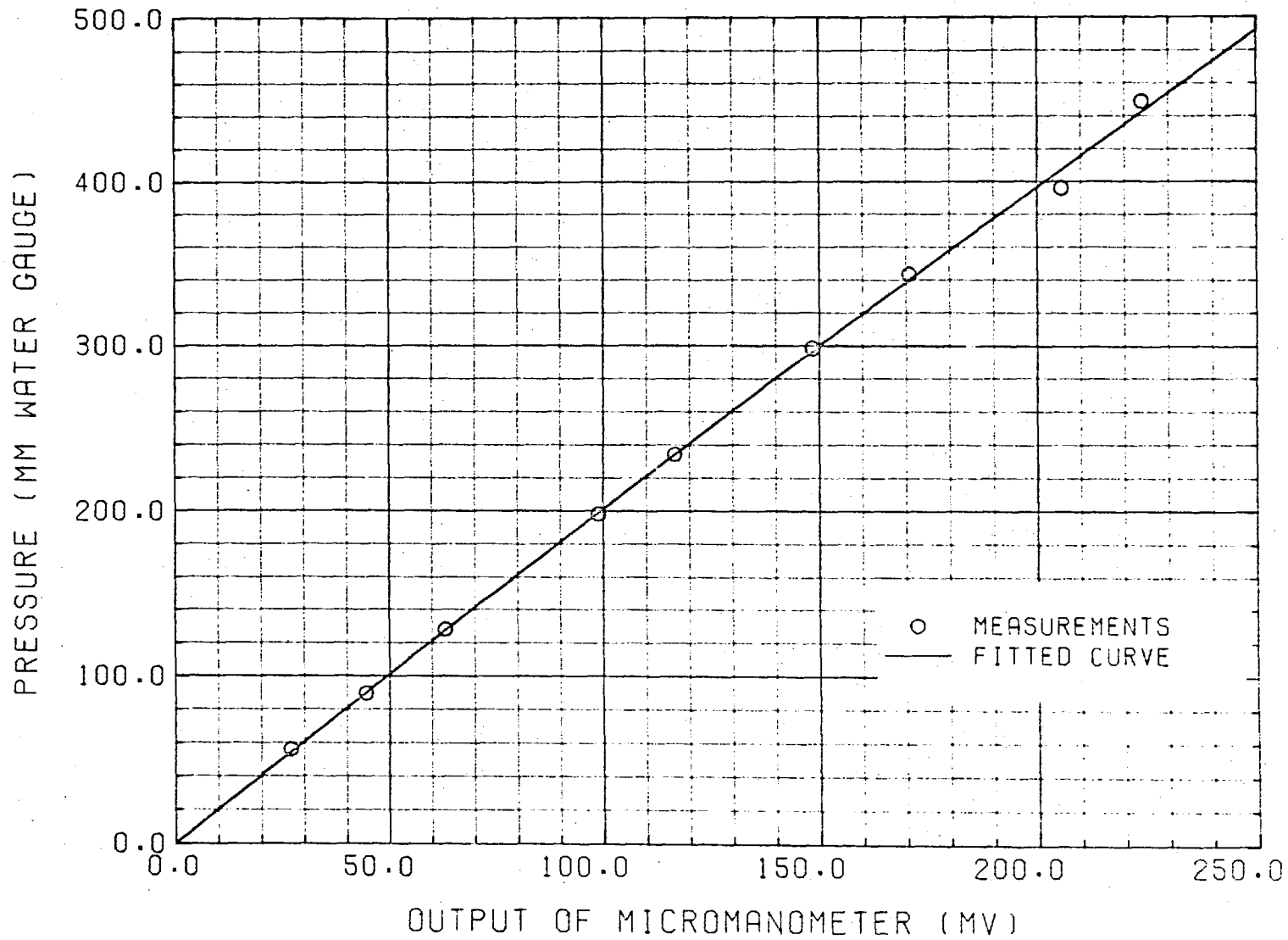
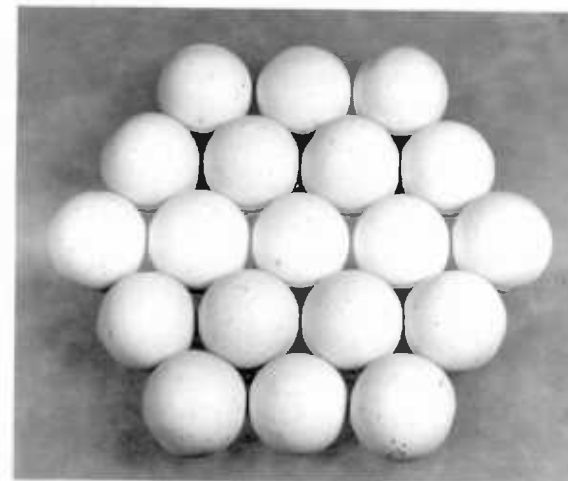


Fig. 4.8 Calibration curve for micromanometer

Dry



Wet



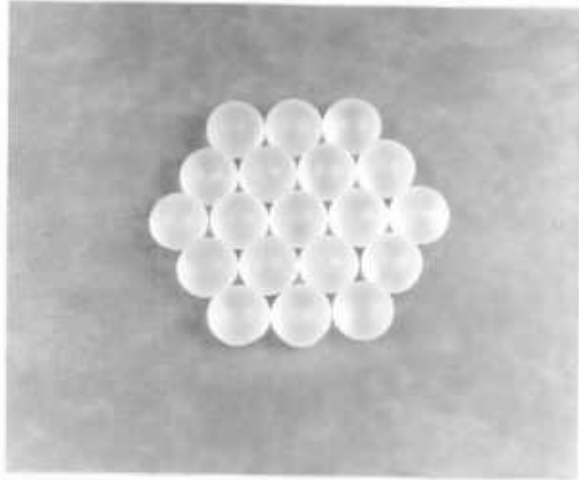
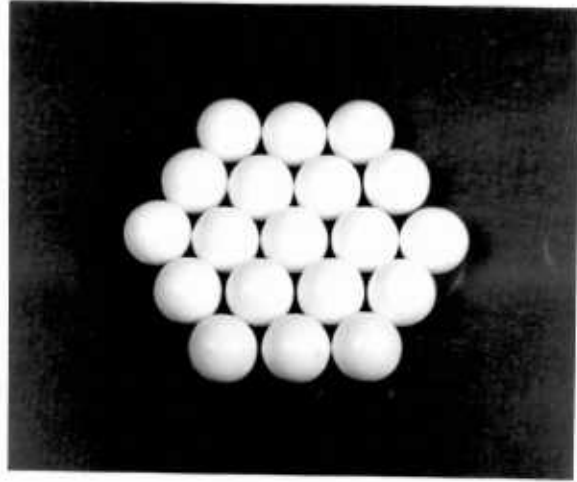
PL13

W13

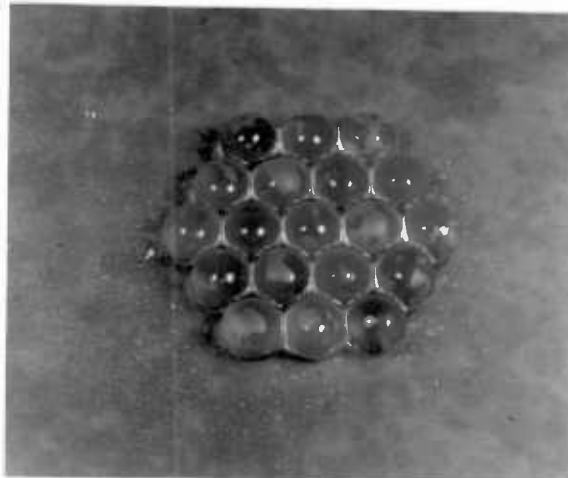
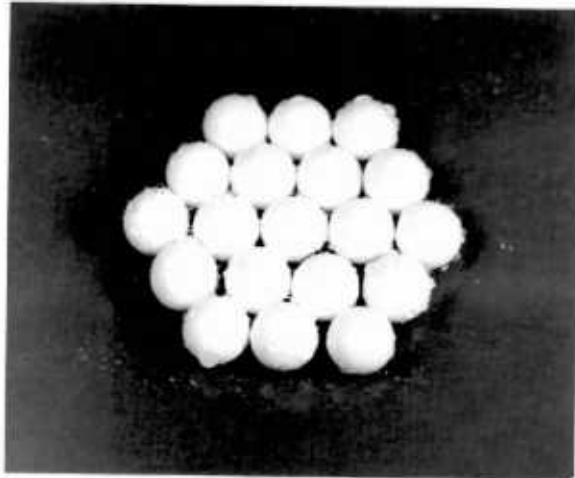
AL13

Plate 3 Appearance of particles in dry and wet states. (Scale 1:1)

Dry



Wet



PL9

G8

C11

Paraffin wax coating

Coke particles and polythene spheres (PL13) were coated by paraffin wax according to the following procedure: Paraffin wax, coagulation point of which is specified as 62°C , was melted in a beaker heated in a boiling water bath. Particles were put into the beaker. Polythene spheres were allowed to warm up only for a few minutes in the beaker because dissolution of the surface of the spheres occurred after prolonged heating in molten wax. Coke particles, on the other hand, were kept in the molten wax for more than ten minutes for better coverage of the open pores by wax. The particles were then picked up one by one with a pair of tweezers specially made for this purpose, cleared of excess wax and cooled in an alcohol water mixture.

It will be seen from Table 3.1 and Plate 3 that the coated film on polythene spheres is thin and uniform. The surface of coated coke, as shown in Plate 3, preserves the roughness of the original coke particles. Therefore, it can be assumed with confidence that the coated particles are identical with their original except for the contact angle of liquid on the surface.

Measurements of physical properties

The density, viscosity, and surface tension were measured for the liquids other than water.

The viscosity was measured by a standard U-tube viscometer⁽⁷²⁾ at room temperature. Measurements were carried out frequently during experiments as the viscosity changed significantly with the room temperature. The averaged viscosity for each run was used in the analyses of the results.

The surface tension was measured by a capillary rise method. Two different sizes of capillaries were used and the difference of the heights of menisci was read to within 0.01mm by a cathetometer. The calibration was made with water.

The density of packing was measured by a replacement method. A 500 ml volumetric flask was used. Distilled and de-gassed water was used as a replacing liquid. The flask was kept in a water bath at $20.0 \pm 0.2^{\circ}\text{C}$. for more than 12 hours before measurements. The somewhat high density of coated coke (Table 3.1) is considered to be due to the penetration of the paraffin wax into the pores of the coke.

The fractional voidage of the column was calculated from the measured column height using the data on apparent density and the weight of the packing.

Measurement of contact angle

The contact angle was measured with a projection microscope. A small prism was used to obtain a horizontal image of a drop for viewing in the vertical optical system of the microscope. The slide glass was coated by the wax in the same way as for the particles. A flat surface of polythene was obtained by pressing polythene spheres against a heated slide glass. The contact angles were measured on these surfaces; ten drops were measured on both edges. The measured contact angle of water (92.6° on polythene, 105.6° on wax) agreed reasonably well with published data ⁽⁷¹⁾ (94° and 108° respectively).

4.3 Experimental Procedures

4.3.1 Experimental procedure for first series of experiments

Preliminary experiments were conducted in the absence of gas flow; water was used as an irrigating liquid. The particles for the packing were weighed and dumped into the column through a funnel which reduced the severity of the impact of the balls on the grid and column wall. The balance was adjusted to zero with the dry bed and calibrated. For experiments in the non-wetting condition, the liquid flow was then started. For experiments in the wetting condition, the packing was taken out of the column, wetted thoroughly, and dumped into the column again after which the column was suspended from the balance and the liquid flow was started. The column was usually irrigated for about 12 hours before the actual hold-up measurements were started according to the following procedure.

The height of the constant head tank was adjusted to set the liquid flow to the required value. Since the weight of the column became steady within 5 minutes, the liquid was flowed for 10 minutes and then stopped. The average weight of the column during the last 5 minutes of liquid flow was determined and recorded as the total hold-up. The column was then allowed to drain for 5 minutes after which its weight was read and recorded as the static hold-up.

The measurements were made for seven to eight different liquid flow rates. The flow rate was changed in a random order and two to three independent measurements on the same flow rates were made. It was necessary to use two sets of capillary tubes of different size to cover the liquid flow range of 0.2 to 10 ml/sec.

In some experiments, the column was allowed to drain for more than 12 hours to measure the static hold-up according to the definition of previous authors.

4.3.2 Experimental procedure for experiments with gas flow (second series)

The column was filled with packing and hung on the balance in the same way as for preliminary experiments. After calibration of the balance, gas was passed through the column. The flow rate of the gas was kept constant for 20 to 30 minutes for the balance to acquire a steady state because a small drift in the load cell output was observed while the diaphragm^g (3, Fig. 4.4) settled to its equilibrium state. The data on the gas flow rate, the gas pressure and the weight of the column were then taken. This procedure was repeated and the data were taken for six to eight different gas flow rates.

The liquid flow was started at the highest flow rate, then the gas flow was introduced. The gas flow rate was increased gradually up to the point of flooding and then kept at just below that for a few minutes. The column was flooded several times in this way. In the case of wetting flows all the packing surface visible through the column wall was wetted by this method. Then, the gas flow was stopped and the column was kept irrigated at a medium liquid flow rate for about 12 hours.

Liquid drops resting on the inner wall of the column above the packing were wiped before each run started. The amount of drops which had accumulated under flooding or near flooding conditions was about 10g for most of the experiments. Each series of experiments was started in the absence of gas flow. The liquid flow rate was kept constant for more than 30 minutes to ensure the steady state. At least one measurement was taken before the introduction of gas. Unlike the preliminary experiments, the column was kept irrigated and no static hold-up was measured. Experiments with gas flow were conducted in such a way that the liquid flow rate was kept constant and the gas flow rate was changed. Normally the gas flow rate was increased in steps up to flooding point.

The gas flow rates were kept constant for at least 30 minutes before measurements were taken. In the experiments at low liquid flow rates it was necessary to keep constant flow rates for more than 60 minutes before the steady state was reached as confirmed by the continuous recording of the outputs of the micromanometer and the load cell.

Experiments were repeated several times on the same column for different conditions such as different distributor arrangements or liquid flow rates. Overnight the column was either kept irrigated without gas flow or allowed to drain. In the latter case, a lid was put on the column to prevent vaporisation of the liquid.

4.4 Data Processing

The data for an experiment consisted of a set of data logger outputs in paper tape and manually recorded data. The former included 15 to 20 consecutive measurements from the load cell, the micromanometer and the six strain gauges in the liquid flow meter, while the latter comprised the readings from the rotameter and Hg-manometer. The data were processed using a CDC 6400 computer.

4.4.1 Calibration curves

The calibration curves for the rotameters and the micromanometer were not linear. Therefore, a generalized curve-fitting method (Appendix II) was applied to generate the calibration curve. In the computer, this curve is represented by a set of parameters and calibration can be carried out simply by a call to a subprogram ("YQ" in Appendix II). The calibration curve for the micromanometer thus obtained is shown in Fig. 4.8.

The calibration curve of the load cell was linear and was obtained by a linear regression between the weight placed on the column and the voltage output of the load cell.

Both the pressure and the weight were calculated on the basis of the averaged values from 15 to 20 measurements.

4.4.2 Correction for the influence of gas pressure on column weight

Due to the imbalance between the diaphragms at the bottom of the column (3, in Fig. 4.4) and underneath the counter-balancing weight (5, in Fig. 4.1), a small change in the load cell output was observed when the gas pressure changed. This change was corrected for in the following way: the column weight was correlated with the gas pressure measured for the dry column using the generalized curve-fitting program (Appendix II). The resulting parameters of the fitted curve were used later to estimate the necessary amount of correction on the column weight for the measured pressure. An example of this correction curve is given in Fig. 4.9.

4.4.3 Calculation of liquid flow rate

Because the draining of the liquid from the container took place at random and the weight of the container decreased suddenly during the draining, a special computer program was developed to calculate the liquid flow rate from the recorded data. The details of the program are shown in Appendix I.

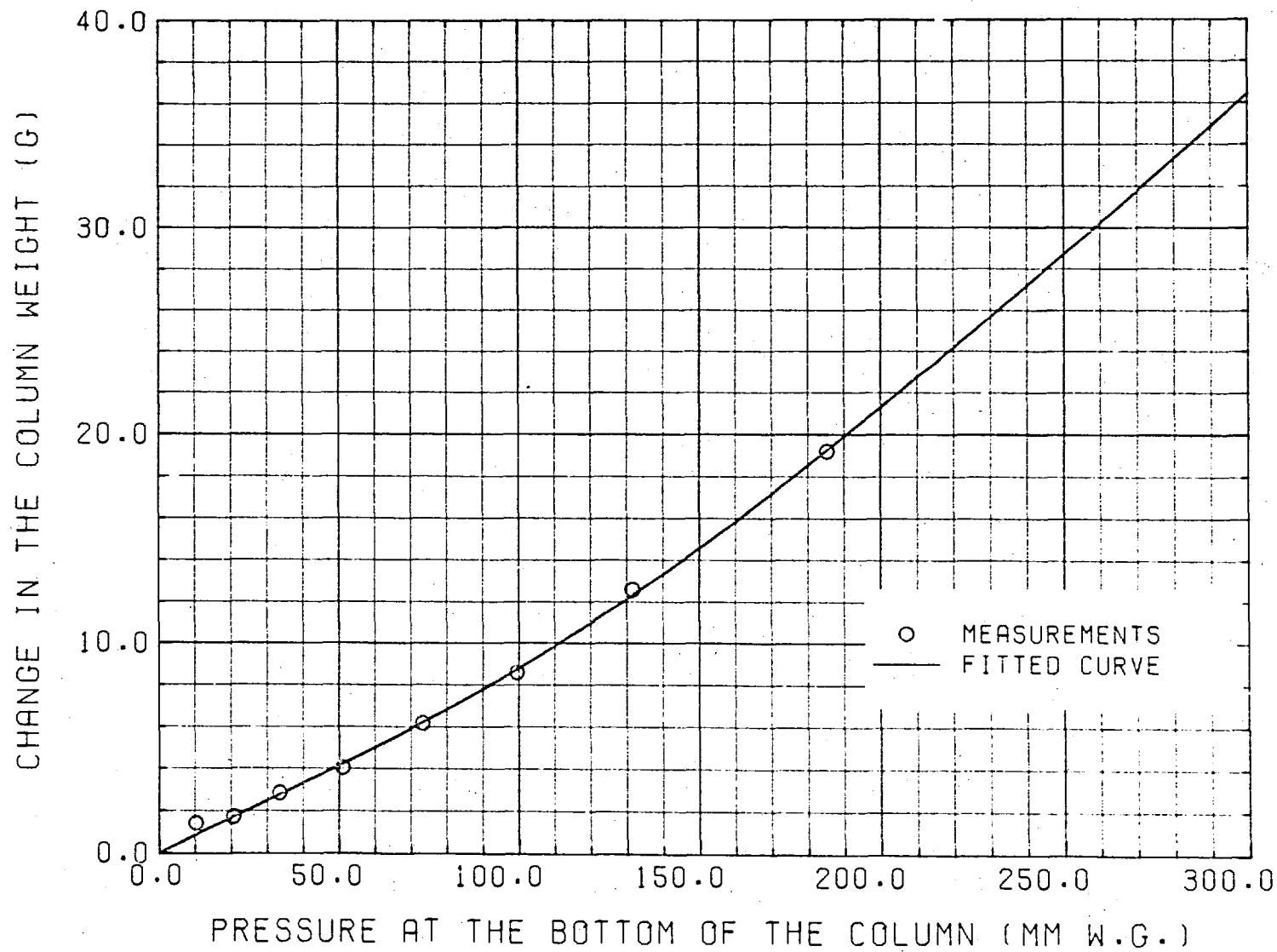


Fig. 4.9 Calibration curve for the effect of the gas pressure on the column weight for Run 340

CHAPTER 5

EXPERIMENTAL RESULTS

In the first series of experiments, the effects of liquid velocity and distributor arrangements on the total hold-up were investigated using 16 different columns in the absence of gas flow while 29 different columns were used for the second series of experiments with gas flow. The total hold-up, the liquid distribution and the gas pressure loss were measured for various velocities of liquid and gas with different distributor arrangements. Table 5.1 shows the summary of the experimental Run numbers classified on the basis of packing and liquid. Each Run number in the Table represents a different column except for Runs 22 to 26 in which the same column was used. It will be seen from the Table that not all the combinations of the five liquids and seven packings were studied but a relatively large number of experiments were repeated for certain combinations.

In this chapter, typical examples of the results are shown with the description of the flow patterns observed during the experiments.

5.1 Experimental Data

The total hold-up, liquid velocity, gas velocity, pressure drop and liquid flow distribution, calculated directly from the measured data, are tabulated in Appendix IV for all the experiments. In these Tables, each set of data is identified by a 6-digit (for the first series of experiments) or a 7-digit (for the second series of experiments) Run number. The full explanation of the make-up of a Run number is given in Appendix IV. In the following, abridged Run numbers are used to refer to a set of experimental data. Two digit numbers represent the first series of experiments while three or more digits are used for the second series.

Liquid	Packing						
	PL13	AL13	W13	PL9	G8	PLM	C11
WATR	13* 22* 120 15* 23* 190 17* 24* 220 26*	14* 130 16*	150 160 180 210 230	18* 140 19*	12* 20* 27* 110	170	---
ETOH	240* 260*	250* 270*	---	280*	290*	---	---
GLY	330 340	310	300 320 380	360	---	---	350 370
CACL	400	---	390	---	---	---	410
ZNCL	---	---	420	430	---	---	440

* Without gas flow

Table 5.1 Summary of experimental Runs

Reference to the system

Reference to a specific system will be made by using symbols for packing and liquid shown in Tables 3.1 and 3.2, e.g. PL13/WATR.

Correction of the influence of the grid

The total hold-up and the gas pressure drop were calculated based on an effective column height H_b :

$$H_b = H_{bt} - (1 - d_p/d_g)H_g \quad (5.1)$$

where H_{bt} is total column height including the grid and d_g and H_g are diameter of spheres and thickness of the grid respectively.

Liquid flow distribution

The liquid flow distribution is shown in terms of the relative flux to three concentric annuli: inner, middle, outer. The relative liquid flux to i 'th annulus Fl_i is calculated by:

$$Fl_i = \frac{Q_i/S_i}{Q/S} \quad (5.2)$$

where Q is the total flow rate, S is the cross-sectional area of the entire column and Q_i and S_i are the flow rate and cross-sectional area of the i 'th annulus. It will be noted from Fig. 4.4 that the cross-sectional area of the middle annulus is twice as much as, that of outer annulus is three times as much as that of inner annulus.

5.2 Experiments in the absence of gas flow

Fig. 5.1 shows the experimental results for Run 17. It can be seen from the Figure that the measured total hold-up for the Run is reproducible to within $\pm 0.05\%$. The liquid distribution does not change significantly with the flow rate.

In the wetting systems, the measured distributions varied from one bed to another. No systematic influence of the distributor arrangement and of the liquid flow rate on the liquid distribution were observed. The measured hold-up did not change significantly with the change in the distributor arrangement.

In the non-wetting systems, the variation of the liquid distributions among different beds was less than that in the wetting system. No systematic influence of liquid flow rate on the distribution was observed but the distributor arrangement influences the performance of the column. Fig. 5.2 shows the effect of the distributor arrangement on total hold-up and liquid distribution. The trend of the variation of the liquid distribution is consistent with the distributor arrangement in that the distributor, '19' gave the most even distribution and '7I' gave the most centralised distribution. The distributor arrangement influenced the static part of the total hold-up but not the dynamic part. The effect of the distributor arrangement can be represented by the number of distribution points rather than its influence on liquid flow distribution; the total hold-up increases with the number of the distribution points.

In Fig. 5.3, plots of the total hold-up against liquid velocity in the absence of gas flow are shown for different columns for the PL13/WATR system. Although the overall scatter is relatively large, approximately 0.7%, the scatter around the fitted curves is as small as 0.2%. This indicates

LIQUID FLOW DISTRIBUTION

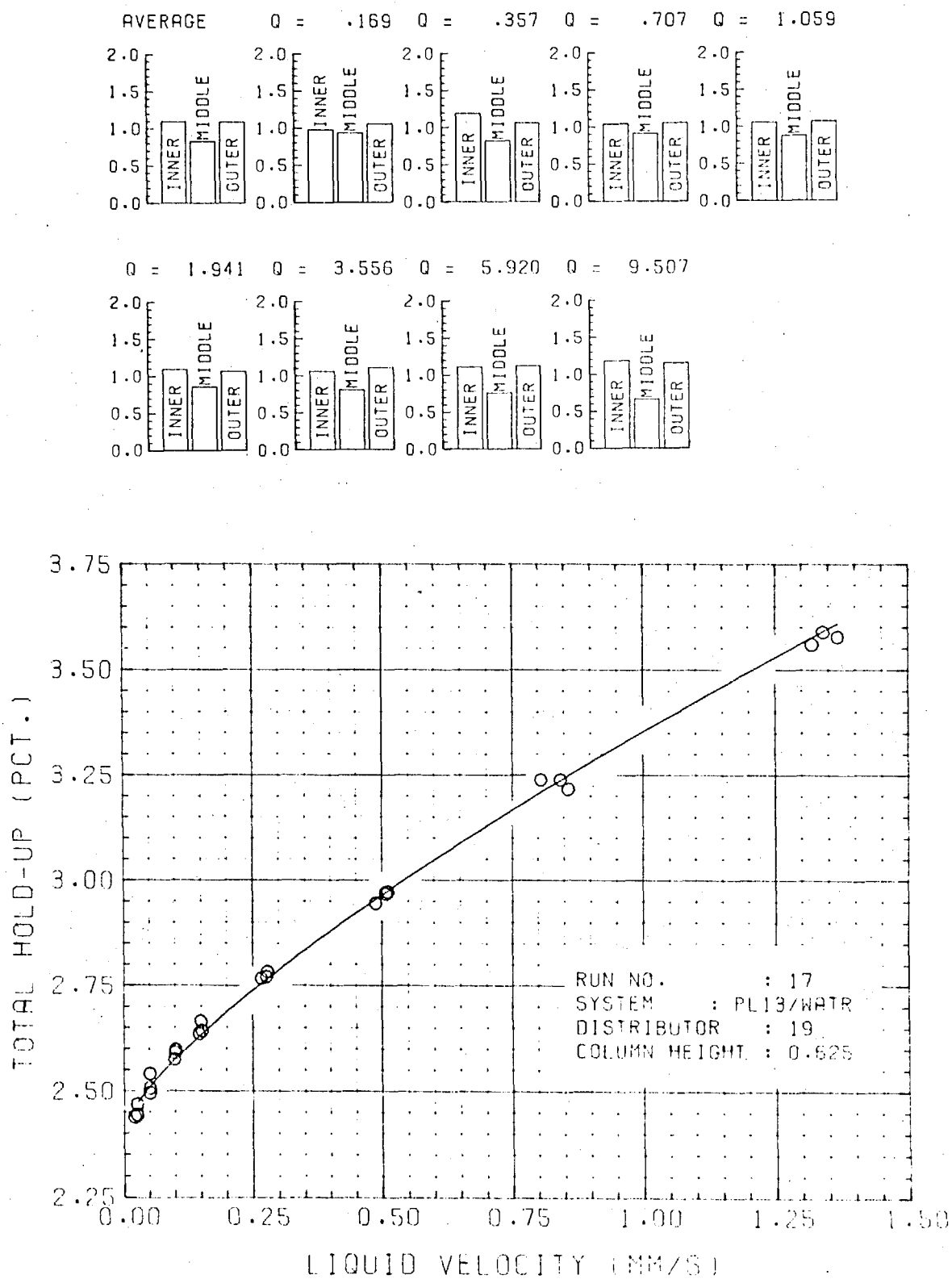


Fig. 5.1 Graphical representation of experimental results for Run 17

LIQUID FLOW DISTRIBUTION

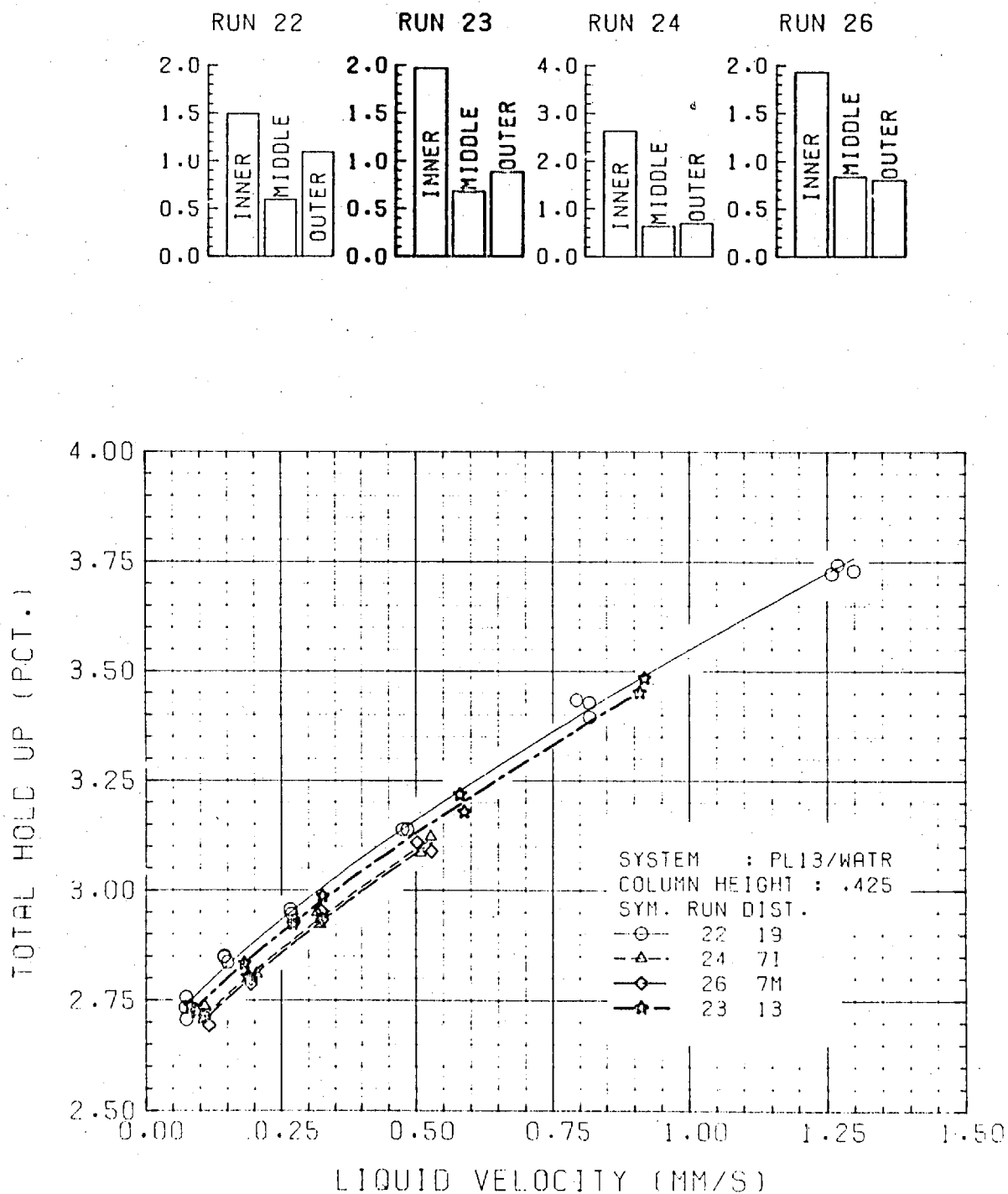


Fig. 5.2 Influence of the distributor arrangement on liquid flow distribution and total hold-up

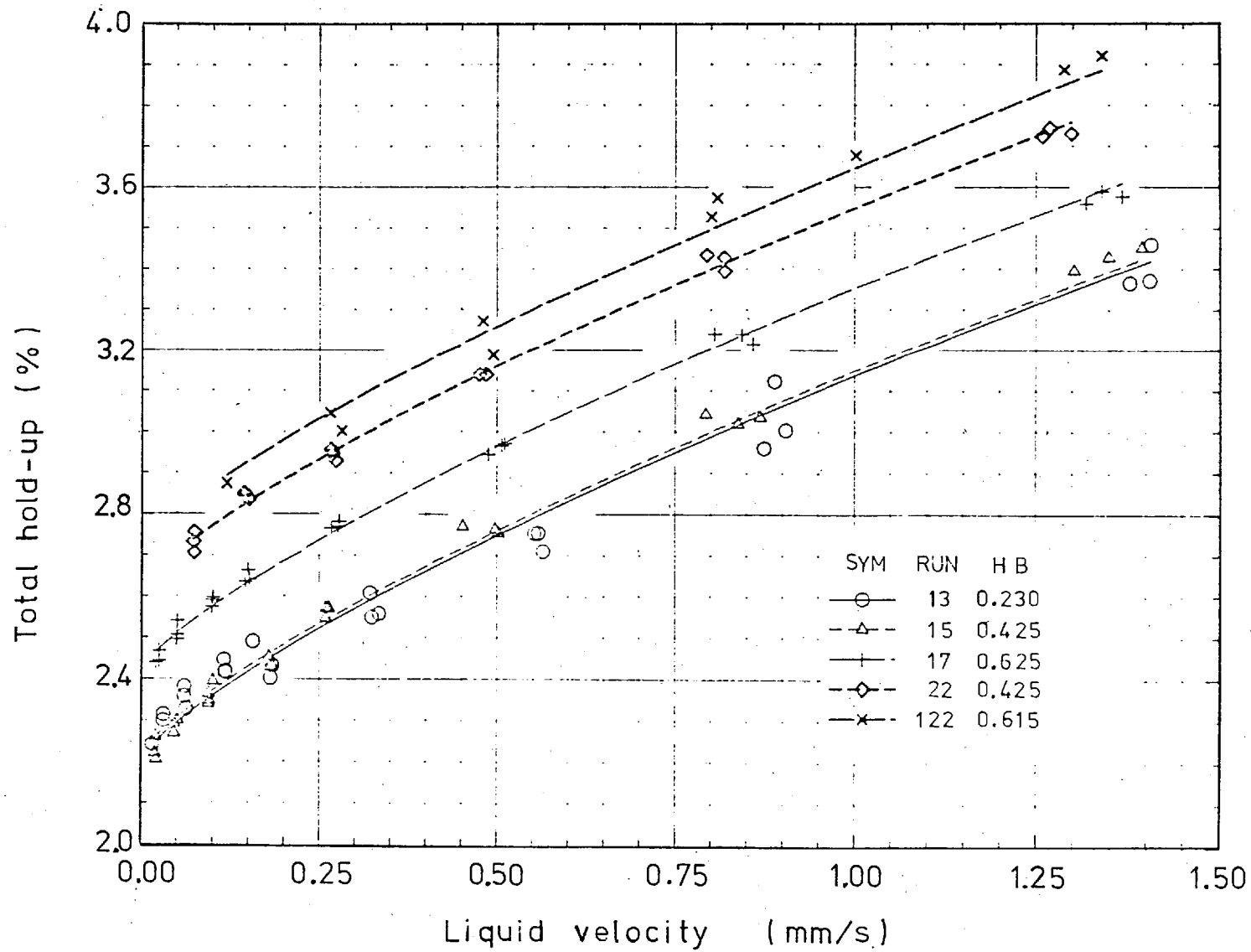


Fig. 5.3 Relationship between total hold-up and liquid velocity for different columns of PL13/WATR system. The same distributor arrangement, '19', was used.

that most of the scatter is due to that in the static hold-up. The overall scatter for the other systems are 1.0% for W13/WATR, 0.8% for W13/GLY, 0.5% for W13/CACL, 0.6% for G8/WATR and less than 0.4% for the rest. It will be noted from Fig. 5.3 that no effect of column height, in the range 0.2~0.6m, on the hold-up could be detected within the scatter of the data.

It will be clear from Figs. 5.2 and 5.3 that the change in total hold-up with the change in distributor arrangement is negligibly small compared with the variation of total hold-up among the various columns.

5.3 Experiments with Gas Flow

Figs. 5.4, 5.5 and 5.6 show typical examples of the variation of the total hold-up, gas pressure drop and liquid flux to the outer annulus with gas velocity. Fluctuations of the column weight and the gas pressure recorded on the strip chart are also shown in the Figures. Clear differences can be seen between non-wetting and wetting systems in that: the region of the loading, i.e. between start of loading and flooding, is much wider in the former than in the latter; that the effect of gas flow on liquid distribution is larger in the former than in the latter. It will be also seen that the changes in liquid distribution take place before any significant increase is observed in the total hold-up.

5.3.1 Change of the flow pattern of the liquid with gas velocity

The observed changes in the flow pattern with gas velocity are described below with reference to the typical results shown in Figs. 5.4, 5.5 and 5.6.

The flow pattern did not change at first (A) until the gas velocity reached the point B. In the vicinity of the point B, in the case of non-wetting systems, liquid slugs, whose size was comparable with that of the pores

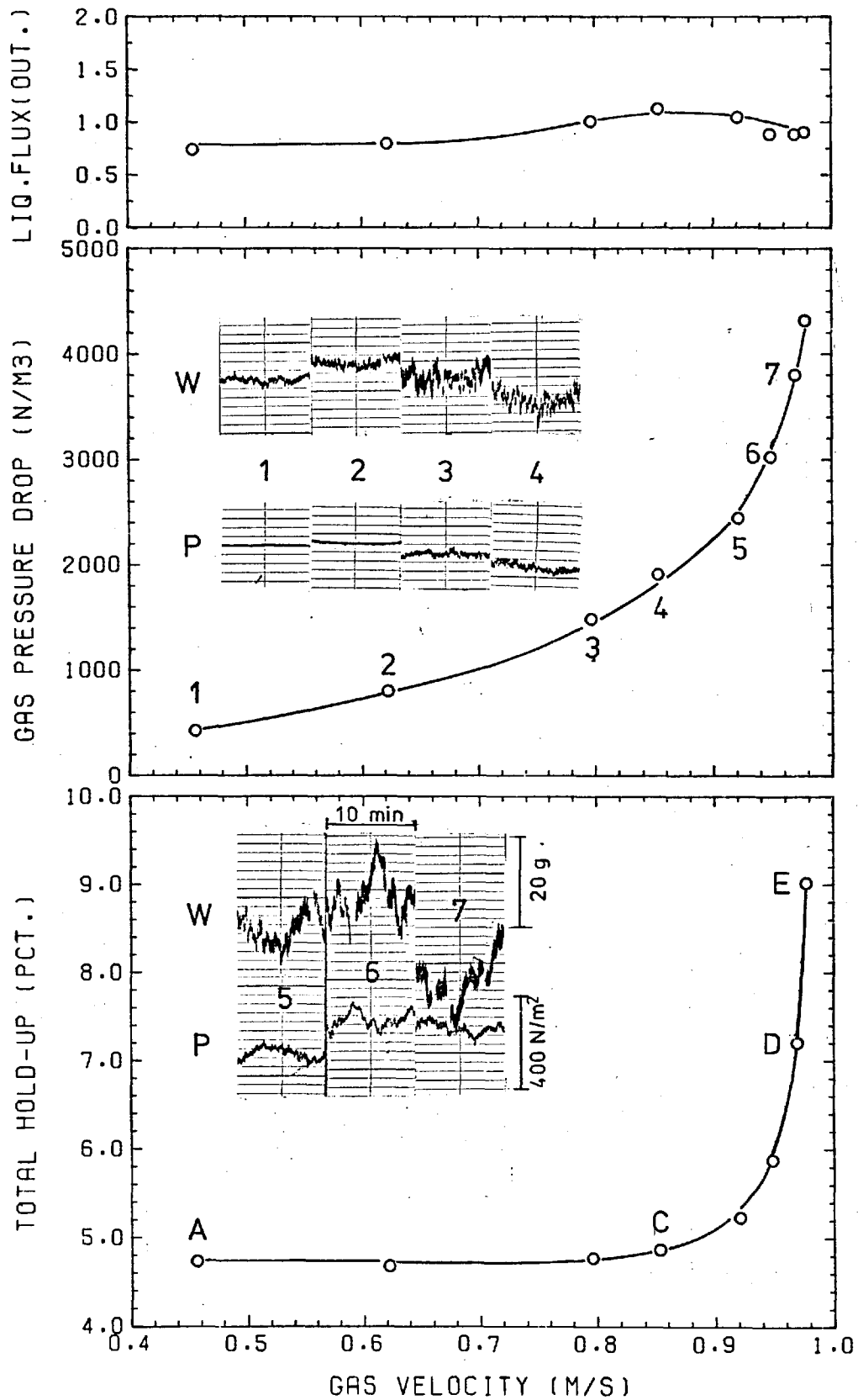


Fig. 5.4 Variation of total hold-up, pressure drop and relative liquid flux to outer annulus with gas velocity, Run 13183 (AL13/WATR). Examples of recorded strip chart show the fluctuations in pressure (P) and column weight (W).

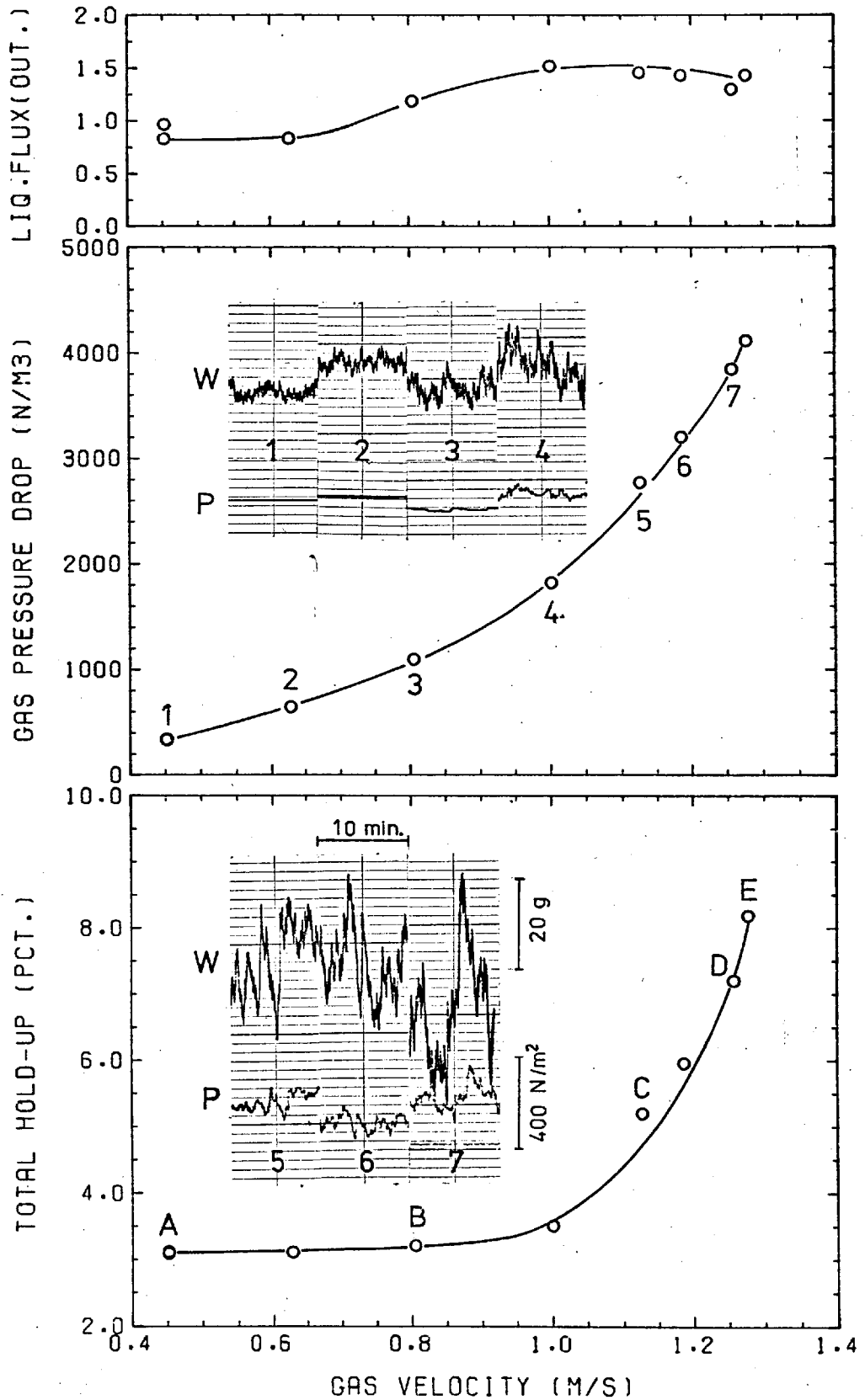


Fig. 5.5 Variation of total hold-up, pressure drop and relative liquid flux to outer annulus with gas velocity, Run 19171 (PL13/WATR). Examples of recorded strip chart show the fluctuations in pressure (P) and column weight (W).

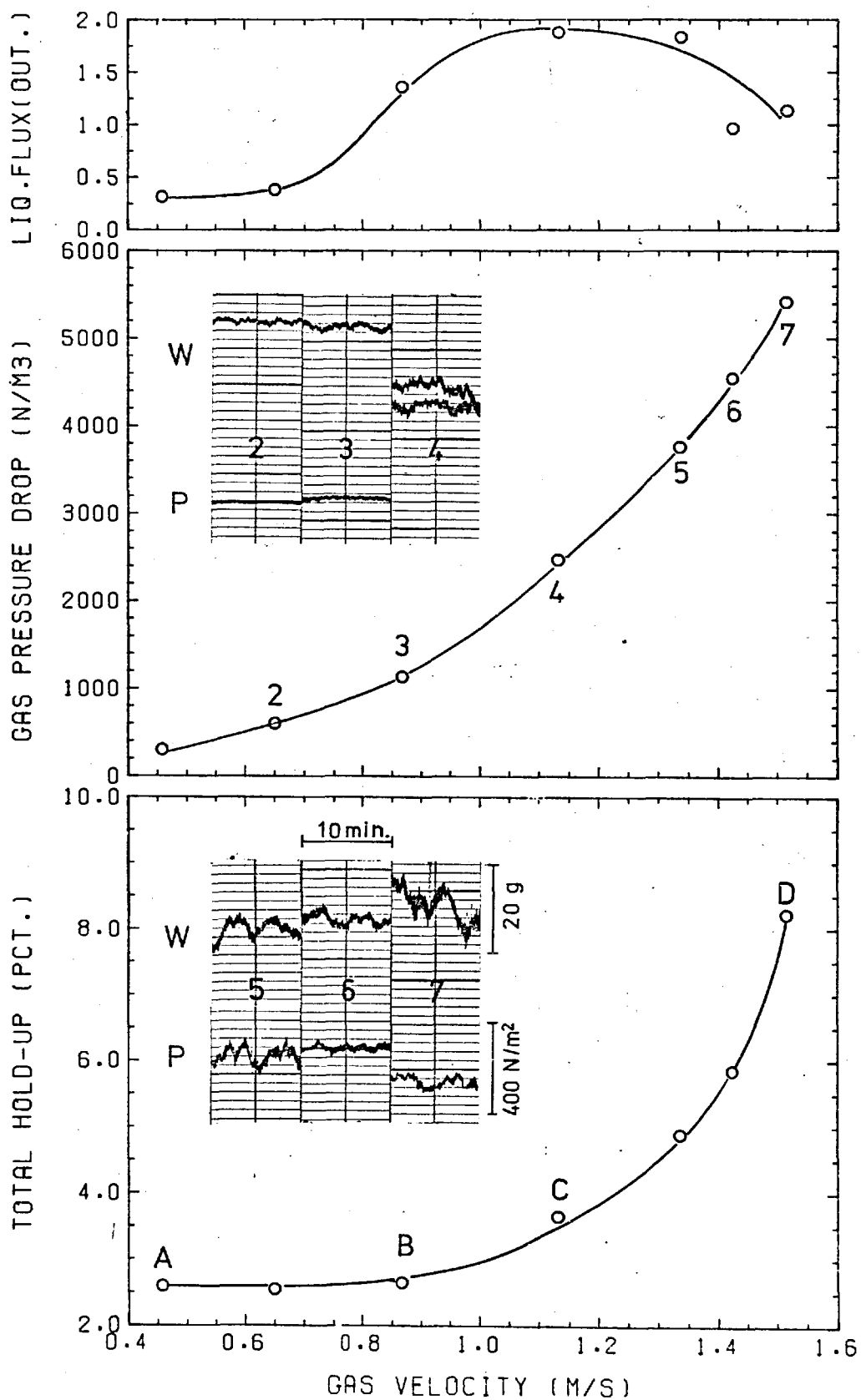


Fig. 5.6 Variation of total hold-up, pressure drop and relative liquid flux to outer annulus with gas velocity, Run 30361 (W13/GLY). Examples of recorded strip chart show the fluctuations in pressure (P) and column weight (W).

of the bed and significantly larger than those observed in the column in the absence of the gas flow, started to appear on the wall of the column occasionally. In the case of wetting systems, the flow pattern did not change significantly.

With a further increase of the gas velocity to near the point C, the slugs became larger and appeared more frequently on the wall. The slugs, in the non-wetting system stayed for a while and then slowly moved away. In the wetting system also the slugs appeared on the wall, however, they remained at the same places where they originated. The slugs appeared at a relatively small number of locations which did not change with the liquid velocity or the liquid distributor arrangement but changed from one bed to another. This appearance of the slugs on the column wall marked the onset of loading.

With a further increase in the gas velocity, the size of the slugs increased and the area in contact with the wall increased until they covered almost the entire column wall (Point D). At the point D, splashes of the liquid could be seen on the top of the column. In the case of non-wetting systems, a displacement of one or two balls on the top surface could be observed occasionally because the packings were lighter than the liquids.

A further small increase in the gas velocity induced the column to flood (E). In case of wetting systems, the liquid accumulated on the top of the column to form a pool. Once the pool had formed, it was necessary to decrease the gas velocity to a value 5 -10% lower than necessary to flood for the pool to disappear. In case of non-wetting systems instead of forming a pool of liquid, the particles at the top of the column started to move in a manner similar to that of a fluidized bed; the depth of the layer of particles in motion increased with the gas velocity.

As shown in Figs. 5.4, 5.5 and 5.6, two types of fluctuations were noted in the recorded traces of the column weight and gas pressure: a fluctuation with a relatively high frequency whose magnitude could be seen on the chart as the width of the recorded trace and a semi-periodical fluctuation with a period of a few minutes. Both fluctuations increased with the gas velocity. The change in the magnitude of the high-frequency fluctuation seemed to correspond to the increase in the size of the slugs with the gas velocity.

5.3.2 Reproducibility of the measurements

The reproducibility of the total hold-up measurements with gas flow was reasonably good for measurements on the same bed. No significant effect was found of the distributor arrangement. The direction of the change in gas velocity, increasing or decreasing, during the experiments did not affect the measured total hold-up except in the region very close to flooding (at a gas velocity within about 10% of that at flooding). The reproducibility of the value of the gas velocity at flooding was better than 10% except for PL13/WATR and W13/WATR systems in which cases the maximum differences in gas velocity at flooding were about 30% (Fig. 5.7) Possible causes, such as gas leak, influence of bed height and influence of distributor arrangement were checked and none of them could satisfactory account for the observed differences.

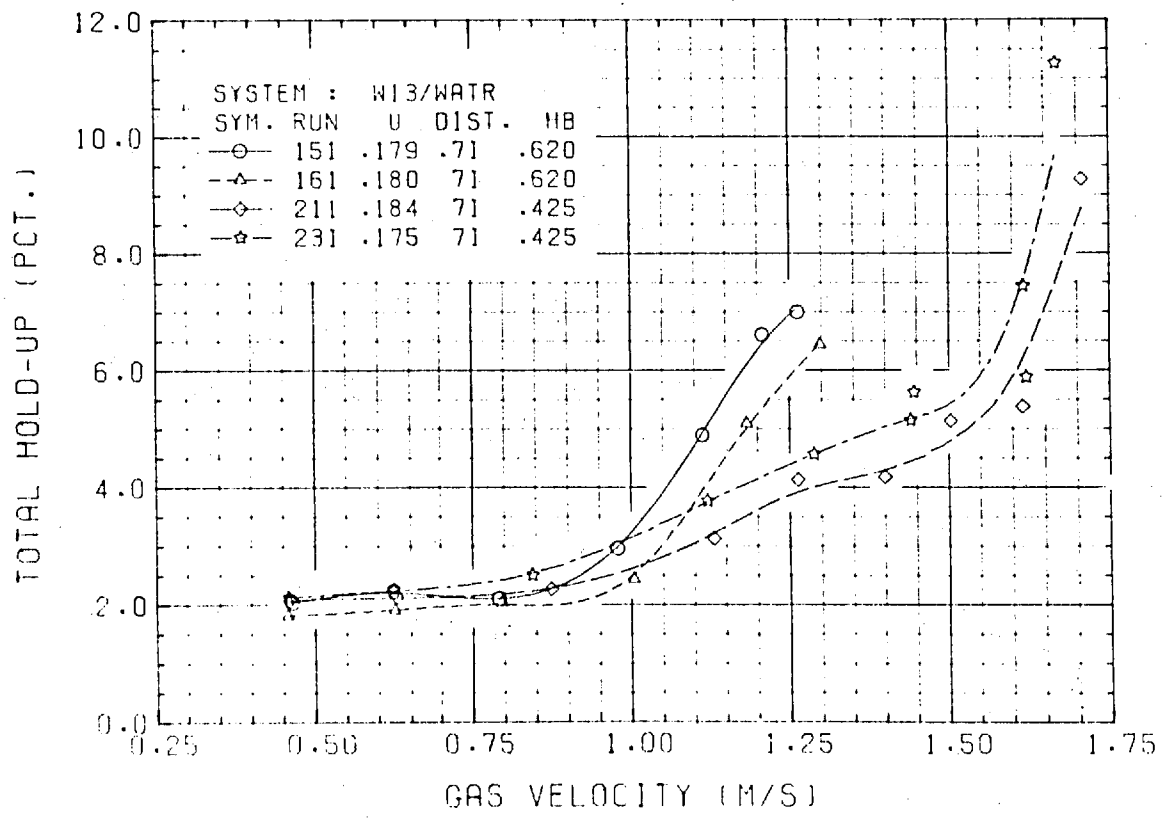
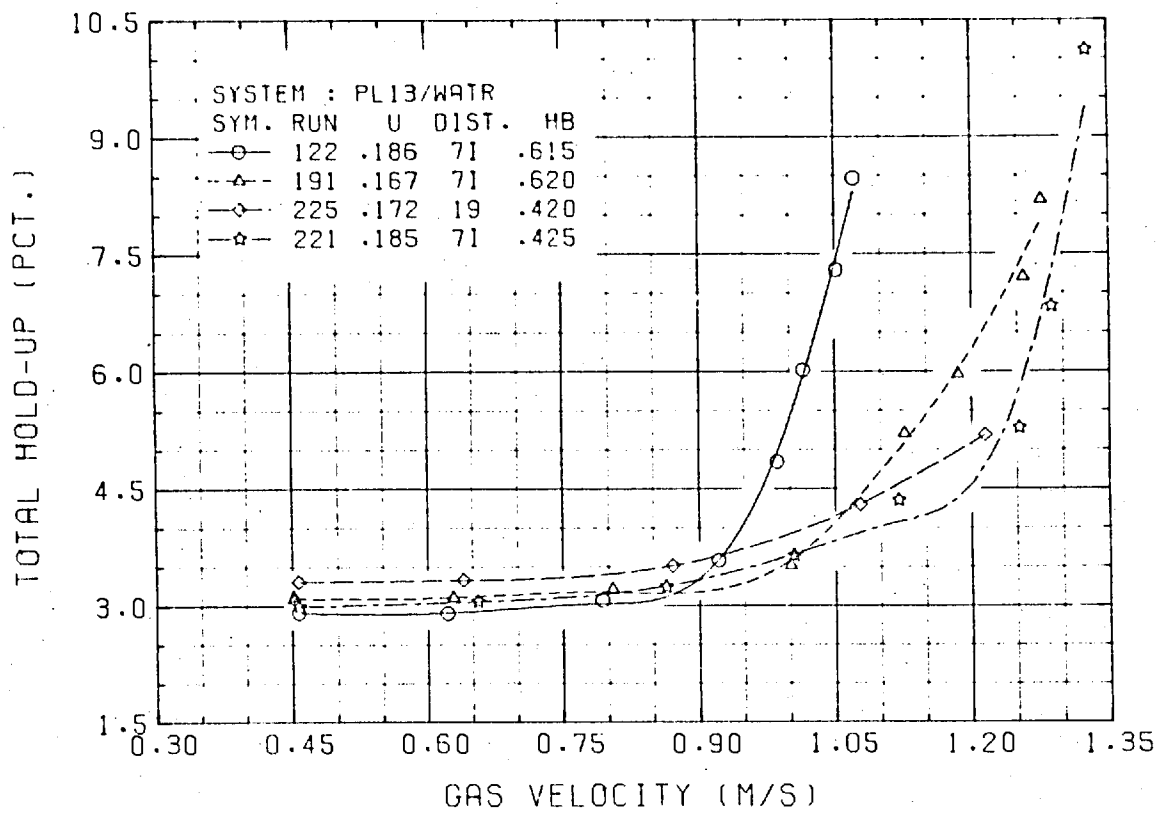


Fig. 5.7 Examples of variation of total hold-up with gas velocity for PL13/WATR and W13/WATR systems. These two systems showed the poorest reproducibility in measurements with gas flow.

CHAPTER 6

DISCUSSION

The total hold-up in the absence of gas flow was divided into the static- and dynamic parts. In Sec. 6.1 the two types of hold-up are correlated with the appropriate dimensionless parameters and mathematical formulae for the correlations are given. The correlations are compared with the experimental data and correlations proposed by previous authors. The pressure drop of the gas is discussed in Sec. 6.2. Due to the complexity of the problem, only the effect of total hold-up on the gas pressure drop is dealt with; no attempt is made to correlate the pressure drop with the hold-up. In Sec. 6.3, the flooding velocities are discussed on the basis of the existing flooding diagrams. The instability of the bed near the point of flooding is discussed in Sec. 6.4 and the effect of the gas flow on the distribution of liquid in Sec. 6.5. Finally, in Sec. 6.6, the blast furnace process is described in the light of the results of this study.

6.1 Hold-up in the Absence of Gas Flow

6.1.1 Calculation of dynamic and static hold-up

It is convenient to discuss the static hold-up and the dynamic hold-up individually since the former is influenced only by static forces while the dynamic forces must also be considered in the latter. The total hold-up, h_t , is divided into the static and dynamic parts by assuming the relationship:

$$h_t = h_s^* + b u^c \quad (6.1)$$

where h_s^* is the static part and the term, $b u^c$, represents the dynamic part.

As already mentioned in Chapter 5, the scatter in the total hold-up among several series of measurements for the same system was mainly due to the difference in the static hold-up. Therefore the measured total hold-up, h_t , is correlated with liquid velocity, u , according to Eq. (6.1) such that b and c are constant for the same combination of packing and liquid while h_s^* was allowed to vary between each series of measured data. Because of the non-linear nature of Eq. (6.1), an iterative method of least squares was applied in which b , c and h_s^* 's were determined to minimize the sum of the squares of the differences between the measured value of h_t and those estimated by Eq. (6.1). The principle of the iterative method is given in Appendix III.

Table 6.1 shows the calculated h_s^* for each experiment from a series of measurements. The measured residual hold-up, h_s , after twelve hours' draining is also shown in the Table. It must be noted that because of the assumed dependency of the total hold-up on liquid velocity, u , in the form of Eq. (6.1), one can not assume without experimental proof that the static part of the hold-up, h_s^* , is the same as the static hold-up, h_s , which is usually defined as the hold-up after the column is allowed to drain for a long time. The difference between h_s^* and h_s in the present study was 0.265%, on an average, which is in reasonable agreement with the data of Gardner⁽²⁸⁾ who first mentioned this difference and reported values between 0.03 and 0.27%. The difference is not very large when compared with the magnitude or the scatter in the static part of the hold-up, h_s^* . However, the difference is too large to be neglected when one compares it with the magnitude of the dynamic hold-up which ranged between 0.02% and 2% in the present experiments.

SYSTEM	RUN	h_s^*	h_s	RUN	h_s^*	h_s	RUN	h_s^*	h_s	RUN	h_s^*	h_s
PL13/WATR	13	2.20	--	15	2.22	--	17	2.42	1.83	22	2.62	--
	23	2.59	--	24	2.55	--	26	2.54	2.31	121	2.71	--
	122	2.63	--	123	2.62	--	124	2.71	2.42	191	2.78	--
	192	2.76	2.51	221	2.57	--	222	2.78	2.52	223	2.78	--
	224	2.84	--									
AL13/WATR	14	4.33	3.74	16	4.34	3.89	131	4.23	4.05	132	4.25	--
	133	4.36	3.82									
W13/WATR	151	1.69	--	152	1.67	--	153	1.70	1.65	161	1.55	--
	162	1.59	--	163	1.54	1.48	181	1.40	--	182	1.51	--
	183	1.53	1.37	211	1.74	--	212	1.90	1.71	213	1.91	--
	231	1.69	1.71	232	1.86	--						
PL9/WATR	18	3.33	--	19	3.32	2.77	141	3.27	2.69	142	3.24	--
	143	3.26	--									
G8/WATR	12	4.55	--	20	4.44	3.85	27	4.44	--	111	4.03	--
	112	4.28	--	113	4.28	3.96	114	4.26	--			
PLM/WATR	171	2.95	2.41	172	2.89	--	173	2.91	--	174	2.94	--
PL13/ETOH	241	2.32	--	242	2.23	--	261	2.26	--	262	2.29	--
AL13/ETOH	251	2.49	--	252	2.41	1.93	271	2.54	--	272	2.54	--
PL9/ETOH	281	3.00	--	282	3.26	--						
G8/ETOH	291	4.10	--	292	4.00	--						
AL13/GLY	311	3.14	--	312	3.13	--	313	3.06	--	314	3.14	--
	315	3.07	--	316	3.18	2.97						
PL13/GLY	332	2.21	--	333	2.25	2.12	342	2.20	--	343	2.18	1.96
W13/GLY	301	1.97	--	302	2.33	2.30	303	2.25	--	304	258	--
	305	2.42	--	306	2.34	--	324	2.68	--	325	2.77	2.67
	382	2.13	2.03									
PL9/GLY	362	2.08	2.12									
C11/GLY	353	3.42	3.25	372	3.67	--						
PL13/CACL	402	2.64	--	403	2.60	2.49						
W13/CACL	392	1.48	--	393	1.53	--	394	1.81	1.53	395	1.93	--
C11/CACL	412	3.86	--	413	3.90	--	414	3.89	3.90			
W13/ZNCL	423	2.40	2.07									
PL9/ZNCL	432	2.85	--									
C11/ZNCL	441	3.19	2.95									

average of the difference $h_s^* - h_s$: 0.265%

Table 6.1 Static part of the hold-up, h_s^* , obtained by least-squares fitting of the data to Eq. (6.1) and measured static hold-up, h_s after 12-hour draining, %.

SYSTEM	Number of data	Least-squares fit by Eq. (6.1)			Static part of hold-up, h_s^* , %		
		Coefficient b	Power c	Correlation Coefficient	Average	Number of runs	Standard deviation
PL13/WATR	170	0.934	0.775	0.9965	2.49	17	0.207
AL13/WATR	74	1.256	0.737	0.9908	4.10	5	0.045
W13/WATR	65	0.636	0.898	0.9875	1.64	14	0.138
PL9/WATR	61	1.449	0.692	0.9960	3.31	5	0.024
G8/WATR	117	1.914	0.810	0.9947	4.37	7	0.166
PLM/WATR	20	1.430	0.608	0.9973	2.92	4	0.021
PL13/ETOH	25	1.655	0.580	0.9965	2.29	4	0.031
AL13/ETOH	19	1.811	0.547	0.9993	2.29	4	0.052
PL9/ETOH	9	1.892	0.610	0.9991	3.15	2	0.133
G8/ETOH	8	1.862	0.765	0.9924	4.06	2	0.046
PL13/GLY	26	2.480	0.493	0.9944	2.21	4	0.027
AL13/GLY	34	5.589	0.613	0.9961	2.91	6	0.042
W13/GLY	51	2.323	0.567	0.9866	2.39	9	0.241
PL9/GLY	6	5.196	0.499	0.9996	2.08	1	---
C11/GLY	13	3.324	0.478	0.9943	3.55	2	0.125
PL13/CACL	11	1.293	0.575	0.9983	2.62	2	0.021
W13/CACL	22	1.083	0.663	0.9989	1.70	4	0.191
C11/CACL	17	1.274	0.644	0.9986	3.88	3	0.015
W13/ZNCL	6	1.899	0.640	0.9990	2.40	1	---
PL9/ZNCL	6	2.560	0.717	0.9992	2.85	1	---
C11/ZNCL	7	1.845	0.836	0.9963	3.19	1	---
OVER ALL	763	---	---	0.9990	---	-	---

Table 6.2 Results of the least squares fit by Eq. (6.1)

Table 6.2 shows the results of the least-squares fit by Eq. (6.1) for all experiments*. It will be noted that the data fit the equation very well, though the scatter in the static part of the hold-up is relatively large. Fig. 6.1 shows typical examples of the plot of the total hold-up vs. liquid velocity.

The dynamic hold-up, h_d , was calculated by subtracting h_s^* , which is given in Table 6.1, from the measured total hold-up, h_t :

$$h_d = h_t - h_s^* \quad (6.2)$$

In the following, h_s^* is referred to as the static hold-up since the difference between h_s^* and h_s is not significant when considering the static hold-up.

6.1.2 Correlation for static hold-up, h_s^*

In Fig. 6.2 the data for wetting flows are plotted on the diagram proposed by Dombrowski and Brownell⁽⁴⁹⁾. The residual saturation, S_r^* , was calculated as h_s^* / ϵ . It can be seen from the Figure that the present experimental data show higher residual saturation than would be expected from the Dombrowski's curve, however, the variation of the residual saturation with the capillary number is almost parallel to the curve. The difference between the estimated and experimental residual saturations is almost equivalent to 1.2% in static hold-up which is significantly larger than experimental error.

* Due to the pores open to the surface, the alumina spheres (AL13) absorbed a small amount of liquid which was estimated to be 0.21% on the basis of a comparison of h_s^* between PL13/ETOH and AL13/ETOH systems. Table 6.2 shows the values after this correction was applied.

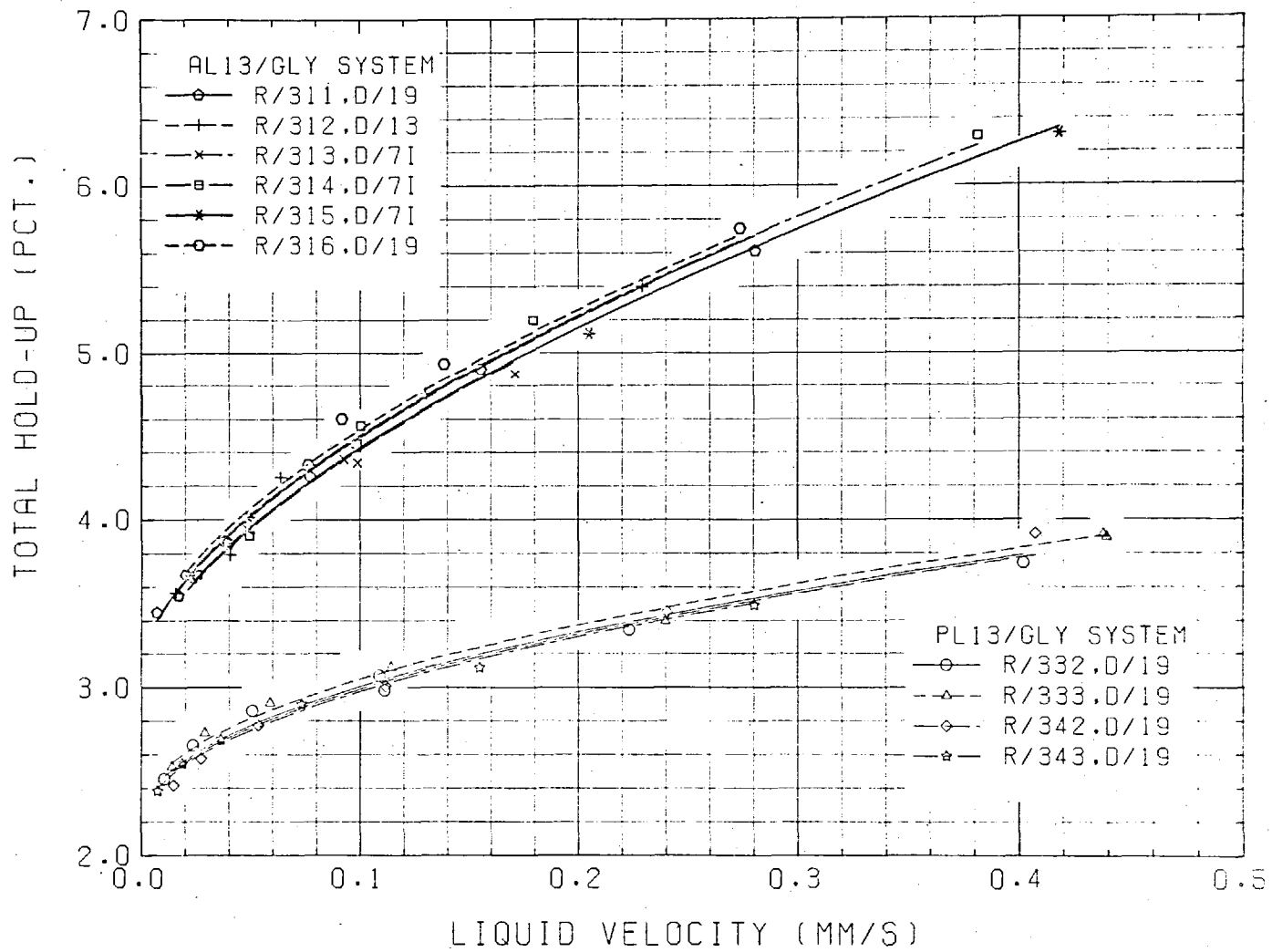


Fig. 6.1 Examples of variation of total hold-up with liquid velocity. The curves are obtained by least-squares fit according to Equation (6.1).

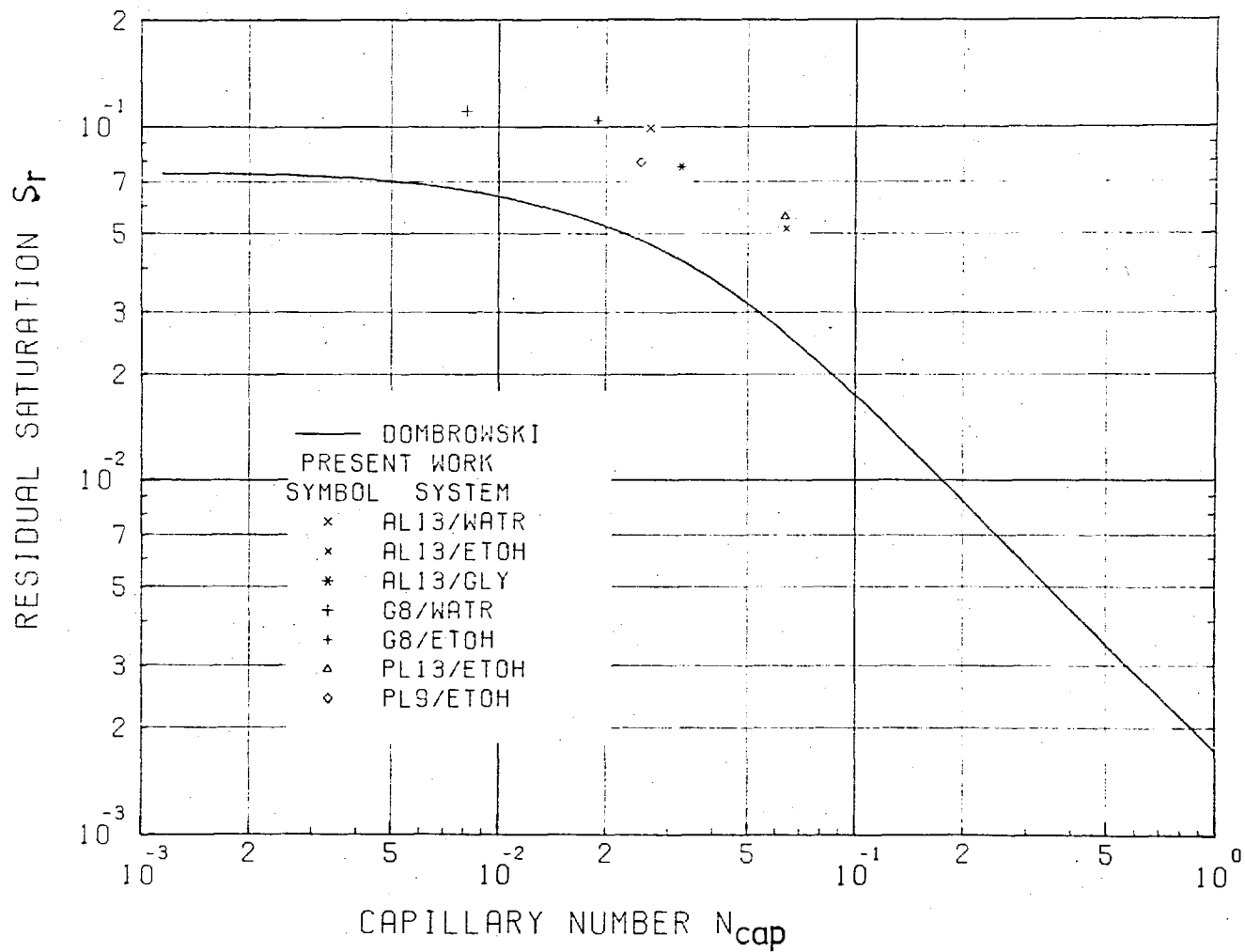


Fig. 6.2 Plot of experimental data for wetting flows on Dombrowski's diagram

Among the forces shown in Chapter 3, three forces, the gravitational force, f_g , the gas-liquid interfacial force, f_s , and the liquid-solid interfacial force, f_{si} , are independent of liquid velocity. Since h_s^* is assumed to be independent of liquid flow rate, it can be correlated with these three forces from which two independent dimensionless numbers can be derived as shown in Chapter 3, i.e.

$$C_p = f_g/f_s \quad (3.10)$$

$$N_c = f_{si}/f_s \quad (3.11)$$

It was pointed out that the capillary number N_{cap} is essentially the same as C_p . For geometrically similar systems, the static hold-up can be assumed the same if both C_p and N_c are the same. However, it is necessary to take the effect of geometry into account if one compares static hold-up among systems of different geometries.

It is difficult to derive a precise correction factor since only two different geometries, i.e. spheres and coke particles, were used in the experiments. Therefore, the correction for the difference in geometry was simply made by choosing an appropriate expression for the characteristic length. Two characteristic lengths given by Eqs. (6.3) and (6.4) are generally used to represent the diameter of packing:

$$d_s = \frac{\phi d_p}{(1 - \epsilon)} \quad (6.3)$$

$$d'_h = \frac{\phi d_p \epsilon}{(1 - \epsilon)} \quad (6.4)$$

d_s is related to the specific surface area of the bed while d'_h is related to the mean hydraulic radius. In order to find a suitable dimensionless parameter, the static part of the hold-up, h_s^* , is correlated with dimensionless parameters by the equation:

$$h_s^* = a C_p^b N_c^c \quad (6.5)$$

The following three variations of C_p were tested:

$$C_{ps} = \frac{\rho_l g d_p^2 \phi^2}{\sigma (1 - \epsilon)^2} \quad (6.6)$$

$$C_{ph} = \frac{\rho_l g d_p^2 \phi^2 \epsilon^2}{\sigma (1 - \epsilon)^2} \quad (6.7)$$

$$N'_{cap} = \frac{\rho_l g d_p^2 \phi^2 \epsilon^3}{180(1 - \epsilon)^2 \sigma} \quad (6.8)$$

C_{ps} and C_{ph} use d_s and d'_h respectively while N'_{cap} is obtained from N_{cap} after appropriate modification. The shape factor, ϕ , of the coke is assumed to be 0.5 based on gas pressure loss measurements (Sec. 6.2). The iterative method of least squares (Appendix III) was applied to obtain a , b and c . The calculated results for the static hold-up and the residual saturation, S_r^* , are given in Table 6.3.

It will be noted from the Table that the correlation coefficient for the equation No. 1 is the best among the correlations for h_s^* and is approximately the same as those for the correlations for S_r^* . The absolute values of b and c are almost the same in the first three equations while

Equation Number	Equation	Correlation Coefficient	Power	
			b	c
1	$h_S^* = a \cdot C_p^b \cdot N_c^c$	0.841	-0.341	0.364
2	$h_S^* = a \cdot C_{ph}^b \cdot N_c^c$	0.758	-0.309	0.291
3	$h_S^* = a \cdot N_{cap}^b \cdot N_c^c$	0.699	-0.272	0.269
4	$S_r^* = a \cdot N_{cap}^b \cdot N_c^c$	0.849	-0.296	0.394
5	$S_r^* = a \cdot C_{ps}^b \cdot N_c^c$	0.855	-0.297	0.487

$$S_r^* = h_S^* / \epsilon$$

Table 6.3 Comparison of various correlations for static hold-up.

the absolute value of c is considerably larger than that of b in the last two equations. If one assumed the same magnitude but different signs for b and c , one will have a new dimensionless parameter as follows:

$$(f_g/f_s)^m \cdot (f_{si}/f_s)^{-m} = (f_g/f_{si})^m$$

The new dimensionless parameter, f_g/f_{si} , can be interpreted as the ratio of the gravitational force to the liquid-solid interfacial force and the parameter is identical to $C_p/2$ when the contact angle, θ , is 0.

Because of its physical significance and simplicity, the new parameter, the modified capillary number, $C_{pm} = f_g/f_{si}$ was preferred to the other possible dimensionless parameters in the correlation for the static hold-up.

It will be clear from Fig. 6.2 that the relationship between $\log(S_r)$ and $\log(N_{cap})$ is no longer linear in the range of the experimental data. Since the static hold-up decreases asymptotically to zero when the capillary number increases to infinity and it approaches a constant value when the capillary number decreases to zero, the following relationship (Equation 6.9) is assumed between h_s^* and C_{pm} .

$$h_s^* = 1/(a + b C_{pm}) \quad (6.9)$$

where C_{pm} is expressed in terms of d_s as follows:

$$C_{pm} = \frac{\rho_l g \phi^2 d_p^2}{(1+\cos\theta)\sigma (1-\epsilon)^2} \quad (6.10)$$

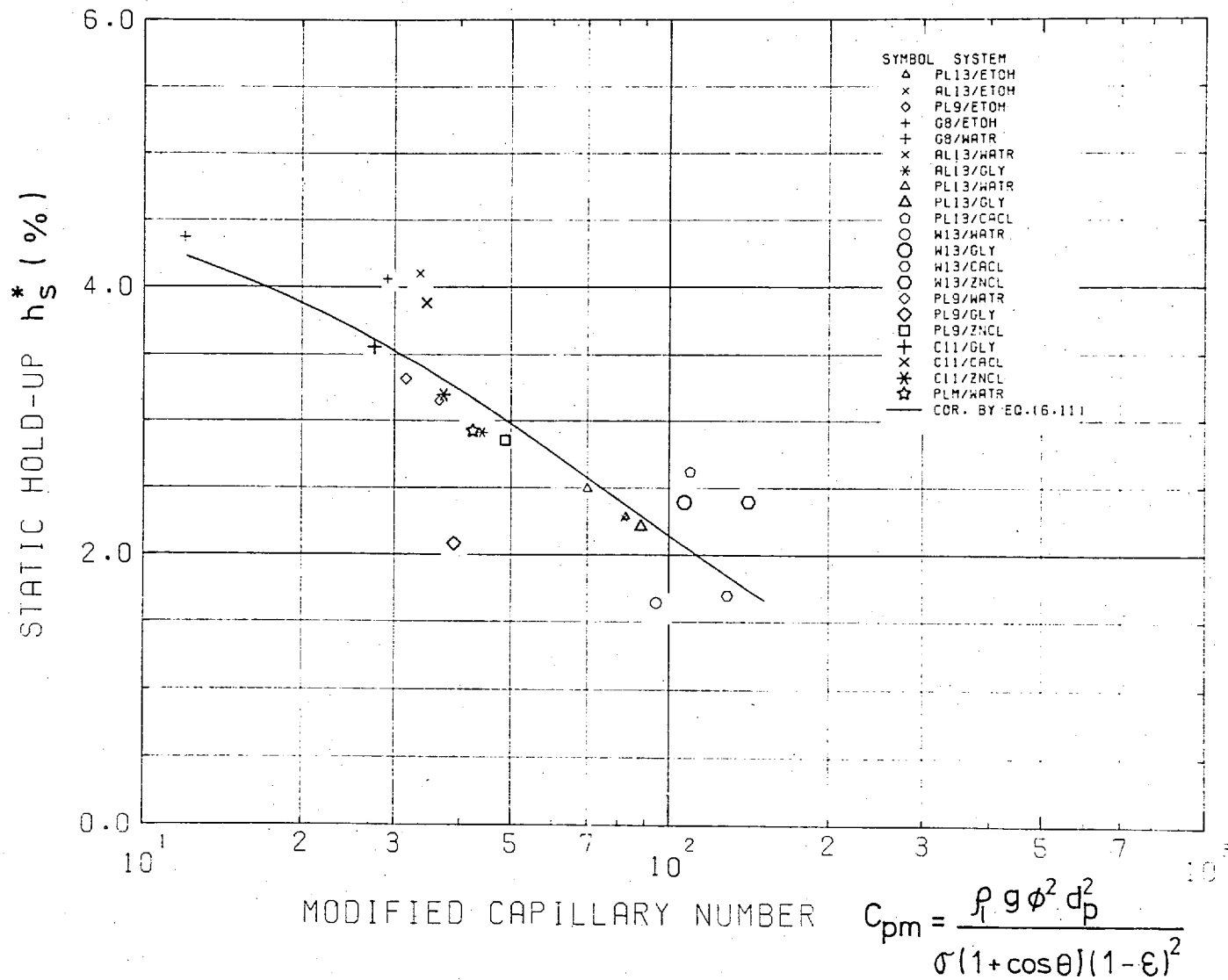


Fig. 6.3 Relationship between static hold-up, h_s^* and modified capillary number, C_{pm}

The constants a and b in Eq. (6.9) are calculated by using the iterative method of least squares. The values obtained for a and b are 0.205 and 0.00263 respectively. and the correlation coefficient is 0.832. Therefore Eq. (6.9) can be rewritten as

$$h_s^* = 1/(0.205 + 0.00263 C_{pm}) \quad (6.11)$$

The relationship between h_s^* and C_{pm} is shown in Fig. 6.3.

6.1.3 Correlation for the dynamic hold-up

The following relationship is assumed between the dynamic hold-up, h_d , and the dimensionless parameters introduced in Chapter 3.

$$h_d = a R_e^b G_a^c C_p^d N_c^e \quad (6.12)$$

where a , b , c , d , and e are constants. These constants were determined by using the iterative method of least squares which is explained in Appendix III.

The constants in Eq. (6.12) were calculated for two cases: d_s was used in the first as the characteristic length while d_h' was used in the second. The correlation coefficient in the first case was 0.952 and 0.922 in the second. With the large number of data (=765) the difference between these two coefficients is statistically significant (more than 99.9% confidence). Therefore, the first case has been chosen. The resulting correlation is shown by Eq. (6.13):

$$h_d(\%) = 605 \left[\frac{\rho_l u d_p \phi}{(1-\epsilon) \mu_l} \right]^{0.648} \left[\frac{\rho_l^2 g d_p^3 \phi^3}{\mu_l^2 (1-\epsilon)^3} \right]^{-0.485} \left[\frac{\rho_l g d_p^2 \phi^2}{\sigma (1-\epsilon)^2} \right]^{0.097} (1+\cos\theta)^{0.648} \dots(6.13)$$

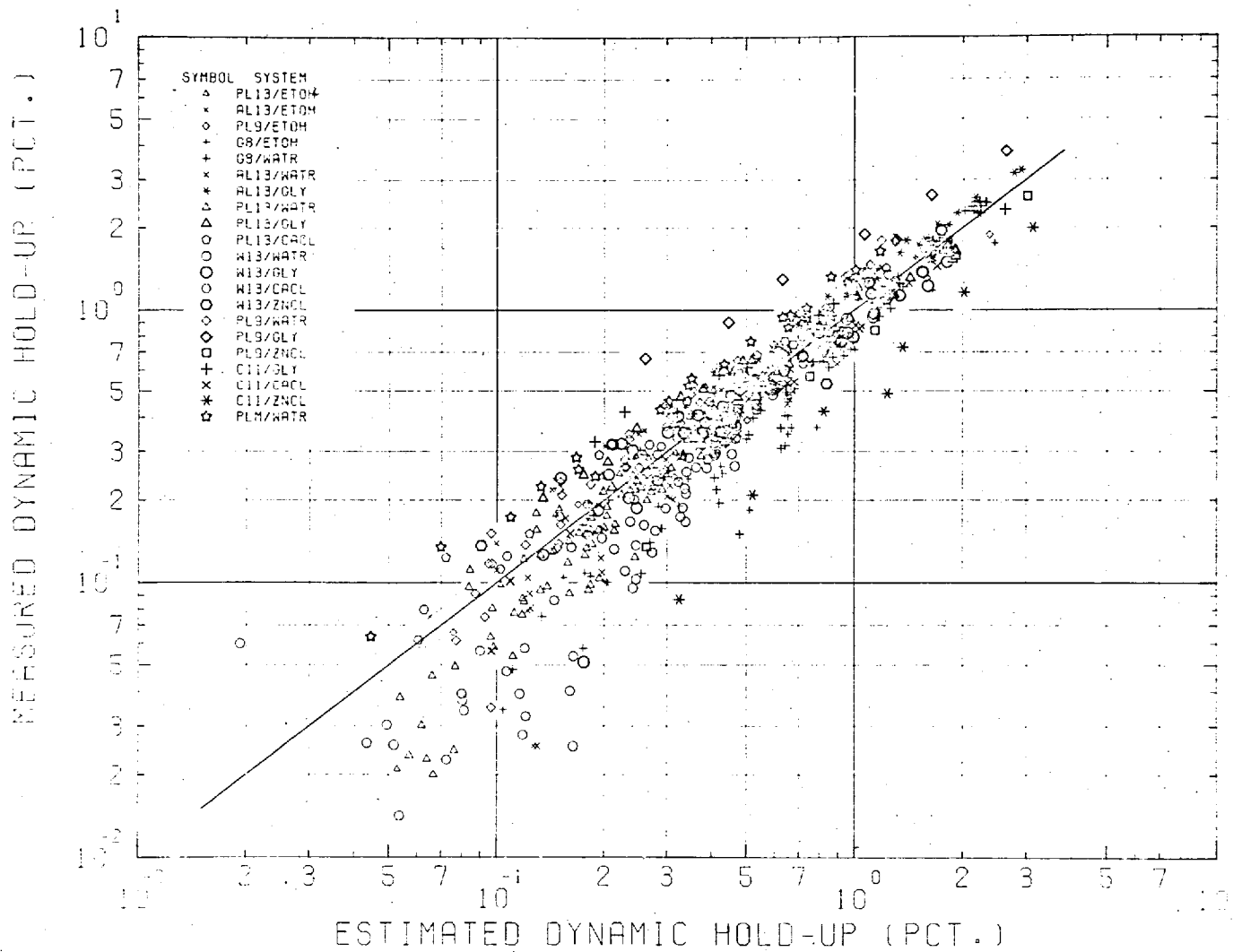


Fig. 6.4 Comparison between measured and estimated dynamic hold-up

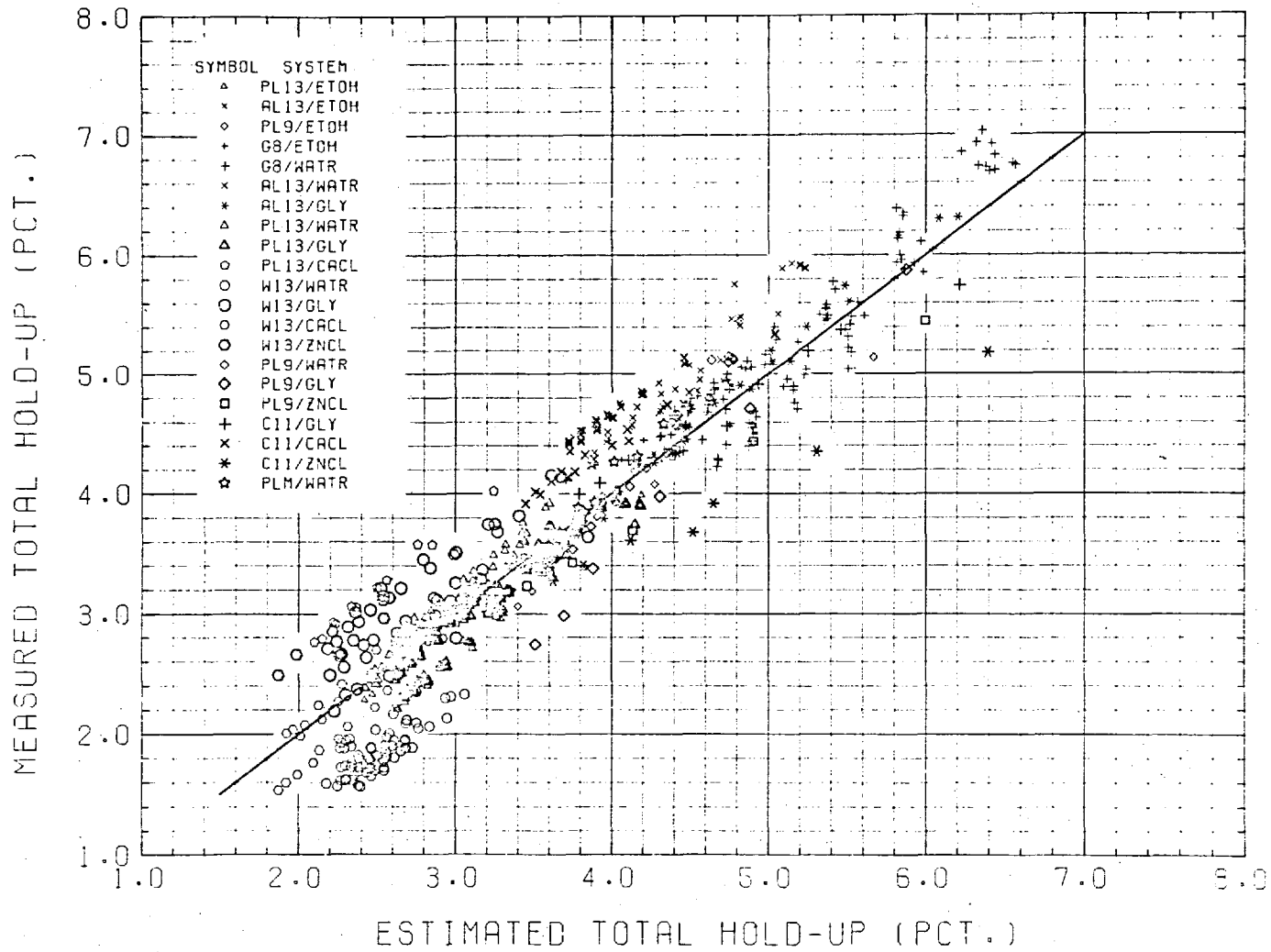


Fig. 6.5 Comparison between measured and estimated total hold-up

The estimated values of the dynamic hold-up by Eq. (6.13) are compared with the measured values in Fig. 6.4. Most of the measured values are within $\pm 0.3\%$ from the estimated values. Eq. (6.13) is valid within the following ranges of the values for dimensionless numbers covered by the experiments:

$$Re_m = \frac{\rho_l \mu d_p \phi}{(1-\epsilon) \mu_l} : 0.002 \sim 35 \quad (6.14)$$

$$Ga_m = \frac{\rho_l^2 g d_p^3 \phi^3}{\mu_l^2 (1-\epsilon)^3} : 4 \times 10^3 \sim 10 \times 10^8 \quad (6.15)$$

$$C_{ps} = \frac{\rho_l g d_p^2 \phi^2}{\sigma (1-\epsilon)^2} : 20 \sim 165 \quad (6.16)$$

$$N_c = 1 + \cos \theta : 0.59 \sim 2.0 \quad (6.17)$$

6.1.4 Correlation for the total hold-up

The total hold-up can be estimated simply by adding the estimated static and dynamic hold-ups. Fig. 6.5 shows the comparison between estimated and measured values of total hold-up. The correlation coefficient is 0.999. Most of the measured values are within $\pm 0.6\%$ from estimated values.

6.1.5 Comparison of estimated hold-up with published experimental data

Table 6.4 shows published data on static hold-up. It will be noted that most of the data are measured on ring packings. The relationship between the static hold-up and

Worker	Material	Packing				Liquid			h_s	C_{pm}		
		d_p (mm)	ϵ (-)	$\frac{a_t}{t}$ (1/m)	ϕ (-)	ρ_l (kg/m ³)	σ (N/m)	θ (deg)				
Schulman et al ^(27,34)	Porcelain R.R.	12.7	0.605	381	0.490	Water	1000	0.073	0	3.25	16.7	
		25.4	0.726	192	0.337	Water	1000	0.073	0	1.50	65.7	
						Water-	1170	0.0774	0	1.41	72.5	
						CaCl ₂	1225	0.0803	0	1.42	73.2	
							1320	0.0863	0	1.35	73.4	
						Water-	1000	0.038	0	0.79	126.3	
						S.A.	1000	0.043	0	0.83	111.6	
							1000	0.0575	0	1.17	83.5	
			38.1	0.715	134	0.334	Water	1000	0.073	0	0.89	134.5
		Porcelain B.S.	12.7	0.66	436	0.368	Water	1000	0.073	0	3.17	12.7
			25.4	0.695	205	0.350	Water	1000	0.073	0	1.10	57.4
							Water-	1160	0.0774	0	1.11	62.7
							CaCl ₂	1300	0.0803	0	1.17	67.7
							Water-	1000	0.043	0	0.94	97.2
						S.A.	1000	0.060	0	1.08	69.7	
Broz and Kolar ⁽³⁸⁾	Spheres	10	0.392	--	1.0	Water	1000	0.0732	0	3.96	18.1	
						Water-	1115	0.0502	0	2.14	29.4	
						glycerol	1186	0.0503	0	2.41	31.3	
							1213	0.0495	0	2.40	32.5	
						Water-	853.2	0.0281	0	2.77	40.2	
Gardner ⁽²⁸⁾	Coke	8.98	0.417	--	0.6	Water	1000	0.073	90°	5.23	11.5	
		15.55	0.456	--	0.6					2.40	39.5	
		19.05	0.462	--	0.6					1.81	60.6	
Warner ⁽⁴⁰⁾	Steel R.R.	6.35	0.72	--	(0.335)	Mercury	13600	0.496	140**	12.70	66.3	
							13600	0.470	140**	11.80	62.8	
Standish ⁽⁴²⁾	Steel R.R.	6.35	0.71	--	(0.335)	Water	1000	0.073	90°	4.03	3.61	
									0	3.41	7.22	
									0	6.65	4.60	
	Porcelain R.R.	6.35	0.624	--	(0.49)	Water	1000	0.073	90°	2.93	9.19	
									0	8.03	2.31	
	Porcelain B.S.	6.35	0.60	--	(0.335)	Water	1000	0.073	90°	3.41	4.63	
									0			
Andrieu ⁽⁴³⁾	Pyrex R.R.	10.0	0.69	--	(0.335)	Water	1000	0.073	90°	5.40	7.84	
			0.68	--	(0.335)				0	2.30	16.6	
	Silvered Pyrex R.R.	10.0	0.69	--	(0.335)	Water	1000	0.073	0	3.50	7.84	

R.R.: Raschig rings, B.S.: Berl saddles * Silicone coated, ** Approximate estimation

Table 6.4 Published data on static hold-up

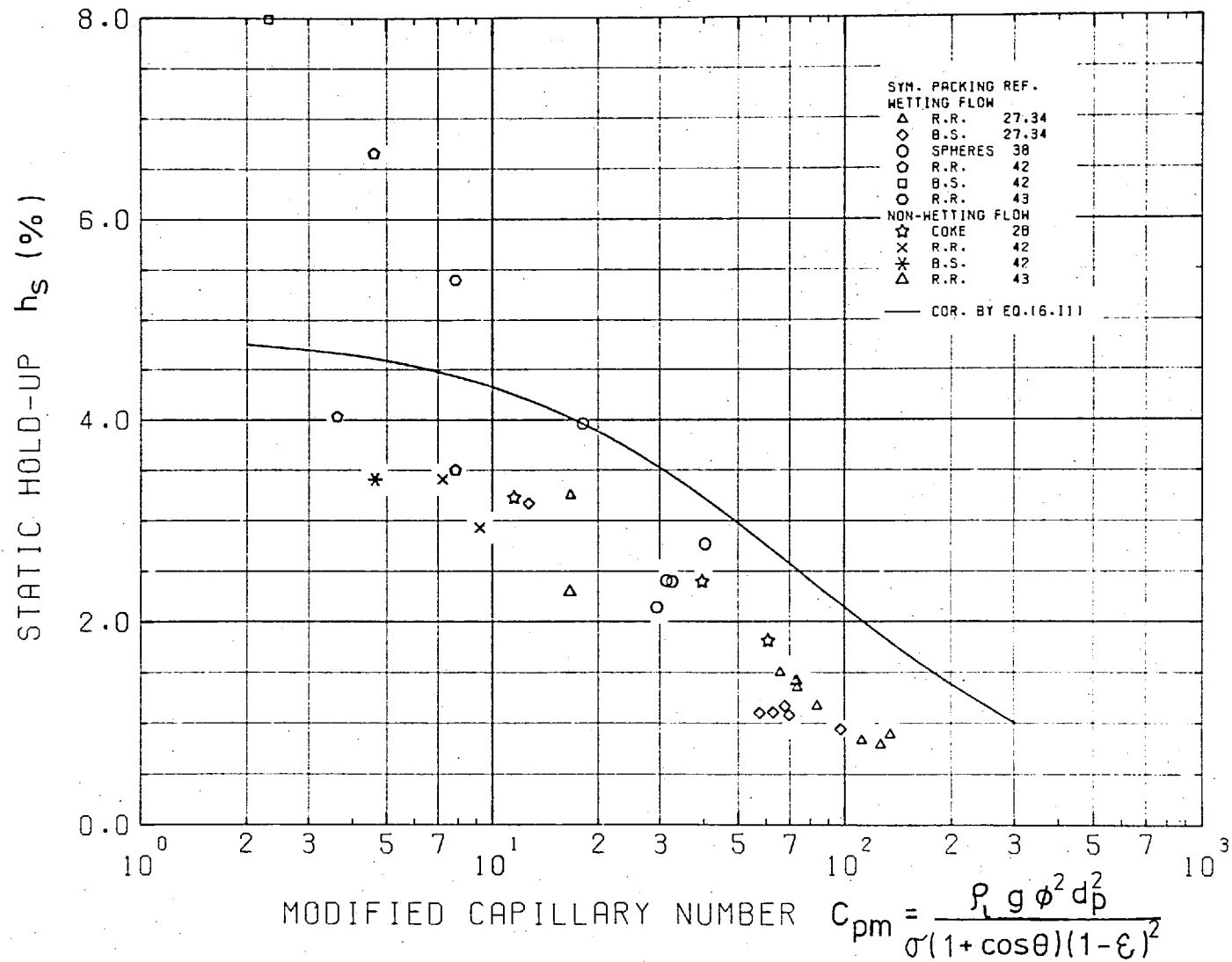


Fig.6.6 Relationship between the static hold-up, h_s , and the modified capillary number for published data. (R.R.: raschig rings, B.S.: berl saddles)

the modified capillary number, C_{pm} , is given in Fig. 6.6. Although the agreement of the data with the proposed correlation, Eq. (6.11), is rather poor, a few comments can be made. The majority of the data on raschig rings would fit the proposed correlation, if the modified capillary number were increased three fold. This indicates that the proposed method of correcting the influence of the geometry of packings is not adequate for the ring packings. However, the correction of the effect of the degree of wetting seems to be satisfactory since non-wetting data show no significant differences from wetting data.

The static hold-up for the 6.35mm steel raschig rings/mercury system measured by Warner⁽⁴⁰⁾ are the largest of all the measurements shown in Table 6.4. The larger difference in static hold-up between his system and present systems can be explained in terms of the different mechanisms of hold-up as follows.

In Fig. 6.7 three different ways in which liquid is held by a tube are shown schematically. The first and the second correspond to wetting and non-wetting systems used in the present study. The third indicates the way

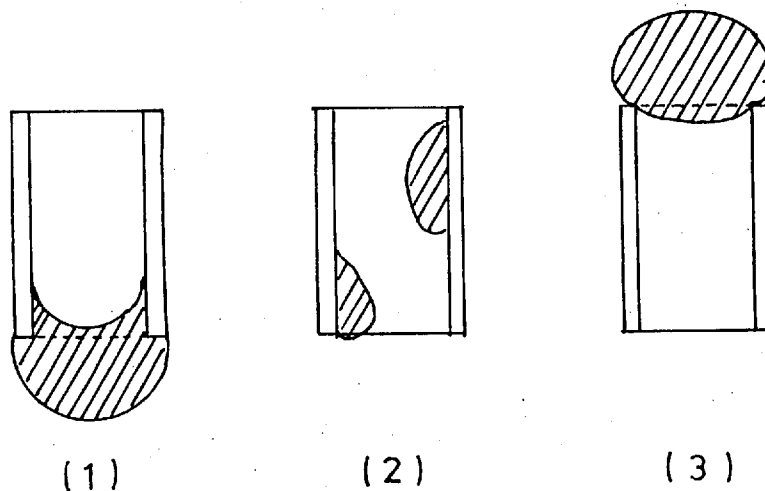


Fig. 6.7 Schematic drawing of three different ways in which liquid is held by a tube.

in which mercury is held in the ring packings. The difference between the second and the third is that the static hold-up decreases with the increase in contact angle, θ , in the second, while in the third it increases with contact angle.

Values of the dynamic hold-up estimated by Eq. (6.13) are compared with the published data on non-wetting systems in Table 6.5. It can be seen from the Table that Eq.(6.13) gives reasonable predictions for the silicone-coated coke/water system measured by Gardner⁽²⁸⁾. Comparison with the data on wetting systems measured by Jesser and Elgin⁽³³⁾ shows that Eq. (6.13) predicts 25 ~ 30% higher values for sphere packings. However, the agreement is poor for Warner's⁽⁴⁰⁾ measurements. The significantly low values are predicted by Eq.(6.13) while the relatively good predictions (b and c) are made by the correlations which are based on wetting systems. In Eq. (6.13), the power on $N_c (=1 + \cos \theta)$ is 0.648, which means that the dynamic hold-up in the wetting system is approximately 50% higher than the non-wetting system in which the contact angle is assumed to be 90° . This difference is significantly higher than those given by previous authors; Andrieu⁽⁴³⁾ reported that the operating hold-up is 10% higher in wetting flow than in non-wetting flow while Standish⁽⁴¹⁾ reported no significant difference between the two systems. In both these studies, ring packings were used. It is difficult to explain precisely the reason for the disagreement between the present study in which spherical packings have been used and the previous studies. It is likely that the effect of the degree of wetting on dynamic hold-up is dependent on the flow condition and the size and shape of the packing.

6.2 Gas Pressure Drop

6.2.1 Gas pressure drop through dry column

The data are plotted in Fig. 6.8 as a relationship

Worker:	Warner ⁽⁴⁰⁾		Gardner ⁽²⁸⁾				Blast furnace		
							Metal	Slag	
Measured data [†]	h_o	7.4	2.3	0.8	2.63	0.50	1.27	--	--
	h_d	--	--	0.53	2.36	0.32	1.09	--	--
Estimated values*	a	6.85	4.3	2.05	5.05	1.61	3.48	1.54	8.24
	b	5.97	2.32	0.33	2.08	0.26	1.25	0.28	0.77
	c	7.55	2.65	0.27	2.03	0.206	1.16	0.22	0.76
	d	2.41	0.97	0.27	1.55	0.25	1.10	0.13	0.62

* a, b, c: h_o estimated by correlations 2, 1 and 3 in Table 2.3 respectively.

d: h_d estimated by Eq. (6.13)

† Detailed data are shown in Table 2.4. Contact angle, θ , are assumed to be 140° , 90° , 125° for Warner's, Gardner's and Blast furnace systems respectively.

Table 6.5 Comparison of measured dynamic and operational hold-ups, %, with values estimated using various correlations.

between the friction factor f_k (Eq. 2.6) and gas Reynolds number Re_g (Eq. 2.7). In Fig. 6.8a both parameters are calculated on the assumption that ϕ is unity for all the packings.

It will be noted from Fig. 6.8a that the data for spherical packings agree well with the correlation proposed by Carman while coke packings follow the trend of Ergun's correlation. The difference between these two correlations seems to be related to the roughness of the surface of the packings; a similar difference is known to exist in the pressure drop correlation between the flows through smooth-walled pipes and rough-walled pipes. It is clear from Fig. 6.8a that the data for the non-spherical coke packings lie above those for spherical packings. Fig. 6.8b shows that a value of the shape factor, ϕ , equal to 0.5 brings the data for coke packings in agreement with the correlation. This value of the shape factor was used in the calculations which follow.

6.2.2 Pressure drop through irrigated column

It has been mentioned in Sec. 2.2.2 that the published correlations for the pressure drop through irrigated columns are summarised in the form of various expressions for the ratio, F , of the pressure drop through the irrigated column to that through the dry column. In all cases cited except one, F is expressed as a function of total hold-up h_t . An additional modification for the fractional voidage, ϵ , of the dry column has been incorporated in some cases. This indicates that F would be a function solely of h_t for a particular column.

In Figs. 6.9 and 6.10 typical examples of the relationship between the ratio, F , and the total hold-up, h_t , are shown. In the calculation of F , the pressure drop, ΔP_d , through the dry column was estimated for the given gas

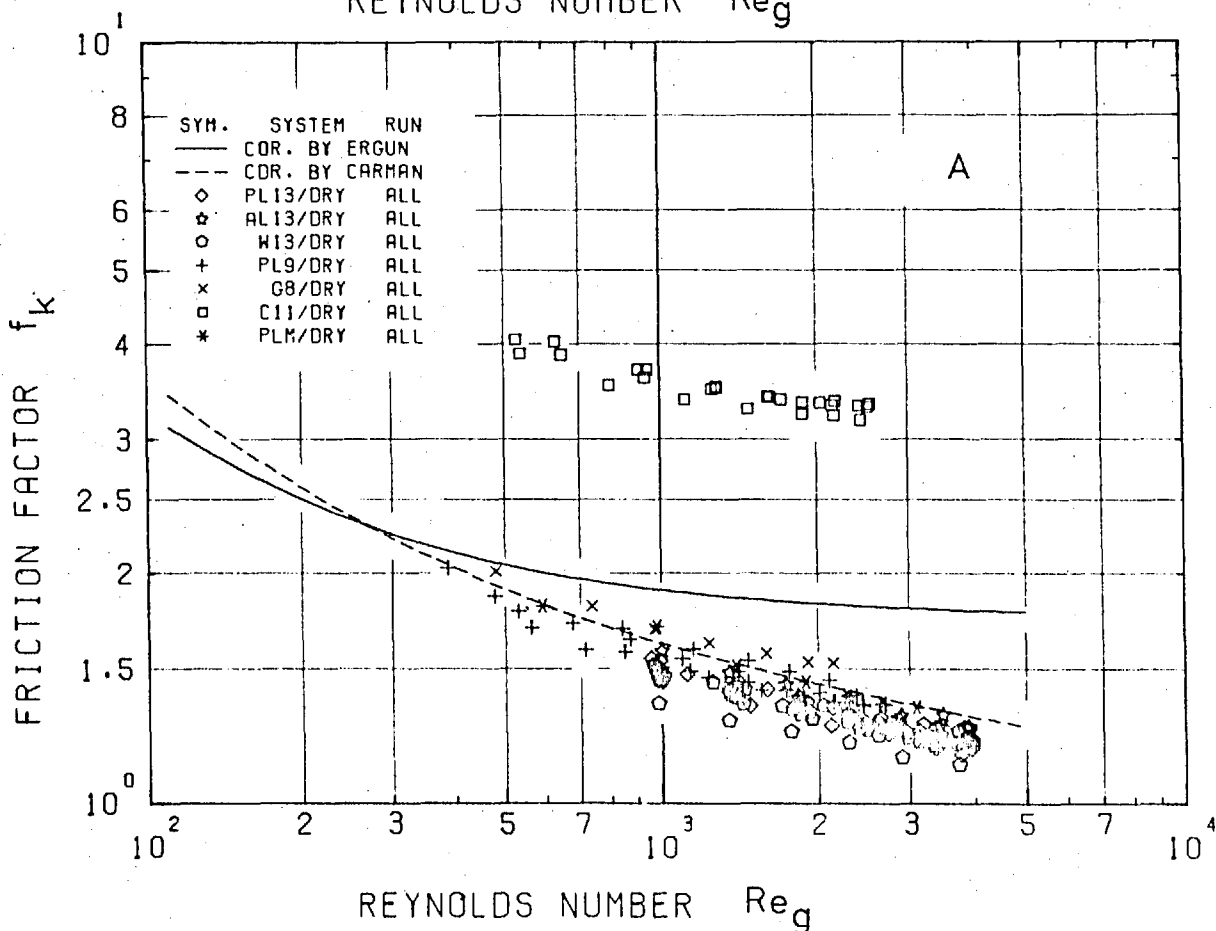
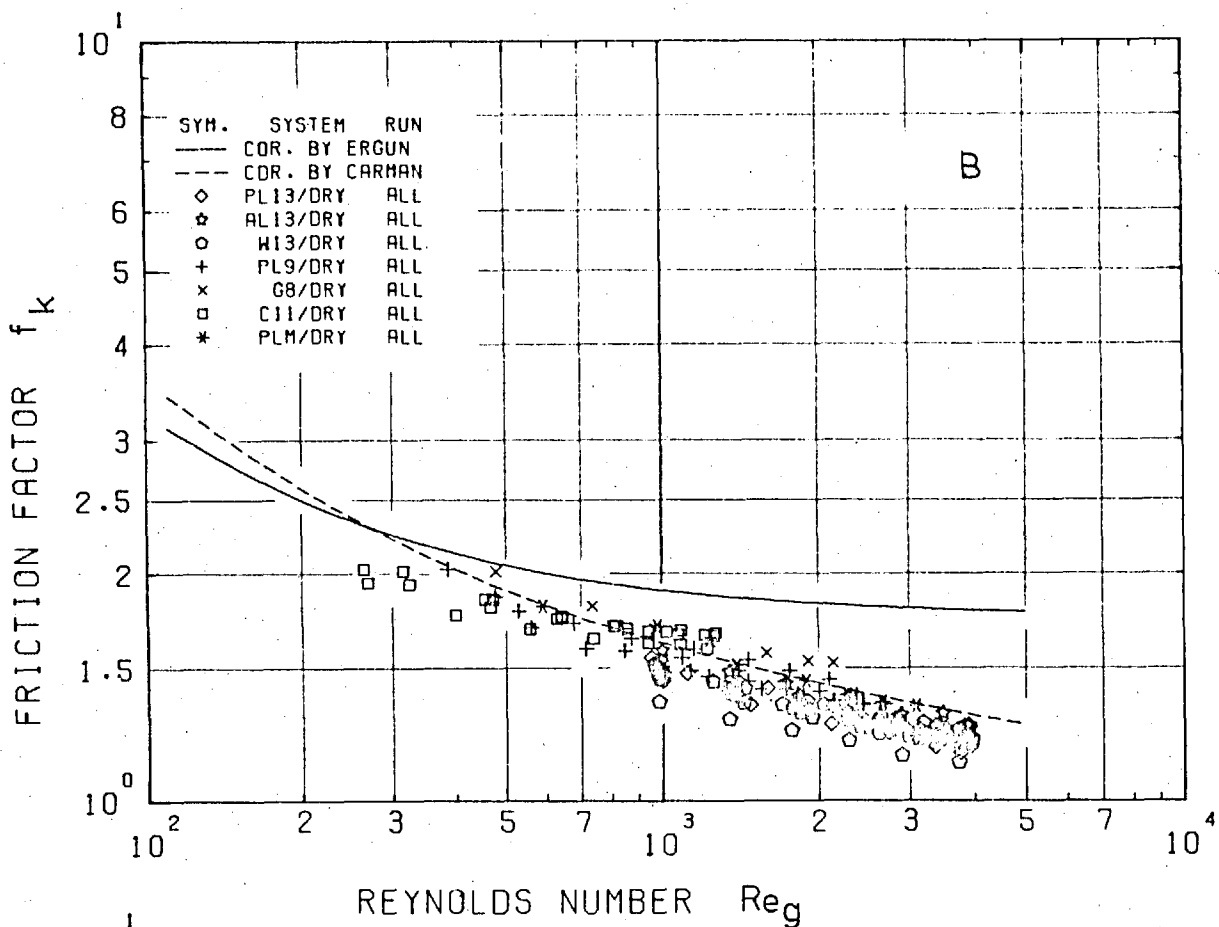


Fig. 6.8 Relationship between friction factor, f_k , and Reynolds number, Re_g , for dry columns.

A: ϕ is assumed to be 1.0 for all packings
 B: ϕ for coke is assumed to be 0.5

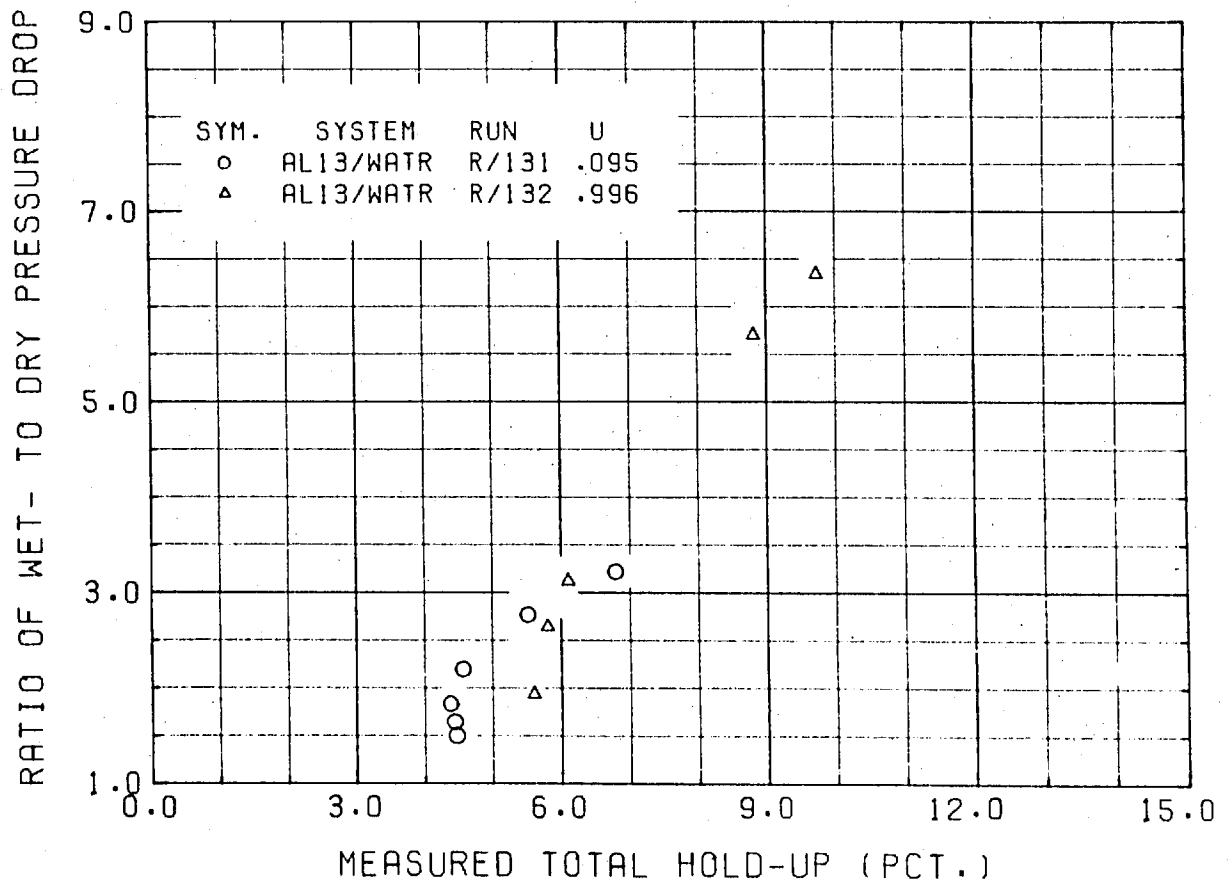
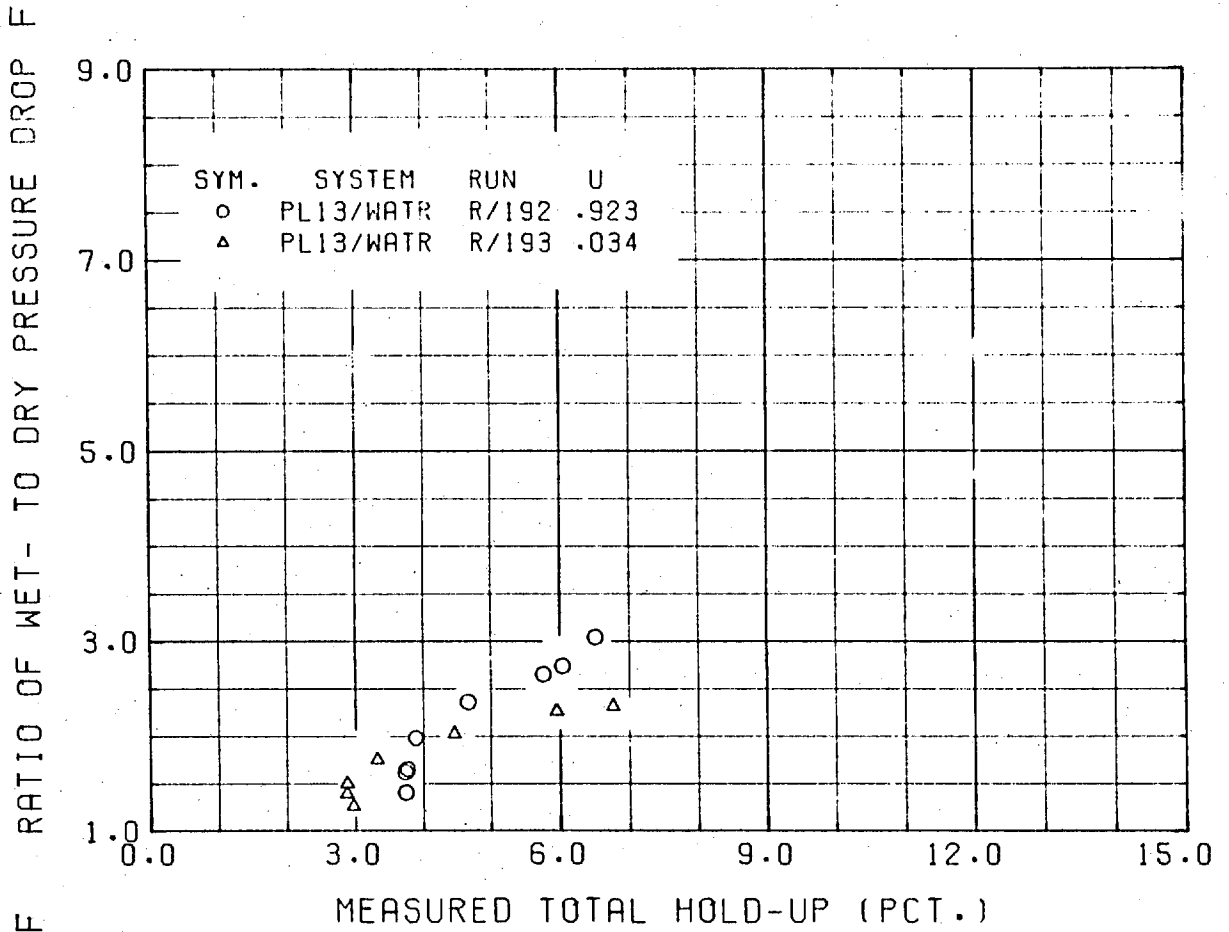
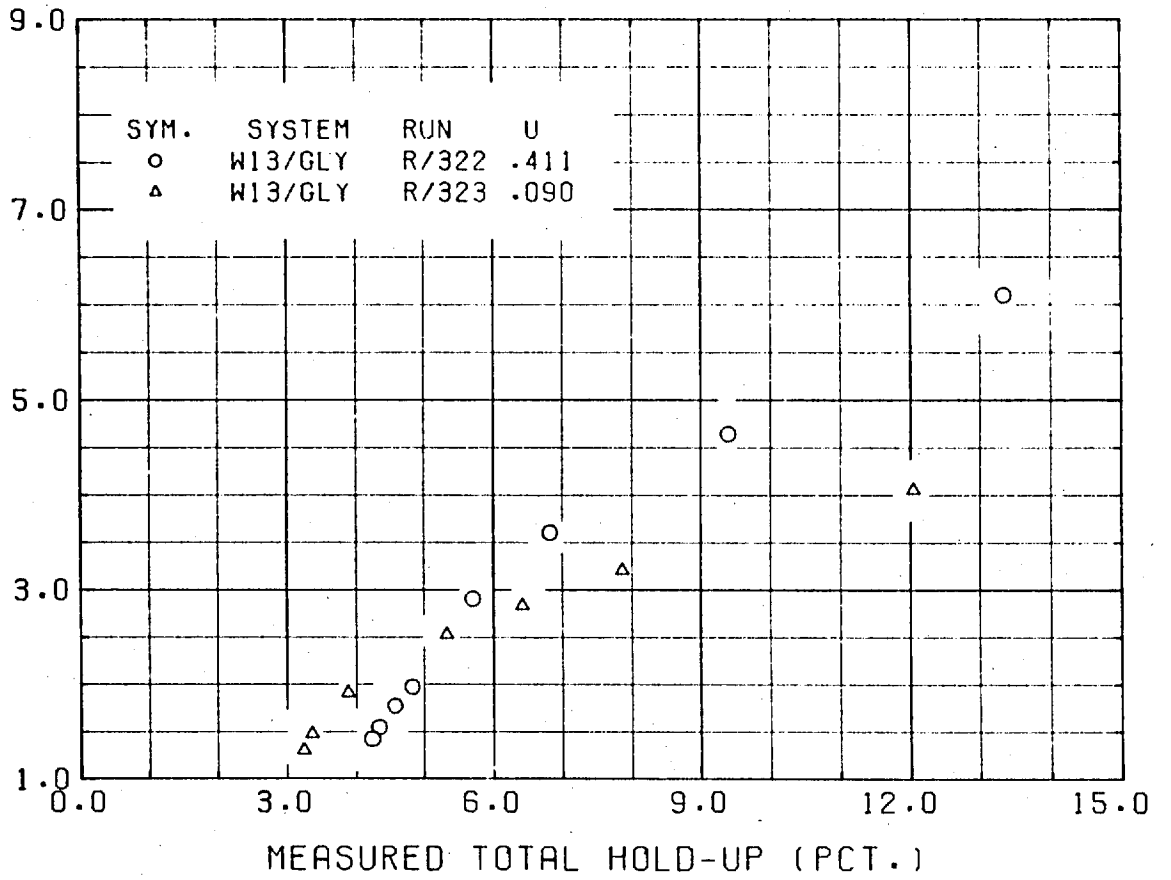


Fig. 6.9 Relationship between the total hold-up and the ratio of the pressure drop through irrigated column to that through dry column.

RATIO OF WET- TO DRY PRESSURE DROP F



RATIO OF WET- TO DRY PRESSURE DROP F

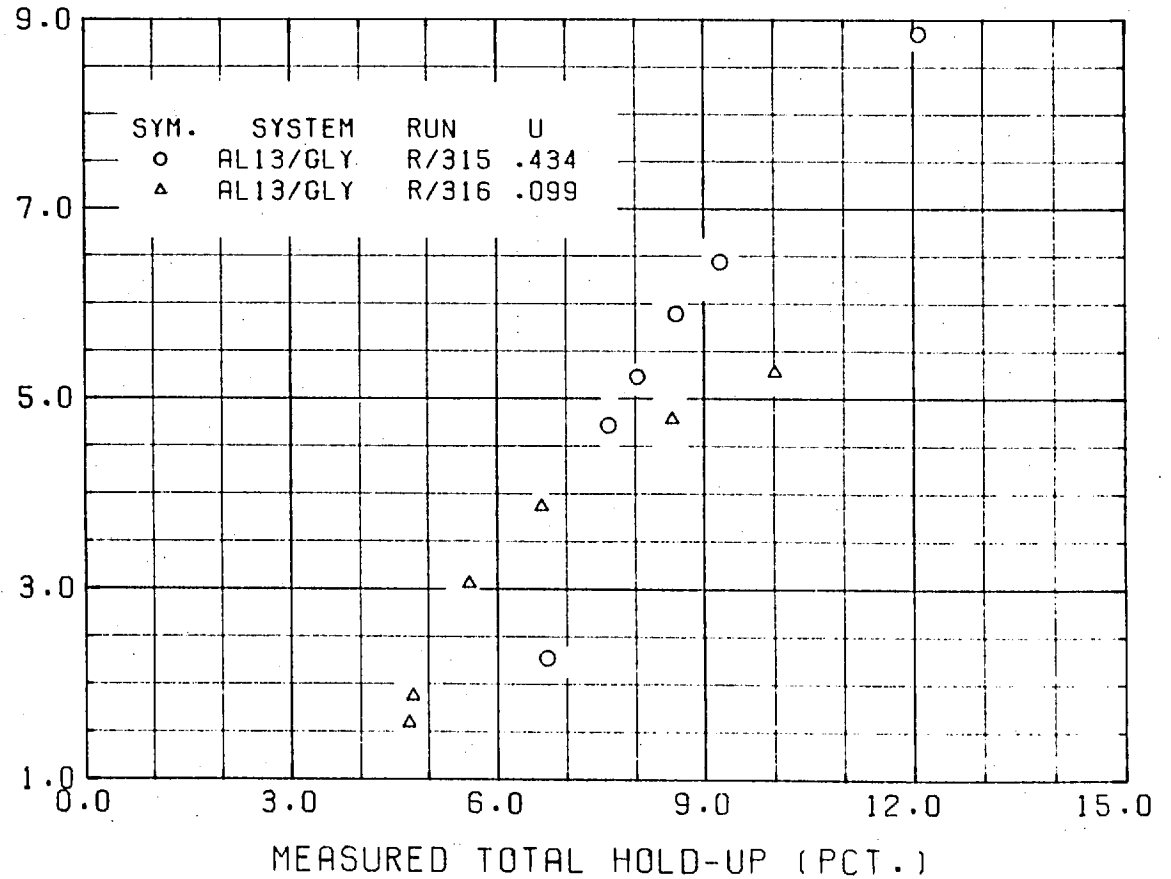


Fig. 6.10 Relationship between the total hold-up and the ratio of the pressure drop through irrigated column to that through dry column.

velocity V using Eq. (6.19).

$$\Delta P_d = a V + b V^2 \quad (6.19)$$

where the constants a and b were determined by the method of least squares based on measured pressure drop through the dry column.

A similar variation in the ratio, F , with the total hold-up, h_t , for the various systems can be observed in these figures. In the region below the loading point, F increases with the gas velocity, although the total hold-up remains virtually constant. Above the loading point F increases with h_t . The rate of increase in F with h_t depends on not only the liquid velocity but also the irrigating liquid; the rate increases with the liquid velocity and is higher with the glycerol solution than with water. Therefore, it is clear that the ratio F is not a unique function of the total hold-up but is influenced also by velocities and physical properties of gas and liquid. The expression for F based on the pressure drop correlation proposed by Jeschar et al.⁽⁸⁾ includes the velocity of liquid, u , and of gas, V , according to the equation:

$$F = \left[\frac{1 + h_t/(1 - \epsilon)}{1 - h_t/\epsilon} \right]^{1.2} \left(1.5 \frac{u}{V} \frac{\epsilon}{h_t} + \frac{\epsilon}{\epsilon - h_t} \right)^{1.8} \quad (2.17)$$

From this equation it can be seen that F increases with u and decreases with V . Therefore, it does not explain the increase in F with gas velocity below the loading point.

In order to study the gas flow through the irrigated column in more detail, the same data shown in Figs. 6.9 and 6.10 are plotted as the relationship between the friction factor, f_k , and the gas Reynolds number, Re_g , in Figs. 6.11

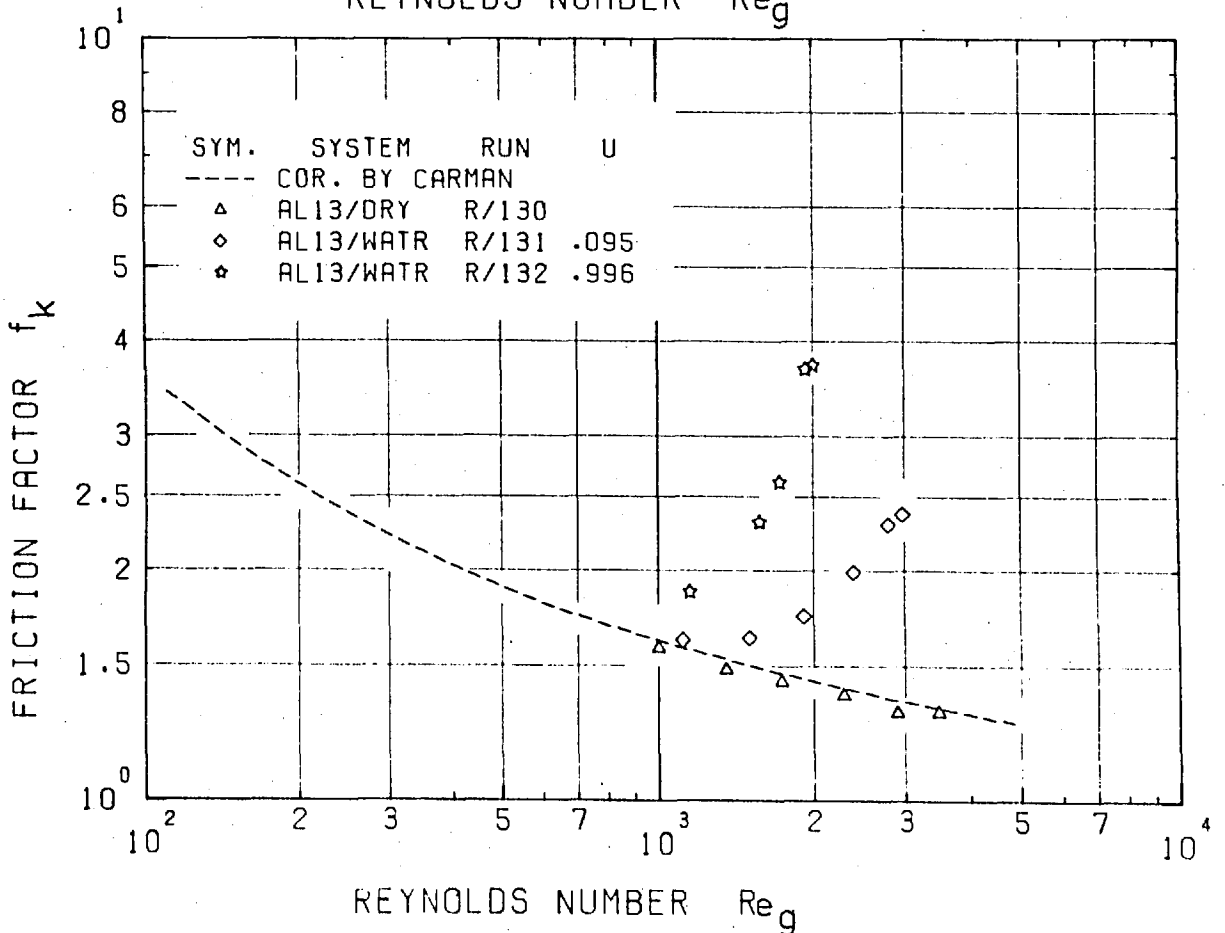
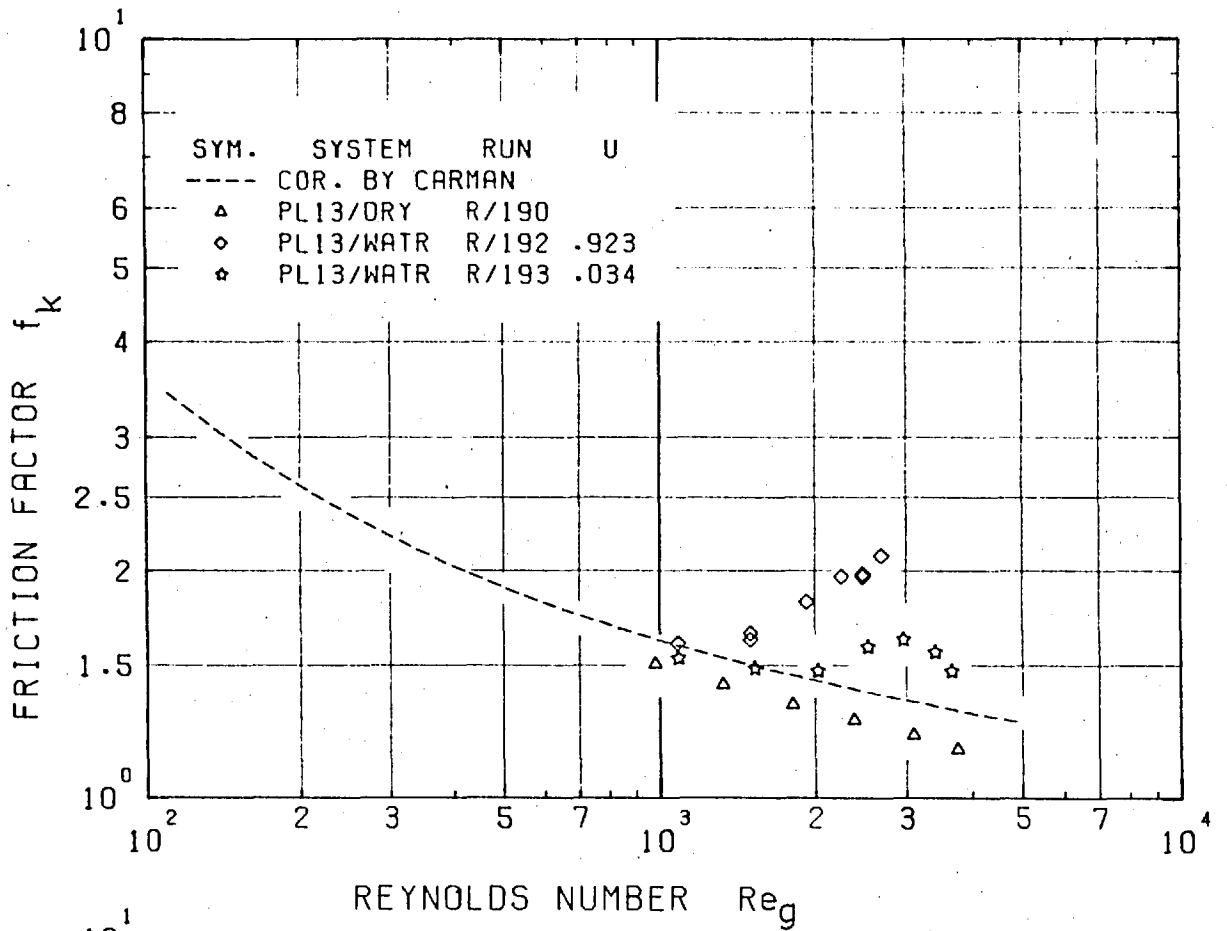


Fig. 6.11 Variation of friction factor f_k with gas Reynolds number Re_g for dry and irrigated columns.

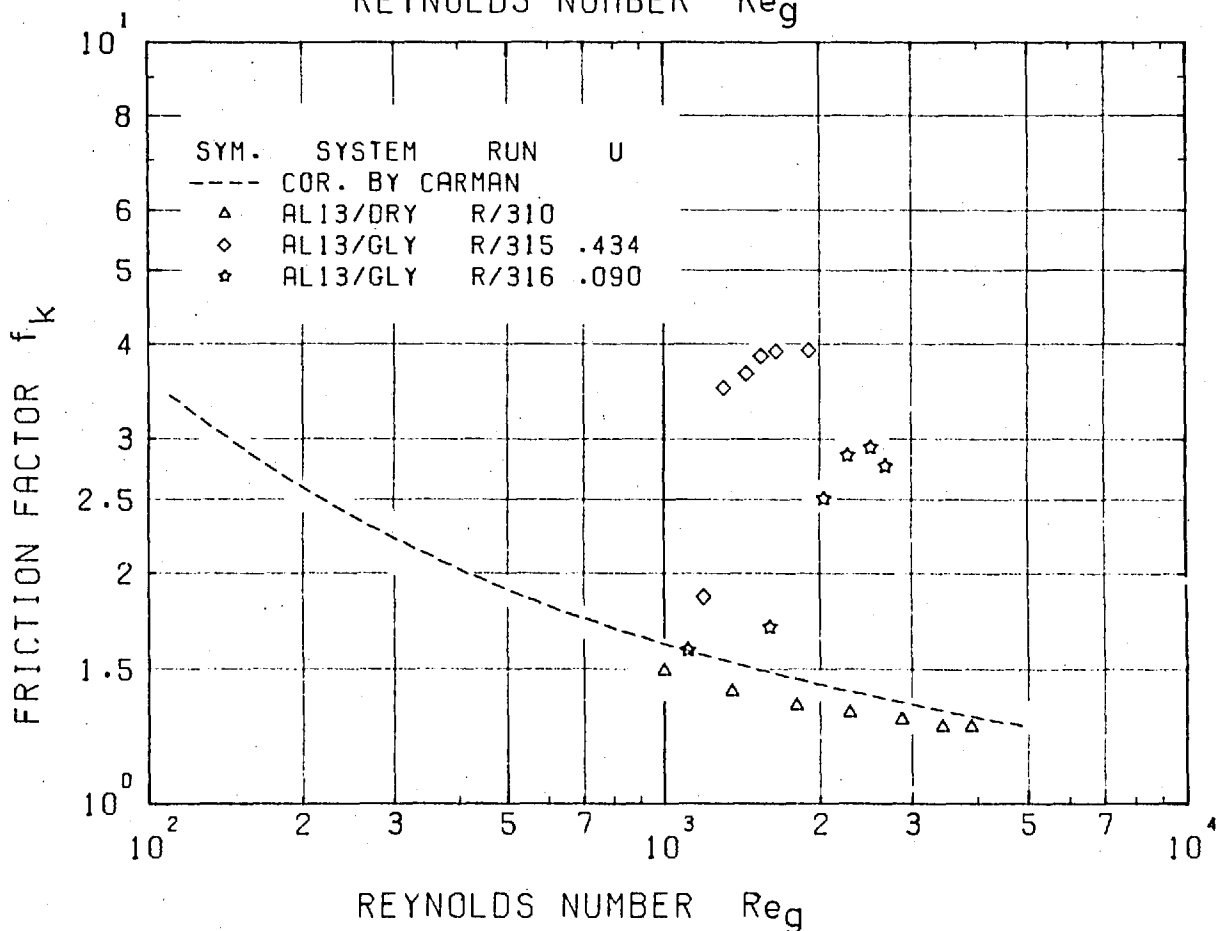
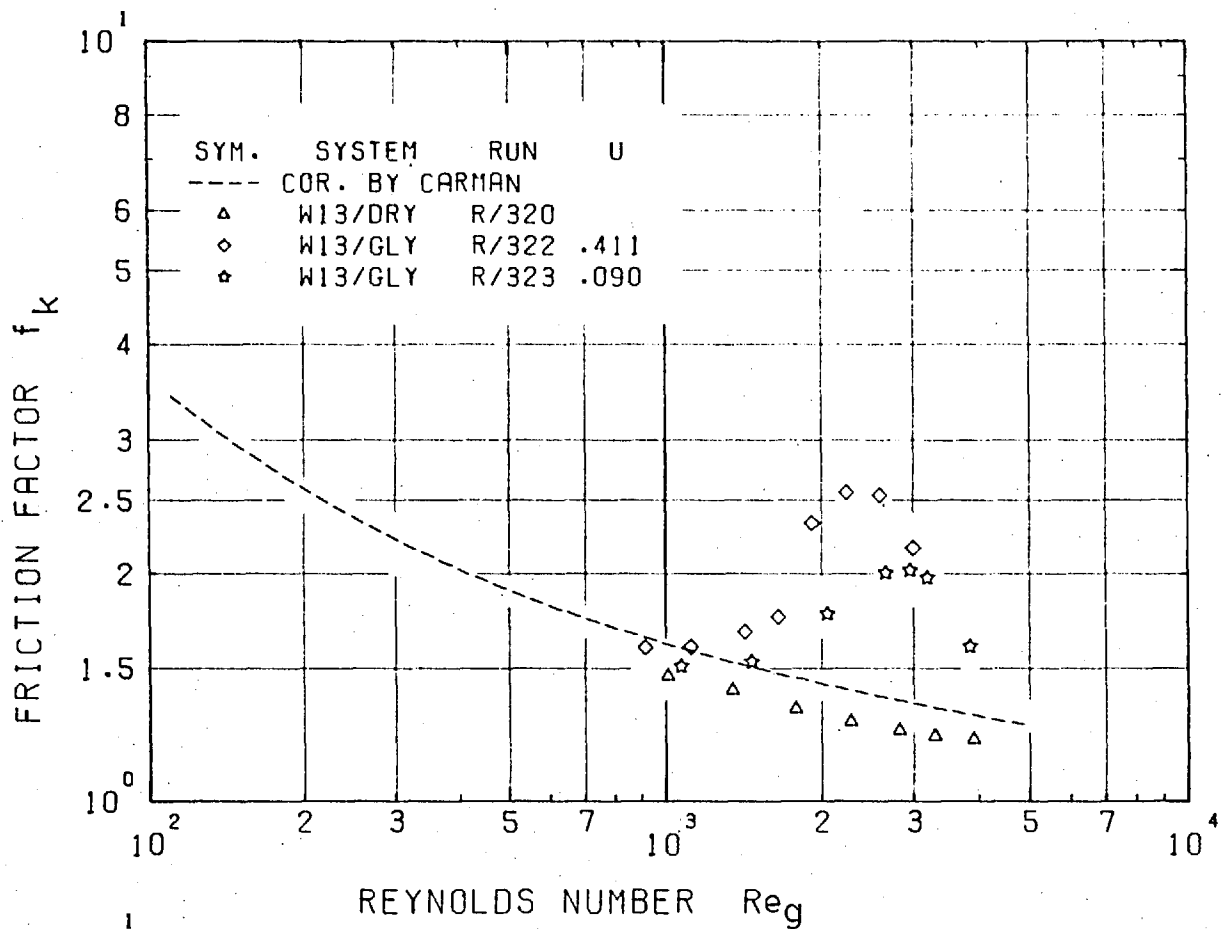


Fig. 6.12 Variation of friction factor f_k with gas Reynolds number Re_g for dry and irrigated columns

and Fig. 6.12. In the calculation of f_k and Re_g , the fractional voidage, ϵ_w of the irrigated bed was used instead of ϵ in Eqs. (2.6) and (2.7) where

$$\epsilon_w = \epsilon - h_t \quad (6.20)$$

The effect of the packing on the gas pressure drop can be expressed in terms of specific surface area and the fractional voidage. Since the effect of the liquid on the fractional voidage was taken into account in the calculation of f_k and Re_g , the displacement of the plots for the irrigated column from those for dry column is caused by the change in the specific surface area of the irrigated packing. The increase in f_k for the same value of Re_g corresponds to the increase in the specific surface area.

The types of variation of f_k with Re_g which were obtained with irrigated columns are shown schematically in Fig. 6.13. At low gas velocities, i.e. at low Re_g ,

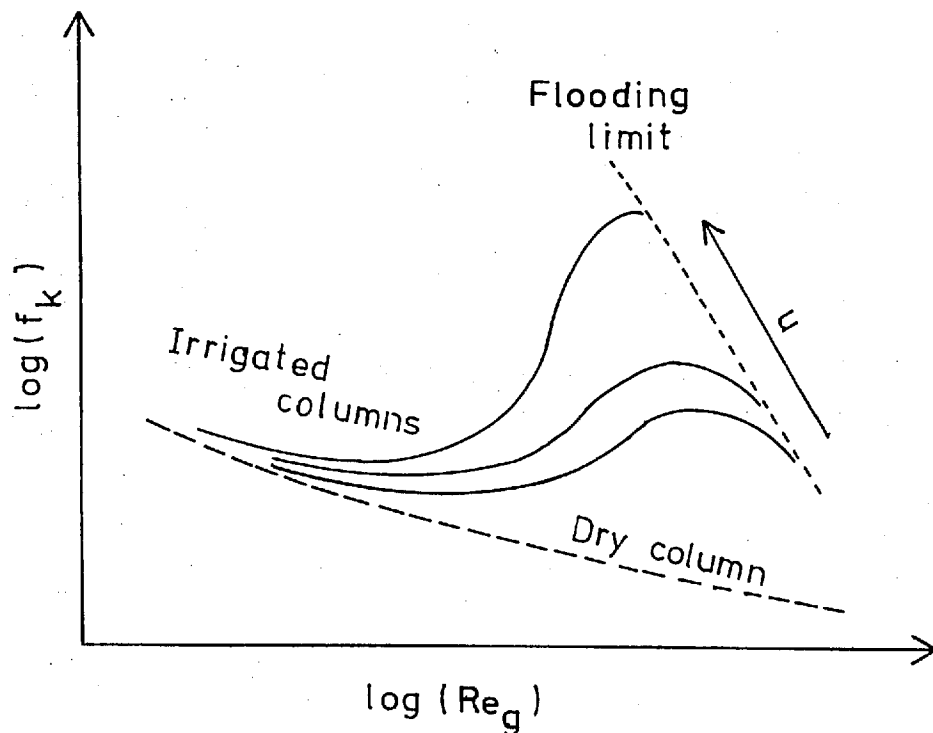


Fig. 6.13 Schematic drawing of the variation of f_k with Re_g

plots for the irrigated column followed the same path as for the dry bed. With the increase in the gas velocity, they levelled off gradually at first and then at an increasing rate. The departure from the curve for the dry column occurred well below the loading point and the displacement from the curve for the dry column reached a maximum approximately when loading started. The departure from the dry bed curve decreased with the further increase in gas velocity with non-wetting flows while this decrease was not very noticeable with wetting flows.

Since the magnitude of the displacement from the dry bed curve, which corresponds to the amount of correction for the change in specific surface, depends on many parameters, e.g. velocities and physical properties of liquid and gas, and since the effects are not linear, further analyses to establish the gas pressure drop correlation for irrigated bed were not attempted.

6.3 Flooding

The flooding velocities were determined from the observation of fluctuations of the column weight, the degree of coverage of the column wall by the liquid slugs and the appearance of the top of the column as described in Sec. 5.3. The flooding velocities determined in this manner were also checked from the curves relating the total hold-up to gas velocity which showed a steep rise near the flooding point. The results of the measurements on flooding velocities are tabulated in Table 6.5 together with the calculated parameters for the flooding diagrams. The data are plotted on the flooding diagrams proposed by Sherwood et al.⁽⁶⁰⁾ and by Mersmann⁽⁵²⁾ in Figs. 6.14 and 6.15 respectively.

Fig. 6.14 shows that the data from the present work agree reasonably well with those of Elliott et al.⁽⁴⁾ and

RUN	SYSTEM	FLOODING VELOCITIES		LIQUID VISCOSITY (NS/M2)	VOID FRACTION (-)	CALCULATED PARAMETERS			
		LIQUID (M/S)	GAS (M/S)			AFTER SHEPWOOD FLOODING FACTOR (-)	AFTER SHEPWOOD FLUID RATIO (-)	AFTER MERSMANN DIMENSIONLESS PRESSURE LOSS	AFTER MERSMANN IRRIGATION DENSITY
11191	G8/WATR	.51471	.630	.00115	.3784	.42604	.02354	.11635	.0002387
11174	G8/WATR	.17950	.782	.00115	.3784	.65642	.00661	.16699	.0000832
11271	G8/WATR	.56704	.604	.00115	.3784	.39160	.02705	.10857	.0002630
11253	G8/WATR	.17530	.759	.00115	.3784	.61838	.00665	.15876	.0000813
11351	G8/WATR	.17949	.762	.00115	.3784	.62328	.00679	.15992	.0000832
11392	G8/WATR	1.30064	.487	.00115	.3784	.25458	.07695	.07672	.0005032
11372	G8/WATR	.49515	.635	.00115	.3784	.43283	.02247	.11788	.0002296
11422	G8/WATR	.03011	.870	.00115	.3784	.81247	.00100	.20031	.0000140
11443	G8/WATR	.11269	.797	.00115	.3784	.68185	.00407	.17246	.0000523
11531	G8/WATR	.03283	.910	.00115	.3784	.88890	.00104	.21643	.0000152
12141	PL13/WATR	.99050	.906	.00113	.4054	.41911	.03150	.08901	.0002502
12152	PL13/WATR	.07532	1.131	.00113	.4054	.65313	.00192	.13189	.0000190
12291	PL13/WATR	.99492	.894	.00113	.4054	.40808	.03206	.08696	.0002513
12272	PL13/WATR	.18619	1.071	.00113	.4054	.58567	.00501	.11955	.0000470
12391	PL13/WATR	.06156	1.132	.00113	.4054	.65428	.00157	.13210	.0000156
12472	PL13/WATR	.30716	1.044	.00113	.4054	.55651	.00848	.11433	.0000776
19171	PL13/WATR	.16678	1.277	.00102	.4054	.81575	.00376	.15116	.0000407
19292	PL13/WATR	.92871	.971	.00102	.4054	.47165	.02756	.09402	.0002267
19381	PL13/WATR	.03367	1.405	.00102	.4054	.98748	.00069	.17897	.0000082
22171	PL13/WATR	.18525	1.288	.00108	.4029	.65873	.00414	.16118	.0000466
22291	PL13/WATR	.05886	1.387	.00108	.4029	.99581	.00122	.18466	.0000148
22391	PL13/WATR	1.01047	1.002	.00108	.4029	.51971	.02906	.10225	.0002541
22471	PL13/WATR	.01767	1.414	.00108	.4029	1.03496	.00036	.19134	.0000044
13183	AL13/WATR	.31388	.977	.00108	.4039	.49335	.00926	.10820	.0000792
13164	AL13/WATR	.09518	1.143	.00108	.4039	.67525	.00240	.14376	.0000240
13291	AL13/WATR	.99605	.705	.00108	.4039	.25689	.04071	.06072	.0002513
13392	AL13/WATR	.06406	1.206	.00108	.4039	.75173	.00153	.15857	.0000162
15171	W13/WATR	.17889	1.263	.00109	.4106	.76569	.00408	.14917	.0000434
15291	W13/WATR	1.01734	1.103	.00109	.4106	.58398	.02657	.11712	.0002467
15392	W13/WATR	.06434	1.365	.00109	.4106	.89436	.00136	.17159	.0000156
16171	W13/WATR	.18022	1.220	.00105	.4106	.70912	.00426	.14180	.0000432
16271	W13/WATR	.01863	1.342	.00105	.4106	.85803	.00040	.16901	.0000045
18361	W13/WATR	.31233	1.428	.00101	.4253	.84583	.00630	.15966	.0000695
21171	W13/WATR	.18429	1.502	.00105	.4106	1.07482	.00354	.19408	.0000441
21291	W13/WATR	1.00726	1.163	.00105	.4106	.64440	.02495	.12115	.0002412
23171	W13/WATR	.17431	1.440	.00113	.4106	1.00254	.00349	.19034	.0000428
23291	W13/WATR	.05842	1.613	.00113	.4106	1.25789	.00104	.23506	.0000143
14171	PL9/WATR	.18189	.832	.00109	.3843	.62561	.00630	.14255	.0000727
14291	PL9/WATR	.93701	.686	.00109	.3843	.42531	.03935	.10307	.0003747
14391	PL9/WATR	.06349	.853	.00109	.3843	.65759	.00214	.14874	.0000254
17272	PLM/WATR	.18167	.915	.00115	.3897	.61729	.00572	.14007	.0000614
33191	PL13/GLY	.44349	.855	.06360	.4106	.65899	.01644	.06391	.0003943
33272	PL13/GLY	.11433	1.140	.06360	.4106	1.17153	.00318	.10536	.0001017
34171	PL13/GLY	.10440	1.177	.05750	.4106	1.22388	.00281	.11426	.0000899
34351	PL13/GLY	.01660	1.484	.05750	.4106	1.94560	.00035	.17488	.0000143
34451	PL13/GLY	.01986	1.525	.05750	.4106	2.05459	.00041	.18394	.0000171
31362	AL13/GLY	.02012	1.184	.06290	.4047	1.34020	.00054	.12192	.0000184
31472	AL13/GLY	.10097	.942	.06290	.4047	.84834	.00340	.108024	.0000924
31591	AL13/GLY	.43352	.622	.06290	.4047	.36997	.02209	.03835	.0003965
31641	AL13/GLY	.09946	.933	.06290	.4047	.83221	.00338	.07886	.0000910
30172	W13/GLY	.06569	1.410	.06570	.4180	1.87558	.00148	.14439	.0000568
30291	W13/GLY	.37728	1.006	.06570	.4180	.85295	.01189	.07776	.0003265
30361	W13/GLY	.02261	1.515	.06570	.4180	1.93443	.00047	.16503	.0000196
32171	W13/GLY	.05762	1.322	.06780	.4106	1.58374	.00138	.13551	.0000519
32291	W13/GLY	.41060	.937	.06780	.4106	.79561	.01389	.07258	.0003701
32251	W13/GLY	.02084	1.476	.06780	.4106	1.97421	.00045	.16608	.0000188
32371	W13/GLY	.08989	1.259	.06780	.4106	1.43639	.00226	.12390	.0000810
38151	W13/GLY	.01792	1.527	.06870	.4180	1.98283	.00037	.17193	.0000157
38291	W13/GLY	.48465	.987	.06870	.4180	.82840	.01556	.07713	.0004256
38381	W13/GLY	.14563	1.333	.06870	.4180	1.51101	.00346	.13359	.0001279
38351	W13/GLY	.01834	1.695	.06870	.4180	2.44313	.00034	.20901	.0000161
36161	PL9/GLY	.06540	.849	.05430	.3950	1.06456	.00244	.11829	.0000663
36291	PL9/GLY	.48887	.549	.05430	.3950	.44514	.02822	.05593	.0006453
35171	C11/GLY	.11247	1.060	.05440	.5242	.91406	.00336	.11402	.0001441
35251	C11/GLY	.03021	1.185	.05440	.5242	1.14235	.00081	.14016	.0000387
35391	C11/GLY	.45018	.889	.05440	.5242	.64293	.01605	.08261	.0005766
37171	C11/GLY	.09760	1.159	.07050	.5242	1.15093	.00267	.12896	.0001363
37351	C11/GLY	.01166	1.353	.07050	.5242	1.56847	.00027	.17218	.0000163
37491	C11/GLY	.28377	.932	.07050	.5242	.74424	.00365	.08627	.0003963
40171	PL13/CACL	.14501	1.449	.00614	.4076	1.09203	.00335	.14554	.0000577
40391	PL13/CACL	1.14395	1.063	.00614	.4076	.58771	.03603	.08276	.0004555
39171	W13/CACL	.15571	1.600	.00466	.4060	1.26881	.00326	.16226	.0000565
39391	W13/CACL	1.19524	1.157	.00466	.4060	.66348	.03458	.08933	.0004337
39451	W13/CACL	.14933	1.603	.00466	.4060	1.27358	.00312	.16283	.0000542
39551	W13/CACL	.03404	1.777	.00466	.4060	1.56507	.00064	.19740	.0000124
41171	C11/CACL	.14386	1.482	.00634	.5179	1.09465	.00325	.18036	.0000890
41391	C11/CACL	1.21833	1.111	.00634	.5179	.61519	.03671	.10594	.0007537
42171	PL9/ZNCL	.24791	1.100	.02860	.3998	.94785	.00900	.10355	.0002221
43291	PL9/ZNCL	1.06375	.750	.02860	.3998	.44063	.05602	.05299	.0009530
44171	C11/ZNCL	.28432	1.373	.02790	.5316	.79821	.00827	.10942	.0002426
44251	C11/ZNCL	.06354	1.557	.02790	.5316	1.02649	.00163	.13836	.0000542
42171	W13/ZNCL	.18577	1.660	.03020	.4180	1.31319	.00447	.11135	.0001150
42391	W13/ZNCL	.87551	1.150	.03820	.4180	.63024	.03039	.05663	.0005421

Table 6.6 Flooding velocities and dimensionless parameters for the flooding diagrams.

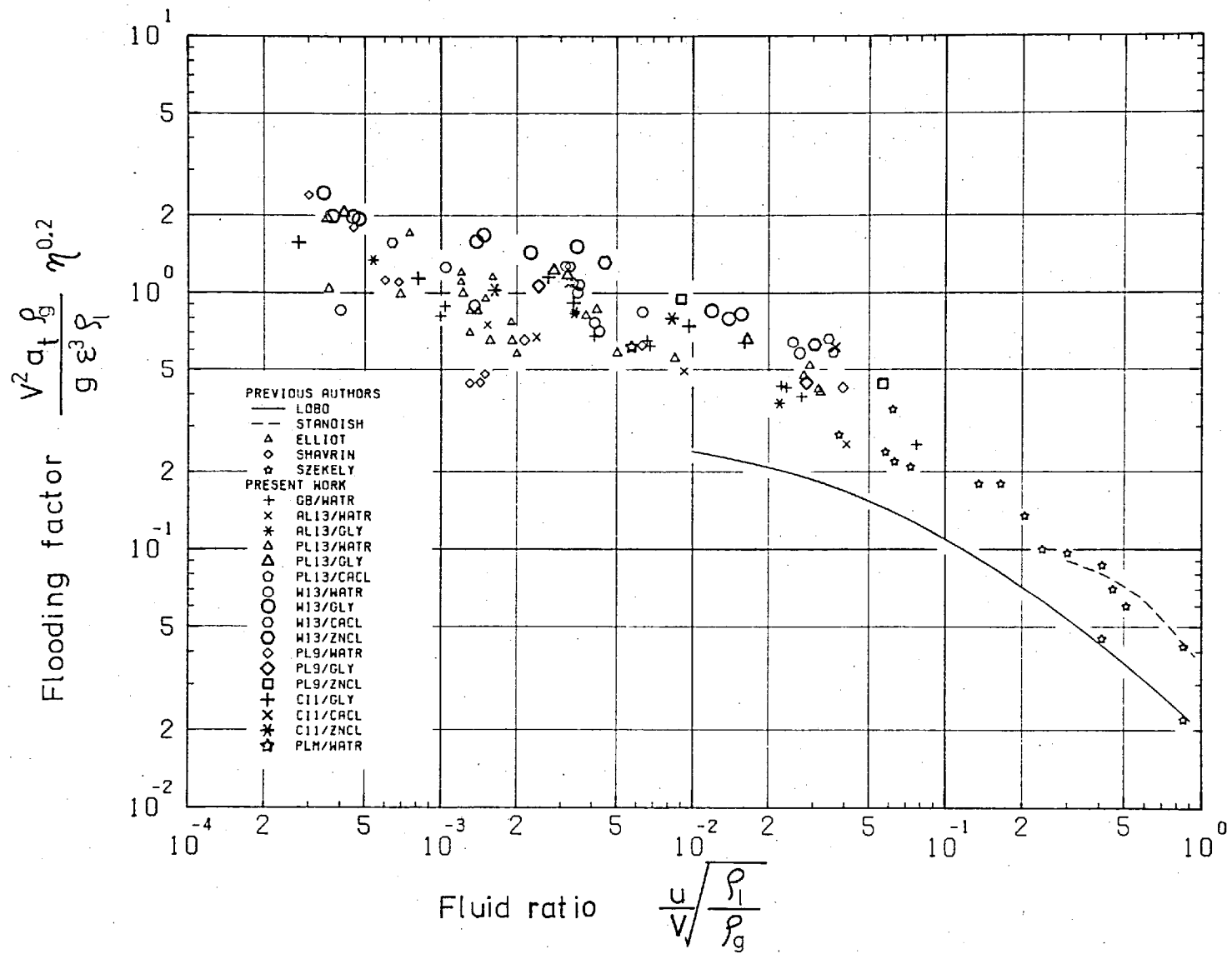


Fig. 6.14 Plots of flooding data on Sherwood diagram

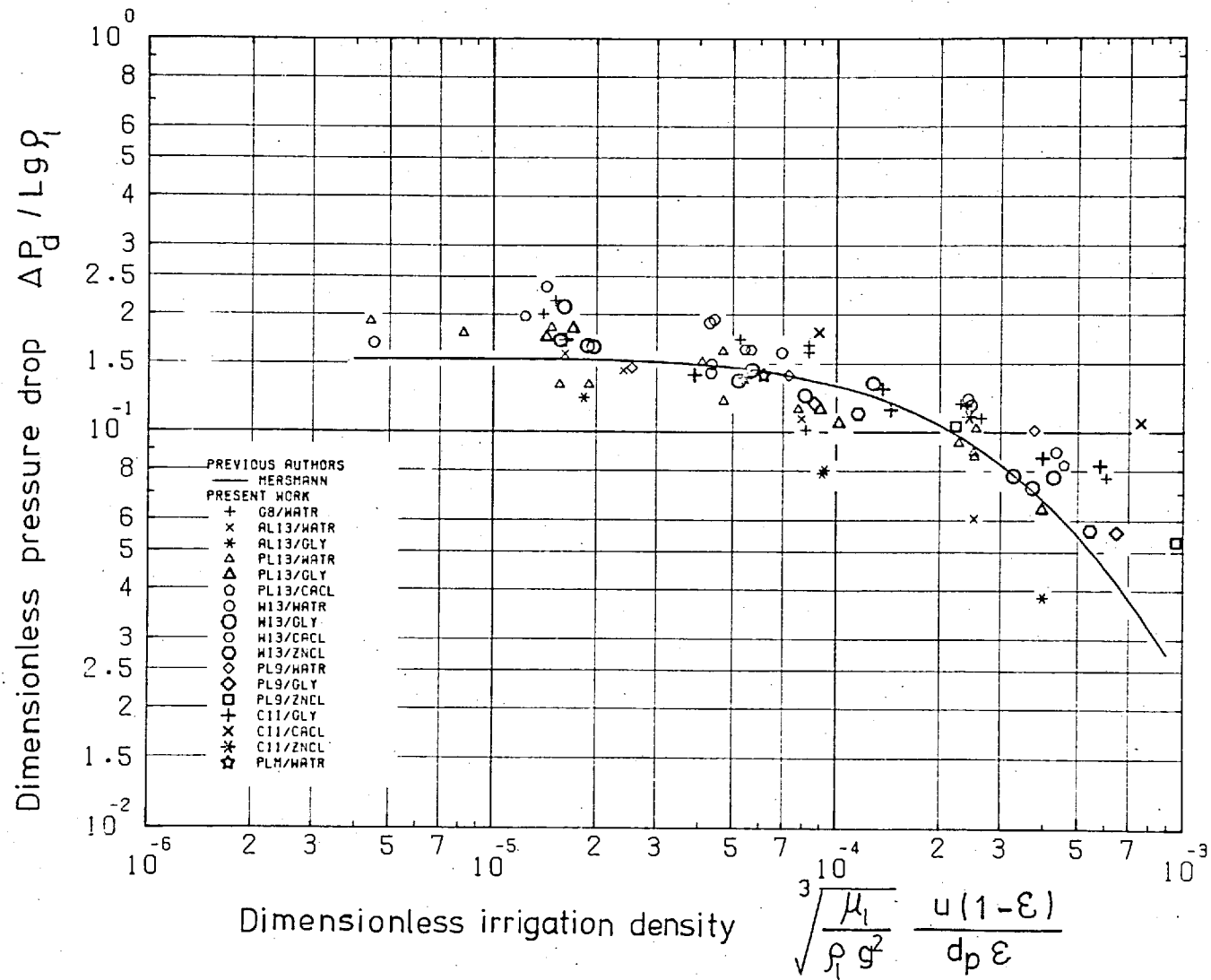


Fig. 6.15 Plots of flooding data on Mersmann's diagram

Shavrin et al⁽⁶⁵⁾. However, their flooding factors for the same fluid ratio are approximately twice as high as those estimated by the correlation given by Lobo et al⁽⁶¹⁾.

Fig. 6.15 shows that the results of this study agree reasonably well with the correlation given by Mersmann⁽⁵²⁾ although the present data indicates somewhat higher dimensionless pressure drops than predicted by this correlation.

It can be seen from Figs. 6.14 and 6.15 that the scatter of the plots in the former is approximately 100% which is twice as much as that in the latter. On this basis, the Mersmann's diagram will be used in further discussions.

It will be seen from Fig. 6.15 that the data points for the non-wetting flow systems are above those for alumina sphere packings (AL13/WATR, AL13/GLY). Due to the scatter in the experimental data, it is difficult to deduce a suitable correction term to account for the degree of wetting from the flooding diagram itself. It will be noted, however, from the correlation for dynamic hold-up shown in Eq. (6.13) that the effect of the degree of wetting on the dynamic hold-up can be accounted for in terms of $(1+\cos\theta)$ and that the powers on u and $(1+\cos\theta)$ are the same. Therefore, it is reasonable to multiply the dimensionless irrigation density in the abscissa by the factor, $(1+\cos\theta)$, to incorporate the influence of the degree of wetting on flooding velocities. To maintain consistency with the original dimensionless irrigation density, the correction factor, $(1+\cos\theta)$, is divided by two to yield $(\cos\frac{\theta}{2})^2$. The modified dimensionless irrigation density then, can be written as follows:

Modified dimensionless irrigation density

$$= \left(\frac{\mu_l}{\rho_l g^2} \right)^{1/3} \frac{u \cos^2(\theta/2) (1-\epsilon)}{d_p \epsilon} \quad (6.21)$$

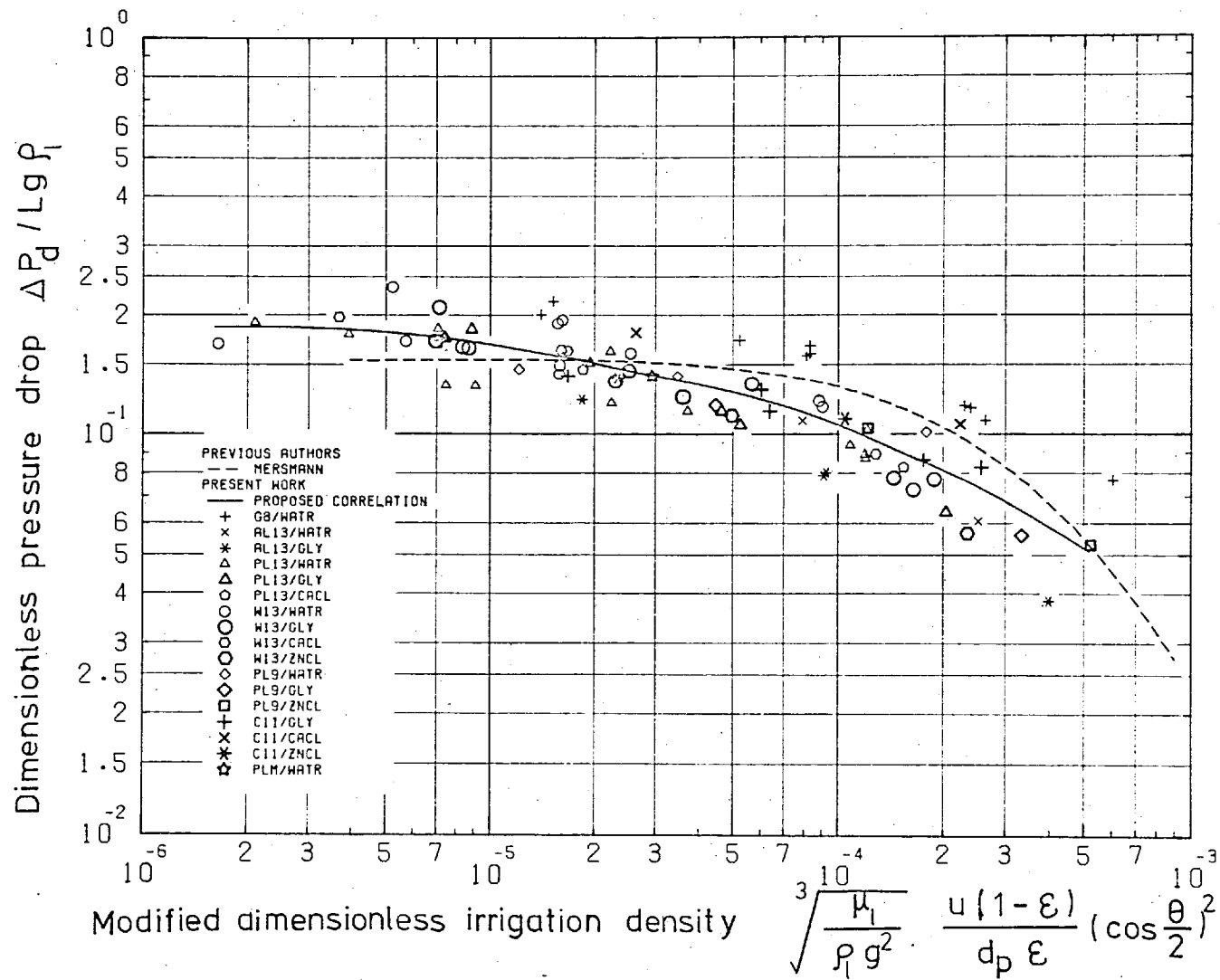


Fig. 6.16 Flooding diagram based on modified dimensionless irrigation density.

The measured flooding data are plotted in Fig. 6.16 as a relationship between the dimensionless pressure drop and the modified dimensionless irrigation density. It can be seen from this Figure that the data for the system G8/WATR have the highest and the data for the system AL13/GLY have the lowest ordinates; both are wetting systems. A comparison between Figs. 6.15 and 6.16 shows that the use of modified irrigation density decreases the scatter of the plotted data. An even further improvement will result if the data on the G8/WATR system which, despite numerous data points, are taken on a single column, are excluded. The solid line shown in the Figure is drawn by the generalized curve fitting program shown in Appendix II. It is clear that the solid line represents the data better than the dotted line which is the original Mersmann correlation. These two curves differ mainly in their slopes, i.e., the Mersmann correlation indicates that the dimensionless pressure does not change in the region where the dimensionless irrigation density is less than 3×10^{-5} while the proposed correlation indicates that the dimensionless pressure increases with the decrease in the modified dimensionless irrigation density. Since Mersmann's correlation is based on a small number of experimental data at low irrigation densities, the present correlation will be more reliable. The scatter of the data about the proposed correlation is approximately $\pm 30\%$ in the ordinate which corresponds to $\pm 15\%$ in the estimated flooding velocity of the gas.

6.4 Instability of the Bed

Fig. 6.17 shows variations of the total hold-up and pressure drop with gas velocity for the PL9/ZNCL system. It should be noted that zinc chloride solution ($\rho_l = 1920 \text{ kg/m}^3$) was the heaviest liquid used in this work. In Runs 431 and 433 the column behaved differently from that described

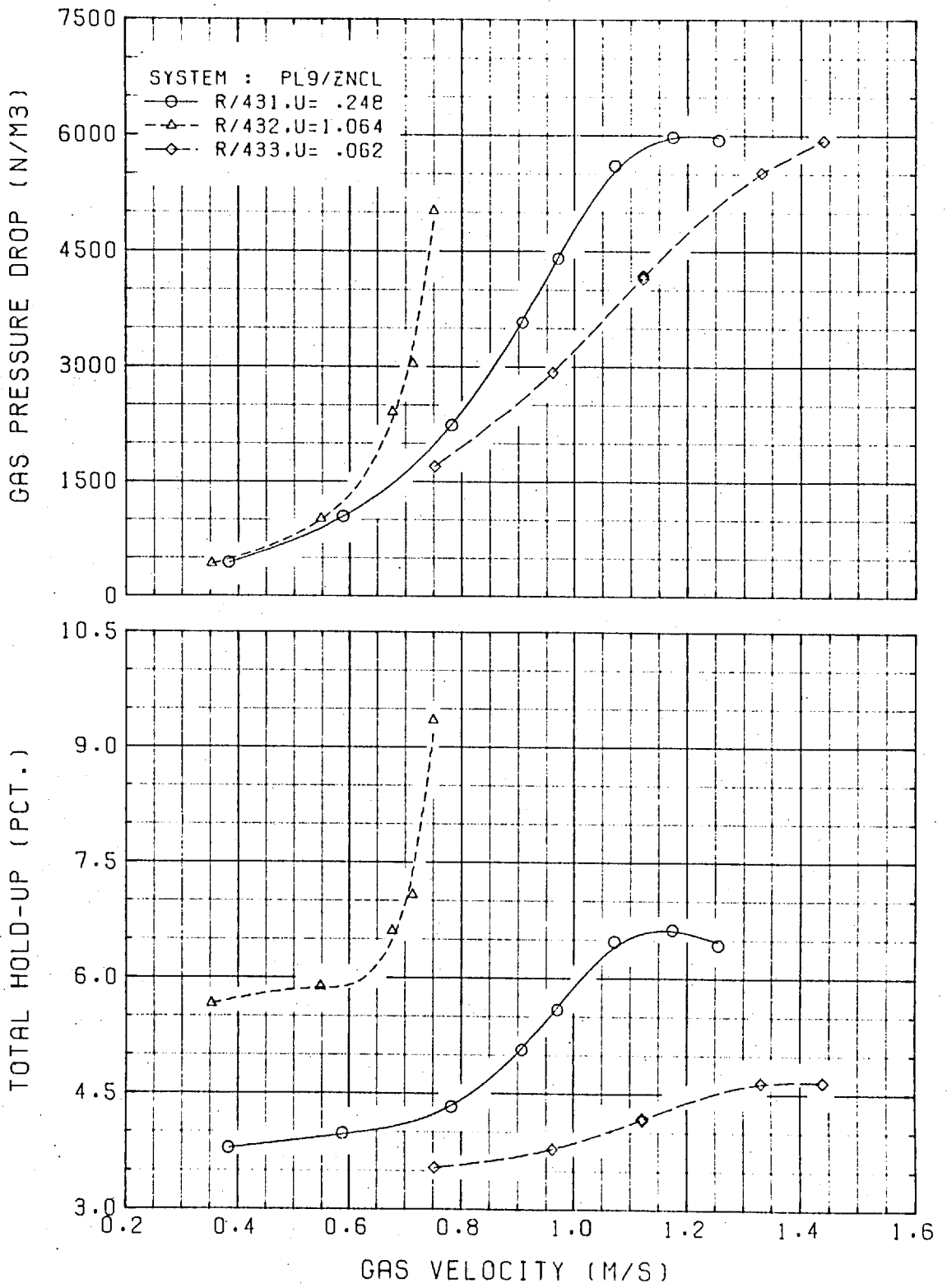


Fig. 6.17 Variations of total hold-up and gas pressure with gas velocity for Run 430 (PL9/ZNCL)

generally in Sec. 5.3. In Run 431 the column behaved the same as described in Sec. 5.3 until the gas velocity reached that at flooding. However, when the column started to flood, it expanded slightly (5-10mm); this instantly stopped the flooding. A further increase in gas velocity caused a further expansion of the column and thus complete flooding was not observed. In Run 433 (lowest liquid velocity), the expansion of the column started before flooding occurred; complete flooding was not observed in this experiment also. It must be noted that this expansion of the column was different from the movement of the particles on top of the column described in Sec. 5.3; in the latter the movement was confined to the top part of the column while in the former the small shift of the packing extended throughout the column. With reference to the instability of the bed, the experiments are classified into three categories: those in which flooding occurred; those in which fluidization occurred before flooding; and those in which flooding and fluidization occurred together.

The condition for fluidization to take place at the point of flooding can be described by considering the balance between the forces as follows:

$$g\{\rho_s(1-\epsilon) + \rho_l h_t\} = \Delta P/L \quad (6.22)$$

By dividing both sides by $\rho_l g$, Eq. (6.22) can be made dimensionless:

$$\frac{\rho_s}{\rho_l} (1-\epsilon) = \frac{\Delta P}{gL\rho_l} - h_t \quad (6.23)$$

Because h_t and ΔP are the values at flooding and hence are difficult to estimate, it is difficult to discuss the problem exactly. However, the modified dimensionless irrigation density determines the flooding velocity of the gas (Fig. 6.16), so that it may be assumed as a first

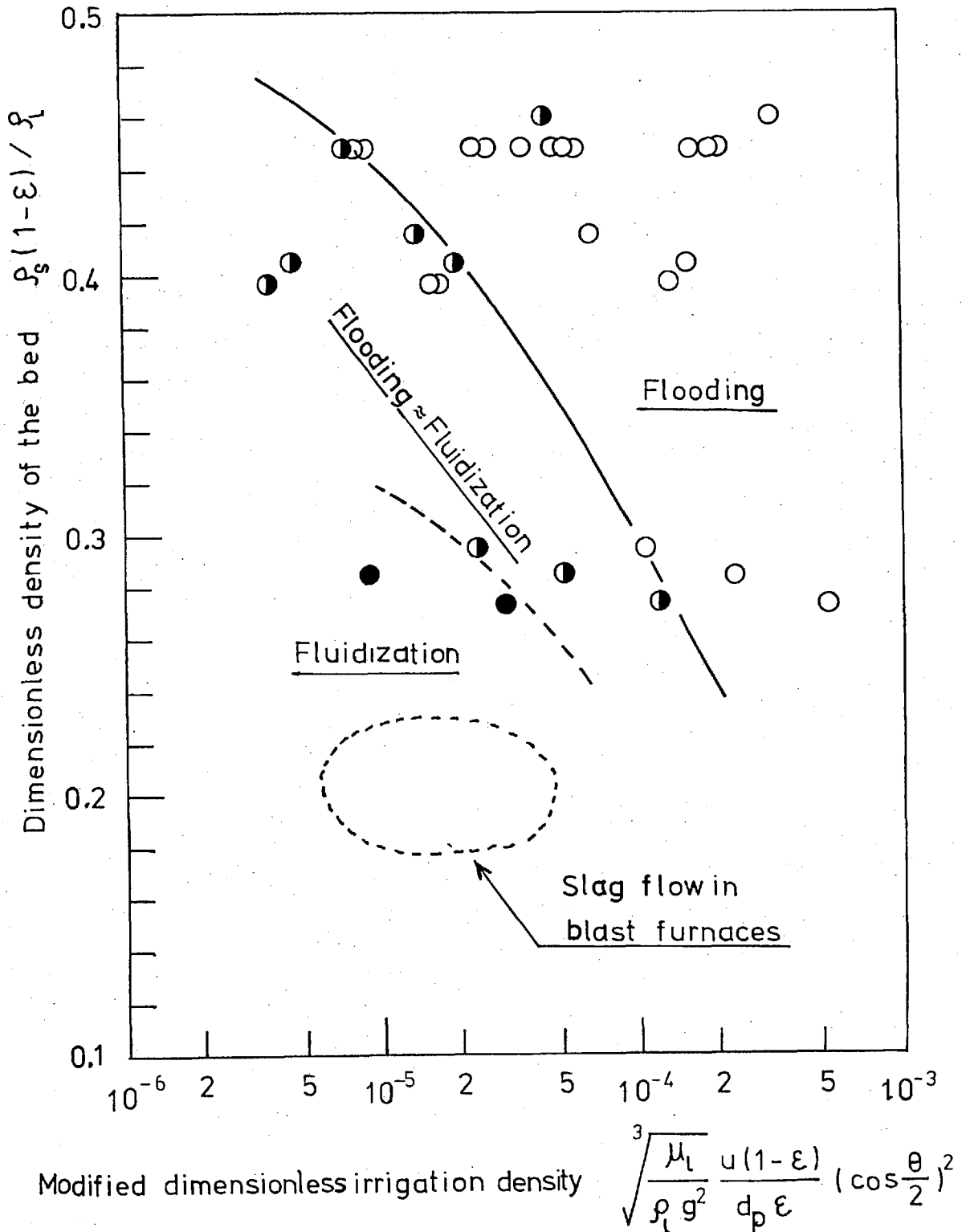


Fig. 6.18 Diagram showing the regions of bed instability. Experimental points: Normal flooding, \circ ; Fluidization together with flooding, \bullet ; Fluidization before onset of flooding \bullet .

approximation that both h_t and $\Delta P/gL\rho_\ell$ at flooding are functions only of the modified dimensionless irrigation density. Under this assumption, Eq. (6.23) becomes

$$\frac{\rho_s}{\rho_\ell} (1-\epsilon) = \frac{\Delta P}{gL\rho_\ell} - h_t = f \left(\begin{array}{l} \text{modified dimensionless} \\ \text{irrigation density} \end{array} \right) \quad \dots (6.24)$$

The left hand side of equation (6.24) may be termed the dimensionless density of the bed.

Fig. 6.18 shows the data plotted in terms of the two dimensionless parameters in Eq. (6.24). It can be seen from the Figure that the data show a consistent trend. Under the conditions corresponding to the bottom left region in the Figure, fluidization will occur before the onset of flooding. The estimated region for the slag flow in blast furnaces is also shown. Although more data will be needed to establish the precise boundaries of these regions, this figure indicates that the coke bed will start to fluidize before it is flooded by slag under the average flow conditions in the furnaces.

6.5 Liquid Distribution

Porter et al.⁽⁷³⁾, in their experimental work on the spreading of liquid in an irrigated column, have shown that the agreement between theory and experiment depends on the sampling area; better agreement was obtained with larger sampling area. From their results on 13mm - Raschig ring packings, they suggested that a sampling area of at least 0.04 m^2 is necessary to obtain reasonably reproducible results. The cross-sectional area of the present column is 0.007 m^2 which is, according to the above results, not large enough for detailed analyses on liquid distribution. The poor reproducibility of the liquid distributions for the wetting columns could be ascribed to

this small cross-sectional area. Therefore, no attempt was made to analyse the liquid distribution in relation to the distributor arrangement or size and height of the packing. It is possible, however, to discuss the distribution of liquid in the column under various flow conditions. A large number of experiments has reduced the uncertainty in the individual experiments and some interesting results have been obtained.

As mentioned in Sec. 5.3, a large influence of gas flow on the liquid distribution was found in the non-wetting systems. Fig. 6.19 shows the variation of the relative liquid flux to the outer annulus in relation to the dimensionless gas pressure drop of the irrigated bed, ΔP_w^* defined by Eq.(6.25).

$$\Delta P_w^* = \Delta P_w / L \quad g \quad \rho_l \quad (6.25)$$

This parameter was preferred to the actual gas velocity because the former represents the effect of gas on liquid flow better than the latter. It is worth noting that the maximum possible value of the liquid flux to the outer annulus is 2.0 since the outer annulus occupies half of the total cross-sectional area of the column. It is clear from Fig. 6.19 that the liquid flux to the outer annulus increased with ΔP_w^* at first. In the region where ΔP_w^* is greater than 0.3 the scatter in the liquid flux is too large to indicate any simple relationship with ΔP_w^* . The difference between wetting and non-wetting systems is remarkable. In non-wetting systems, the influence of gas flow was so strong that in most cases more than 80% of the liquid flowed to the outer half annulus when ΔP_w^* is 0.2; in the wetting system the change was significantly smaller.

It was mentioned in Chapter 5 that the influence of the liquid distribution on the measured hold-up and pressure drop was, if at all, very small compared with the experimental

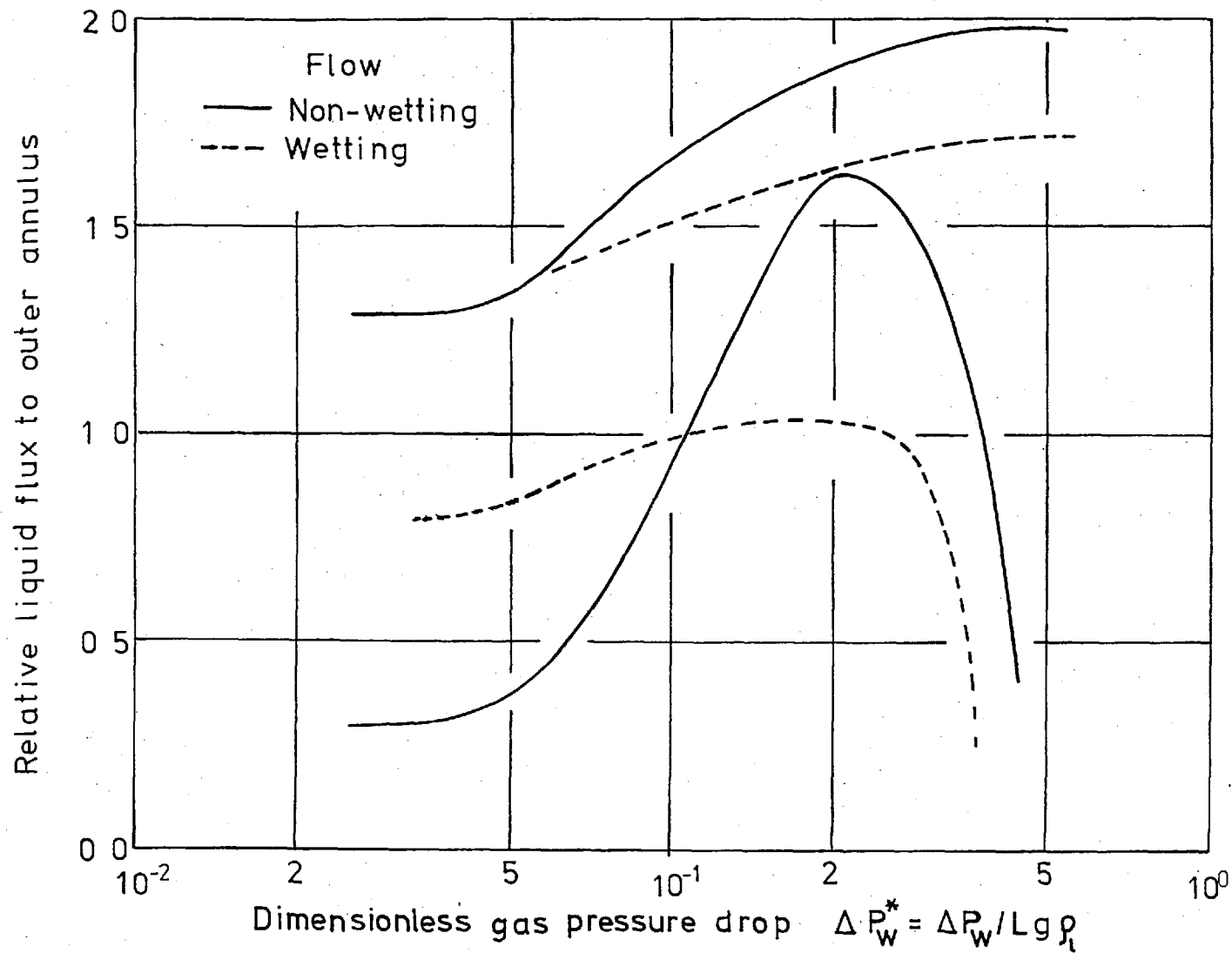


Fig. 6.19 Variation of relative liquid flux to outer annulus with dimensionless gas pressure drop ΔP_w^* . The curves show approximately upper and lower limit of all the measured data.

error. However, this does not necessarily mean that larger changes in liquid distribution do not influence the performance of the columns. It is possible that the remarkably similar change in the flow distribution with gas velocity affected the performance of the column so similarly that no significant differences were detected in the measured data. Further investigations would be required to assess the influence of the liquid distribution on the performance of the columns.

6.6 Possibility of the occurrence of the Flooding in the Blast Furnace

Since the proposed flooding diagram, based on the present experimental data, does not differ greatly from the correlation given by Mersmann⁽⁵²⁾ no significant change is anticipated in the discussions on the possibility of the occurrence of flooding, if the discussions are based on the data averaged over the cross-sectional area of the furnace.

The present study, however, leads to a picture different from that described by Elliott et al.⁽⁴⁾ when the flow conditions reach close to or exceed the flooding limit. They suggested that, in case this happened in the furnace locally, either or both metal and slag might be carried upwards by the gas and due to the lower temperature there the liquid would solidify in the voids of coke bed. This would reduce the permeability locally and the diverted gas stream, which would normally flow through that area, would force another region of the furnace to flood with further disruption of gas flow. The whole process would be unstable and, once started, would tend to build up.

From the results of present investigation the possible phenomena can be described differently as follows. From Fig. 6.18 it can be seen that the coke bed tends to fluidize before flooding would occur. The coke bed moves downwards

continuously, albeit slowly during the normal operation of the furnace. When the flow approaches the flooding conditions the coke-bed tends to be held and since the bed below it is moving downwards the void fraction of the bed would increase. The bed in such a case would be highly unstable and a small change in the balancing forces could cause the collapse of the loosely supported bed. The collapse, if large enough, could be detected as a slip and would be followed by a temporary channelling of the bed. The process is not necessarily 'unstable' according to Elliott's definition of the word since the loosening of the bed would counteract the tendency for flooding. It will be noted that this description of the process coincides well with the observations from the experimental blast furnace when attempts were made to initiate flooding⁽⁶⁷⁾. Evidently, the limiting conditions of the flow to prevent the occurrence of this phenomena are different from those for flooding and further studies are needed to quantify the conditions.

Since the coke bed cannot move upwards without pushing the whole stack upwards, the loosening of the bed would take time to develop. If the change in the flow conditions is rapid enough, flooding would occur as described by Elliott et al⁽⁴⁾. Since the furnace is operated under constant conditions, this rapid change is unlikely to occur in normal operations, however, the slip and channelling mentioned above could cause changes in flow conditions which would be rapid enough to start and propagate the flooding as described by Elliott et al.

The drastic change of the liquid flow distributions in non-wetting systems with the gas velocity suggests that the radial distribution of the liquids in the blast furnace can change significantly as they descend through the coke bed in the presence of the ascending gas stream. The change in the liquid distribution would be more complicated in the

region near the raceway since the gas flow there is not parallel to the liquid flow. Further studies of the liquid distribution under such circumstances are necessary to understand fully the real situation in the blast furnace since the occurrence of slip and channelling depends on the local conditions of flows of the liquid and gas.

CHAPTER 7

CONCLUSIONS

Irrigated packed columns were studied, with and without a counter-current flow of gas, at low liquid superficial velocities (0.02 - 1.0 mm/s) for different degrees of wetting between the liquids and packings. Seven packing materials and five liquids were used in the experiments to obtain a range of particle sizes (8-13mm), contact angles (0-114°), liquid densities (807-1920 kg/m³) and viscosities (0.0009-0.064 Ns/m²). The total hold-up, liquid distribution, gas pressure drop and flooding velocities were measured for various liquid and gas velocities.

(1) The measured total hold-up was related to the liquid velocity by the equation

$$h_t = h_s^* + b u^c$$

where b and c are constants. The values of the constants and the static hold-up, h_s^* , were determined by a least-square technique.

(2) The static hold-up for both non-wetting and wetting flows was correlated with the modified capillary number, $C_{pm} (= \rho g d_p^2 \phi^2 / (1-\xi)^2 \sigma (1+\cos\theta))$ by the equation

$$h_s^* = 1 / (0.205 + 0.00263 C_{pm})$$

Published measurements of the static hold-up for raschig ring packings confirm the validity of the correction term for the degree of wetting but a further correction for the shape factor would be necessary to obtain accurate predictions for ring packings using this equation.

(3) The measured dynamic hold-up, determined as the difference between h_t and h_s^* , were correlated by the equation

$$h_d = 605 \text{ Re}_m^{0.648} \text{ Ga}_m^{-0.485} \text{ C}_{ps}^{0.097} \text{ N}_c^{0.648}$$

The value of the dynamic hold-up estimated from this equation compared reasonably well with those measured by Gardner⁽²⁸⁾.

(4) The effect of the total hold-up on the ratio of the gas pressure drop through the irrigated bed to that through the dry bed at the same gas velocity depended on both the liquid and gas flow conditions and could not be predicted satisfactorily using existing correlations.

(5) The measured flooding velocities were correlated better by Mersmann's flooding diagram rather than the Sherwood diagram.

(6) The dimensionless irrigation density on the abscissa of Mersmann's diagram was multiplied by the factor, $(\cos \frac{\theta}{2})^2$, to take into account the degree of wetting and a modified correlation curve was proposed.

(7) A systematic effect of the gas flow on liquid flow distribution was observed; the relative liquid flux to the peripheral region of the bed increased with gas velocity until it reached a maximum after which the distribution became almost random. The changes in the liquid distribution with gas flow for non-wetting flows were remarkably larger than for the wetting flows.

(8) With reference to the instability of the bed the experiments are classified into three categories: those in which flooding occurred; those in which fluidization occurred; and those in which flooding and fluidization occurred together. The results were correlated in terms of the

dimensionless density of the bed and the modified dimensionless irrigation density and the boundaries of three regions were identified in the diagram. The diagram indicated that in blast furnaces the fluidization of the coke bed is likely to start before the onset of flooding by the slag.

(9) A new explanation for the malfunctioning of blast furnaces in relation to the instability of the bed was given. Disturbances in the smooth descent of the coke bed followed by the slip and temporary channelling would be more likely to occur than flooding.

APPENDIX I

METHOD FOR COMPUTING LIQUID FLOW RATES

I.1 Introduction

As shown in Fig.4.5, the weight change of each of six containers, 6, was measured by a pair of strain gauges, 3, fixed on the cantilever, 4,. The electrical signals from the strain gauges were measured and recorded by a data logger.

Fig. A1-1 shows typical examples of the change of the weight signal with time. Data A show a steady increase of weight with time whereas in Data B a rapid decrease of weight in the middle disrupts the overall tendency of increase. The disruption is caused by the draining of liquid from the container.

A computer program was written to process the data which include those obtained during the draining. The principle of the liquid flow computation is given in the following, together with a list of the program.

I.2 Principle of the Method

The weight signal increases linearly with time (except during the draining) and the rate of increase is proportional to the liquid flow rate. If the data during the draining are excluded, the relationship between the weight signal x and time t can be shown as:

$$x + \hat{x} = a + bt \quad (A1-1)$$

where

- a, b = constants
- \hat{x} = 0 before draining
- \hat{x} = x_0 after draining

The parameters a , b and x_0 can be determined by the method of least squares as follows. For a given set of data (x_i, t_i)

$$\begin{aligned} i &= 1 \text{ to } n, & \text{before draining} \\ i &= n+1 \text{ to } m, & \text{after draining} \end{aligned}$$

the sum E of the squared error is

$$E = \sum_{i=1}^n (a + bt_i - x_i)^2 + \sum_{i=n+1}^m (a + bt_i - x_i - x_0)^2 \quad (\text{A1-2})$$

By equating the partial differentials of E with respect to a , b and x_0 to zero and after rearrangement one can show that

$$a \cdot m + b \cdot \sum_{i=1}^m t_i - (m - n) x_0 = \sum_{i=1}^m x_i,$$

$$a \cdot \sum_{i=1}^m t_i + b \cdot \sum_{i=1}^m t_i^2 - x_0 \sum_{i=n+1}^m t_i = \sum_{i=1}^m t_i x_i,$$

$$a \cdot (m - n) + b \cdot \sum_{i=n+1}^m t_i - (m - n) x_0 = \sum_{i=n+1}^m x_i \quad (\text{A1-3})$$

Equations (A1-3) are solved for a , b and x_0 and the liquid flow rate can be calculated from the value of b .

I.3 Program and Calculated Results

A listing of the program, in the form of a subroutine is given in Table A1-1. It consists of two parts; in the first, the data are screened to identify the occurrence of draining and to eliminate those during the draining; in the second, the linear regression calculation is carried

Table A1-1 Listing of computer program for the calculation of liquid flow rate

```

00100 SUBROUTINE QFLOW(DATA,TIME,NO,TINT,SENS,D,IER,M,N,B)
00110C DATA: WEIGHT SIGNAL, NO: NUMBER OF DATA, TINT: TIME INTERVAL (1/S)
00120C SENS: SIGNAL SENSITIVITY (G/WEIGHT SIGNAL), Q: LIQUID FLOW RATE (G/S)
00130C THE CONTENT OF DATA MAY BE DESTROYED
00140 DIMENSION DATA(I),A(9),B(3),NORDR(3),TIME(I)
00150 M=0
00160 N=0
00170 IER=0
00190 IGO=1
00190C DATA SCREENING
00200 DO 100 I=2,NO
00210 GO TO(10,20,30,40),IGO
00220 10 IF(DATA(I)-DATA(I-1)).LT.-50.)GO TO 11
00230 M=M+1
00240 DATA(M)=DATA(I-1)
00250 TIME(M)=FLOAT(I-1)
00260 GO TO 100
00270 11 IF(M.GE.3)GO TO 12
00280 M=0
00290 IGO=4
00300 GO TO 100
00310 12 IGO=2
00320 N=M
00330 GO TO 100
00340 20 IF(DATA(I)-DATA(I-1)).LT.-10.)GO TO 100
00350 IGO=3
00360 GO TO 100
00370 30 IF(DATA(I)-DATA(I-1)).LT.-50.)GO TO 200
00380 M=M+1
00390 DATA(M)=DATA(I-1)
00400 TIME(M)=FLOAT(I-1)
00410 GO TO 100
00420 40 IF(DATA(I)-DATA(I-1)).LT.-50.)GO TO 100
00430 IGO=1
00440 100 CONTINUE
00450 200 IF(M.NE.3)GO TO 300
00460 M=N
00470 N=0
00480 300 IF(M.LT.4)GO TO 990
00490C CALCULATION OF COEFFICIENTS
00500 DO 310 I=1,3
00510 B(I)=0.
00520 DO 310 J=1,3
00530 K=I+3*(J-1)
00540 A(K)=0.
00550 310 CONTINUE
00560 A(1)=FLOAT(M)
00570 IF(N.NE.0)GO TO 320
00580 N1=3
00590 N2=4
00600 GO TO 330
00610 320 N1=4
00620 N2=5
00630 330 DO 340 I=1,M
00640 A(2)=A(2)+TIME(I)
00650 A(N2)=A(N2)+TIME(I)**2
00660 B(1)=B(1)+DATA(I)
00670 340 B(2)=B(2)+DATA(I)*TIME(I)
00680 A(N1)=A(2)
00690 IF(N.EQ.0)GO TO 400
00700 DO 350 I=N+1,M
00710 A(6)=A(6)+TIME(I)
00720 350 B(3)=B(3)+DATA(I)
00730 A(3)=FLOAT(M-N)
00740 A(7)=-A(3)
00750 A(8)=-A(6)
00760 A(9)=A(7)
00770 NO=3
00780 GO TO 500
00790 400 NO=2
00800C SOLVE SIMULTANEOUS EQUATION
00810 500 CALL ESIMQ(A,8,NO,IER,NORDR)
00820 IF(IER.NE.0)GO TO 990
00830 Q=B(2)*SENS/TINT
00840 RETURN
00850 990 IER=1
00860C UNABLE TO CALCULATE Q
00870 RETURN
00880 END

```

out according to Equation (A1-3).

It is clear from Fig. A1-1 that calculated regression lines are very satisfactory even when there is an intervening period of drainage of the liquid.

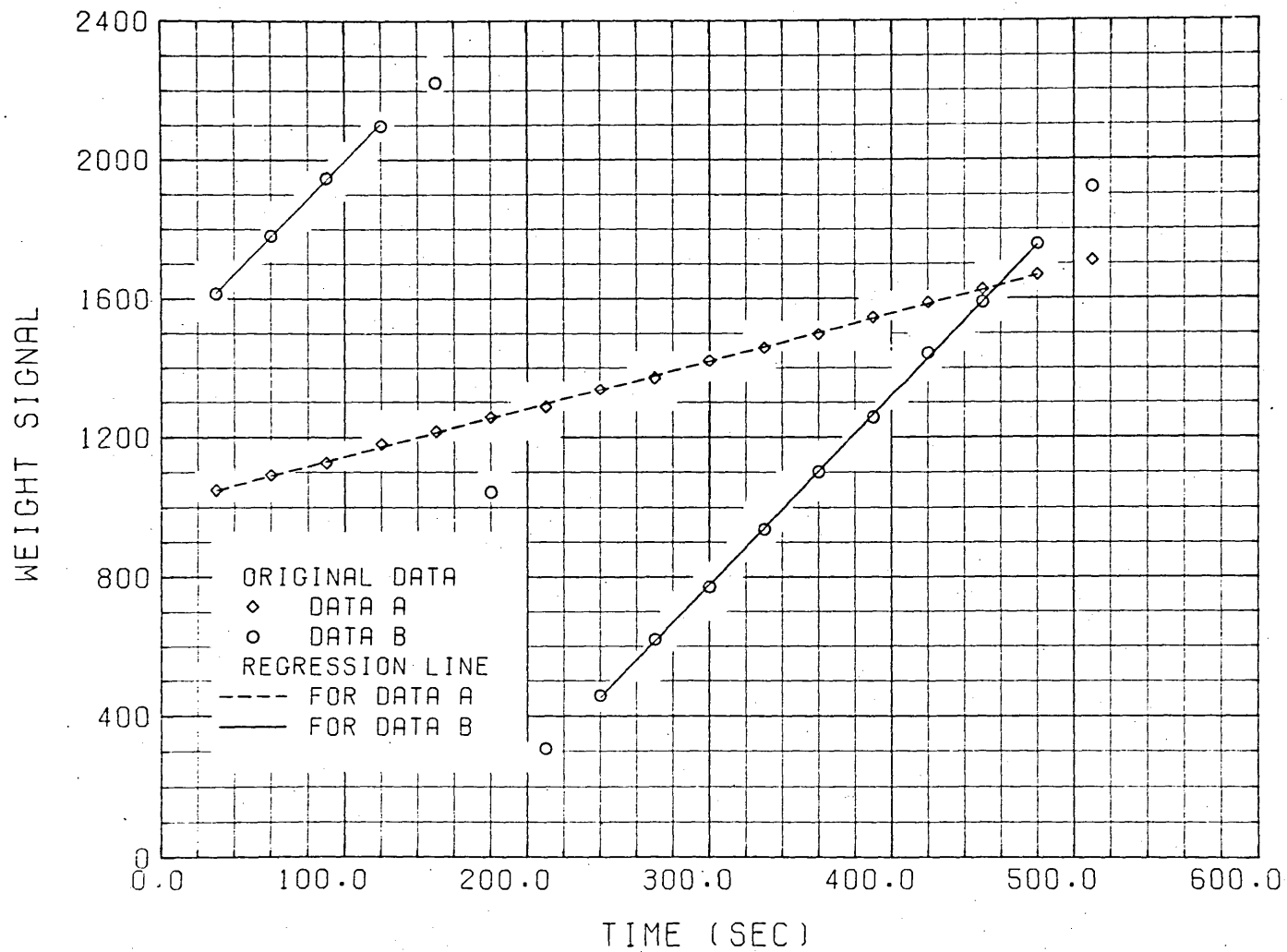


Fig. A1-1 Variation of the weight of the container with time in two typical cases.

APPENDIX II

GENERALIZED CURVE-FITTING

II.1. Introduction

A generalized curve-fitting method was applied to obtain the various calibration curves for processing the data. The principle of the method and the computer program will be described.

II.2. Parametric Interpolation⁽⁷⁴⁾

The whole curve is divided into segments and each segment is expressed mathematically by a third order polynomial. The four parameters that are needed to determine the third order polynomial are the values of y and y' ($= dy/dx$) at both ends of the segment.

For the i 'th segment, which represents the part of the curve between $x = x_i$ and $x = x_{i+1}$, the curve is given by the equation:

$$y_{i,i+1}(t) = y_i p_0(t) + y_{i+1} q_0(t) + y'_i d_i p_1(t) + y'_{i+1} d_i q_1(t) \quad (A2-1)$$

where subscripts i and $i+1$ show the positions corresponding to x_i and x_{i+1} and

$$\begin{aligned} d_i &= x_{i+1} - x_i & p_0(t) &= 1 - q_0(t) \\ t &= (x - x_i)/d_i & q_1(t) &= t^2(t - 1) \\ q_0(t) &= t^2(3 - 2t) & p_1(t) &= t(t - 1)^2 \end{aligned} \quad (A2-2)$$

II 3. Conditional Least-Square Method

Fig. A2-1 shows the physical model of the method proposed by Hosaka⁽⁷⁴⁾. The curve is represented by an elastic string, ℓ , to which is connected from each data point a spring whose length is assumed to be zero under no load. The whole system is in equilibrium when the sum, U of the elastic strain energies of both the string and springs, given by Equation (A2-3) has a minimum value.

$$U = \frac{k}{2} \left\{ \sum_j (y_j - \bar{y}_j)^2 + \lambda \int y''^2 dx \right\} \quad (\text{A2-3})$$

where \bar{y}_j is the ordinate of a data point
 y_j is the ordinate of the corresponding point on the string,
 k is the spring constant and
 λ is the strength of the string relative to that of spring

If one divides the whole curve into n segments, this curve is determined by $(n + 1)$ sets of (y_i, y'_i) at the intersections and at both ends of the curve. The elastic strain energy, U , will be minimum when

$$\partial U / \partial y_i = 0 \quad , \quad (\text{A2-4})$$

$$\partial U / \partial y'_i = 0 \quad . \quad (\text{A2-5})$$

Although it is possible to determine y_i 's and y'_i 's from Eqs.(A2-4) and (A2-5), the latter is substituted by Equation (A2-6) which stipulates that the curve be continuous up to the second order differential:

$$y''_{i-1,i} (1) = y''_{i,i+1} (0) \quad (\text{A2-6})$$

This condition makes the interpolated curve smoother.

From the above discussion it will be clear that this method of curve fitting is essentially a least-square method with the condition that the curve be expressed by connected segments of a third-order polynomial which are continuous up to the second-order differential at the points of connection and with the constraint that the curve is bent according to the value of the parameter λ .

II.4. Mathematical Formulation

Equation (A2-3) is rewritten as

$$U = \frac{k}{2} \left\{ \sum_i \sum_j (y_i^j)^2 + \lambda \sum_i \int_{x_i}^{x_{i+1}} +1 (y''_{i,i+1})^2 dx \right\} \quad (\text{A2-7})$$

where y_i^j is the value of y on the i 'th segment of the curve corresponding to the data point $(\bar{x}_i^j, \bar{y}_i^j)$ and expressed as:

$$y_i^j = y_i p_0(t_i^j) + y_{i+1} q_0(t_i^j) + y'_i d_i p_i(t_i^j) + y'_{i+1} d_i q_i(t_i^j) \quad \dots(\text{A2-8})$$

$$t_i^j = (\bar{x}_i^j - x_i)/d_i \quad (\text{A2-9})$$

By differentiating Equation (A2-1) with respect to x , one can get

$$y''_{i,i+1} = A_i t + B_i \quad (\text{A2-10})$$

where

$$A_i = 6(y'_i + y'_{i+1})/d_i - 12(y_{i+1} - y_i)/d_i^2 \quad (\text{A2-11})$$

$$B_i = 6(y_{i+1} - y_i)/d_i^2 - 4y'_i/d_i - 2y'_{i+1}/d_i \quad (\text{A2-12})$$

Then,

$$\int_{x_i}^{x_{i+1}} (y''_{i,i+1})^2 dx = d_i \int_0^1 (y_{i,i+1})^2 dt$$

$$= d_i (A_i^2/3 + A_i B_i + B_i^2) \quad (\text{A2-13})$$

It can be shown that in Equations (A2-7) and (A2-8), y_i and y'_i will appear only when i in the summation \sum_i equals either $i-1$ or i . Therefore, one can write, at the minimum value of U

$$\frac{\partial U}{\partial y_i} = \frac{k}{2} \frac{\partial}{\partial y_i} \left\{ \sum_j (y_{i+1}^j - \bar{y}_{i+1}^j)^2 + \sum_j (y_i^j - \bar{y}_i^j)^2 \right.$$

$$\left. + \lambda \int_{x_{i-1}}^{x_i} (y''_{i-1,i})^2 dx + \lambda \int_{x_i}^{x_{i+1}} (y''_{i,i+1})^2 dx \right\} = 0 \quad \dots(\text{A2-14})$$

Substitution for A_i and B_i from Equations (A2-11) and (A2-12) in Equation (A2-13) and using the resulting expression and Equation (A2-8) one can rewrite Equation (A2-13) as

$$\left\{ \sum_j P_o(t_{i-1}^j) q_o(t_{i-1}^j) - 12\lambda/d_{i-1}^3 \right\} y_{i-1}$$

$$+ \left\{ \sum_j q_o(t_{i-1}^j)^2 + \sum_j P_o(t_{i-1}^j)^2 + 12\lambda(1/d_{i-1}^3 + 1/d_i^3) \right\} y_i$$

$$+ \left\{ \sum_j p_o(t_i^j) q_o(t_i^j) - 12\lambda/d_i^3 \right\} y_{i+1}$$

$$+ \left\{ \sum_j d_{i-1} P_o(t_{i-1}^j) q_o(t_{i-1}^j) - 6\lambda/d_{i-1}^2 \right\} y'_{i-1}$$

$$+ \left\{ \sum_j d_{i-1} q_1(t_{i-1}^j) q_o(t_{i-1}^j) + \sum_j d_i P_i(t_i^j) P_o(t_i^j) - 6\lambda(1/d_{i-1}^2 - 1/d_i^2) \right\} y'_i$$

$$+ \left\{ \sum_j d_i P_o(t_i^j) q_o(t_i^j) + 6\lambda/d_i^2 \right\} y'_{i+1}$$

$$= \sum_j \bar{y}_{i-1}^j q_o(t_{i-1}^j) + \sum_j \bar{y}_i^j P_o(t_i^j) \quad (\text{A2-15})$$

It is clear from Equation (A2-10) that Equation (A2-6) is satisfied when

$$A_{i-1} = B_i, \quad (\text{A2-16})$$

which, using Equations (A2-11) and (A2-12), can be written as

$$\begin{aligned} & 6 \frac{y_{i-1}}{d_{i-1}^2} - 6 \left(\frac{1}{d_{i-1}^2} - \frac{1}{d_i^2} \right) y_i - 6 \frac{y_{i+1}}{d_i^2} \\ & + 2 \frac{y_{i-1}}{d_{i-1}} + 4 \left(\frac{1}{d_{i-1}} + \frac{1}{d_i} \right) y'_i + 2 \frac{y_{i+1}}{d_i} = 0 \quad (\text{A2-17}) \end{aligned}$$

Equations (A2-15) and (A2-17) provide $2(n+1)$ linear equation in y_i 's and y'_i 's and can be solved simultaneously for y_i 's and y'_i 's.

II.5. Computer Program

Two subprograms were written:

"SMR" to obtain parameters, y_i , y'_i and
 "YQ" to obtain y and y' from the fitted curve for a given x value.

Tables A2-1 and A2-2 show the form of calling "SMR" and "YQ" respectively. Table A2-3 shows listings of the programs "SMR" and "YQ" as well as associated ones used in either program.

TABLE A2-1 - Calling form of subroutine SMR

CALL SMR(XD,AD,X,ND,NX,RAMDA,IZ,A,B,DL,K,KK,IF,NF,XF,IER,NORDR)

<u>Variable</u>	<u>Size</u>	<u>Input/ Output</u>	<u>Explanation</u>
XD	ND	I	Data for x_j (independent)
AD	ND	I	Data for y_j (dependent)
X	NX	*I/O	x at the boundary of segments
ND	--	I	Number of data points
NX	--	I	Number of segments + 1
RAMDA	--	I	Smoothing factor (λ) ≥ 0.0
IZ	--	**	(see the footnote)
NF	--	I	Number of fixed points
IF	(+)	I	Position of fixed points
XF	(+)	I	Data of fixed points
A	(2*NX)	O	y and y' values
B	((2*NX)**2)	}	Working vectors
DL	(NX)		
K	(NX)		
KK	(NX)		
NORDR	(2*NX)		
IER	--	O	ERROR indicator

+ : as many as necessary

* : when IZ = 2, X must be given, otherwise it will be determined by the programme

** : parameter IZ determines the method of choosing X.

IZ = 1 : every data point is taken as X, thus NX=ND.

IZ = 2 : X is assumed to have been given outside the programme

IZ = 3 : X is determined by data points, evenly spaced

TABLE A2-2 - Calling form of subroutine YQ

CALL YQ(X,A,NX,XD,YD,YDD,IER)

<u>Variable</u>	<u>Size</u>	<u>Input/output</u>	<u>Explanation</u>
X	NX	I	} as for SMR
A	2*NX	I	
NX	--	I	
XD	--	I	value of x where y is needed
YD	--	O	value of y at given x
YDD	--	O	value of dy/dx at given x
IER	--	O	ERROR indicator, = 0 when normal; = 9 when XD is outside the range of X.

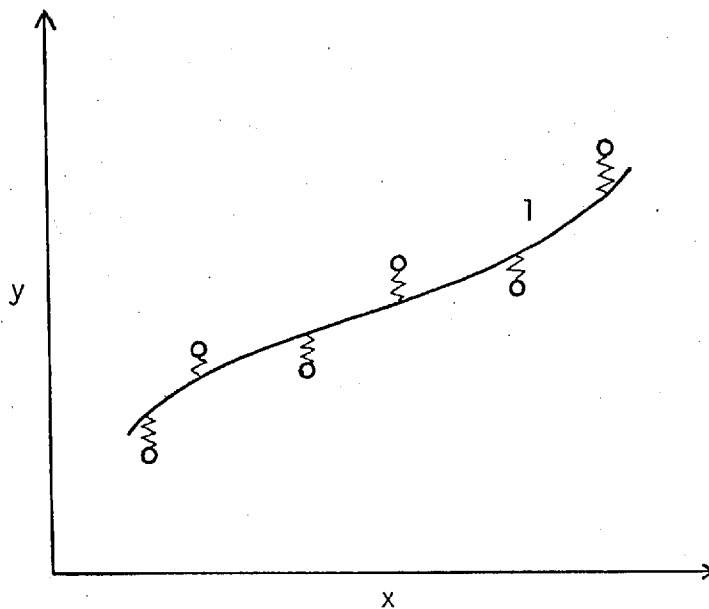


Fig. A2-1 Physical model of generalized curve fitting; hypothetical springs are connected from data points (O) to the elastic string l

Table A2-3 Listings of computer programs for generalized curve fitting

```

00100 SUBROUTINE NMR(XD,AD,X,NO,NX,ROO,IZ,A,B,DL,K,KK,IF,NF,XF,IER,
00110 *NOROR)
0115C GENERALIZED CURVE-FITTING PROGRAM
00120 DIMENSION X0(1),AD(1),X(9),A(1),B(1),DL(1),K(1),KK(1),IF(1)
00130 *XF(1),NOROR(1)
00140 NXX=NX*2
00150 NXX2=NXX*NXX
00160 DO 11 I=1,NXX2
00170 11 B(I)=0.
00180 DO 10 I=2,NO
00190 YOBIX=X0(I)
00200 YOBIX=AD(I)
00210 11=1-1
00220 DO 20 11=1,11
00230 11=11-1
00240 12=1-11
00250 IF(X0(12)-YOBIX)30,30,20
00260 30 IF(11-1)10,10,40
00270 20 CONTINUE
00280 11=1-1
00290 40 DO 50 J=1,111
00300 J1=[-J*]
00310 J2=J1-1
00320 XD(J1)=XD(J2)
00330 AD(J1)=AD(J2)
00340 50 CONTINUE
00350 J1=J1-1
00360 XD(J1)=YOBIX
00370 AD(J1)=YOBIX
00380 10 CONTINUE
00390 NX1=NX-1
00400C IZ=1(X'S=X0'S),=2(X'S ARE GIVEN),=3(EQUAL INCREMENT)
00410 IF(IZ-2)60,90,70
00420 60 COX=(XD(NO)-X0(1))/10000.
00430 INX=1
00440 X(1)=X0(1)
00450 DO 100 I=2,NO
00460 IF((X0(I))-X(INX))LT.OOX)GO TO 101
00470 INX=INX+1
00480 X(INX)=X0(I)
00490 GO TO 100
00500 101 IF(1.NE.NO)GO TO 100
00510 X(INX)=X0(I)
00520 100 CONTINUE
00530 NX=INX
00540 NX1=INX-1
00550 NXX=NX*2
00560 NXX2=NXX*NXX
00570 GO TO 90
00580 70 DX=(XD(NO)-X0(1))/FLOAT(INX1)
00590 X(1)=X0(1)
00600 X(INX)=X0(NO)
00610 DO 80 I=2,NX1
00620 X(I)=X0(I)+FLOAT(I-1)*DX
00630 80 CONTINUE
00640 90 K(1)=0
00650 KK(1)=1
00660 DL(1)=X(2)-X(1)
00670 RAMOA=ROO*(X(NX)-X(1))**3
00680 DO 110 I=2,NX1
00690 K(I)=0
00700 KK(I)=0
00710 DL(I)=X(I+1)-X(I)
00720 110 CONTINUE
00730 IS=1
00740 DO 120 11=1,NX1
00750 DO 130 I=1S,NO
00760 IF(X0(I).GT.X(I+1))GO TO 140
00770 K(11)=K(11)+1
00780 130 IE=1
00790 140 KK(11+1)=KK(11)+K(11)
00800 120 15=1E+1
00810 DO 180 IR=1,NX
00820 IF(IR-1)90,190,200
00830 200 SX1=0.
00840 SX2=0.
00850 SX3=0.
00860 SX4=0.
00870 IM=IR-1
00880 JE=K(IM)
00890 IF(JE.LT.1)GO TO 211
00900 DO 210 J=1,JE
00910 SX1=SX1+PQ(1,IM,J,X0,X,DL,KK)*PQ(2,IM,J,X0,X,DL,KK)
00920 210 SX2=SX2+PQ(2,IM,J,X0,X,DL,KK)*PQ(3,IM,J,X0,X,DL,KK)=OL(IM)
00930 211 SX1=SX1-12.*RAMOA/OL(IM)**3
00940 SX2=SX2-6.*RAMOA/OL(IM)**2
00950 SX3=6./OL(IM)
00960 SX4=2./OL(IM)
00970 CALL NCOLW(N1,N2,N3,N4,IR,IM,NX)
00980 B(N1)=SX1
00990 B(N2)=SX2
01000 B(N3)=SX3
01010 B(N4)=SX4
01020 190 SX1=0.
01030 SX2=0.
01040 SX3=0.
01050 SX4=0.
01060 IM=IR
01070 JE=K(IM)
01080 IF(NX-IR)240,240,220
01090 220 IF(JE.LT.1)GO TO 221
01100 DO 230 J=1,JE
01110 SX1=SX1+PQ(1,IM,J,X0,X,DL,KK)**2
01120 230 SX2=SX2+PQ(1,IM,J,X0,X,DL,KK)*PQ(3,IM,J,X0,X,DL,KK)=OL(IM)
01130 221 SX1=SX1+12.*RAMOA/OL(IM)**3
01140 SX2=SX2+6.*RAMOA/OL(IM)**2
01150 SX3=6./OL(IM)**2
01160 SX4=4./OL(IM)
01170 240 IF(IR-1)260,260,250
01180 250 IM=IR-1
01190 JE=K(IM)
01200 IF(JE.LT.1)GO TO 271

```

Table A2-3 (continued)

```

01210 DO 270 J=1,JE
01220 SX1= SX1+PQ(2,IM,J,XD,X,DL, KK)##2
01230 270 SX2= SX2+PQ(2,IM,J,XD,X,DL, KK)##PQ(4,IM,J,XD,X,DL, KK)=DL(IM)
01240 271 SX1= SX1+12.*RAMOA/OL(IM)##3
01250 SX2= SX2-6.*RAMOA/OL(IM)##2
01260 SX3= SX3-6./OL(IM)##2
01270 SX4= SX4+4./OL(IM)
01280 250 CALL NCOLW(N1,N2,N3,N4,IR,IR,NX)
01290 B(N1)=SX1
01300 B(N2)=SX2
01310 B(N3)=SX3
01320 B(N4)=SX4
01330 IF(NX.LE. IR)GO TO 290
01340 SX1=0.
01350 SX2=0.
01360 SX3=0.
01370 SX4=0.
01380 IM=IR
01390 JE=K(IM)
01400 IF(JE.LT. I)GO TO 301
01410 DO 300 J=1,JE
01420 SX1= SX1+PQ(1,IM,J,XD,X,DL, KK)##PQ(2,IM,J,XD,X,DL, KK)
01430 300 SX2= SX2+PQ(1,IM,J,XD,X,DL, KK)##PQ(4,IM,J,XD,X,DL, KK)=DL(IM)
01440 301 SX1= SX1-12.*RAMOA/OL(IM)##3
01450 SX2= SX2+6.*RAMOA/OL(IM)##2
01460 SX3= -6./OL(IM)##2
01470 SX4= 2./OL(IM)
01480 CALL NCOLW(N1,N2,N3,N4,IR,IR+1,NX)
01490 B(N1)=SX1
01500 B(N2)=SX2
01510 B(N3)=SX3
01520 B(N4)=SX4
01530 290 SX1=0.
01540 SX2=0.
01550 IF(1R-1)330,330,310
01560 310 IM=IR-1
01570 JE=K(IM)
01580 IF(JE.LT. I)GO TO 330
01590 DO 320 J=1,JE
01600 IN=KK(IM)+J-1
01610 320 SX1= SX1+AQ(IN)##PQ(2,IM,J,XD,X,DL, KK)
01620 330 IF(NX-IR)340,340,350
01630 350 IM=IR
01640 JE=K(IM)
01650 IF(JE.LT. I)GO TO 340
01660 DO 360 J=1,JE
01670 IN=KK(IM)+J-1
01680 360 SX1= SX1+AQ(IN)##PQ(1,IM,J,XD,X,DL, KK)
01690 340 A(IR)=SX1
01700 IRI=IR+NX
01710 A(IRI)=SX2
01720 180 CONTINUE
01730 IF(NF.LE. 0)GO TO 370
01740 DO 400 J=1,NXX
01750 DO 400 I=1,NF
01760 IFS=IF(I)

```

```

01770 NB=J+NXX=(IFS-1)
01780 400 A(J)=A(J)-XF(I)##B(NB)
01790 NXX=NXX-NXX
01800 JX=0
01810 DO 410 J=1,NXXX
01820 IC=(J-1)/NXX+1
01830 IR=J-(IC-1)##NXX
01840 DO 420 I=1,NF
01850 IF(IC.EQ. IF(I))GO TO 410
01860 420 IF(IR.EQ. IF(I))GO TO 410
01870 JX=JX+1
01880 B(JX)=B(J)
01890 410 CONTINUE
01900 JX=0
01910 DO 470 J=1,NXX
01920 DO 480 I=1,NF
01930 480 IF(J.EQ. IF(I))GO TO 470
01940 JX=JX+1
01950 A(JX)=A(J)
01960 470 CONTINUE
01970 NXX=NXX-NF
01980 370 CALL ESIMQ(B,A,NXX,IER,NORDR)
01990 IF(NF.LE. 0)GO TO 550
02000 NX2=2*NX
02010 JX=NXX
02020 DO 510 I=1,NX2
02030 J=NX2-I+1
02040 DO 540 IJJ=J
02050 IJ=IJJ
02060 540 IF(J.EQ. IF(IJ))GO TO 530
02070 A(IJ)=A(IJX)
02080 JX=JX-1
02090 GO TO 510
02100 530 A(IJ)=XF(IJ)
02110 510 CONTINUE
02120 550 RETURN
02130 END

```

```

02140 FUNCTION PQ(K,I,J,XD,X,DL, KK)
02150 DIMENSION XO(I),X(I),DL(I),KK(I)
02160 ND=KK(I)+J-1
02170 T=(XD(ND)-X(I))/DL(I)
02180 GO TO (1,2,3,4),K
02190 1 PQ=1.-T##T##(3.-2.*T)
02200 GO TO 10
02210 2 PQ=T##T##(3.-2.*T)
02220 GO TO 10
02230 3 PQ=T##T-I.##2
02240 GO TO 10
02250 4 PQ=T##T-(T-1).1
02260 10 RETURN
02270 END

```

Table A2-3 (continued)

```

02280 SUBROUTINE NCOLW(N1,N2,N3,N4,I,J,N)
02290 N1=2*(J-1)*N+1
02300 N2=2*(N+J-1)*N+1
02310 N3=2*(J-1)*N+I+N
02320 N4=2*(N+J-1)*N+I+N
02330 RETURN
02340 END

```

```

00100 SUBROUTINE ESIMQ(A,B,N,KS,NORDR)
0105C TO SOLVE LINEAR SIMULTANEOUS EQUATIONS
0106C BY ELIMINATION METHOD
00110 DIMENSION A(1),B(1),NORDR(1)
00120 DO 10 J=1,N
00130 10 NORDR(J)=J
00140 TOL=0.
00150 KS=0
155 IF(N.EQ.1)GO TO 200
00160 JJ=-N
00170 DO 65 J=1,N
00180 JY=J+1
00190 JJ=JJ+N+1
00200 BIGA=0.
00210 IT=JJ-J
00220 DO 30 ICOL=J,N
00230 DO 30 IROW=J,N
00240 ICR=ICOL+N*(IROW-1)
00250 IF(ABS(BIGA).GE.ABS(A(ICR))) GO TO 30
00260 BIGA=A(ICR)
00270 IMAX=ICOL
00280 MAXIR=IROW
00290 30 CONTINUE
00300 IF(ABS(BIGA).GT.TOL)GO TO 40
00310 KS=1
00320 RETURN
00330 40 IR1=N*(J-1)
00340 IR2=N*(MAXIR-1)
00350 DO 130 KR=1,N
00360 IR1=1+IR1
00370 IR2=1+IR2
00380 SAVE=A(IR1)
00390 A(IR1)=A(IR2)
00400 130 A(IR2)=SAVE
00410 ISAVE=NORDR(J)
00420 NORDR(J)=NORDR(MAXIR)
00430 NORDR(MAXIR)=ISAVE
00440 I1=J+N*(J-2)
00450 IT=IMAX-J
00460 DO 50 K=J,N
00470 I1=I1+N
00480 I2=I1+IT
00490 SAVE=A(I1)
00500 A(I1)=A(I2)
00510 A(I2)=SAVE

```

```

00520 50 A(I1)=A(I1)/BIGA
00530 SAVE=B(IMAX)
00540 B(IMAX)=B(J)
00550 B(J)=SAVE/BIGA
00560 IF(J.EQ.N)GO TO 70
00570 IQS=N*(J-1)
00580 DO 65 IX=JY,N
00590 IXJ=IQS+IX
00600 IT=J-IX
00610 DO 60 JX=JY,N
00620 IXJX=N*(JX-1)+IX
00630 JJX=IXJX+IT
00640 60 A(IXJX)=A(IXJX)-A(IXJ)*A(JJX)
00650 65 B(IX)=B(IX)-B(J)*A(IXJ)
00660 70 NY=N-1
00670 IT=N*N
00680 DO 80 J=1,NY
00690 IA=IT-J
00700 IB=N-J
00710 IC=N
00720 DO 80 K=1,J
00730 B(IB)=B(IB)-A(IA)*B(IC)
00740 IA=IA-N
00750 90 IC=IC-1
00760 DO 100 J=1,N
00770 DO 110 KK=J,N
00780 K=KK
00790 IF(NORDR(K).EQ.J)GO TO 120
00800 110 CONTINUE
00810 K=K+1
00820 120 SAVE=B(J)
00830 B(J)=B(K)
00840 B(K)=SAVE
00850 100 NORDR(K)=NORDR(J)
00860 RETURN
864 200 B(1)=B(1)/A(1)
866 RETURN
00870 END

```

APPENDIX III

ITERATIVE METHOD FOR LEAST SQUARES

III.1 Introduction

In the course of the analysis of the experimental data, a least square method was applied to fit a nonlinear relation among the experimental data and calculated parameters. Because of the nonlinear nature of the equation to be fitted, an iterative method was applied instead of an ordinary linear regression method.

The principle of the iterative method (75) is explained below together with a computer program for the case in which a correlation between dynamic hold-up and dimensionless parameters was obtained.

III.2 Mathematical Formulation

The assumed relation between dynamic hold-up h_d , and dimensionless parameters Re , Ga , C_p , N_c was

$$h_d = a \cdot Re^b \cdot Ga^c \cdot C_p^d \cdot N_c^e \quad (6.12)$$

For the sake of convenience, Equation (6.12) is rewritten as

$$y = a \cdot k^b \cdot l^c \cdot m^d \cdot n^e \quad (A3-2)$$

The problem is to obtain the values of the constant, a , and powers, b , c , d , e for a given set of data $(\bar{y}_i, k_i, l_i, m_i, n_i)$ such that the sum, E , of the squares of the errors

$$E = \sum_i (\bar{y}_i - y_i)^2 \quad (A3-3)$$

will be minimum, where

$$y_i = a \cdot k_i^b \cdot l_i^c \cdot m_i^d \cdot n_i^e \quad (A3-4)$$

If reasonable approximate values can be assigned to a , b , c , d and e , then Equation (A3-2) can be expanded

In the form of Taylor series. Neglecting the terms of the second and higher order, one can write

$$\begin{aligned}
 y_i = y_i|_o &+ (a-a_o) \frac{\partial y_i}{\partial a} |_o + (b-b_o) \frac{\partial y_i}{\partial b} |_o \\
 &+ (c-c_o) \frac{\partial y_i}{\partial c} |_o + (d-d_o) \frac{\partial y_i}{\partial d} |_o + (e-e_o) \frac{\partial y_i}{\partial e} |_o \\
 &\dots\dots\dots (A3-5)
 \end{aligned}$$

where $|_o$ shows that the values are based on the estimates $a_o, b_o, c_o, d_o,$ and e_o .

After substituting for y_i from Equation (A3-5) into Equation (A3-3) one can see that the minimum value of E can be obtained by choosing the differences, $(a-a_o), (b-b_o), (c-c_o), (d-d_o)$ and $(e-e_o)$ such that

$$\frac{\partial E}{\partial(a-a_o)} = \frac{\partial E}{\partial(b-b_o)} = \frac{\partial E}{\partial(c-c_o)} = \frac{\partial E}{\partial(d-d_o)} = \frac{\partial E}{\partial(e-e_o)} = 0$$

..... (A3-6)

From Equations (A3-4), (A3-5), (A3-6) a linear simultaneous equation of the form

$$\begin{pmatrix} a_{11} & & a_{15} \\ & a_{21} & \\ & & a_{ij} \\ a_{51} & & a_{55} \end{pmatrix} \begin{pmatrix} x_1 \\ x_2 \\ \\ x_5 \end{pmatrix} = \begin{pmatrix} b_1 \\ \\ \\ b_5 \end{pmatrix} \tag{A3-7}$$

can be derived where,

$$\begin{aligned}
 a_{ij} &= \sum_k \frac{\partial y_i}{\partial x_k} |_o \cdot \frac{\partial y_i}{\partial x_j} |_o \\
 b_{ij} &= \sum_k (\bar{y}_i - y_i|_o) \cdot \frac{y_i}{x_k} |_o
 \end{aligned}$$

$$x_1 = a - a_0, \quad x_2 = b - b_0, \quad x_3 = c - c_0, \quad x_4 = d - d_0, \quad x_5 = e - e_0.$$

After solving Equation (A3-7) one can make a correction for a_0 , b_0 , c_0 , d_0 , e_0 , and repeat the procedure until the ratios of the variance of the errors of estimate to that of original data for subsequent iterations differ less than the prescribed value ($=10^{-15}$ in the present work).

III.3 Computer program

A listing of the computer program is given in Table A3-1. The main program which handles the input data and lists the results is excluded.

Note that in the program, h_d is represented by YD; Re , G_a , C_p , N_c by XD; and a to e by A0.

Table A3-1 Listing of computer programs for iterative method of least squares

```

00100 SUBROUTINE FFIT(XD,YD,ND,AD,N,DFITN,AIJ,A,B,NORDR,SNAME,NITR)
00110C LEAST SQUARE FIT BY ITERATIVE METHOD
00120C XD,YD : INPUT DATA
00130C ND : NUMBER OF DATA
00140C AQ : COEFFICIENTS TO BE DETERMINED
00150C N : NUMBER OF AOS
00160C DFITN : DEGREE OF FITNESS (=1.-STANDARD ERROR OF ESTIMATE /
00170C STANDARD DEVIATION OF YD)
00180C AIJ : PARTIAL DEFFERENTIALS
00190C A,B,NORDR : WORKING VECTOR OF MINIMUM SIZE OF (N*N),(N),(N)
00200C NITER : MAXIMUM NUMBER OF ITERATION / RETURN WITH ACTUAL
00210C NUMBER OF ITERATION
00220 EXTERNAL SNAME
00230 DIMENSION XO(4,90D),YO(11,AD(1),AIJ(1),A(1),B(1),NORDR(1),KID(1),JK(3)
00240 MAXITR=NITR
00250 CERROR=1.0E-15
00260 SY=0.
00270 DO 10 I=1,ND
00280 10 SY=SY+YD(I)
00290 AY=SY/FLOAT(ND)
00300 SY=0.
00310 DO 20 I=1,ND
00320 20 SY=SY+(YD(I)-AY)**2
00330 DO 100 I=1,MAXITR
00340 SB=0.
00350 DO 30 J=1,N
00360 DO 40 K=1,N
00370 (J=J+(K-1))*N
00380 40 A(IJ)=0.
00390 30 B(IJ)=0.
00400 DO 110 J=1,ND
00410 CALL SNAME(XO(1,J),YO(J),AD,AIJ,BIJ,N)
00420 CALL ARRANGE(N,AIJ,BIJ,A,B)
00430 110 SB=SB+BIJ**2
00440 CALL ESIMQ(A,B,N,IER,NORDR)
00450 DO 120 J=1,N
00460 120 A(IJ)=B(IJ)+A0(J)
00470 SBR=SB/SY
00480 IF(1.EQ.1160 TO 130
00490 NITR=I
00500 IF(ABS(SBR0-SBR).LE.CERROR)GO TO 200
00510 130 SBR0=SBR
00520 100 CONTINUE
00530 200 DFITN=1.-SQRT(SBR)
00540 RETURN
00550 END

```

```

00560 FUNCTION QFUNS(XD,AD,N)
00570C TO CALCULATE FITTED VALUE FOR A GIVEN XD
00580 DIMENSION AO(1),XD(1)
00590 QFUN=AD(1)
00600 DO 10 I=1,N-1
00610 10 QFUN=QFUN+XD(I)**AD(I+1)
00620 QFUNS=QFUN
00630 RETURN
00640 END

```

```

00650 SUBROUTINE FFUNS(XC,YD,AD,AIJ,BIJ,N)
00660C TO CALCULATE PARTIAL DIFFERENTIALS (AOS)
00670 DIMENSION XD(1),AO(1),AIJ(1)
00680 BIJ=YD-QFUNS(XD,AD,N)
00690 C=1.
00700 DO 10 I=1,N-1
00710 10 C=C+XD(I)**AD(I+1)
00720 AIJ(1)=C
00730 C=C+AO(1)
00740 DO 20 I=1,N-1
00750 20 AIJ(I+1)=C+ALOG(XD(I))
00760 RETURN
00770 END

```

```

00780 SUBROUTINE ARRANGE(N,AIJ,BIJ,A,B)
00790C TO CONSTRUCT MATRIX A AND VECTOR B FOR
00800C SIMULTANEDUS EQUATION A * X = B
00810 DIMENSION AIJ(1),B(1),A(N,N)
00820 DO 10 I=1,N
00830 10 B(I)=B(I)+AIJ(I)*BIJ
00840 DO 20 J=1,N
00850 20 A(I,J)=A(I,J)+AIJ(I)*A(J)
00860 10 CONTINUE
00870 RETURN
00880 END

```

***** EXAMPLE OF CALL TO FFIT IN MAIN PROGRAMME *****

```

00420 DO 250 I=1,5
00430 NITR=5
00440 CALL FFIT(XD,YD,ND,AD,5,DFITS,AIJ,A,B,NORDR,FFUNS,NITR)
00450 IITR=I
00460 IF(NITR.LT.5)GO TO 260
00470 PRINT 10D3,I,DFITN,AD(NNR+1)
00480 1003 FORMAT(1X,'ITERATION IN PROGRESS. I =',I2,'DFITN = ',
00490+*F8.3,' ,PDNER = ',F8.3)
00500 250 CONTINUE
00510 260 PRINT *,'END ITERATION'

```

APPENDIX IV

EXPERIMENTAL DATA

In this Appendix, a complete tabulation of the experimental data is given. The data for the experiments are compiled according to the combination of packing and liquid. Since the distributor arrangement (DIST), the effective bed height (HB), fractional voidage (EPS) and viscosity of liquid (VIS) varied for a given combination of packing and liquid, they are given at the beginning of each set of data. Each measurement, identified by a Run number, consists of the total hold-up, the superficial velocities of liquid and gas, the pressure drop of the gas and the liquid distribution in terms of the relative liquid fluxes (defined by Eq. (5.2)) to three concentric annuli in the column cross-section.

Six-digit Run numbers are used for the first series of experiments and seven-digit Run numbers are used for the second series of experiments. The make-up of the Run numbers is described below.

First series of experiments: 6 digit numbers (e.g. 134311)

- | | | |
|---------------------------|---|--|
| The first two digits (13) | : | number indicating a particular column (except Runs 20~26 in which the same column was used). |
| The third digit (4) | : | Liquid flow range |
| The fourth digit (3) | : | Repeat measurement over the same liquid flow range. |
| The last two digits (11) | : | Number showing the chronological order of the measurements. |

Second series of experiments: 7 digit number (e.g. 1219101)

- The first two digits (12) : Number indicating a particular column.
- The third digit (1) : Particular series of measurements on the same column.
- The fourth digit (9) : Liquid flow range
- The fifth digit (1) : Repeat measurements over the same liquid flow range.
- The last two digits (01) : Number showing the sequence of measurements on the same liquid flow rate with different gas velocities. 01 indicates measurements without gas flow.

A particular series of measurements is referred to by its abridged Run number. Two digit Run numbers which correspond to the first two digits of the full Run number are used to refer to the first series of experiments. Three or more digit Run numbers, e.g. 110, 111 or 11172, are used for the second series of experiments. In this case Run 110 is used to identify the particular column while Run 111 and Run 11172 are used to identify the specific sets of data.

EXPERIMENTAL RESULTS FOR ■■ PL13/WATR ■■ SYSTEM

NO. 1

EXPERIMENTAL RESULTS FOR ■■ PL13/WATR ■■ SYSTEM

NO. 2

PACKING : PLASTIC SPHERES

AVERAGE SIZE = 13.2 (MM) . APPARENT DENSITY = 921. (KG/M3)

LIQUID : WATER

DENSITY = 1000. (KG/M3) . NOMINAL VISCOSITY = .0010 (NS/M2)

SURFACE TENSION = .0732 (N/M) . CONTACT ANGLE = 92.6 (DEG.)

RUN NO.	TOTAL HOLD-UP (PCT.)	LIQUID VELOCITY (MM/S)	GAS VELOCITY (M/S)	PRESSURE DROP (N/M3)	RELATIVE LIQUID FLUX		
					INNER (-)	MIDDLE (-)	OUTER (-)
*** RUN 13 *** . DIST = 19 . HB = .230 . EPS = .4106 . VIS = .00085							
134311	2.490	.1560	0	0	.952	.959	1.048
137312	3.122	.8986	0	0	1.122	.901	1.026
138313	3.459	1.4069	0	0	1.114	.820	1.079
135314	2.608	.3212	0	0	1.007	.959	1.029
136315	2.755	.5526	0	0	1.045	.934	1.032
134416	2.432	.1833	0	0	.997	.949	1.039
135417	2.549	.3234	0	0	1.010	.958	1.029
136418	2.755	.5578	0	0	1.095	.904	1.034
137419	3.004	.9044	0	0	1.036	.907	1.051
138420	3.371	1.4051	0	0	1.119	.913	1.020
138521	3.365	1.3776	0	0	1.030	.897	1.060
137522	2.960	.8740	0	0	1.024	.878	1.074
135523	2.558	.3342	0	0	1.007	.893	1.070
136524	2.711	.5646	0	0	.971	.884	1.088
134525	2.403	.1812	0	0	1.011	.952	1.032
130126	2.241	.0156	0	0	1.057	.763	1.134
132127	2.417	.1175	0	0	1.021	.671	1.203
131128	2.329	.0629	0	0	.945	.787	1.156
130229	2.299	.0309	0	0	.713	.868	1.172
132230	2.446	.1159	0	0	.940	.787	1.158
131231	2.358	.0604	0	0	1.038	.789	1.124
131332	2.382	.0602	0	0	.959	.841	1.118
132333	2.417	.1173	0	0	1.079	.754	1.132
130334	2.314	.0312	0	0	.845	.858	1.145
*** RUN 15 *** . DIST = 19 . HB = .425 . EPS = .4106 . VIS = .00093							
152101	2.349	.0951	0	0	1.596	.814	.921
151102	2.293	.0453	0	0	1.569	.785	.949
150103	2.261	.0205	0	0	1.287	.901	.971
153104	2.453	.1799	0	0	1.441	.861	.945
150205	2.204	.0209	0	0	1.580	.628	1.042
152206	2.341	.0937	0	0	1.409	.668	1.075
153207	2.429	.1807	0	0	1.380	.852	.970
151208	2.269	.0459	0	0	1.522	.739	.994
151309	2.300	.0510	0	0	1.402	1.017	.861
153310	2.437	.1821	0	0	1.602	.835	.907
152311	2.365	.0943	0	0	1.575	.766	.939
150312	2.220	.0192	0	0	1.652	.745	.942
157113	3.043	.7927	0	0	1.287	.724	1.091
156114	2.771	.4521	0	0	1.247	.739	1.085
158115	3.427	1.3493	0	0	1.345	.747	1.047
155116	2.571	.2592	0	0	1.369	.695	1.071
155217	2.571	.2530	0	0	1.297	.708	1.087
158218	3.451	1.3345	0	0	1.271	.786	1.041
156219	2.755	.5019	0	0	1.263	.712	1.096

RUN NO.	TOTAL HOLD-UP (PCT.)	LIQUID VELOCITY (MM/S)	GAS VELOCITY (M/S)	PRESSURE DROP (N/M3)	RELATIVE LIQUID FLUX		
					INNER (-)	MIDDLE (-)	OUTER (-)
*** RUN 17 *** . DIST = 19 . HB = .625 . EPS = .4156 . VIS = .00035							
157220	3.035	.8683	0	0	1.209	.768	1.080
158321	3.395	1.3019	0	0	1.275	.758	1.069
155322	2.547	.2587	0	0	1.311	.817	1.015
154123	2.395	.1003	0	0	1.382	.577	1.079
156324	2.763	.4974	0	0	1.268	.712	1.095
157325	3.019	.8378	0	0	1.265	.709	1.098
*** RUN 17 *** . DIST = 19 . HB = .625 . EPS = .4156 . VIS = .00035							
178101	3.588	1.3397	0	0	1.264	.625	1.150
174102	2.642	.1520	0	0	1.276	.828	1.020
177103	3.238	.8056	0	0	1.246	.710	1.109
175104	2.782	.2789	0	0	1.251	.742	1.082
176105	2.945	.4879	0	0	1.089	.776	1.117
178206	3.577	1.3674	0	0	1.103	.650	1.189
176207	2.967	.5071	0	0	.979	.831	1.120
174208	2.665	.1502	0	0	.777	.821	1.130
177209	3.258	.8429	0	0	1.153	.772	1.033
175210	2.771	.2766	0	0	1.159	.835	1.052
175311	2.766	.2670	0	0	.866	.935	1.054
178312	3.559	1.3183	0	0	1.182	.709	1.125
174313	2.635	.1463	0	0	1.109	.876	1.046
177314	3.216	.8582	0	0	.916	.789	1.186
176315	2.972	.5109	0	0	1.124	.814	1.080
170116	2.468	.0256	0	0	.946	1.025	1.077
172116	2.597	.1009	0	0	1.084	.675	1.071
171118	2.541	.0508	0	0	1.213	.909	1.063
171219	2.507	.0502	0	0	1.139	.806	1.079
170220	2.444	.0254	0	0	.974	.690	1.089
172221	2.575	.0986	0	0	1.028	.712	1.051
172322	2.590	.0996	0	0	.874	.636	1.048
170323	2.439	.0207	0	0	1.010	.692	1.069
171324	2.495	.0500	0	0	1.199	.828	1.045
*** RUN 22 *** . DIST = 19 . HB = .425 . EPS = .4011 . VIS = .00106							
224102	2.836	.1509	0	0	1.694	.659	.979
223103	2.756	.0740	0	0	1.353	.704	1.071
225104	2.956	.2663	0	0	1.351	.686	1.145
227105	3.434	.861	0	0	1.624	.556	1.072
228106	3.743	1.2588	0	0	1.580	.481	1.130
223207	2.707	.0741	0	0	1.325	.605	1.018
225208	2.946	.2582	0	0	1.533	.684	1.023
227209	3.427	.8179	0	0	1.395	.630	1.164
225210	3.138	.4751	0	0	1.499	.569	1.114
224211	2.849	.1444	0	0	1.808	.610	.977
228212	3.723	1.2593	0	0	1.441	.419	1.218
227313	3.394	.8186	0	0	1.694	.502	1.118
223314	2.733	.0730	0	0	1.465	.685	1.045
225315	2.929	.2727	0	0	1.323	.651	1.114
225316	3.138	.4842	0	0	1.531	.502	1.137
228317	3.730	1.2583	0	0	1.442	.444	1.202
224318	2.849	.1444	0	0	1.611	.594	.990
*** RUN 23 *** . DIST = 13 . HB = .425 . EPS = .4106 . VIS = .00108							
238101	3.451	.9097	0	0	2.352	.586	.809

EXPERIMENTAL RESULTS FOR ■■ PL13/WATR ■■ SYSTEM

NO. 3

EXPERIMENTAL RESULTS FOR ■■ PL13/WATR ■■ SYSTEM

NO. 4

RUN NO.	TOTAL HOLD-UP (PCT.)	LIQUID VELOCITY (MM/S)	GAS VELOCITY (M/S)	PRESSURE DROP (N/M3)	RELATIVE LIQUID FLUX		
					INNER (-)	MIDDLE (-)	OUTER (-)
237102	3.178	.5879	0	0	1.800	.716	.913
236103	2.922	.2708	0	0	1.861	.657	.930
234104	2.723	.0934	0	0	1.659	.768	.929
235105	2.803	.1871	0	0	1.665	.755	.935
238206	3.484	.9185	0	0	1.868	.506	1.021
236207	2.986	.3265	0	0	1.872	.660	.924
235208	2.833	.1816	0	0	2.129	.738	.790
237209	3.218	.5797	0	0	2.355	.573	.816
234210	2.737	.0820	0	0	2.126	.807	.748
*** RUN 24 *** . O1ST = 71 . HB = .425 . EPS = .4106 . VIS = .00109							
245101	2.737	.1081	0	0	1.999	.787	.803
248102	3.122	.5269	0	0	3.036	.444	.668
247103	2.949	.3160	0	0	2.703	.624	.568
246104	2.803	.1911	0	0	2.811	.660	.610
246205	2.910	.2046	0	0	2.703	.566	.704
248206	3.095	.5077	0	0	3.027	.569	.593
247207	2.922	.3223	0	0	2.404	.762	.682
245208	2.707	.1052	0	0	2.297	.648	.789
*** RUN 26 *** . O1ST = 7M . HB = .425 . EPS = .4106 . VIS = .00108							
258101	3.109	.5018	0	0	1.665	.591	1.036
256102	2.786	.1937	0	0	1.857	.957	.745
257103	2.933	.3258	0	0	1.749	.861	.841
255104	2.593	.1163	0	0	1.961	.945	.718
257205	2.952	.3241	0	0	1.857	.880	.793
255206	2.713	.1080	0	0	2.160	.830	.722
256207	2.796	.1936	0	0	2.010	.846	.763
259208	3.088	.5282	0	0	2.154	.760	.768
*** RUN 120 ***							
*** GAS PRESSURE DROP THROUGH DRY BED *** HB = .615 . EPS = .4054							
1200002	0	0	.515	315.7	0	0	0
1200003	0	0	.737	612.3	0	0	0
1200004	0	0	.984	1020.5	0	0	0
1200005	0	0	1.279	1620.1	0	0	0
1200006	0	0	1.616	2470.0	0	0	0
*** RUN 121 *** . O1ST = 19 . HB = .615 . EPS = .4054 . VIS = .00102							
1219101	3.920	1.3396	0	0	1.086	.705	1.160
1218101	3.573	.8089	0	0	1.021	.823	1.108
1217101	3.273	.4800	0	0	1.186	.988	.951
1216101	3.045	.2649	0	0	1.022	1.224	.950
1215101	2.976	.1197	0	0	1.125	1.361	.740
1214101	3.677	1.0017	0	0	1.160	.792	1.031
1214102	3.745	.9770	.430	389.1	1.224	.819	1.043
1214103	3.789	.9805	.558	720.8	.752	.455	1.427
1214104	4.007	.9718	.737	1467.0	.198	.149	1.902
1214105	4.544	1.0186	.795	1893.2	.288	.172	1.758
1214106	5.341	1.0292	.853	2532.2	.466	.233	1.560
1214107	6.743	.9958	.906	3331.1	.750	.259	1.549
1213201	3.885	1.2885	0	0	1.057	.771	1.129
1218201	3.527	.8006	0	0	1.055	.848	1.082
1217201	3.189	.4941	0	0	1.010	.945	1.037
1216201	3.032	.2810	0	0	.889	1.117	.971

RUN NO.	TOTAL HOLD-UP (PCT.)	LIQUID VELOCITY (MM/S)	GAS VELOCITY (M/S)	PRESSURE DROP (N/M3)	RELATIVE LIQUID FLUX		
					INNER (-)	MIDDLE (-)	OUTER (-)
1215201	2.837	.1457	0	0	.816	1.242	.918
1215202	2.896	.1241	.457	379.5	.911	1.004	1.035
1215203	2.837	.0752	.673	845.1	.926	.718	1.205
1215204	2.899	.0692	.799	1302.8	.338	.462	1.563
1215205	3.268	.0745	.923	1859.3	.159	.124	1.833
1215206	4.087	.0717	.993	2412.6	.712	.419	1.361
1215207	5.375	.0634	1.048	3077.5	.724	.569	1.968
1215208	6.373	.0714	1.091	3602.2	.319	.412	1.500
1215209	8.767	.0531	1.191	4413.8	.841	.631	1.292
*** RUN 122 *** . O1ST = 71 . HB = .615 . EPS = .4054 . VIS = .00105							
1226101	2.917	.2305	0	0	1.652	1.151	.695
1227101	3.105	.3931	0	0	1.617	.952	.829
1228101	3.245	.6209	0	0	2.078	.319	.695
1229101	3.601	1.0158	0	0	1.825	.354	.758
1229102	3.748	.9907	.459	428.9	1.554	.878	.895
1229103	3.762	.9855	.597	784.5	1.319	.558	1.111
1229104	3.867	.9975	.737	1396.9	.190	.246	1.744
1229105	4.188	.9948	.798	1741.3	.336	.161	1.748
1229106	5.772	.9922	.862	2551.3	.510	.242	1.540
1229107	7.821	1.0089	.894	3351.8	.741	.243	1.351
1229201	3.197	.5193	0	0	1.811	1.042	.778
1228201	3.013	.3176	0	0	1.591	1.114	.757
1226201	2.786	.1002	0	0	1.591	1.166	.705
1227201	2.885	.1884	0	0	1.358	1.170	.782
1227202	2.915	.1867	.457	379.5	1.531	1.184	.715
1227203	2.905	.1859	.622	704.8	1.506	.981	.849
1227204	3.068	.1893	.793	1285.2	.673	.722	1.288
1227205	3.578	.1936	.922	1919.9	.394	.237	1.481
1227206	4.842	.1841	.986	2696.4	.534	.260	1.320
1227207	6.013	.1771	1.015	3214.7	.603	.389	1.321
1227208	7.291	.1852	1.052	3809.5	.591	.405	1.512
1227209	8.462	.1876	1.071	4203.3	.620	.314	1.565
*** RUN 123 *** . O1ST = 71 . HB = .615 . EPS = .4054 . VIS = .00103							
1237101	2.642	.0150	0	0	1.593	.741	.941
1238101	2.676	.0346	0	0	1.859	.892	.735
1239101	2.747	.0614	0	0	1.828	.943	.762
1239102	2.749	.0603	.457	352.4	1.030	1.015	.935
1239103	2.745	.0615	.623	651.8	1.814	.653	.927
1239104	2.749	.0618	.793	1168.8	.609	.817	1.252
1239105	2.986	.0614	.921	1723.7	.333	.406	1.539
1239106	5.306	.0604	1.048	3072.8	.511	.436	1.492
1239107	6.649	.0608	1.118	3804.7	.676	.558	1.391
1239108	7.629	.0646	1.132	4160.3	.425	.371	1.588
*** RUN 124 *** . O1ST = 13 . HB = .615 . EPS = .4054 . VIS = .00113							
1249101	3.615	.9489	0	0	1.162	.990	.958
1249201	3.576	.9200	0	0	.843	.975	1.075
1248201	3.303	.5193	0	0	.873	1.118	.976
1245201	2.802	.0874	0	0	1.123	.884	1.038
1246201	2.926	.1387	0	0	1.559	.908	.876
1247201	3.087	.3174	0	0	1.307	.710	1.083
1247202	3.133	.3149	.459	389.1	1.302	.731	1.071

EXPERIMENTAL RESULTS FOR ■■ PL13/WATR ■■ SYSTEM

NO. 5

EXPERIMENTAL RESULTS FOR ■■ PL13/WATR ■■ SYSTEM

NO. 6

RUN NO.	TOTAL	LIQUID	GAS	PRESSURE	RELATIVE LIQUID FLUX		
	HOLD-UP (PCT.)	VELOCITY (MM/S)	VELOCITY (M/S)	DROP (N/M3)	INNER (-)	MIDDLE (-)	OUTER (-)
1247203	3.199	.2669	.618	744.7	1.743	.807	.877
1247204	3.206	.3204	.624	743.1	1.209	.822	1.047
1247205	3.227	.3270	.738	1130.6	.816	.525	1.362
1247206	3.514	.3266	.858	1734.9	.291	.267	1.698
1247207	4.312	.3177	.917	2221.3	.555	.199	1.652
1247209	5.851	.3059	.984	3048.8	.701	.252	1.569
1247209	6.961	.3128	1.018	3581.4	.591	.305	1.573
1247210	8.443	.2723	1.044	4145.9	.807	.356	1.470

■■■ RUN190 ■■■

■■■ GAS PRESSURE DROP THROUGH DRY BED ■■ HB = .620 . EPS = .4106

1900001	0	0	.457	242.0	0	0	0
1900002	0	0	.618	414.4	0	0	0
1900003	0	0	.844	721.3	0	0	0
1900004	0	0	1.107	1164.2	0	0	0
1900005	0	0	1.440	1849.0	0	0	0
1900006	0	0	1.752	2560.8	0	0	0

■■■ RUN 191 ■■■ . DIST = 71 . HB = .620 . EPS = .4106 . VIS = .00104

1919101	3.353	.5181	0	0	2.184	.716	.785
1918101	3.096	.3181	0	0	2.186	.819	.721
1917101	3.028	.1850	0	0	2.244	.907	.647
1916101	2.875	.0936	0	0	1.552	1.227	.682
1917102	3.112	.1790	.452	336.9	1.177	1.190	.829
1917103	3.085	.1900	.452	335.3	.925	1.109	.965
1917104	3.101	.1709	.629	645.3	1.439	1.045	.832
1917105	3.210	.1745	.805	1097.7	.577	.946	1.182
1917106	3.510	.1639	1.001	1822.1	.116	.657	1.515
1917107	5.204	.1586	1.126	2771.2	.215	.702	1.455
1917108	5.960	.1658	1.185	3199.8	.188	.757	1.429
1917109	7.209	.1684	1.257	3842.0	.222	.958	1.294
1917110	8.186	.1390	1.277	4110.9	.085	.814	1.428

■■■ RUN 192 ■■■ . DIST = 71 . HB = .615 . EPS = .4054 . VIS = .00102

1927101	3.284	.3997	0	0	1.946	.839	.789
1926101	3.121	.2219	0	0	2.097	.842	.736
1925101	2.967	.1273	0	0	2.550	.807	.607
1924101	2.855	.0510	0	0	2.092	1.149	.550
1928101	3.397	.6764	0	0	2.088	.849	.734
1929101	3.757	1.0071	0	0	1.139	.995	.963
1929102	3.842	1.0499	.456	405.0	1.362	.968	.905
1929103	3.879	.9457	.522	760.6	.532	.812	1.279
1927201	3.165	.3896	0	0	1.550	.857	.904
1929201	3.599	1.0172	0	0	.960	.821	1.131
1929202	3.723	1.0034	.454	376.3	1.167	.939	.988
1929203	3.732	.9180	.629	725.5	.481	.520	1.477
1929204	3.759	.8610	.629	741.5	.553	.777	1.290
1929205	3.883	.9002	.804	1326.7	.211	.307	1.700
1929206	4.657	.8573	.918	1977.3	.068	.318	1.741
1929207	5.751	.8529	.980	2475.4	.023	.311	1.760
1929208	6.029	1.0546	.971	2519.4	.072	.300	1.751
1929209	6.513	1.0824	1.038	3144.5	.085	.434	1.653

■■■ RUN 193 ■■■ . DIST = 71 . HB = .615 . EPS = .4054 . VIS = .00102

1939101	2.880	.0655	0	0	2.300	.983	.582
---------	-------	-------	---	---	-------	------	------

RUN NO.	TOTAL	LIQUID	GAS	PRESSURE	RELATIVE LIQUID FLUX		
	HOLD-UP (PCT.)	VELOCITY (MM/S)	VELOCITY (M/S)	DROP (N/M3)	INNER (-)	MIDDLE (-)	OUTER (-)
1938101	2.848	.0354	0	0	1.973	1.018	.655
1937101	2.784	.0183	0	0	1.355	1.095	.819
1938102	2.965	.0359	.464	350.8	1.892	1.019	.700
1938103	2.869	.0360	.656	666.5	1.380	1.068	.836
1938104	2.876	.0347	.865	1135.3	.899	1.110	.972
1938105	3.319	.0322	1.071	1908.7	.035	.960	1.353
1938106	4.452	.0357	1.213	2737.9	.074	.959	1.316
1938107	5.953	.0316	1.336	3627.7	.321	.925	1.280
1938108	6.768	.0287	1.405	4058.2	.588	.743	1.309

■■■ RUN220 ■■■

■■■ GAS PRESSURE DROP THROUGH DRY BED ■■ HB = .425 . EPS = .4106

2200001	0	0	.464	244.6	0	0	0
2200002	0	0	.634	433.8	0	0	0
2200003	0	0	.856	754.5	0	0	0
2200004	0	0	1.154	1285.3	0	0	0
2200005	0	0	1.460	1977.5	0	0	0
2200006	0	0	1.782	2838.2	0	0	0

■■■ RUN 221 ■■■ . DIST = 71 . HB = .425 . EPS = .4106 . VIS = .00108

2219101	3.052	.4738	0	0	2.189	.885	.579
2218101	2.906	.3155	0	0	2.182	1.004	.614
2216101	2.573	.1004	0	0	2.304	1.237	.522
2217101	2.816	.1859	0	0	1.891	1.190	.590
2217102	2.932	.1927	.457	360.0	2.022	1.150	.571
2217103	3.059	.1843	.656	740.7	1.297	1.273	.737
2217104	3.245	.1856	.964	1412.2	.458	.309	1.516
2217105	3.640	.1767	1.005	1979.8	.140	.116	1.842
2217106	4.357	.1863	1.119	2697.4	.016	.047	1.926
2217107	5.280	.1821	1.252	3493.5	.001	.064	1.921
2217108	10.106	.1723	1.327	4935.7	.017	.059	1.918
2217109	6.828	.2020	1.288	4278.0	.015	.045	1.927

■■■ RUN 222 ■■■ . DIST = 71 . HB = .420 . EPS = .4029 . VIS = .00110

2228101	2.867	.0399	0	0	1.917	1.190	.583
2227101	2.816	.0168	0	0	1.597	1.283	.636
2229101	2.880	.0546	0	0	1.693	1.285	.601
2229102	2.981	.0548	.452	359.6	1.494	1.248	.591
2229103	2.994	.0532	.636	712.2	1.338	1.164	.574
2229104	3.139	.0549	.873	1433.6	1.141	.600	1.205
2229105	3.744	.0553	1.119	2568.4	.013	.149	1.863
2229106	4.083	.0881	1.326	3306.3	0	.762	1.491
2229107	5.985	.0545	1.387	4371.0	.015	.228	1.815
2229108	8.049	.0512	1.419	4829.6	0	.202	1.837

■■■ RUN 223 ■■■ . DIST = 71 . HB = .420 . EPS = .4029 . VIS = .00106

2238101	3.488	.5505	0	0	1.821	.961	.817
2237101	3.250	.3996	0	0	2.503	.771	.644
2236101	3.072	.2298	0	0	2.502	.960	.527
2239101	3.670	1.0097	0	0	2.251	.793	.715
2239102	4.006	1.0380	.457	406.3	2.857	.898	.446
2239103	4.140	1.0007	.630	852.2	.756	.883	1.160
2239104	4.278	.9855	.803	1482.7	.433	.351	1.598
2239105	6.056	1.0085	.950	2749.2	.071	.217	1.803
2239106	7.393	1.0254	1.002	3467.4	.028	.239	1.804

EXPERIMENTAL RESULTS FOR ** PL13/WATR ** SYSTEM

NO. 7

RUN NO.	TOTAL HOLD-UP (PCT.)	LIQUID VELOCITY (MM/S)	GAS VELOCITY (M/S)	PRESSURE DROP (N/M3)	RELATIVE LIQUID FLUX		
					INNER (-)	MIDDLE (-)	OUTER (-)
2239107	10.730	1.0047	1.043	4646.5	.286	.476	1.570
*** RUN 224 *** . DIST = 71 . HB = .420 . EPS = .4029 . VIS = .00109							
2249101	2.967	.0628	0	0	2.085	.927	.688
2248101	2.900	.0335	0	0	2.008	1.036	.645
2247101	2.860	.0178	0	0	2.121	.950	.660
2247102	2.927	.0178	.466	354.9	2.070	.935	.699
2247103	2.893	.0169	.625	637.4	2.256	1.082	.541
2247104	3.035	.0176	.869	1307.6	.463	1.137	1.098
2247105	4.194	.0183	1.153	2811.3	0	1.028	1.338
2247106	4.436	.0169	1.373	3714.9	0	.219	1.911
2247107	7.407	.0183	1.412	4896.3	.040	.894	1.393
2249102	7.854	.0545	1.370	4887.0	.008	.317	1.764
*** RUN 225 *** . DIST = 19 . HB = .420 . EPS = .4029 . VIS = .00108							
2259101	3.179	.1728	0	0	2.067	.774	.788
2259102	3.310	.1742	.458	361.9	2.106	.762	.783
2259103	3.330	.1730	.641	723.8	1.816	.710	.913
2259104	3.512	.1732	.871	1466.3	.568	.513	1.452
2259105	4.295	.1677	1.077	2535.7	.016	.202	1.830
2259106	5.189	.1726	1.215	3497.7	.008	.293	1.776

EXPERIMENTAL RESULTS FOR ** W13/WATR ** SYSTEM

NO. 1

PACKING : MAX-COATED SPHERES
 AVERAGE SIZE = 13.3 (MM) . APPARENT DENSITY = 921. (KG/M3)
 LIQUID : WATER
 DENSITY = 1000.(KG/M3) . NOMINAL VISCOSITY = .0010 (NS/M2)
 SURFACE TENSION = .0732 (N/M) . CONTACT ANGLE = 105.6 (DEG.)

RUN NO.	TOTAL HOLD-UP (PCT.)	LIQUID VELOCITY (MM/S)	GAS VELOCITY (M/S)	PRESSURE DROP (N/M3)	RELATIVE LIQUID FLUX		
					INNER (-)	MIDDLE (-)	OUTER (-)
*** RUN150 ***							
*** GAS PRESSURE DROP THROUGH DRY BED ** HB = .620 . EPS = .4105							
1500001	0	0	.580	368.5	0	0	0
1500002	0	0	.891	789.3	0	0	0
1500003	0	0	1.236	1418.8	0	0	0
1500004	0	0	1.533	2078.4	0	0	0
1500005	0	0	1.825	2858.2	0	0	0
*** RUN 151 *** . DIST = 71 . HB = .620 . EPS = .4106 . VIS = .00110							
1519101	1.956	.5025	0	0	.633	.948	1.162
1518101	1.855	.3083	0	0	.574	.891	1.121
1517101	1.785	.1824	0	0	.830	.865	1.214
1516101	1.691	.0987	0	0	.541	.846	1.221
1516102	2.015	.8988	.464	316.3	.494	.634	1.002
1516103	2.042	.013	.459	316.3	.422	.841	1.421
1517102	2.031	.828	.464	322.7	.416	.834	1.355
1518102	2.131	.3219	.464	329.0	.543	.785	1.252
1517103	2.225	.835	.623	577.3	.475	.513	1.483
1517104	2.099	.1794	.791	972.8	.284	.394	1.622
1517105	2.957	.1760	.978	1728.8	.354	.270	1.776
1517106	4.890	.1769	1.113	2756.9	.336	.523	1.625
1517107	6.604	.1766	1.208	3680.7	.329	.418	1.632
1517108	6.991	.1771	1.263	3935.3	.326	.505	1.540
1517201	1.889	.1849	0	0	.553	.834	1.235
1518201	1.974	.1180	0	0	.545	.314	1.178
1516201	1.823	.0991	0	0	.525	.879	1.208
1519201	2.119	.5170	0	0	.704	.925	1.152
*** RUN 152 *** . DIST = 71 . HB = .620 . EPS = .4106 . VIS = .00108							
1529101	2.302	.3389	0	0	.355	.753	1.204
1528101	2.094	.8299	0	0	.780	.884	1.152
1527101	1.949	.3881	0	0	.543	.873	1.205
1526101	1.821	.2302	0	0	.517	.878	1.210
1526102	2.051	.2312	.459	317.9	.429	.675	1.399
1529102	2.625	.9948	.462	344.8	.593	.725	1.312
1529103	2.709	.9932	.624	639.0	.473	.537	1.470
1529104	2.798	.9884	.793	1059.2	.178	.289	1.721
1529105	4.034	.9780	.986	2170.1	.016	.264	1.792
1529106	5.448	1.0508	1.049	2785.4	.017	.227	1.914
1529107	6.955	1.0988	1.103	3427.6	.021	.255	1.594
*** RUN 153 *** . DIST = 71 . HB = .620 . EPS = .4105 . VIS = .00109							
1539101	1.728	.0614	0	0	.570	.800	1.275
1538101	1.739	.0335	0	0	.552	.915	1.207
1537101	1.726	.0171	0	0	.615	.745	1.298
1539201	1.757	.0625	0	0	.631	.828	1.239
1539202	1.899	.0638	.459	310.0	.340	.575	1.492
1539203	1.969	.0624	.634	590.0	.307	.500	1.547

EXPERIMENTAL RESULTS FOR W13/WATR SYSTEM

NO. 2

EXPERIMENTAL RESULTS FOR W13/WATR SYSTEM

NO. 3

RUN NO.	TOTAL HOLD-UP (PCT.)	LIQUID VELOCITY (MM/S)	GAS VELOCITY (M/S)	PRESSURE DROP (N/M3)	RELATIVE LIQUID FLUX		
					INNER (-)	MIDDLE (-)	OUTER (-)
1539204	1.987	.0631	.802	960.1	.234	.298	1.697
1539205	2.281	.0621	.986	1572.2	.023	.244	1.801
1539206	4.840	.0631	1.205	3095.4	.078	.307	1.745
1539207	6.078	.0724	1.292	3777.2	.104	.639	1.532
1539208	6.651	.0635	1.365	4180.5	.270	.642	1.476

*** RUN 160 ***

GAS PRESSURE DROP THROUGH DRY BED					HB = .620	EPS = .4106
1600001	0	0	.462	240.4	0	0
1600002	0	0	.623	414.4	0	0
1600003	0	0	.791	634.3	0	0
1600004	0	0	1.053	1074.0	0	0
1600005	0	0	1.330	1635.5	0	0
1600006	0	0	1.720	2625.7	0	0

*** RUN 161 ***

GAS PRESSURE DROP THROUGH DRY BED					HB = .620	EPS = .4106	VIS = .00108
1619101	1.885	.5101	0	0	1.001	.798	1.131
1618101	1.723	.2954	0	0	.893	.807	1.161
1617101	1.653	.1897	0	0	.958	.876	1.096
1616101	1.575	.1018	0	0	.899	.966	1.060
1616102	1.769	.0991	.459	303.7	.764	.890	1.155
1617102	1.814	.1843	.457	305.3	.731	.869	1.178
1618102	1.899	.3146	.457	311.6	.839	.746	1.217
1619102	2.056	.5159	.457	317.9	.901	.675	1.241
1617103	1.903	.1821	.625	564.7	.687	.783	1.245
1617104	2.033	.1804	.796	950.6	.789	.717	1.252
1617105	2.431	.1793	1.004	1591.2	.076	.359	1.713
1617106	5.083	.1774	1.183	2980.0	.042	.404	1.697
1617107	6.433	.1778	1.298	3736.0	.274	.748	1.405
1618103	6.056	.3273	1.220	3468.7	.182	.447	1.623
1618201	1.903	.3138	0	0	.843	.826	1.167
1617201	1.716	.1791	0	0	.887	.881	1.117
1617301	1.692	.1529	0	0	.925	.901	1.092
1619301	1.944	.4987	0	0	1.041	.911	1.048
1618301	1.783	.2892	0	0	.990	.862	1.095

*** RUN 162 ***

GAS PRESSURE DROP THROUGH DRY BED					HB = .620	EPS = .4106	VIS = .00107
1629101	1.619	.0638	0	0	.882	.973	1.064
1628101	1.623	.0340	0	0	.835	1.138	.979
1627101	1.616	.0161	0	0	.723	1.006	1.090
1627102	1.801	.0171	.457	308.4	.792	.806	1.202
1627103	1.842	.0183	.624	559.9	.769	.770	1.224
1627104	1.935	.0171	.876	1165.7	.164	.537	1.581
1627105	2.818	.0171	1.112	2105.3	.039	.228	1.808
1627106	5.354	.0154	1.339	3598.4	.016	.398	1.705
1627107	5.956	.0268	1.444	3960.6	0	.007	1.968
1629102	5.234	.0638	1.293	3380.1	.036	.506	1.634
1629103	5.989	.0632	1.347	3798.2	.174	.471	1.611

*** RUN 163 ***

GAS PRESSURE DROP THROUGH DRY BED					HB = .620	EPS = .4106	VIS = .00105
1639201	2.323	1.2916	0	0	.489	.502	1.485
1639201	2.065	.8034	0	0	.435	.502	1.487
1637201	1.962	.4652	0	0	.467	.535	1.473
1636201	1.723	.2592	0	0	.479	.644	1.402

*** RUN 180 ***

RUN NO.	TOTAL HOLD-UP (PCT.)	LIQUID VELOCITY (MM/S)	GAS VELOCITY (M/S)	PRESSURE DROP (N/M3)	RELATIVE LIQUID FLUX		
					INNER (-)	MIDDLE (-)	OUTER (-)
1800001	0	0	.469	214.5	0	0	0
1800002	0	0	.676	413.7	0	0	0
1800003	0	0	.924	732.4	0	0	0
1800004	0	0	1.269	1281.0	0	0	0
1800005	0	0	1.562	1834.2	0	0	0
1800006	0	0	1.787	2312.2	0	0	0

*** RUN 181 ***

GAS PRESSURE DROP THROUGH DRY BED					HB = .640	EPS = .4301	VIS = .00107
1818101	1.888	.7651	0	0	.664	.580	1.379
1819101	2.137	1.2382	0	0	.690	.543	1.393
1817101	1.700	.4342	0	0	.681	.571	1.378
1816101	1.566	.2133	0	0	.697	.614	1.381

*** RUN 182 ***

GAS PRESSURE DROP THROUGH DRY BED					HB = .635	EPS = .4253	VIS = .00100
1828101	1.700	.3215	0	0	1.503	.969	.857
1829101	1.807	.5241	0	0	1.450	.894	.921
1828102	1.845	.3296	.462	274.9	1.223	1.132	.849
1828103	1.960	.3275	.691	611.6	.547	.886	1.229
1828104	2.089	.3256	.922	1147.5	.109	.427	1.650
1828105	3.010	.3243	1.111	1901.1	.005	.187	1.843
1828106	3.903	.3243	1.181	2333.5	.004	.119	1.886
1827201	1.658	1.141	0	0	1.528	1.074	.783
1829201	1.903	.4965	0	0	1.331	.963	.918
1826201	1.569	.0429	0	0	1.708	1.073	.724

*** RUN 183 ***

GAS PRESSURE DROP THROUGH DRY BED					HB = .635	EPS = .4253	VIS = .00101
1834101	1.594	.0040	0	0	.397	.690	1.393
1835101	1.620	.0892	0	0	.620	.821	1.246
1837101	1.825	.4375	0	0	.747	.707	1.273
1838101	2.049	.8169	0	0	.647	.654	1.339
1839101	2.314	1.2850	0	0	.684	.636	1.340
1836101	1.745	.3303	0	0	.767	.761	1.232
1836102	1.963	.3245	.467	270.3	.692	.735	1.274
1836103	2.083	.3238	.573	591.5	.440	.657	1.406
1836104	2.296	.3181	.921	1190.7	.087	.377	1.698
1835105	3.334	.3149	1.125	2027.7	.007	.184	1.894
1836106	3.916	.3149	1.200	2285.7	0	0	0
1836107	5.461	.3181	1.338	3830.0	0	0	0
1835108	6.479	.2511	1.428	3681.8	.577	.565	1.417
1835109	6.513	.3232	1.426	3704.9	.578	.567	1.416

*** RUN 210 ***

GAS PRESSURE DROP THROUGH DRY BED					HB = .425	EPS = .4106	
2100001	0	0	.457	216.9	0	0	0
2100002	0	0	.623	380.7	0	0	0
2100003	0	0	.919	634.6	0	0	0
2100004	0	0	1.057	1015.3	0	0	0
2100005	0	0	1.340	1543.7	0	0	0
2100006	0	0	1.725	2455.1	0	0	0

*** RUN 211 ***

GAS PRESSURE DROP THROUGH DRY BED					HB = .71	EPS = .4106	VIS = .00105
2118101	2.006	.3481	0	0	1.071	.915	1.055
2119101	2.115	.5203	0	0	1.334	.856	.983
2116101	1.797	1.030	0	0	1.048	.964	1.013
2117101	1.880	.1914	0	0	1.031	1.018	.986

EXPERIMENTAL RESULTS FOR ■■ H13/WATR ■■ SYSTEM

NO. 4

EXPERIMENTAL RESULTS FOR ■■ H13/WATR ■■ SYSTEM

NO. 5

RUN NO.	TOTAL HOLD-UP (PCT.)	LIQUID VELOCITY (MM/S)	GAS VELOCITY (M/S)	PRESSURE DROP (N/M3)	RELATIVE LIQUID FLUX		
					INNER (-)	MIDDLE (-)	OUTER (-)
2117102	2.075	.1914	.461	304.6	1.074	.933	1.024
2117103	2.120	.1911	.629	549.2	1.020	.763	1.147
2117104	2.263	.1850	.875	1073.0	.694	.332	1.523
2117105	3.125	.1814	1.131	2030.6	-.020	.237	1.808
2117106	4.131	.1835	1.263	2725.1	.007	.304	1.770
2117107	4.177	.1822	1.399	3098.9	.014	.007	1.953
2117108	5.134	.1791	1.502	3712.7	0	.007	1.960
2117109	5.377	.1855	1.615	4137.3	0	.035	1.942
2117110	9.262	.1794	1.707	5281.8	.012	.088	1.912
■■■ RUN 212 ■■■ . DIST = 71 . HB = .425 . EPS = .4106 . VIS = .00105							
2127101	2.169	.3898	0	0	1.523	.744	.989
2126101	2.035	.2253	0	0	1.357	.809	1.005
2128101	2.351	.6359	0	0	1.485	.655	1.057
2129101	2.580	1.0121	0	0	1.443	.691	1.049
2129102	2.800	1.0193	.464	325.4	1.153	.725	1.122
2129103	2.962	1.0045	.631	599.9	1.160	.734	1.117
2129104	3.039	.9999	.792	964.5	.884	.485	1.364
2129105	3.490	1.0018	.973	1569.1	.382	.272	1.664
2129106	5.775	1.0095	1.096	2817.4	.759	.480	1.409
2129107	7.260	1.0131	1.163	3555.8	.363	.530	1.511
2129108	8.213	1.0217	1.253	4151.1	.240	.432	1.613
2129109	8.755	1.0351	1.332	4649.5	.131	.457	1.634
2129110	11.853	.9609	1.365	5399.5	.121	.435	1.651
■■■ RUN 213 ■■■ . DIST = 71 . HB = .425 . EPS = .4106 . VIS = .00105							
2139101	1.959	.0532	0	0	1.615	.914	.854
2138101	1.946	.0349	0	0	1.534	.899	.894
2137101	1.925	.0183	0	0	1.705	.799	.902
2137102	2.052	.0164	.462	311.5	1.270	.783	1.060
2137103	2.142	.0175	.630	556.1	1.202	.418	1.308
2137104	2.192	.0183	.872	1043.0	.648	.385	1.508
2137105	2.677	.0162	1.135	1887.5	.178	.339	1.700
2137106	2.248	.0157	1.419	2519.7	.026	.009	1.946
■■■ RUN 230 ■■■							
■■■ GAS PRESSURE DROP THROUGH DRY BED ■■ HB = .425 . EPS = .4106							
2300001	0	0	.463	237.7	0	0	0
2300002	0	0	.528	417.7	0	0	0
2300003	0	0	.855	726.8	0	0	0
2300004	0	0	1.110	1163.0	0	0	0
2300005	0	0	1.375	1714.4	0	0	0
2300006	0	0	1.590	2245.2	0	0	0
2300007	0	0	1.828	2909.7	0	0	0
■■■ RUN 231 ■■■ . DIST = 71 . HB = .425 . EPS = .4106 . VIS = .00111							
2319101	2.089	.5099	0	0	1.693	.576	1.036
2318101	1.910	.3043	0	0	1.622	.640	1.021
2316101	1.730	.0974	0	0	1.464	.681	1.048
2317101	1.800	.1684	0	0	1.622	.664	1.005
2317102	2.125	.1805	.459	309.2	1.408	.614	1.109
2317103	2.252	.1784	.524	563.0	1.185	.682	1.141
2317104	2.504	.1756	.844	1063.7	.300	.733	1.406
2317105	3.769	.1791	1.121	2212.9	.024	.212	1.822
2317106	4.566	.1814	1.288	2898.2	.004	.317	1.763

RUN NO.	TOTAL HOLD-UP (PCT.)	LIQUID VELOCITY (MM/S)	GAS VELOCITY (M/S)	PRESSURE DROP (N/M3)	RELATIVE LIQUID FLUX		
					INNER (-)	MIDDLE (-)	OUTER (-)
2317107	5.148	.1769	1.440	3440.4	0	.473	1.659
2317108	5.882	.1749	1.621	4111.9	.002	.480	1.653
2317109	11.255	.1684	1.668	5549.4	.050	.768	1.458
2317110	7.446	.1675	1.617	4931.0	.166	.689	1.479
2317111	6.406	.1705	1.539	4451.1	.079	1.004	1.312
2317112	5.632	.1643	1.445	3899.6	0	.816	1.455
■■■ RUN 232 ■■■ . DIST = 71 . HB = .425 . EPS = .4106 . VIS = .00113							
2329101	1.896	.0584	0	0	1.504	.512	1.139
2328101	1.880	.0282	0	0	1.526	.513	1.131
2327101	1.883	.0128	0	0	1.375	.936	1.170
2329102	2.159	.0506	.457	336.9	1.469	.558	1.123
2329103	2.252	.0579	.663	683.0	1.226	.475	1.256
2329104	2.527	.0579	.906	1356.8	.294	.231	1.719
2329105	3.673	.0590	1.153	2450.5	0	.175	1.856
2329106	3.613	.0574	1.392	3140.5	0	.129	1.880
2329107	4.623	.0625	1.613	3938.8	.018	.158	1.858
2329108	5.649	.0562	1.694	4356.5	0	.435	1.691
2329109	6.503	.0559	1.803	4792.5	.007	.028	1.945
2329110	4.749	.0584	1.596	3888.1	.008	.274	1.789

EXPERIMENTAL RESULTS FOR ** PL9/WATR ** SYSTEM

NO. 1

PACKING : PLASTIC SPHERES

AVERAGE SIZE = 9.0 (MM) . APPARENT DENSITY = 921. (KG/M3)
 LIQUID : WATER
 DENSITY = 1000.(KG/M3) . NOMINAL VISCOSITY = .0010 (NS/M2)
 SURFACE TENSION = .0732 (N/M) . CONTACT ANGLE = 92.6 (DEG.)

RUN NO.	TOTAL HOLD-UP (PCT.)	LIQUID VELOCITY (MM/S)	GAS VELOCITY (M/S)	PRESSURE DROP (N/M3)	RELATIVE LIQUID FLUX		
					INNER (-)	MIDDLE (-)	OUTER (-)
*** RUN 18 ***	. DIST = 19 . HB = .294 . EPS = .4040 . VIS = .00093						
185117	4.234	.5230	0	0	.995	.640	1.230
187118	4.580	.8544	0	0	.878	.668	1.252
188119	5.098	1.3979	0	0	1.032	.701	1.181
184120	3.706	.1606	0	0	.791	.612	1.316
185121	3.927	.3056	0	0	.765	.671	1.289
184222	3.705	.1668	0	0	.861	.675	1.254
185223	3.879	.3016	0	0	.885	.632	1.272
188224	5.113	1.3995	0	0	1.269	.698	1.103
187225	4.580	.8813	0	0	.974	.663	1.223
186226	4.191	.5332	0	0	.882	.669	1.251
187327	4.551	.8864	0	0	.945	.645	1.244
185328	3.913	.3020	0	0	.920	.661	1.243
188329	5.122	1.2234	0	0	.782	.671	1.283
186330	4.292	.5381	0	0	.882	.646	1.265
184331	3.798	.1651	0	0	.855	.605	1.296
183532	3.812	.1855	0	0	.694	.684	1.304
182533	3.534	.0955	0	0	.575	.826	1.255
181534	3.543	.0499	0	0	.515	.916	1.221
180535	3.442	.0248	0	0	.864	.756	1.203
182636	3.658	.1003	0	0	.745	.749	1.247
180637	3.475	.0254	0	0	.910	.821	1.147
183638	3.855	.1889	0	0	.955	.763	1.168
181639	3.557	.0505	0	0	.717	.753	1.254
182740	3.573	.0998	0	0	.812	.790	1.199
181741	3.533	.0512	0	0	.731	.733	1.261
180742	3.442	.0255	0	0	.688	.629	1.341
183743	3.831	.1874	0	0	.826	.716	1.240
*** RUN 19 ***	. DIST = 19 . HB = .599 . EPS = .4003 . VIS = .00098						
195205	3.875	.2748	0	0	.601	.271	1.591
198207	5.149	1.3373	0	0	.629	.351	1.532
195208	4.241	.4868	0	0	.985	.371	1.535
197209	4.642	.3299	0	0	.521	.330	1.582
194210	3.658	.1398	0	0	.519	.320	1.588
195311	3.923	.2200	0	0	.535	.364	1.555
196412	5.137	1.3729	0	0	.501	.332	1.587
196313	4.241	.5084	0	0	.636	.295	1.564
194314	3.723	.1465	0	0	.610	.287	1.578
197315	4.555	.8486	0	0	.595	.297	1.577
194415	3.711	.1474	0	0	.594	.322	1.562
196417	4.241	.5114	0	0	.586	.352	1.546
198418	5.149	1.3941	0	0	.620	.319	1.555
195419	3.912	.2657	0	0	.578	.357	1.546
197420	4.555	.8450	0	0	.755	.348	1.492
190121	3.344	.0231	0	0	.618	.232	1.610

EXPERIMENTAL RESULTS FOR ** PL9/WATR ** SYSTEM

NO. 2

RUN NO.	TOTAL HOLD-UP (PCT.)	LIQUID VELOCITY (MM/S)	GAS VELOCITY (M/S)	PRESSURE DROP (N/M3)	RELATIVE LIQUID FLUX INNER (-)	MIDDLE (-)	OUTER (-)
192122	3.582	.0923	0	0	.393	.281	1.655
191123	3.480	.0491	0	0	.515	.316	1.592
192224	3.598	.0926	0	0	.481	.309	1.608
190225	3.353	.0246	0	0	.336	.328	1.645
191226	3.452	.0476	0	0	.393	.300	1.643
190327	3.410	.0210	0	0	.225	.305	1.697
192328	3.582	.0942	0	0	.418	.277	1.649
191329	3.457	.0482	0	0	.320	.359	1.631
*** RUN 140 ***	*** GAS PRESSURE DROP THROUGH DRY BED *** HB = .594 . EPS = .3912						
1400001	0	0	.312	246.0	0	0	0
1400002	0	0	.441	450.7	0	0	0
1400003	0	0	.569	708.3	0	0	0
1400004	0	0	.713	1038.5	0	0	0
1400005	0	0	.914	1613.0	0	0	0
1400006	0	0	1.124	2316.3	0	0	0
1400007	0	0	1.312	3004.7	0	0	0
1400008	0	0	1.546	4018.4	0	0	0
1400009	0	0	1.132	2296.5	0	0	0
1400010	0	0	.251	173.4	0	0	0
1400011	0	0	.549	681.8	0	0	0
1400012	0	0	.750	1175.5	0	0	0
1400013	0	0	.954	1809.5	0	0	0
1400014	0	0	1.148	2484.7	0	0	0
1400015	0	0	1.370	3354.7	0	0	0
*** RUN 141 ***	. DIST = 71 . HB = .594 . EPS = .3912 . VIS = .00108						
1415101	3.536	-1004	0	0	1.304	.647	1.124
1417101	3.726	-1843	0	0	1.321	.587	1.154
1418101	3.935	-3170	0	0	1.238	.667	1.132
1419101	4.213	-5183	0	0	1.383	.634	1.104
1419102	4.253	-5204	.278	368.2	1.088	.730	1.144
1418102	3.947	-3019	.277	351.7	1.041	.778	1.130
1417102	3.750	-1855	.281	355.0	1.004	.620	1.241
1415102	3.609	-0989	.287	350.0	1.142	.684	1.155
1417103	3.636	-1918	.414	705.0	.731	.470	1.424
1417104	3.545	-1794	.537	1163.9	.291	.193	1.744
1417105	3.571	-1780	.675	1840.8	.004	.114	1.889
1417106	7.064	-1915	.801	3800.5	.128	.354	1.698
1417107	9.951	-1651	.832	5202.2	.365	.574	1.482
*** RUN 142 ***	. DIST = 71 . HB = .584 . EPS = .3843 . VIS = .00103						
1429101	4.793	.9848	0	0	1.148	.746	1.113
1428101	4.341	.6361	0	0	1.043	.782	1.127
1427101	4.058	.3801	0	0	1.254	.798	1.046
1427102	4.135	.1968	.284	386.2	.917	.691	1.225
1429102	4.304	.6330	.282	387.9	.695	.686	1.303
1429103	4.817	1.0148	.281	419.8	1.008	.570	1.203
1429104	4.679	.9760	.414	876.6	.430	.616	1.435
1429104	4.619	.9862	.517	1346.7	.358	.230	1.698
1429105	4.829	1.0282	.632	1973.1	.133	.419	1.655
1429106	5.846	.9245	.667	2517.9	.073	.283	1.757
1429107	9.474	.9963	.686	3858.9	.129	.282	1.745

EXPERIMENTAL RESULTS FOR ■■ PL9/WATR ■■ SYSTEM

NO. 3

RUN NO.	TOTAL	LIQUID	GAS	PRESSURE	RELATIVE LIQUID FLUX		
	HOLD-UP (PCT.)	VELOCITY (MM/S)	VELOCITY (M/S)	DROP (N/M ³)	INNER (-)	MIDDLE (-)	OUTER (-)
1427103	6.144	.3723	.749	3138.5	-.096	.325	1.728
■■■ RUN 143 ■■■ . DIST = 7I . HB = .584 . EPS = .3843 . VIS = .00109							
1439101	3.555	-.0613	0	0	1.297	.797	1.033
1438101	3.463	.0320	0	0	1.319	.727	1.072
1437101	3.386	.0161	0	0	1.282	.639	1.130
1437102	3.403	.0137	-.284	344.2	-.964	-.988	1.271
1438102	3.427	.0315	-.286	349.3	-.645	-.815	1.245
1439102	3.514	-.0632	-.284	357.7	-.817	-.698	1.253
1439103	3.451	.0629	-.413	720.4	1.497	-.571	1.106
1439104	3.321	-.0635	-.571	1316.5	-.182	-.155	1.805
1439105	3.753	-.0627	.753	2369.4	-.116	-.225	1.781
1439106	6.289	-.0690	.828	3719.5	.405	-.299	1.642
1439107	8.785	-.0596	.853	4416.4	.032	-.221	1.815
1437103	7.910	-.0116	.929	4886.6	-.043	-.440	1.669

EXPERIMENTAL RESULTS FOR ■■ PLM/WATR ■■ SYSTEM

NO. 1

PACKING : PLASTIC SPHERES(MIXI)
 AVERAGE SIZE = 10.6 (MM) . APPARENT DENSITY = 921. (KG/H³)
 LIQUID : WATER
 DENSITY = 1000.(KG/M³) . NOMINAL VISCOSITY = .0010 (NS/M²)
 SURFACE TENSION = .0732 (N/M) . CONTACT ANGLE = 92.6 (DEG.)

RUN NO.	TOTAL	LIQUID	GAS	PRESSURE	RELATIVE LIQUID FLUX		
	HOLD-UP (PCT.)	VELOCITY (MM/S)	VELOCITY (M/S)	DROP (N/M ³)	INNER (-)	MIDDLE (-)	OUTER (-)
■■■ RUN 170 ■■■							
■■■ GAS PRESSURE DROP THROUGH DRY BED ■■ HB = .594 . EPS = .3897							
1700001	0	0	.326	224.5	0	0	0
1700002	0	0	.541	574.5	0	0	0
1700003	0	0	.767	1012.0	0	0	0
1700004	0	0	1.044	1750.0	0	0	0
1700005	0	0	1.255	2380.7	0	0	0
1700006	0	0	1.466	3122.0	0	0	0
1700007	0	0	1.706	4066.3	0	0	0
■■■ RUN 171 ■■■ . DIST = 19 . HB = .594 . EPS = .3897 . VIS = .00108							
1718101	4.268	.7877	0	0	1.035	.729	1.162
1719101	4.586	1.2772	0	0	.606	.561	1.410
1717101	3.885	.4871	0	0	.760	.865	1.170
1714101	3.189	-.0758	0	0	.823	1.121	.992
1716101	3.576	.2730	0	0	.756	.941	1.125
1715101	3.372	.1444	0	0	.724	1.009	1.094
■■■ RUN 172 ■■■ . DIST = 7I . HB = .594 . EPS = .3897 . VIS = .00114							
1725101	3.179	-.0611	0	0	1.114	1.212	.837
1727101	3.455	-.1921	0	0	1.242	1.104	.861
1729101	3.852	-.5119	0	0	1.273	.775	1.054
1729201	3.757	-.5019	0	0	1.315	.609	1.142
1727201	3.419	-.1862	0	0	.755	1.030	1.070
1727202	3.495	-.1887	.329	364.9	.739	.880	1.169
1727203	3.450	-.1846	.464	698.4	.953	.755	1.175
1727204	3.386	-.1838	.626	1271.2	.300	.607	1.484
1727205	4.310	-.1716	.806	2423.6	.249	.506	1.564
1727206	5.494	-.1863	.863	3027.9	.412	.541	1.488
1727207	7.433	-.1750	.915	3924.3	.775	.843	1.179
1729202	7.409	-.5160	.823	3554.5	.150	.473	1.617
■■■ RUN 173 ■■■ . DIST = 7I . HB = .594 . EPS = .3897 . VIS = .00115							
1737101	3.678	.3424	0	0	.863	.902	1.112
1736101	3.372	.1524	0	0	.853	.986	1.065
1735101	3.137	-.0426	0	0	.577	1.182	1.036
1738101	3.930	-.5987	0	0	1.000	.737	1.169
1739101	4.313	-.9733	0	0	1.163	.749	1.107
■■■ RUN 174 ■■■ . DIST = 7I . HB = .594 . EPS = .3897 . VIS = .00115							
1749101	3.198	-.0621	0	0	.852	1.075	1.010
1748101	3.113	-.0316	0	0	1.603	.933	.847
1747101	3.075	-.0158	0	0	1.185	1.318	.746
1746101	3.003	-.0079	0	0	.532	1.210	1.033

EXPERIMENTAL RESULTS FOR ■■ AL13/WATR ■■ SYSTEM

NO. 1

PACKING : ALUMINA SPHERES
 AVERAGE SIZE = 13.1 (MM) . APPARENT DENSITY = 3465. (KG/M3)
 LIQUID : WATER
 DENSITY = 1000.(KG/M3) . NOMINAL VISCOSITY = .0010 (NS/M2)
 SURFACE TENSION = .0732 (N/M) . CONTACT ANGLE = 0 (DEG.)

RUN NO.	TOTAL HOLD-UP (PCT.)	LIQUID VELOCITY (MM/S)	GAS VELOCITY (M/S)	PRESSURE DROP (N/M3)	RELATIVE LIQUID FLUX		
					INNER (-)	MIDDLE (-)	OUTER (-)
*** RUN 14 *** . DIST = 19 . HB = .245 . EPS = .4189 . VIS = .00086							
145416	5.102	.5413	0	0	.389	1.024	1.196
144417	4.630	.1681	0	0	.404	1.134	1.123
145419	4.831	.3072	0	0	.448	1.111	1.123
147419	5.757	.8841	0	0	.373	1.058	1.181
148420	5.908	1.4086	0	0	.287	1.166	1.142
148521	5.928	1.3409	0	0	.354	1.288	1.044
146522	5.150	.5431	0	0	.334	1.007	1.225
147523	5.464	.8632	0	0	.413	1.060	1.166
145524	4.825	.2973	0	0	.370	1.228	1.076
144525	4.655	.1517	0	0	.377	1.206	1.087
146625	5.142	.5409	0	0	.339	1.655	.822
144627	4.659	.1430	0	0	.491	1.411	.922
148528	5.887	1.2596	0	0	.296	1.461	.957
147629	5.433	.9299	0	0	.238	1.734	.807
145630	4.858	.2987	0	0	.409	1.407	.952
141131	4.427	.0576	0	0	.898	.714	1.217
142132	4.530	.1085	0	0	1.043	.671	1.195
140133	4.352	.0290	0	0	1.253	1.069	.878
140234	4.352	.0280	0	0	1.138	1.084	.908
142335	4.533	.1055	0	0	1.252	.773	1.062
141235	4.436	.0553	0	0	1.114	.754	1.120
142337	4.552	.1087	0	0	.881	.757	1.197
140338	4.408	.0271	0	0	1.299	.528	1.198
141339	4.450	.0547	0	0	1.396	.756	1.025
*** RUN 16 *** . DIST = 19 . HB = .455 . EPS = .4189 . VIS = .00095							
165422	4.827	.2912	0	0	.324	1.917	.665
164523	4.641	.1571	0	0	.154	2.030	.615
168524	5.891	1.3818	0	0	.717	1.611	.723
165525	4.936	.2939	0	0	.400	2.026	.572
166526	5.084	.5466	0	0	.479	1.922	.610
168527	5.891	1.3903	0	0	.608	1.643	.739
164628	4.635	.1603	0	0	.206	1.896	.718
167629	5.425	.8682	0	0	.733	1.514	.779
168730	5.090	.5200	0	0	.571	1.685	.726
167731	5.410	.8919	0	0	.674	1.618	.733
166832	5.094	.5238	0	0	.603	1.736	.684
164733	4.641	.1434	0	0	.242	1.933	.745
168734	5.922	1.3444	0	0	.562	1.601	.781
164835	4.650	.1376	0	0	.255	1.859	.724
167836	5.472	.8694	0	0	.750	1.583	.729
165937	4.845	.2860	0	0	.352	1.919	.654
161139	4.435	.0534	0	0	.556	1.706	.718
160139	4.430	.0256	0	0	.344	2.049	.577
163140	4.752	.1857	0	0	.387	1.940	.630

EXPERIMENTAL RESULTS FOR ■■ AL13/WATR ■■ SYSTEM

NO. 2

RUN NO.	TOTAL HOLD-UP (PCT.)	LIQUID VELOCITY (MM/S)	GAS VELOCITY (M/S)	PRESSURE DROP (N/M3)	RELATIVE LIQUID FLUX		
					INNER (-)	MIDDLE (-)	OUTER (-)
162141	4.619	.0992	0	0	.416	1.792	.712
162242	4.616	.0980	0	0	.337	1.798	.734
161243	4.529	.0510	0	0	.604	1.870	.600
160244	4.442	.0252	0	0	.436	1.914	.629
163245	4.731	.1898	0	0	.185	1.972	.678
161346	4.498	.0510	0	0	.518	2.150	.456
163347	4.721	.1920	0	0	.269	1.840	.732
162348	4.600	.1007	0	0	.328	1.758	.762
160349	4.417	.0251	0	0	.263	2.099	.573

*** RUN 130 ***

*** GAS PRESSURE DROP THROUGH DRY BED ***					HB = .445 . EPS = .4039		
1300002	0	0	.463	279.9	0	0	0
1300003	0	0	.623	473.8	0	0	0
1300004	0	0	.802	753.7	0	0	0
1300005	0	0	1.057	1242.9	0	0	0
1300006	0	0	1.336	1857.8	0	0	0
1300007	0	0	1.610	2657.7	0	0	0

*** RUN 131 ***

*** DIST = 71 . HB = .445 . EPS = .4039 . VIS = .00109							
1319101	4.859	.4950	0	0	.918	1.363	.509
1316101	4.694	.3083	0	0	1.015	1.069	.959
1317101	4.561	.1771	0	0	.981	1.217	.879
1316101	4.428	.0971	0	0	.647	1.253	.969
1318201	4.675	.3018	0	0	.922	1.052	1.000
1319301	4.951	.5125	0	0	1.004	1.065	.965
1316301	4.463	.1026	0	0	.908	1.501	.728
1317301	4.577	.1860	0	0	1.116	1.322	.759
1318301	4.726	.3181	0	0	.939	1.199	.904
1318302	4.735	.3195	.456	427.5	1.332	1.251	.739
1318303	4.678	.3170	.622	800.0	.679	1.514	.796
1318304	4.767	.3126	.796	1485.3	1.025	.996	1.001
1318305	4.872	.3116	.853	1904.0	.638	1.009	1.122
1318306	5.233	.3164	.921	2441.8	1.158	.859	1.041
1318307	5.877	.3170	.948	3016.9	1.356	1.004	.885
1318308	7.206	.3119	.969	3901.5	1.434	.963	.884
1318309	9.017	.3049	.977	4317.2	1.234	1.033	.904
1318401	4.926	.3035	0	0	.867	.900	1.112
1318401	4.517	.1005	0	0	.766	1.386	.847
1317401	4.637	.1896	0	0	.880	1.259	.886
1318401	4.834	.3108	0	0	.395	1.055	1.175
1319401	5.027	.5160	0	0	.605	1.095	1.080
1319402	5.100	.5348	.457	478.2	.676	1.557	.754
1318402	4.853	.3131	.457	458.4	1.051	1.055	.950
1317402	4.631	.1833	.457	440.8	1.010	1.261	.842
1316402	4.466	.1005	.459	429.7	.947	1.457	.742
1315403	4.437	.0970	.618	777.9	1.126	1.291	.783
1316404	4.377	.0981	.792	1337.7	1.413	1.120	.795
1316405	4.564	.0965	.980	2336.0	1.902	1.212	.573
1316406	5.519	.0953	1.114	3724.3	1.597	.806	.925
1316407	6.797	.0837	1.143	4537.5	1.086	.906	1.039

*** RUN 132 ***

*** DIST = 71 . HB = .445 . EPS = .4039 . VIS = .00105							
1321101	5.509	1.0251	0	0	.777	1.185	.966

EXPERIMENTAL RESULTS FOR ■■ AL13/WATR ■■ SYSTEM

NO. 3

RUN NO.	TOTAL HOLD-UP (PCT.)	LIQUID VELOCITY (MM/S)	GAS VELOCITY (M/S)	PRESSURE DROP (N/M3)	RELATIVE LIQUID FLUX		
					INNER (-)	MIDDLE (-)	OUTER (-)
1328101	5.126	.6439	0	0	1.153	1.318	.758
1327101	4.872	.3897	0	0	1.157	1.029	.936
1326101	4.723	.2106	0	0	.815	1.186	.954
1326102	4.621	.2253	.459	443.0	1.098	1.213	.842
1327102	4.834	.3956	.457	462.8	1.118	1.365	.740
1328102	5.154	.8196	.457	495.8	1.096	1.469	.684
1329102	5.608	.9315	.459	555.3	1.255	1.117	.849
1329103	5.801	1.0229	.624	1273.8	.372	1.230	1.074
1329104	6.106	1.0315	.676	1725.5	.379	.772	1.356
1329105	8.914	.9807	.701	3360.7	.588	.726	1.314
1329106	9.728	1.0137	.705	3775.0	.526	.707	1.346
1327103	8.535	.3673	.911	4281.9	.841	.999	1.060
*** RUN 133 *** . DIST = 71 . HB = .445 . EPS = .4039 . VIS = .00108							
1339101	4.583	.0632	0	0	.185	1.395	1.039
1338101	4.529	.0336	0	0	.211	1.171	1.166
1337101	4.469	.0169	0	0	.239	1.372	1.039
1337102	4.488	.0174	.454	423.1	.428	1.025	1.186
1338102	4.383	.0236	.457	412.1	.844	1.589	.696
1339102	4.393	.0604	.457	418.7	.989	1.288	.830
1339201	4.342	.0635	0	0	.531	1.386	.924
1339202	4.450	.0635	.452	416.5	1.208	.990	.941
1339203	4.374	.0673	.623	786.7	.944	1.235	.880
1339204	4.260	.0625	.792	1364.1	1.590	.580	1.070
1339205	4.247	.0642	.979	2241.2	1.680	.814	.894
1339206	4.669	.0632	1.114	3219.7	.368	.930	1.262
1339207	5.728	.0635	1.205	4526.5	.125	.360	1.699
1337202	4.919	.0152	1.359	4859.3	.038	.032	1.937

EXPERIMENTAL RESULTS FOR ■■ G8/WATR ■■ SYSTEM

NO. 1

PACKING : GLASS SPHERES
 AVERAGE SIZE = 8.1 (MM) . APPARENT DENSITY = 2500. (KG/M3)
 LIQUID : WATER
 DENSITY = 1000. (KG/M3) . NOMINAL VISCOSITY = .0010 (NS/M2)
 SURFACE TENSION = .0732 (N/M) . CONTACT ANGLE = 0 (DEG.)

RUN NO.	TOTAL HOLD-UP (PCT.)	LIQUID VELOCITY (MM/S)	GAS VELOCITY (M/S)	PRESSURE DROP (N/M3)	RELATIVE LIQUID FLUX		
					INNER (-)	MIDDLE (-)	OUTER (-)
*** RUN 12 *** . DIST = 19 . HB = .210 . EPS = .4000 . VIS = .00085							
126311	5.714	.5684	0	0	.745	.773	1.582
124312	5.061	.1989	0	0	1.015	.360	1.397
125319	5.297	.3195	0	0	.784	.607	1.322
128314	6.935	1.3343	0	0	1.301	.669	1.211
127215	6.347	.9124	0	0	1.041	.364	1.386
127416	6.386	.8757	0	0	1.308	.248	1.469
124417	4.948	.1543	0	0	.484	.422	1.403
128418	6.854	1.2458	0	0	.850	.928	1.101
125419	5.400	.3140	0	0	.593	.385	1.523
127520	6.321	.9102	0	0	.819	.643	1.288
126421	5.778	.5567	0	0	1.029	.459	1.331
125522	5.351	.3083	0	0	.811	.254	1.531
126523	5.496	.5352	0	0	1.127	.429	1.317
128524	7.032	1.3725	0	0	.565	.849	1.245
124525	4.997	.1557	0	0	.670	.384	1.498
120334	4.654	.0306	0	0	.910	.569	1.303
121335	4.793	.0617	0	0	.798	.517	1.373
122336	4.867	.1173	0	0	.633	.463	1.462
123337	5.045	.2129	0	0	.754	.484	1.408
123438	5.061	.2318	0	0	1.209	.395	1.310
121439	4.706	.0621	0	0	1.001	.472	1.332
122440	4.884	.1186	0	0	.825	.608	1.307
120441	4.699	.0315	0	0	1.224	.534	1.220
123542	5.116	.2179	0	0	1.046	.433	1.342
121543	4.738	.0602	0	0	.995	.568	1.275
122544	4.923	.1185	0	0	1.137	.395	1.334
120545	4.657	.0289	0	0	1.059	.546	1.257
*** RUN 20 *** . DIST = 19 . HB = .307 . EPS = .4057 . VIS = .00099							
204206	4.864	.1553	0	0	2.371	.438	.995
205207	5.169	.2687	0	0	1.671	.379	1.166
208208	6.924	1.3499	0	0	1.208	.732	1.102
208309	6.832	1.3668	0	0	1.258	.736	1.083
206210	5.586	.5025	0	0	1.169	.598	1.198
207211	6.188	.8435	0	0	1.139	.825	1.066
206312	5.549	.4991	0	0	1.627	.258	1.255
205313	5.131	.2892	0	0	1.215	.686	1.129
204314	4.915	.1549	0	0	1.823	.699	.917
208415	6.740	1.2731	0	0	1.198	.671	1.143
207316	5.161	.8322	0	0	1.277	.853	1.004
205417	5.112	.2861	0	0	1.269	.688	1.109
206418	5.563	.4982	0	0	1.230	1.018	.918
207419	6.138	.8356	0	0	1.393	.708	1.055
204420	4.786	.1380	0	0	1.650	.915	.822
201121	4.579	.0518	0	0	2.587	.921	.523

EXPERIMENTAL RESULTS FOR G8/WATR SYSTEM

NO. 2

EXPERIMENTAL RESULTS FOR G8/WATR SYSTEM

NO. 3

RUN NO.	TOTAL HOLD-UP (PCT.)	LIQUID VELOCITY (MM/S)	GAS VELOCITY (M/S)	PRESSURE DROP (N/M3)	RELATIVE LIQUID FLUX		
					INNER (-)	MIDDLE (-)	OUTER (-)
202122	4.740	.1000	0	0	2.028	.765	.805
200123	4.487	.0132	0	0	2.506	.543	.784
202224	4.657	.1001	0	0	2.099	.619	.873
201225	4.547	.0474	0	0	2.552	.327	.902
200226	4.496	.0266	0	0	2.392	.432	.891
202327	4.680	.0979	0	0	1.743	.627	.988
200328	4.473	.0120	0	0	2.649	.495	.766
201329	4.570	.0502	0	0	2.365	.724	.720
*** RUN 27 *** DIST = 19 . HB = .587 . EPS = .4004 . V15 = .00100							
277101	5.958	.8315	0	0	.142	.703	1.478
276102	5.468	.4876	0	0	.205	.741	1.432
274103	4.908	.1464	0	0	.189	.714	1.455
275104	5.089	.2579	0	0	.109	.695	1.493
278105	6.634	1.3109	0	0	.183	.690	1.472
277206	5.999	.8247	0	0	.231	.811	1.381
278207	6.730	1.2924	0	0	.212	.599	1.519
276208	5.449	.4799	0	0	.354	.893	1.289
275209	5.093	.2748	0	0	.249	.879	1.333
274210	4.893	.1489	0	0	.218	.840	1.357
275311	5.089	.2862	0	0	.109	.666	1.511
277312	5.939	.9085	0	0	.156	.778	1.426
274313	4.871	.1485	0	0	.124	.810	1.417
278314	6.705	1.3425	0	0	.316	1.036	1.213
276315	5.504	.4608	0	0	.559	.710	1.334
270116	4.614	.0273	0	0	.148	.647	1.510
272117	4.770	.0992	0	0	.176	.606	1.527
271118	4.681	.0523	0	0	.483	.654	1.388
271219	4.706	.0528	0	0	.335	.926	1.337
272220	4.639	.0277	0	0	.256	.609	1.498
272221	4.795	.0995	0	0	.288	.805	1.365
270322	4.605	.0261	0	0	.193	.700	1.462
272323	4.828	.0997	0	0	.221	.764	1.413
271324	4.745	.0453	0	0	.171	.887	1.354
*** RUN 110 ***							
*** GAS PRESSURE DROP THROUGH DRY BED *** HB = .567 . EPS = .3784							
1100001	0	0	.335	384.0	0	0	0
1100002	0	0	.316	806.0	0	0	0
1100003	0	0	.681	1292.0	0	0	0
1100004	0	0	.655	1965.5	0	0	0
1100005	0	0	1.116	3073.5	0	0	0
1100006	0	0	1.238	4169.0	0	0	0
1100007	0	0	1.489	5114.4	0	0	0
*** RUN 111 *** DIST = 71 . HB = .557 . EPS = .3784 . V15 = .00103							
1119101	5.195	.5253	0	0	1.084	1.096	.624
1118101	4.760	.3125	0	0	1.063	.851	1.077
1117101	4.498	.1952	0	0	.139	1.082	1.244
1116101	4.094	.0554	0	0	.455	.854	1.256
1115102	5.222	.8174	.405	564.5	.393	1.012	1.222
1114103	5.414	.9129	.414	1032.6	.821	.856	1.137
1113104	5.511	.6005	.487	1459.9	.411	.317	1.055
1112105	5.720	.9208	.569	2025.3	.771	1.204	.957

RUN NO.	TOTAL HOLD-UP (PCT.)	LIQUID VELOCITY (MM/S)	GAS VELOCITY (M/S)	PRESSURE DROP (N/M3)	RELATIVE LIQUID FLUX		
					INNER (-)	MIDDLE (-)	OUTER (-)
1119106	5.977	.5195	.629	2522.0	.312	.783	1.371
1119107	5.855	.5011	.622	2634.1	.037	.900	1.391
1119108	7.438	.5108	.630	3583.7	.013	.914	1.391
1119201	5.223	.5142	0	0	.101	.592	1.493
1119301	5.043	.5136	0	0	1.367	1.131	.802
1119201	4.710	.3229	0	0	.996	1.393	.820
1117201	4.436	.1807	0	0	.266	1.275	1.082
1116201	4.224	.0939	0	0	.856	.980	1.067
1117202	4.528	.1835	.331	605.4	.120	1.187	1.135
1117203	4.536	.1777	.408	904.6	.001	.770	1.484
1117204	4.605	.1814	.487	1285.1	.092	.859	1.398
1117205	4.692	.1793	.567	1736.5	.434	1.324	.995
1117205	4.840	.1794	.623	2179.3	0	.971	1.501
1117207	4.901	.1815	.651	2390.3	.001	.994	1.346
1117208	4.944	.1809	.681	2629.0	0	1.002	1.341
1117209	5.046	.1811	.709	2966.2	.002	1.061	1.304
1117210	5.083	.1771	.729	3144.4	.008	1.206	1.311
1117211	5.230	.1747	.743	3412.5	.011	1.025	1.324
1117212	6.773	.1609	.692	3594.1	0	.101	1.637
1117301	4.396	.1733	0	0	0	.547	1.622
1117401	4.513	.1650	0	0	.001	.747	1.499
1117402	4.941	.1655	.677	2693.0	.457	.429	1.542
1117403	5.016	.1842	.706	2985.2	.745	.416	1.453
1117404	5.098	.1849	.731	3249.9	.903	.351	1.737
1117405	5.218	.1829	.742	3533.5	.001	.380	1.725
1117406	5.397	.1826	.761	3858.7	.005	.491	1.855
1117407	5.534	.1855	.775	4168.3	.004	.426	1.897
1117408	6.639	.1847	.786	5967.0	.005	.387	1.419
1117409	9.051	.1749	.752	5794.1	.028	.547	1.919
1118302	8.518	.3075	.677	5828.7	.133	.732	1.953
1118301	4.867	.3102	0	0	.442	.956	1.223
1116501	4.279	.3071	0	0	.653	.919	1.544
1117501	4.555	.3026	0	0	.977	.950	1.410
1116501	4.809	.3016	0	0	.743	.923	1.312
1116501	5.320	.3125	0	0	.618	.934	1.547
*** RUN 112 *** DIST = 13 . HB = .557 . EPS = .3784 . V15 = .00110							
1125101	4.643	.1900	0	0	.711	.429	1.469
1126101	5.039	.3024	0	0	.468	.562	1.455
1127101	5.486	.5232	0	0	.548	.574	1.421
1128101	6.109	.8289	0	0	.506	.759	1.321
1127102	5.526	.5740	.335	782.7	.475	.578	1.444
1127103	5.705	.5706	.408	1164.0	.375	.547	1.497
1127104	5.778	.5713	.486	1522.3	.348	.525	1.519
1127105	5.004	.5594	.566	2226.0	.337	.493	1.548
1127106	6.440	.5753	.680	2668.7	.596	.802	1.264
1127107	6.604	.5633	.690	2890.1	.635	.739	1.290
1127108	6.646	.5596	.600	3014.7	.540	.704	1.344
1127109	8.013	.5627	.604	4953.3	.374	.394	1.591
1127201	5.609	.5495	0	0	.116	.692	1.493
1128301	5.044	.3837	0	0	.355	.997	1.230
1127301	5.491	.3771	0	0	.307	.896	1.309

EXPERIMENTAL RESULTS FOR ■■ GB/WATR ■■ SYSTEM

NO. 4

EXPERIMENTAL RESULTS FOR ■■ GB/WATR ■■ SYSTEM

NO. 5

RUN NO.	TOTAL HOLD-UP (PCT.)	LIQUID VELOCITY (MM/S)	GAS VELOCITY (M/S)	PRESSURE DROP (N/M3)	RELATIVE LIQUID FLUX		
					INNER (-)	MIDDLE (-)	OUTER (-)
1126301	4.991	.3458	0	0	.126	.811	1.416
1125301	4.590	.1800	0	0	.263	.657	1.466
1125302	4.665	.1750	.331	559.0	.191	.622	1.511
1125303	4.633	.1766	.408	970.3	.050	.893	1.391
1125304	4.682	.1776	.486	1364.6	0	.624	1.576
1125305	4.789	.1770	.564	1857.6	0	.959	1.367
1125306	4.879	.1766	.619	2266.5	0	.814	1.457
1125307	5.023	.1761	.677	2767.3	.027	.630	1.561
1125308	5.223	.1708	.736	3479.9	.045	.650	1.545
1125309	6.181	.1756	.752	4552.2	.130	.780	1.434
1125310	6.684	.1725	.759	4682.0	.127	.885	1.370
1126302	6.572	.3418	.613	3542.2	.024	.768	1.478
1127302	8.222	.5653	.609	4323.9	.170	.712	1.463
1128302	7.361	.8714	.513	2843.4	.249	1.190	1.147
*** RUN 113 *** .01ST = 19 . HB = .567 . EPS = .3784 . VIS = .00110							
1139101	6.746	1.3159	0	0	.344	1.262	1.064
1138101	5.934	.7973	0	0	.108	1.226	1.165
1137101	5.419	.5194	0	0	.117	1.490	.999
1136101	4.956	.2899	0	0	.168	1.397	1.039
1135101	4.690	.1849	0	0	.492	1.258	1.017
1135102	4.782	.1829	.330	639.9	.511	1.539	.837
1135103	4.705	.1831	.408	947.8	.127	1.099	1.238
1135104	4.750	.1874	.483	1316.2	.121	.713	1.479
1135105	4.819	.1791	.554	1809.1	.525	1.225	1.027
1135105	4.869	.1794	.621	2181.0	.518	1.014	1.159
1135107	5.081	.1780	.677	2755.2	.014	1.298	1.153
1135108	5.220	.1791	.707	3054.8	.040	1.162	1.227
1135109	5.345	.1769	.736	3395.2	.026	1.192	1.215
1135110	5.691	.1761	.762	3952.1	.041	1.327	1.126
1135111	6.211	.1729	.737	4076.5	.030	1.405	1.080
1138102	6.721	.7753	.512	2352.2	.054	.986	1.332
1135201	4.593	.1729	0	0	.433	1.111	1.127
1136201	4.899	.2773	0	0	.172	.633	1.511
1137201	5.374	.4394	0	0	.058	.758	1.472
1138201	5.880	.7527	0	0	.395	.624	1.442
1139201	5.761	1.3006	0	0	.273	.711	1.429
1139202	6.368	1.3119	.304	752.4	.212	.773	1.411
1139203	7.052	1.3002	.359	1058.5	.195	.803	1.398
1139204	7.216	1.3070	.410	1437.3	.131	.576	1.560
1139205	7.533	1.3042	.459	1921.6	.139	.734	1.459
1139206	7.876	1.2889	.484	2393.4	.080	.896	1.379
1139207	8.832	1.3002	.475	2990.4	.185	1.126	1.201
1139208	10.522	1.2970	.487	4133.7	.159	1.062	1.250
1139209	10.156	1.2957	.483	3881.2	.207	1.084	1.220
1137202	5.835	.5035	.332	668.2	.003	1.154	1.245
1137203	5.937	.4344	.459	1624.1	.012	1.001	1.337
1137204	6.368	.4971	.565	2488.9	.022	1.176	1.225
1137205	6.507	.4951	.594	2922.7	.025	1.220	1.197
1137206	6.704	.4980	.610	3147.8	.021	1.139	1.248
1137207	7.299	.4827	.635	3729.0	.013	1.016	1.327
*** RUN 114 *** .01ST = 19 . HB = .567 . EPS = .3784 . VIS = .00111							

RUN NO.	TOTAL HOLD-UP (PCT.)	LIQUID VELOCITY (MM/S)	GAS VELOCITY (M/S)	PRESSURE DROP (N/M3)	RELATIVE LIQUID FLUX		
					INNER (-)	MIDDLE (-)	OUTER (-)
1144101	4.590	.1222	0	0	.340	1.101	1.165
1143101	4.446	.0624	0	0	.329	1.005	1.229
1142101	4.356	.0305	0	0	.566	1.217	1.021
1141101	4.331	.0159	0	0	.289	1.099	1.185
1142201	4.456	.0311	0	0	.882	.858	1.135
1142202	4.438	.0306	.331	601.3	.162	1.039	1.262
1142203	4.324	.0312	.459	1081.0	.138	1.109	1.232
1142204	4.423	.0302	.622	1997.7	.016	.521	1.637
1142205	4.458	.0285	.678	2407.6	0	1.017	1.343
1142206	4.608	.0303	.737	2962.8	.024	1.371	1.103
1142207	4.625	.0301	.768	3258.5	.027	2.001	.712
1142208	4.740	.0312	.829	3848.3	.058	3.079	.039
1142209	6.547	.0411	.870	3338.1	.211	2.937	.075
1142210	5.345	.0299	.867	4728.7	.157	2.808	.179
1142211	6.084	.0179	.896	5230.2	.184	2.942	.076
1144301	4.705	.1125	0	0	.330	1.403	.981
1144302	4.645	.1107	.331	617.5	.325	1.275	1.062
1144303	4.643	.1098	.458	1136.3	.083	1.332	1.108
1144304	4.740	.1109	.621	2122.2	.037	2.158	.612
1144305	4.797	.1114	.678	2556.3	.013	2.040	.693
1144306	4.852	.1139	.738	3090.8	.027	2.419	.454
1144307	5.053	.1118	.797	3763.6	.011	1.843	.615
1144308	5.785	.1204	.768	3964.2	.044	1.957	.791
1144401	4.406	.1136	0	0	.452	1.126	1.111
*** RUN 115 *** .01ST = 71 . HB = .567 . EPS = .3784 . VIS = .00115							
1154101	4.456	.0608	0	0	.461	1.362	.965
1153101	4.396	.0336	0	0	.765	1.084	1.031
1153102	4.369	.0329	.331	612.3	.344	1.362	1.003
1153103	4.314	.0327	.459	1091.4	.771	1.182	.072
1153104	4.346	.0336	.621	1937.3	.324	.753	1.382
1153105	4.623	.0323	.735	2342.0	0	.826	1.453
1153106	4.784	.0357	.796	3088.9	.203	1.404	1.048
1153107	5.505	.0326	.863	3369.2	0	1.075	1.300
1153108	6.362	.0340	.898	4056.7	.204	1.079	1.227
1153109	8.484	.0288	.930	7312.7	.252	1.104	1.136

EXPERIMENTAL RESULTS FOR ■■ PL13/ETOH ■■ SYSTEM

NO. 1

PACKING : PLASTIC SPHERES

AVERAGE SIZE = 13.2 (MM) . APPARENT DENSITY = 921. (KG/M3)

LIQUID : ETHANOL - WATER

DENSITY = 807.(KG/M3) . NOMINAL VISCOSITY = .0016 (NS/M2)

SURFACE TENSION = .0240 (N/M) . CONTACT ANGLE = 0 (DEG.)

RUN NO.	TOTAL HOLD-UP (PCT.)	LIQUID VELOCITY (MM/S)	GAS VELOCITY (M/S)	PRESSURE DROP (N/M3)	RELATIVE LIQUID FLUX		
					INNER (-)	MIDDLE (-)	OUTER (-)
*** RUN 241 *** . DIST = 19 . HB = .425 . EPS = .4106 . VIS = .00161							
2418101	3.477	.5672	0	0	1.151	.825	1.064
2417101	3.132	.3040	0	0	1.537	.894	.893
2419101	3.988	.9913	0	0	.772	.759	1.232
2416101	2.872	.1399	0	0	1.422	.868	.946
2415101	2.601	.0502	0	0	1.363	.863	.968
2416201	2.840	.0880	0	0	2.231	1.085	.541
2413101	2.979	.2008	0	0	1.452	.629	1.084
2414201	3.513	.0558	0	0	1.381	1.182	.764
2418201	3.483	.4483	0	0	1.111	1.356	.742
2417201	3.058	.3148	0	0	.808	1.111	1.002
2419201	3.938	.9789	0	0	.659	.994	1.124
*** RUN 242 *** . DIST = 19 . HB = .425 . EPS = .4106 . VIS = .00161							
2429101	2.867	.0960	0	0	1.190	.681	1.142
2426101	2.329	.0115	0	0	.806	1.401	.817
2428101	2.527	.0481	0	0	.829	1.052	1.029
2427101	2.407	.0199	0	0	1.021	.989	1.609
*** RUN 251 *** . DIST = 19 . HB = .425 . EPS = .4106 . VIS = .00156							
2519101	2.712	.0951	0	0	.733	1.367	.870
2517101	2.449	.0210	0	0	.877	1.391	.817
2518101	2.551	.0448	0	0	.731	1.523	.775
2516101	2.294	.0042	0	0	.853	1.016	1.037
*** RUN 262 *** . DIST = 19 . HB = .425 . EPS = .4106 . VIS = .00156							
2629101	3.922	.9289	0	0	1.149	.432	1.307
2624101	2.535	.0391	0	0	.931	1.162	.925
2627101	3.070	.3054	0	0	1.308	1.001	.903
2626101	2.835	.1478	0	0	.822	1.111	.397
2628101	3.457	.5759	0	0	1.300	.712	1.084
2625101	2.597	.0761	0	0	.798	1.173	.959

EXPERIMENTAL RESULTS FOR ■■ AL13/ETOH ■■ SYSTEM

NO. 1

PACKING : ALUMINA SPHERES

AVERAGE SIZE = 13.1 (MM) . APPARENT DENSITY = 3465. (KG/M3)

LIQUID : ETHANOL - WATER

DENSITY = 807.(KG/M3) . NOMINAL VISCOSITY = .0016 (NS/M2)

SURFACE TENSION = .0240 (N/M) . CONTACT ANGLE = 0 (DEG.)

RUN NO.	TOTAL HOLD-UP (PCT.)	LIQUID VELOCITY (MM/S)	GAS VELOCITY (M/S)	PRESSURE DROP (N/M3)	RELATIVE LIQUID FLUX		
					INNER (-)	MIDDLE (-)	OUTER (-)
*** RUN 251 *** . DIST = 19 . HB = .430 . EPS = .4130 . VIS = .00151							
2518101	4.039	.7166	0	0	1.370	.877	.959
2519101	4.303	1.0027	0	0	1.257	.626	1.152
2517101	3.384	.2735	0	0	1.105	1.079	.922
2515101	2.847	.0495	0	0	1.099	.755	1.124
2518201	3.762	.5571	0	0	1.480	.892	.912
2516101	3.059	.1261	0	0	1.326	.979	.972
*** RUN 252 *** . DIST = 19 . HB = .430 . EPS = .4130 . VIS = .00151							
2529101	2.912	.1065	0	0	.683	.755	1.263
2526101	2.546	.0114	0	0	1.448	.528	1.030
2528101	2.762	.0453	0	0	1.075	.769	1.126
2527101	2.644	.0203	0	0	1.356	.349	1.298
*** RUN 271 *** . DIST = 19 . HB = .430 . EPS = .4130 . VIS = .00157							
2718101	3.852	.5614	0	0	.599	.393	1.516
2715101	2.953	.0616	0	0	1.093	.686	1.168
2717101	3.478	.3085	0	0	.493	.716	1.352
2719101	4.368	1.0104	0	0	.937	.288	1.468
2716101	3.197	.1511	0	0	.770	.662	1.292
*** RUN 272 *** . DIST = 19 . HB = .430 . EPS = .4130 . VIS = .00157							
2729101	3.059	.0967	0	0	1.072	.520	1.219
2726101	2.615	.0058	0	0	.904	1.084	1.022
2728101	2.888	.0460	0	0	1.103	.756	1.128
2727101	2.758	.0194	0	0	.816	.959	1.075

EXPERIMENTAL RESULTS FOR ■■ C8/ETOH ■■ SYSTEM

NO. 1

PACKING : GLASS SPHERES
 AVERAGE SIZE = 8.1 (MM) . APPARENT DENSITY = 2500. (KG/M3)
 LIQUID : ETHANOL - WATER
 DENSITY = 807.(KG/M3) . NOMINAL VISCOSITY = .0016 (NS/M2)
 SURFACE TENSION = .0240 (N/M) . CONTACT ANGLE = 0 (DEG.)

RUN NO.	TOTAL HOLD-UP (PCT.)	LIQUID VELOCITY (MM/S)	GAS VELOCITY (M/S)	PRESSURE DROP (N/M3)	RELATIVE LIQUID FLUX		
					INNER (-)	MIDDLE (-)	OUTER (-)
■■■ RUN 291 ■■■ . DIST = 19 . HB = .391 . EPS = .3890 . VIS = .00158							
2915101	4.291	.0845	0	0	.829	.802	1.187
2919101	5.851	.9476	0	0	1.031	.632	1.223
2916101	4.446	.1233	0	0	.257	.475	1.580
2918101	5.278	.5140	0	0	.522	.295	1.603
2917101	4.613	.2396	0	0	.812	.534	1.357
■■■ RUN 292 ■■■ . DIST = 19 . HB = .391 . EPS = .3890 . VIS = .00158							
2929101	4.370	.1641	0	0	1.082	.467	1.309
2925101	4.106	.0133	0	0	1.746	.825	.867
2927101	4.241	.0458	0	0	1.230	.850	1.021

EXPERIMENTAL RESULTS FOR ■■ PL9/ETOH ■■ SYSTEM

NO. 1

PACKING : PLASTIC SPHERES
 AVERAGE SIZE = 9.0 (MM) . APPARENT DENSITY = 921. (KG/M3)
 LIQUID : ETHANOL - WATER
 DENSITY = 807.(KG/M3) . NOMINAL VISCOSITY = .0016 (NS/M2)
 SURFACE TENSION = .0240 (N/M) . CONTACT ANGLE = 0 (DEG.)

RUN NO.	TOTAL HOLD-UP (PCT.)	LIQUID VELOCITY (MM/S)	GAS VELOCITY (M/S)	PRESSURE DROP (N/M3)	RELATIVE LIQUID FLUX		
					INNER (-)	MIDDLE (-)	OUTER (-)
■■■ RUN 281 ■■■ . DIST = 19 . HB = .414 . EPS = .3951 . VIS = .00161							
2819101	3.388	.0909	0	0	.974	.744	1.174
2816101	3.063	.0049	0	0	1.169	.860	1.057
2818101	3.295	.0422	0	0	1.689	.531	1.064
2817101	3.190	.0170	0	0	1.242	.849	1.023
■■■ RUN 282 ■■■ . DIST = 19 . HB = .414 . EPS = .3951 . VIS = .00161							
2829101	5.146	.9945	0	0	.996	.349	1.410
2825101	3.506	.0441	0	0	.970	.840	1.239
2828101	4.571	.5371	0	0	.800	.451	1.413
2827101	4.077	.2473	0	0	1.022	.508	1.304
2826101	3.806	.1167	0	0	1.105	.906	1.030

EXPERIMENTAL RESULTS FOR ** PL13/GLY ** SYSTEM

NO. 1

PACKING : PLASTIC SPHERES
 AVERAGE SIZE = 13.2 (MM) . APPARENT DENSITY = 921. (KG/M3)
 LIQUID : GLYCEROL - WATER
 DENSITY = 1210.(KG/M3) . NOMINAL VISCOSITY = .0640 (NS/M2)
 SURFACE TENSION = .0652 (N/M) . CONTACT ANGLE = 88.1 (DEG.)

RUN NO.	TOTAL HOLD-UP (PCT.)	LIQUID VELOCITY (MM/S)	GAS VELOCITY (M/S)	PRESSURE DROP (N/M3)	RELATIVE LIQUID FLUX		
					INNER (-)	MIDDLE (-)	OUTER (-)
*** RUN 330 ***							
*** GAS PRESSURE DROP THROUGH DRY BED *** HB = .425 . EPS = .4106							
3300001	0	0	.463	253.8	0	0	0
3300002	0	0	.646	459.2	0	0	0
3300003	0	0	.855	756.8	0	0	0
3300004	0	0	1.079	1149.1	0	0	0
3300005	0	0	1.295	1578.3	0	0	0
3300006	0	0	1.556	2215.2	0	0	0
3300007	0	0	1.832	2925.9	0	0	0
*** RUN 331 *** . DIST = 19 . HB = .425 . EPS = .4106 . VIS = .06370							
3319101	3.911	.3813	0	0	1.765	1.252	.594
3319102	4.057	.3901	.378	249.2	1.724	1.251	.608
3319103	4.254	.4119	.489	433.8	1.528	1.004	.827
3319104	4.556	.4318	.628	761.5	1.230	1.486	.628
3319105	5.349	.4748	.758	1756.0	.699	.499	1.417
3319106	7.509	.4924	.840	3073.5	.418	.371	1.591
3319107	12.477	.4601	.855	4524.9	.696	.759	1.258
*** RUN 332 *** . DIST = 19 . HB = .425 . EPS = .4106 . VIS = .07180							
3328101	3.343	.2233	0	0	1.474	1.142	.759
3329101	3.741	.4020	0	0	1.689	.977	.790
3327101	2.983	.1113	0	0	1.598	1.385	.568
3324101	2.456	.0104	0	0	1.590	.971	.833
3325101	2.657	.0234	0	0	1.789	.959	.771
3326101	2.860	.0505	0	0	2.043	.725	.827
3327201	3.069	.1088	0	0	1.793	.874	.819
3327202	3.137	.1106	.452	316.1	1.634	.912	.849
3327203	3.222	.1138	.634	632.2	2.260	.945	.617
3327204	3.906	.1128	.805	1479.1	1.391	.251	1.339
3327205	4.806	.1165	.951	2535.9	.238	.235	1.736
3327206	6.241	.1177	1.081	3576.6	.057	.714	1.499
3327207	8.036	.1135	1.125	4358.0	.941	.898	1.090
3327208	10.210	.1154	1.140	4984.9	1.019	.699	1.187
*** RUN 333 *** . DIST = 19 . HB = .425 . EPS = .4106 . VIS = .05360							
3337101	3.118	.1143	0	0	1.835	.934	.767
3334101	2.528	.0140	0	0	1.671	1.061	.747
3338101	3.395	.2397	0	0	2.496	.809	.623
3335101	2.907	.0587	0	0	2.118	1.021	.618
3339101	3.895	.4395	0	0	2.607	1.412	.212
3339201	3.911	.4380	0	0	1.406	1.435	.601
3335101	2.728	.0289	0	0	1.184	1.117	.871
*** RUN 340 ***							
*** GAS PRESSURE DROP THROUGH DRY BED *** HB = .425 . EPS = .4106							
3400001	0	0	.446	237.7	0	0	0
3400002	0	0	.655	475.3	0	0	0
3400003	0	0	.856	770.7	0	0	0

EXPERIMENTAL RESULTS FOR ** PL13/GLY ** SYSTEM

NO. 2

RUN NO.	TOTAL HOLD-UP (PCT.)	LIQUID VELOCITY (MM/S)	GAS VELOCITY (M/S)	PRESSURE DROP (N/M3)	RELATIVE LIQUID FLUX		
					INNER (-)	MIDDLE (-)	OUTER (-)
3400004	0	0	1.082	1174.5	0	0	0
3400005	0	0	1.328	1689.1	0	0	0
3400006	0	0	1.559	2293.6	0	0	0
3400007	0	0	1.819	3032.0	0	0	0
*** RUN 341 *** . DIST = 19 . HB = .425 . EPS = .4106 . VIS = .06870							
3417101	2.907	.1074	0	0	1.048	1.850	.458
3417102	3.058	.1060	.456	354.6	1.422	1.397	.620
3417103	3.154	.1028	.625	632.2	2.649	.969	.472
3417104	4.046	.1028	.805	1730.6	.784	.909	1.136
3417105	4.444	.1105	.920	2339.8	.162	.353	1.688
3417106	6.387	.1075	1.064	3544.3	.735	.638	1.553
3417107	8.393	.1070	1.138	4548.0	.097	1.215	1.176
3417108	10.965	.0943	1.177	5279.5	.096	1.000	1.310
*** RUN 342 *** . DIST = 19 . HB = .425 . EPS = .4106 . VIS = .06280							
3427101	3.008	.1117	0	0	1.527	1.626	.442
3429101	3.914	.4076	0	0	1.451	1.709	.416
3428101	3.453	.2405	0	0	1.454	1.782	.370
3424101	2.418	.0147	0	0	1.536	1.505	.517
3426101	2.775	.0533	0	0	1.901	1.121	.531
3425101	2.574	.0272	0	0	1.292	1.345	.699
3425102	2.654	.0245	.451	316.1	2.575	1.322	.279
3425103	2.668	.0239	.677	731.5	1.877	1.438	.439
3425104	2.986	.0177	.920	1577.5	.362	.665	1.433
3425105	4.334	.0128	1.199	3212.0	.074	.406	1.691
*** RUN 343 *** . DIST = 19 . HB = .425 . EPS = .4106 . VIS = .06380							
3436101	2.898	.0731	0	0	2.145	1.093	.564
3435101	2.690	.0352	0	0	2.280	1.187	.460
3434101	2.385	.0073	0	0	.780	2.488	.168
3438101	3.115	.1548	0	0	2.225	1.464	.309
3439101	3.491	.2802	0	0	1.946	1.648	.289
3435101	2.547	.0187	0	0	.990	2.147	.305
3435102	2.618	.0185	.459	327.7	1.578	1.677	.396
3435103	2.654	.0178	.677	747.6	2.289	1.114	.506
3435104	3.003	.0168	.931	1767.5	.467	.620	1.420
3435105	4.850	.0173	1.214	3574.3	0	.295	1.780
3435106	7.430	.0153	1.484	5327.9	.179	.945	1.323
3435107	8.272	.0139	1.615	5849.4	2.005	.907	.735
*** RUN 344 *** . DIST = 19 . HB = .425 . EPS = .4106 . VIS = .05750							
3445101	2.500	.0182	0	0	1.473	1.453	.564
3445102	2.551	.0191	.659	662.2	1.715	1.647	.369
3445103	3.005	.0171	.937	1533.7	.358	.293	1.666
3445105	5.863	.0199	1.411	4469.5	.554	1.233	1.009
3445106	7.507	.0233	1.625	5477.9	2.114	.755	.783

EXPERIMENTAL RESULTS FOR ■■ W13/GLY ■■ SYSTEM

NO. 1

PACKING : MAX-COATED SPHERES
 AVERAGE SIZE = 13.3 (MM) . APPARENT DENSITY = 921. (KG/M3)
 LIQUID : GLYCEROL - WATER
 DENSITY = 1210.(KG/M3) . NOMINAL VISCOSITY = .0640 (NS/M2)
 SURFACE TENSION = .0652 (N/M) . CONTACT ANGLE = 96.6 (DEG.)

RUN NO.	TOTAL HOLD-UP (PCT.)	LIQUID VELOCITY (MM/S)	GAS VELOCITY (M/S)	PRESSURE DROP (N/M3)	RELATIVE LIQUID FLUX		
					INNER (-)	MIDDLE (-)	OUTER (-)
*** RUN300 ***							
*** GAS PRESSURE DROP THROUGH DRY BED *** HB = .430 . EPS = .4180							
3000001	0	0	.462	225.8	0	0	0
3000002	0	0	.650	417.4	0	0	0
3000003	0	0	.861	702.4	0	0	0
3000004	0	0	1.115	1117.5	0	0	0
3000005	0	0	1.397	1683.1	0	0	0
3000006	0	0	1.621	2225.9	0	0	0
3000007	0	0	1.830	2784.6	0	0	0
*** RUN 301 *** . DIST = 71 . HB = .430 . EPS = .4180 . VIS = .06430							
3018101	2.794	.1794	0	0	2.297	1.283	.396
3019101	3.345	.3768	0	0	1.919	1.372	.468
3017101	2.496	.0833	0	0	2.170	1.752	.149
3016101	2.374	.0334	0	0	.697	1.979	.504
3017201	2.482	.0721	0	0	1.419	1.689	.438
3017202	2.528	.0721	.457	305.6	1.228	1.443	.657
3017203	2.539	.0729	.624	561.0	.392	2.099	.529
3017204	2.686	.0699	.865	1154.0	.112	.773	1.444
3017205	4.169	.0670	1.117	2700.3	.051	.055	1.913
3017206	4.905	.0656	1.238	3425.5	.011	.018	1.945
3017207	6.028	.0614	1.366	4285.3	.492	.505	1.483
3017208	9.440	.0511	1.410	5560.2	1.025	.771	1.140
*** RUN 302 *** . DIST = 71 . HB = .430 . EPS = .4180 . VIS = .07280							
3028101	3.255	.1674	0	0	2.429	1.027	.510
3025101	2.648	.0163	0	0	1.570	1.629	.430
3026101	2.737	.0383	0	0	2.325	1.311	.372
3027101	2.839	.0777	0	0	2.449	1.237	.373
3028201	3.125	.1785	0	0	1.957	1.655	.280
3029101	3.554	.3726	0	0	2.362	1.474	.255
3029102	3.573	.3852	.452	314.7	2.549	1.359	.254
3029103	3.657	.3930	.620	595.2	3.302	.890	.303
3029104	4.614	.3863	.821	1594.2	.585	.375	1.532
3029105	5.187	.3753	.920	2159.8	.328	.545	1.512
3029106	9.071	.3567	1.006	3920.4	.504	.583	1.431
*** RUN 303 *** . DIST = 71 . HB = .430 . EPS = .4180 . VIS = .06290							
3039101	2.937	.1441	0	0	4.190	.670	.142
3035101	2.490	.0105	0	0	3.378	.764	.362
3038101	2.757	.0834	0	0	3.104	1.373	.070
3037101	2.634	.0442	0	0	3.763	.890	.149
3036101	2.553	.0215	0	0	2.587	1.575	.118
3036102	2.591	.0220	.458	301.0	2.605	1.250	.315
3036103	2.547	.0231	.651	593.8	2.235	1.350	.391
3036104	2.648	.0212	.857	1133.5	.601	.549	1.360
3036105	3.646	.0240	1.131	2469.9	.069	.100	1.879
3036106	4.891	.0258	1.336	3763.0	.177	.132	1.833

EXPERIMENTAL RESULTS FOR ■■ W13/GLY ■■ SYSTEM

NO. 2

RUN NO.	TOTAL HOLD-UP (PCT.)	LIQUID VELOCITY (MM/S)	GAS VELOCITY (M/S)	PRESSURE DROP (N/M3)	RELATIVE LIQUID FLUX		
					INNER (-)	MIDDLE (-)	OUTER (-)
3036107	8.859	.0236	1.424	4547.6	1.682	.687	.972
3036108	8.225	.0185	1.515	5414.2	1.556	.500	1.134
*** RUN 304 *** . DIST = 19 . HB = .430 . EPS = .4180 . VIS = .06570							
3047101	3.149	.0635	0	0	1.007	1.483	.707
3045101	2.764	.0149	0	0	.982	1.338	.804
3048101	3.383	.1322	0	0	1.293	1.303	.721
3046101	2.932	.0349	0	0	1.023	1.421	.738
3049101	3.746	.2538	0	0	.319	1.513	.917
3046201	3.136	.0709	0	0	.775	1.411	.826
3044101	2.707	.0086	0	0	.853	1.297	.877
3049201	3.681	.2594	0	0	1.540	1.419	.565
3046301	3.117	.1439	0	0	1.341	1.318	.696
*** RUN 305 *** . DIST = 13 . HB = .430 . EPS = .4180 . VIS = .06570							
3057101	2.955	.0640	0	0	.905	1.734	.585
3059101	3.364	.2278	0	0	1.545	1.792	.333
3058101	3.133	.1388	0	0	.414	2.041	.558
3055101	2.659	.0166	0	0	2.001	1.363	.453
3056101	2.775	.0297	0	0	2.291	1.354	.359
*** RUN 306 *** . DIST = 71 . HB = .430 . EPS = .4180 . VIS = .06570							
3068101	2.941	.0941	0	0	2.961	1.054	.317
3067101	2.781	.0514	0	0	3.149	1.262	.123
3066101	3.106	.1662	0	0	3.161	1.359	.959
3069101	2.661	.0188	0	0	2.659	.983	.392
*** RUN320 ***							
*** GAS PRESSURE DROP THROUGH DRY BED *** HB = .425 . EPS = .4106							
3200001	0	0	.469	246.9	0	0	0
3200002	0	0	.624	417.7	0	0	0
3200003	0	0	.826	687.6	0	0	0
3200004	0	0	1.053	1058.4	0	0	0
3200005	0	0	1.306	1578.3	0	0	0
3200006	0	0	1.526	2097.5	0	0	0
3200007	0	0	1.814	2856.6	0	0	0
*** RUN 321 *** . DIST = 19 . HB = .425 . EPS = .4106 . VIS = .06370							
3218101	3.165	.1571	0	0	1.146	1.294	.776
3217101	2.819	.0612	0	0	1.277	1.020	.900
3217102	2.920	.0639	.453	346.1	1.451	1.223	.719
3217103	3.063	.0607	.635	692.2	1.415	1.027	.653
3217104	3.354	.0618	.805	1227.6	.359	.642	1.277
3217105	4.659	.0591	.999	2515.1	.039	.146	1.836
3217106	5.972	.0594	1.186	3655.0	.005	.351	1.745
3217108	8.201	.0505	1.296	4790.3	.069	1.773	.842
3217109	11.412	.0479	1.322	5997.1	1.386	1.850	.349
*** RUN 322 *** . DIST = 19 . HB = .425 . EPS = .4106 . VIS = .06310							
3229101	4.144	.3804	0	0	.570	1.187	.901
3229102	4.229	.3967	.380	263.1	.865	1.134	.969
3229103	4.334	.4182	.464	394.6	.980	1.095	.953
3229104	4.573	.4196	.586	673.8	.438	.982	1.205
3229105	4.825	.4175	.676	955.9	.934	.651	1.244
3229106	5.703	.4114	.766	1746.7	.180	.346	1.686
3229107	6.818	.4214	.863	2579.0	.165	.407	1.653
3229108	9.392	.4256	.923	3895.0	.447	1.218	1.057

EXPERIMENTAL RESULTS FOR ■■ W13/GLY ■■ SYSTEM

NO. 3'

RUN NO.	TOTAL HOLD-UP (PCT.)	LIQUID VELOCITY (MM/S)	GAS VELOCITY (M/S)	PRESSURE DROP (N/M3)	RELATIVE LIQUID FLUX		
					INNER (-)	MIDDLE (-)	OUTER (-)
3229109	13.339	.3743	.937	5254.1	.508	1.243	1.021
3225102	4.158	.0218	.940	1968.3	0	.523	1.642
3225103	5.368	.0244	1.339	4111.9	.906	1.395	.790
3225104	9.545	.0163	1.476	5826.3	2.602	.758	.629
■■■ RUN 323 ■■■ .DIST = 71 . HB = .425 . EPS = .4105 . VIS = .06820							
3237101	3.134	.0990	0	0	2.957	1.268	.185
3237102	3.241	.1025	.458	327.7	.994	1.991	.394
3237103	3.357	.0950	.625	623.0	1.753	1.715	.313
3237104	3.664	.0892	.852	1416.8	.738	1.042	1.069
3237105	5.325	.0901	1.071	2773.6	.079	.763	1.462
3237106	6.411	.0871	1.158	3578.9	.680	1.293	.932
3237107	7.368	.0880	1.192	4259.6	1.574	1.364	.590
3237108	12.041	.0773	1.253	5957.9	1.509	1.317	.640
■■■ RUN 324 ■■■ .DIST = 71 . HB = .425 . EPS = .4105 . VIS = .07730							
3247101	3.214	.0734	0	0	2.500	1.193	.383
3248101	3.915	.2597	0	0	2.050	1.307	.465
3248101	3.510	.1536	0	0	2.238	1.201	.467
3246101	3.036	.0394	0	0	2.211	1.038	.580
3245101	2.887	.0184	0	0	2.912	.840	.465
■■■ RUN 325 ■■■ .DIST = 19 . HB = .425 . EPS = .4105 . VIS = .06780							
3259101	4.153	.3596	0	0	1.425	1.301	.677
3259101	3.744	.2242	0	0	.605	1.491	.835
3257101	3.453	.1103	0	0	.718	1.551	.753
3255101	3.211	.0532	0	0	1.625	1.297	.613
3255101	3.011	.0262	0	0	1.980	1.132	.594
■■■ RUN 360 ■■■							
■■■ GAS PRESSURE DROP THROUGH DRY BED ■■■ HB = .430 . EPS = .4180							
3600001	0	0	.456	225.8	0	0	0
3600002	0	0	.679	465.2	0	0	0
3600003	0	0	.967	887.2	0	0	0
3600004	0	0	1.243	1398.0	0	0	0
3600005	0	0	1.501	1979.6	0	0	0
3600006	0	0	1.798	2764.1	0	0	0
■■■ RUN 381 ■■■ .DIST = 19 . HB = .430 . EPS = .4180 . VIS = .07330							
3810101	2.260	.0142	0	0	.537	1.513	.848
3810102	2.387	.0153	.453	291.9	.598	1.489	.844
3810103	2.417	.0164	.682	661.4	1.086	1.202	.856
3810104	2.506	.0164	.915	1363.8	.850	.728	1.229
3810105	4.376	.0194	1.197	2987.6	.028	.494	1.645
3810106	5.376	.0182	1.347	4036.7	.877	.629	1.276
3810107	7.178	.0198	1.421	4647.9	.750	.784	1.222
3810108	7.549	.0202	1.463	4793.9	.595	.873	1.220
3810109	8.295	.0176	1.527	5277.4	.829	1.218	.827
■■■ RUN 382 ■■■ .DIST = 19 . HB = .430 . EPS = .4180 . VIS = .05460							
3827101	2.921	.0933	0	0	1.127	1.237	.818
3827201	2.433	.0905	0	0	1.025	1.246	.847
3828101	3.325	.0220	0	0	.093	1.422	.753
3824101	3.199	.0131	0	0	.736	1.408	.840
3826101	3.493	.0509	0	0	.953	1.423	.762
3825101	3.243	.0252	0	0	1.190	1.079	.894
3823101	3.633	.4771	0	0	.647	1.866	.625

EXPERIMENTAL RESULTS FOR ■■ W13/GLY ■■ SYSTEM

NO. 4

RUN NO.	TOTAL HOLD-UP (PCT.)	LIQUID VELOCITY (MM/S)	GAS VELOCITY (M/S)	PRESSURE DROP (N/M3)	RELATIVE LIQUID FLUX		
					INNER (-)	MIDDLE (-)	OUTER (-)
3829102	3.933	.5009	.367	228.1	.909	1.618	.654
3829103	3.988	.5002	.513	456.1	1.454	1.132	.772
3829104	4.490	.4874	.675	1040.0	.777	.775	1.220
3829105	4.552	.4828	.763	1434.5	.420	.619	1.437
3829106	5.347	.4632	.886	2253.3	.197	.868	1.357
3829107	7.631	.4738	.965	3329.7	.376	1.169	1.111
3829108	12.826	.4843	.987	5277.4	.377	.974	1.231
■■■ RUN 383 ■■■ .DIST = 19 . HB = .430 . EPS = .4180 . VIS = .05870							
3838101	3.025	.1345	0	0	1.229	1.289	.750
3838102	3.171	.1380	.448	314.7	.929	1.282	.856
3838103	3.244	.1423	.671	736.6	.908	.965	1.093
3838104	3.866	.1472	.924	1799.4	.195	.269	1.729
3838105	6.578	.1532	1.127	3587.4	.378	.691	1.407
3838106	8.797	.1504	1.266	4734.6	.668	.492	1.432
3838107	10.517	.1428	1.333	5252.3	.340	.442	1.573
3835102	7.734	.0171	1.533	5129.1	.477	1.553	.938
3835103	9.568	.0220	1.695	5993.5	1.157	1.272	.792
3835104	8.537	.0176	1.632	5758.6	1.073	1.552	.653
3835105	6.056	.0166	1.305	3975.1	.836	.778	1.208

EXPERIMENTAL RESULTS FOR ** AL13/GLY ** SYSTEM

NO. 1

PACKING : ALUMINA SPHERES
 AVERAGE SIZE = 13.1 (MM) . APPARENT DENSITY = 3465. (KG/M3)
 LIQUID : GLYCEROL - WATER
 DENSITY = 1210.(KG/M3) . NOMINAL VISCOSITY = .0640 (NS/M2)
 SURFACE TENSION = .0652 (N/M) . CONTACT ANGLE = 0 (DEG.)

RUN NO.	TOTAL	LIQUID	GAS	PRESSURE	RELATIVE LIQUID FLUX		
	HOLD-UP (PCT.)	VELOCITY (MM/S)	VELOCITY (M/S)	DROP (N/M3)	INNER (-)	MIDDLE (-)	OUTER (-)
*** RUN310 ***							
*** GAS PRESSURE DROP THROUGH DRY BED *** HB = .425 , EPS = .4047							
3100001	0	0	.463	263.1	0	0	0
3100002	0	0	.628	452.3	0	0	0
3100003	0	0	.837	763.8	0	0	0
3100004	0	0	1.058	1186.0	0	0	0
3100005	0	0	1.327	1806.7	0	0	0
3100006	0	0	1.587	2487.4	0	0	0
3100007	0	0	1.803	3172.8	0	0	0
*** RUN 311 *** . DIST = 19 . HB = .425 . EPS = .4047 . VIS = .06240							
3118101	4.935	.1385	0	0	1.266	1.516	.598
3115101	3.549	.0169	0	0	3.285	.721	.419
3119101	5.610	.2805	0	0	1.123	1.528	.638
3117101	4.260	.0769	0	0	1.180	1.508	.633
3116101	3.870	.0379	0	0	1.052	1.395	.746
3114101	3.450	.0070	0	0	1.978	.786	.820
*** RUN 312 *** . DIST = 13 . HB = .425 . EPS = .4047 . VIS = .06220							
3128101	4.754	.1301	0	0	1.288	1.826	.399
3127101	4.254	.0637	0	0	2.099	1.344	.424
3129101	5.399	.2291	0	0	1.673	1.410	.527
3126101	3.793	.0405	0	0	1.589	.911	.865
3125101	3.568	.0155	0	0	2.471	.802	.644
*** RUN 313 *** . DIST = 71 . HB = .425 . EPS = .4047 . VIS = .06920							
3138101	4.339	.0389	0	0	1.695	1.420	.514
3139101	4.674	.1711	0	0	1.601	1.293	.623
3137101	3.941	.0488	0	0	1.059	1.268	.823
3136101	3.581	.0222	0	0	1.203	1.353	.724
3138201	4.358	.0326	0	0	1.303	1.854	.376
3135201	3.653	.0212	0	0	1.831	1.413	.473
3135202	3.815	.0211	.459	359.2	1.121	1.092	.910
3135203	3.848	.0204	.653	745.3	1.066	1.091	.929
3136204	3.892	.0204	.866	1289.3	.752	.724	1.265
3136205	4.564	.0201	1.051	2658.9	2.213	.298	1.030
3136206	5.513	.0190	1.157	4135.0	1.725	.383	1.151
3136207	8.297	.0197	1.184	5574.8	1.270	.242	1.399
*** RUN 314 *** . DIST = 71 . HB = .425 . EPS = .4047 . VIS = .06890							
3148101	5.198	.1793	0	0	2.057	1.036	.630
3149101	5.296	.3813	0	0	2.302	.982	.581
3147101	4.562	.1002	0	0	1.078	1.600	.610
3145101	3.672	.0254	0	0	.904	.834	1.140
3146101	3.905	.0495	0	0	.382	1.168	1.109
3147201	4.472	.0987	0	0	1.625	1.328	.593
3147202	4.666	.0975	.438	422.3	1.025	1.791	.509
3147203	4.685	.1023	.645	844.5	1.267	1.619	.534
3147204	5.950	.1026	.847	2385.9	.797	.715	1.250

EXPERIMENTAL RESULTS FOR ** AL13/GLY ** SYSTEM

NO. 2

RUN NO.	TOTAL	LIQUID	GAS	PRESSURE	RELATIVE LIQUID FLUX		
	HOLD-UP (PCT.)	VELOCITY (MM/S)	VELOCITY (M/S)	DROP (N/M3)	INNER (-)	MIDDLE (-)	OUTER (-)
3147205	7.183	.1000	.929	3721.9	1.207	.783	1.121
3147206	10.070	.1024	.942	4977.2	1.481	1.193	.783
*** RUN 315 *** . DIST = 71 . HB = .425 . EPS = .4047 . VIS = .06560							
3157101	4.433	.0988	0	0	1.117	1.843	.755
3155101	4.015	.0490	0	0	.716	1.942	.619
3155101	3.656	.0236	0	0	.524	1.124	1.033
3158101	5.116	.2048	0	0	.735	1.434	.775
3159101	6.307	.4178	0	0	1.630	1.158	.691
3159102	6.713	.4237	.462	623.0	1.651	.822	.398
3159103	8.034	.4375	.539	1857.5	1.227	.870	1.011
3159104	7.611	.4249	.490	1423.7	.677	1.216	.981
3159105	8.593	.4287	.565	2270.5	1.141	.820	1.070
3159106	9.225	.4415	.593	2692.8	.751	.843	1.187
3159107	12.082	.4448	.622	4024.2	1.205	.615	1.175
*** RUN 316 *** . DIST = 19 . HB = .425 . EPS = .4047 . VIS = .06290							
3168101	4.905	.1554	0	0	.617	1.492	.829
3167101	4.326	.0762	0	0	1.368	1.317	.787
3165101	3.672	.0203	0	0	1.889	1.419	.444
3166101	3.859	.0393	0	0	.593	.839	1.244
3169101	5.745	.2738	0	0	2.105	.827	.581
3164101	4.603	.0315	0	0	1.427	1.398	.619
3164102	4.715	.1005	.456	422.3	1.055	1.243	.838
3164103	4.776	.1029	.657	934.5	.799	1.314	.880
3164104	5.594	.1016	.814	2238.2	1.290	.502	1.218
3164105	6.642	.0983	.878	3233.7	.928	.548	1.309
3164106	8.536	.0954	.917	4340.3	1.115	.570	1.172
3164107	10.010	.0960	.933	4935.7	.881	.759	1.150

EXPERIMENTAL RESULTS FOR ** PL9/GLY ** SYSTEM

NO. 1

PACKING : PLASTIC SPHERES

AVERAGE SIZE = 9.0 (MM) . APPARENT DENSITY = 921. (KG/M3)
 LIQUID : GLYCEROL - WATER
 DENSITY = 1210.(KG/M3) . NOMINAL VISCOSITY = .0640 (NS/M2)
 SURFACE TENSION = .0652 (N/M) . CONTACT ANGLE = 88.1 (DEG.)

RUN NO.	TOTAL HOLD-UP (PCT.)	LIQUID VELOCITY (MM/S)	GAS VELOCITY (M/S)	PRESSURE DROP (N/M3)	RELATIVE LIQUID FLUX		
					INNER (-)	MIDDLE (-)	OUTER (-)

*** RUN360 ***

*** GAS PRESSURE DROP THROUGH DRY BED ** HB = .400 . EPS = .3870

3600001	0	0	.363	313.8	0	0	0
3600002	0	0	.461	475.6	0	0	0
3600003	0	0	.627	826.2	0	0	0
3600004	0	0	.792	1265.1	0	0	0
3600005	0	0	1.003	1929.5	0	0	0
3600006	0	0	1.207	2696.8	0	0	0
3600007	0	0	1.382	3429.9	0	0	0
3600008	0	0	1.577	4344.4	0	0	0
3600009	0	0	1.703	5018.6	0	0	0

*** RUN 361 *** . DIST = 19 . HB = .400 . EPS = .3870 . VIS = .05270

3613101	3.543	.0614	0	0	1.448	1.276	.684
3615102	3.590	.0644	.253	257.4	2.410	.977	.549
3616103	3.619	.0677	.362	502.6	1.348	1.373	.660
3616104	3.724	.0701	.525	1046.9	.646	.987	1.132
3616105	4.622	.0716	.681	2385.5	.403	.529	1.501
3616106	6.086	.0672	.806	4008.5	.089	.049	1.902
3616107	7.643	.0579	.849	4959.7	1.161	.271	1.406
3616108	8.171	.0582	.961	5587.9	.103	.179	1.817
3616109	8.034	.0661	1.083	5915.9	.305	.174	1.749

*** RUN 362 *** . DIST = 19 . HB = .405 . EPS = .3950 . VIS = .05430

3626101	3.376	.0584	0	0	1.126	1.232	.821
3628101	4.709	.2552	0	0	.790	1.690	.649
3627101	3.975	.1312	0	0	.478	1.562	.834
3624101	2.745	.0149	0	0	.443	1.111	1.135
3625101	2.987	.0342	0	0	.517	.954	1.190
3629101	5.873	.5316	0	0	1.338	1.212	.761
3629102	5.887	.5445	.115	72.6	1.352	1.372	.658
3629103	6.025	.5110	.194	186.4	1.289	1.368	.681
3629104	6.118	.4601	.310	428.6	1.278	1.371	.683
3629105	5.296	.4484	.456	978.2	.871	.846	1.144
3629106	8.548	.4500	.482	2721.7	.166	.252	1.749
3629107	15.085	.5192	.549	4552.2	.110	.316	1.728

EXPERIMENTAL RESULTS FOR ** PL9/ZNCL ** SYSTEM

NO. 1

PACKING : PLASTIC SPHERES

AVERAGE SIZE = 9.0 (MM) . APPARENT DENSITY = 921. (KG/M3)
 LIQUID : ZNCL2 - WATER
 DENSITY = 1920.(KG/M3) . NOMINAL VISCOSITY = .0340 (NS/M2)
 SURFACE TENSION = .0809 (N/M) . CONTACT ANGLE = 84.5 (DEG.)

RUN NO.	TOTAL HOLD-UP (PCT.)	LIQUID VELOCITY (MM/S)	GAS VELOCITY (M/S)	PRESSURE DROP (N/M3)	RELATIVE LIQUID FLUX		
					INNER (-)	MIDDLE (-)	OUTER (-)

*** RUN430 ***

*** GAS PRESSURE DROP THROUGH DRY BED ** HB = .411 . EPS = .4060

4300001	0	0	.359	272.0	0	0	0
4300002	0	0	.575	613.2	0	0	0
4300003	0	0	.767	1018.8	0	0	0
4300004	0	0	.990	1622.5	0	0	0
4300005	0	0	1.236	2398.0	0	0	0
4300006	0	0	1.453	3194.9	0	0	0
4300007	0	0	1.650	4027.7	0	0	0
4300008	0	0	1.823	4836.5	0	0	0

*** RUN 431 *** . DIST = 19 . HB = .411 . EPS = .4060 . VIS = .03280

4319101	5.217	.9251	0	0	1.586	1.213	.678
4317101	3.676	.2348	0	0	1.567	1.515	.497
4317102	3.788	.2357	.383	439.0	1.676	1.467	.491
4317103	3.978	.2378	.589	1040.8	1.455	1.050	.823
4317104	4.328	.2442	.783	2235.7	1.190	.572	1.211
4317105	5.059	.2532	.907	3576.7	.294	.369	1.634
4317106	5.589	.2466	.971	4404.7	.256	.435	1.605
4317107	6.475	.2490	1.072	5604.9	.133	.359	1.694
4317108	6.629	.2441	1.174	5977.1	.208	.279	1.718
4317109	6.432	.2727	1.256	5938.9	.273	.282	1.695

*** RUN 432 *** . DIST = 19 . HB = .411 . EPS = .4060 . VIS = .03000

4327101	3.695	.2277	0	0	1.028	1.079	.780
4324101	2.987	.0236	0	0	1.032	1.611	.414
4325101	3.232	.0557	0	0	.934	1.794	.538
4326101	3.423	.1195	0	0	1.095	1.305	.789
4328101	4.434	.5053	0	0	1.510	1.005	.932
4329101	5.446	1.0190	0	0	1.118	1.121	.824
4329102	5.656	1.0403	.353	419.9	1.116	.969	.936
4329103	5.879	1.0610	.548	1004.5	.992	.772	1.153
4329104	6.604	1.0775	.677	2407.5	.836	.469	1.584
4329105	7.070	1.0799	.713	3035.1	.44	.277	1.741
4329106	9.342	1.0601	.750	5013.1	.193	.360	1.673

*** RUN 433 *** . DIST = 19 . HB = .407 . EPS = .3998 . VIS = .02860

4335102	3.538	.0567	.752	1698.7	.391	.952	1.239
4335103	3.780	.0548	.961	2925.1	.399	.247	1.674
4335104	4.158	.0531	1.121	4141.9	.254	.094	1.784
4335105	4.180	.0659	1.121	4182.9	.104	.108	1.859
4335106	4.646	.0642	1.331	5515.4	.005	.227	1.819
4335107	4.655	.0660	1.439	5929.8	0	.178	1.851

EXPERIMENTAL RESULTS FOR ■■ C11/GLY ■■ SYSTEM

NO. 1

EXPERIMENTAL RESULTS FOR ■■ C11/GLY ■■ SYSTEM

NO. 2

PACKING : MAX-COATED COKE
 AVERAGE SIZE = 11.0 (MM) . APPARENT DENSITY = 1210. (KG/M3)
 LIQUID : GLYCEROL - WATER
 DENSITY = 1210.(KG/M3) . NOMINAL VISCOSITY = .0640 (NS/M2)
 SURFACE TENSION = .0652 (N/M) . CONTACT ANGLE = 96.6 (DEG.)

RUN NO.	TOTAL HOLD-UP (PCT.)	LIQUID VELOCITY (MM/S)	GAS VELOCITY (M/S)	PRESSURE DRDP (N/M3)	RELATIVE LIQUID FLUX		
					INNER (-)	MIDDLE (-)	OUTER (-)
3700007	0	0	1.744	3276.9	0	0	0
*** RUN 371 *** . DIST = 19 . HB = .410 . EPS = .5242 . VIS = .06090							
3717101	4.453	.1000	0	0	1.093	.248	1.440
3717102	4.637	.1017	.403	361.2	1.001	.234	1.480
3717103	4.831	.1024	.613	841.9	1.279	.254	1.374
3717104	5.519	.1105	.853	1923.1	.064	.112	1.870
3717105	7.531	.1074	1.036	3360.6	.379	.177	1.724
3717106	10.279	.0981	1.140	4625.9	0	.224	1.821
3717107	15.153	.0642	1.159	5989.3	.346	.185	1.732
3717108	9.007	.0989	1.039	3965.7	.303	.298	1.675
*** RUN 372 *** . DIST = 19 . HB = .410 . EPS = .5242 . VIS = .07460							
3727101	4.726	.0764	0	0	.973	.306	1.444
3724101	3.994	.0071	0	0	.652	.005	1.758
3725101	4.086	.0162	0	0	.740	.185	1.608
3726101	4.282	.0324	0	0	.528	.149	1.692
3728101	4.916	.1462	0	0	1.441	.287	1.300
3729101	5.374	.2444	0	0	1.293	.592	1.160
3727201	4.626	.0660	0	0	.852	.167	1.572
3727202	5.403	.0666	.834	1889.6	.136	.120	1.842
3727103	7.465	.0728	1.036	3477.8	.192	.231	1.752
*** RUN 373 *** . DIST = 19 . HB = .410 . EPS = .5242 . VIS = .07830							
3735101	4.185	.0146	0	0	1.085	.423	1.341
3735102	4.350	.0108	.455	480.8	.648	.592	1.372
3735103	4.424	.0075	.675	1040.5	.228	.485	1.605
3735104	5.044	.0149	.910	2114.4	.005	.101	1.911
3735105	6.089	.0142	1.134	3422.8	.010	.052	1.931
3735106	7.648	.0121	1.237	4439.3	0	.003	1.979
3735107	8.879	.0111	1.280	5008.6	0	.057	1.925
3735108	11.983	.0110	1.353	6216.5	.006	.007	1.977
*** RUN 374 *** . DIST = 19 . HB = .410 . EPS = .5242 . VIS = .07050							
3749101	5.699	.2254	0	0	1.762	.235	1.224
3749102	5.761	.2315	.375	368.3	.941	.575	1.289
3749103	5.983	.2555	.460	564.5	1.025	.278	1.445
3749104	6.140	.2653	.565	858.7	.987	.420	1.370
3749105	6.521	.2818	.675	1325.1	.702	.700	1.292
3749106	7.409	.3111	.805	2246.0	1.231	.203	1.422
3749107	8.458	.3225	.879	2913.3	.331	.153	1.755
3749108	11.212	.3187	.932	4037.5	.320	.469	1.563

RUN NO.	TOTAL HOLD-UP (PCT.)	LIQUID VELOCITY (MM/S)	GAS VELOCITY (M/S)	PRESSURE DRDP (N/M3)	RELATIVE LIQUID FLUX		
					INNER (-)	MIDDLE (-)	OUTER (-)
*** RUN350 ***							
*** GAS PRESSURE DROP THROUGH DRY BED *** HB = .410 . EPS = .5242							
3500001	0	0	.464	299.0	0	0	0
3500002	0	0	.671	581.2	0	0	0
3500003	0	0	.900	1002.2	0	0	0
3500004	0	0	1.156	1595.4	0	0	0
3500005	0	0	1.347	2109.6	0	0	0
3500006	0	0	1.557	2788.9	0	0	0
3500007	0	0	1.814	3690.7	0	0	0
*** RUN 351 *** . DIST = 19 . HB = .410 . EPS = .5242 . VIS = .05560							
3517101	4.501	.1116	0	0	.392	.680	1.409
3517102	4.728	.1095	.455	485.6	.449	.644	1.411
3517103	4.871	.1172	.623	911.3	.268	.636	1.478
3517104	5.323	.1127	.803	1667.1	.293	.578	1.505
3517105	6.535	.1022	.979	2851.1	.028	.122	1.875
3517106	7.642	.1159	1.029	3485.0	.349	.227	1.704
3517107	10.097	.1172	1.060	4508.7	.065	.168	1.834
*** RUN 352 *** . DIST = 19 . HB = .410 . EPS = .5242 . VIS = .05390							
3525101	3.918	.0307	0	0	.500	.271	1.628
3525102	4.057	.0311	.460	461.6	.366	.619	1.455
3525103	4.145	.0334	.787	1009.4	.346	.177	1.736
3525104	4.899	.0342	.932	2202.9	.714	.275	1.554
3525105	7.024	.0299	1.163	3965.7	.085	.043	1.908
3525106	11.261	.0225	1.205	5487.0	.145	.128	1.833
*** RUN 353 *** . DIST = 19 . HB = .410 . EPS = .5242 . VIS = .05440							
3539101	5.195	.2385	0	0	.545	.386	1.539
3539102	4.302	.0575	0	0	.477	.601	1.429
3534101	3.838	.0112	0	0	.110	.383	1.685
3535101	3.997	.0287	0	0	.252	.548	1.537
3537101	4.556	.1327	0	0	.698	.600	1.355
3539101	5.747	.4834	0	0	.879	.514	1.348
3539102	5.956	.5032	.353	325.3	.587	.548	1.425
3539103	6.117	.4745	.457	569.3	.501	.508	1.478
3539104	6.292	.4548	.624	1119.4	.312	.428	1.591
3539105	7.465	.4476	.738	1970.9	.574	.542	1.433
3539106	8.222	.4228	.831	2662.2	.089	.159	1.832
3539107	13.241	.3981	.889	4592.4	.239	.309	1.672
*** RUN370 ***							
*** GAS PRESSURE DROP THROUGH DRY BED *** HB = .410 . EPS = .5242							
3700001	0	0	.385	208.1	0	0	0
3700002	0	0	.572	413.8	0	0	0
3700003	0	0	.799	767.8	0	0	0
3700004	0	0	1.056	1291.6	0	0	0
3700005	0	0	1.346	2037.9	0	0	0
3700006	0	0	1.550	2657.4	0	0	0

EXPERIMENTAL RESULTS FOR W13/CACL SYSTEM

NO. 1

PACKING : MAX-COATED SPHERES

AVERAGE SIZE = 13.3 (MM) . APPARENT DENSITY = 921. (KG/M3)

LIQUID : CACL2 - WATER

DENSITY = 1350.(KG/M3) . NOMINAL VISCOSITY = .0059 (NS/M2)

SURFACE TENSION = .0888 (N/M) . CONTACT ANGLE = 114.1 (DEG.)

RUN NO.	TOTAL HOLD-UP (PCT.)	LIQUID VELOCITY (MM/S)	GAS VELOCITY (M/S)	PRESSURE DROP (N/M3)	RELATIVE LIQUID FLUX		
					INNER (-)	MIDDLE (-)	OUTER (-)

*** RUN 390 ***

*** GAS PRESSURE DROP THROUGH DRY BED *** MB = .430 . EPS = .4180

3900001	0	0	.466	225.8	0	0	0
3900002	0	0	.575	440.2	0	0	0
3900003	0	0	.916	768.6	0	0	0
3900004	0	0	1.231	1306.8	0	0	0
3900005	0	0	1.565	2020.6	0	0	0
3900006	0	0	1.782	2577.1	0	0	0

*** RUN 391 *** . DIST = 19 . MB = .430 . EPS = .4180 . VIS = .00535

3917101	1.595	.1624	0	0	.750	.464	1.422
3917102	1.787	.1618	.448	276.0	.561	.356	1.653
3917103	1.865	.1634	.676	606.6	.427	.283	1.642
3917104	2.030	.1624	.928	1147.2	.435	.172	1.709
3917105	2.662	.1598	1.223	2235.0	.019	.058	1.918
3917106	3.975	.1451	1.475	3466.6	.011	.148	1.865
3917107	5.714	.1484	1.584	4604.6	.723	1.297	.915
3917108	6.718	.1491	1.716	5405.1	.390	1.221	1.074

*** RUN 392 *** . DIST = 19 . MB = .430 . EPS = .4180 . VIS = .00568

3927101	1.768	.1470	0	0	.647	.528	1.417
3929101	2.222	.5685	0	0	.444	.569	1.459
3928101	1.960	.2957	0	0	.623	.523	1.428
3926101	1.669	.0736	0	0	.632	.605	1.376
3925101	1.800	.0331	0	0	.596	.541	1.429
3924101	1.537	.0137	0	0	.540	.575	1.429

*** RUN 393 *** . DIST = 19 . MB = .430 . EPS = .4180 . VIS = .00569

3936101	1.867	.1792	0	0	.579	.519	1.445
3937101	2.062	.3583	0	0	.416	.644	1.422
3938101	2.753	.6754	0	0	.478	.628	1.411
3939101	2.734	1.2243	0	0	.465	.550	1.464
3939102	2.984	1.3233	.350	207.5	.568	.532	1.441
3939103	3.039	1.2214	.562	494.9	.462	.546	1.457
3939104	3.053	1.1938	.782	1001.2	.447	.583	1.450
3939105	3.776	1.1543	1.042	2020.6	.143	.432	1.645
3939106	5.545	1.1936	1.130	3181.5	.523	.333	1.573
3939107	9.626	1.1731	1.157	5526.0	.636	.418	1.488

*** RUN 394 *** . DIST = 71 . MB = .422 . EPS = .4060 . VIS = .00565

3948101	2.733	.8068	0	0	.977	.986	1.322
3949101	3.164	1.4254	0	0	.649	.629	1.353
3947101	2.463	.4684	0	0	.914	1.103	.871
3946101	2.753	.2439	0	0	.755	1.098	1.008
3944101	1.847	.0550	0	0	.580	1.509	.634
3943101	2.176	.1504	0	0	.581	1.393	.913
3945102	2.406	.1512	.451	304.4	.454	1.175	1.081
3945103	2.416	.1518	.674	673.9	.342	1.145	1.137
3945104	2.478	.1524	.914	1234.0	.685	.518	1.412

EXPERIMENTAL RESULTS FOR W13/CACL SYSTEM

NO. 2

RUN NO.	TOTAL HOLD-UP (PCT.)	LIQUID VELOCITY (MM/S)	GAS VELOCITY (M/S)	PRESSURE DROP (N/M3)	RELATIVE LIQUID FLUX		
					INNER (-)	MIDDLE (-)	OUTER (-)
3945105	3.573	.1475	1.176	2556.2	.101	.348	1.711
3945106	5.173	.1483	1.477	4424.6	.012	.842	1.455
3945107	7.001	.1451	1.603	5581.9	.519	.617	1.404
*** RUN 395 *** . DIST = 19 . MB = .422 . EPS = .4060 . VIS = .00466							
3956101	2.076	.0798	0	0	.588	.788	1.278
3959101	2.696	.5653	0	0	.695	.694	1.298
3958101	2.413	.2926	0	0	.640	.748	1.283
3957101	2.245	.1466	0	0	.646	.720	1.299
3954101	2.007	.0157	0	0	.748	.764	1.239
3955101	2.039	.0335	0	0	.524	.744	1.324
3955102	2.222	.0348	.451	313.7	.706	.794	1.298
3955103	2.304	.0388	.683	694.8	.416	.822	1.312
3955104	2.485	.0340	.919	1331.6	.277	.255	1.711
3955105	3.404	.0324	1.209	2663.1	.006	.347	1.749
3955106	3.793	.0340	1.490	3922.7	.072	.399	1.694
3955107	4.601	.0321	1.714	5105.5	.110	.858	1.391
3955108	6.050	.0322	1.777	5798.0	.118	.561	1.389

EXPERIMENTAL RESULTS FOR ** C11/CACL ** SYSTEM

NO. 1

PACKING : WAX-COATED COKE
 AVERAGE SIZE = 11.0 (MM) APPARENT DENSITY = 1210. (KG/M3)
 LIQUID : CACL2 - WATER
 DENSITY = 1350. (KG/M3) NOMINAL VISCOSITY = .0059 (NS/M2)
 SURFACE TENSION = .0888 (N/M) CONTACT ANGLE = 114.1 (DEG.)

RUN NO.	TOTAL HOLD-UP (PCT.)	LIQUID VELOCITY (MM/S)	GAS VELOCITY (M/S)	PRESSURE DROP (N/M3)	RELATIVE LIQUID FLUX		
					INNER (-)	MIDDLE (-)	OUTER (-)
*** RUN 410 ***							
*** GAS PRESSURE DROP THROUGH DRY BED *** HB = .420 . EPS = .5364							
4100001	0	0	.451	280.2	0	0	0
4100002	0	0	.694	579.1	0	0	0
4100003	0	0	.938	994.7	0	0	0
4100004	0	0	1.194	1549.1	0	0	0
4100005	0	0	1.491	2332.6	0	0	0
4100006	0	0	1.766	3191.8	0	0	0
*** RUN 411 *** . DIST = 19 . HB = .420 . EPS = .5364 . VIS = .00621							
4117101	3.868	.1350	0	.844	.585	1.316	
4117102	3.998	.1371	.465	427.3	.647	.623	1.358
4117103	4.207	.1395	.697	894.3	.696	.673	1.311
4117104	4.575	.1457	.920	1667.1	.260	.247	1.721
4117105	5.710	.1485	1.198	3247.9	.201	.012	1.886
4117106	7.204	.1485	1.331	4244.9	.161	.013	1.899
4117107	5.733	.1447	1.435	5540.8	.002	.172	1.854
4117108	11.162	.1430	1.482	6259.9	.003	.396	1.714
*** RUN 412 *** . DIST = 19 . HB = .420 . EPS = .5364 . VIS = .00656							
4129101	4.180	.1339	0	.498	.520	1.372	
4129101	4.401	.2692	0	.537	.472	1.489	
4129101	4.742	.5281	0	.574	.374	1.536	
4129101	4.102	.0570	0	.613	.465	1.468	
4129101	3.918	.0142	0	.490	.533	1.463	
4129101	4.013	.0312	0	.449	.558	1.465	
*** RUN 413 *** . DIST = 19 . HB = .420 . EPS = .5364 . VIS = .00620							
4137101	4.538	.3441	0	.497	.413	1.558	
4137101	4.182	.0952	0	.553	.454	1.493	
4137101	4.324	.1726	0	.526	.482	1.460	
4137101	4.842	.6623	0	.651	.274	1.572	
4137101	5.342	1.2150	0	.681	.241	1.585	
4137102	5.489	1.2105	.353	315.2	.555	.247	1.621
4137103	5.740	1.2329	.623	931.6	.330	.295	1.667
4137104	6.373	1.2477	.896	2141.1	.598	.121	1.695
4137105	8.523	1.2193	1.053	3789.6	.227	.095	1.825
4137106	13.380	1.1813	1.111	6409.4	.422	.657	1.412
*** RUN 414 *** . DIST = 71 . HB = .405 . EPS = .5179 . VIS = .00640							
4147101	4.235	.1439	0	0	1.933	.913	.747
4147101	4.438	.2805	0	0	1.410	.978	.882
4147101	4.747	.5340	0	0	1.285	.846	1.006
4147101	4.136	.0755	0	0	2.343	.926	.603
4147101	3.994	.0167	0	0	2.660	.590	.700
4147201	4.290	.1514	0	0	1.792	.930	.784
4148002	4.455	.1565	.454	472.2	1.915	.952	.724
4148103	4.600	.1510	.675	1038.8	1.089	.759	1.126
4148204	5.197	.1507	.929	2121.2	.130	.138	1.832

EXPERIMENTAL RESULTS FOR ** C11/CACL ** SYSTEM

NO. 2

RUN NO.	TOTAL HOLD-UP (PCT.)	LIQUID VELOCITY (MM/S)	GAS VELOCITY (M/S)	PRESSURE DROP (N/M3)	RELATIVE LIQUID FLUX		
					INNER (-)	MIDDLE (-)	OUTER (-)
4146205	6.549	.1464	1.153	3656.3	.092	.168	1.825
4146206	8.728	.1415	1.271	5140.6	.003	.347	1.745
4146207	10.076	.1495	1.359	6109.2	.154	.401	1.020
4146208	10.698	.1428	1.535	6813.8	.369	.825	1.825
*** RUN 415 *** . DIST = 19 . HB = .405 . EPS = .5179 . VIS = .00634							
4155101	4.280	.0302	0	0	1.008	.489	1.523
4155201	4.329	.0313	0	0	1.015	.517	1.503
4155202	4.497	.0312	.460	472.2	.687	.465	1.445
4155203	4.623	.0316	.688	1031.5	.703	.431	1.498
4154204	4.998	.0313	.931	1968.6	.190	.099	1.840
4155205	6.048	.0302	1.213	3629.7	.368	.004	1.836
4155206	7.143	.0296	1.495	5397.3	.256	.010	1.873
4155207	8.749	.0257	1.705	6893.7	1.091	.585	1.855

EXPERIMENTAL RESULTS FOR **W13/ZNCL** **SYSTEM**

NO. 1

PACKING : WAX-COATED SPHERES
 AVERAGE SIZE = 13.3 (MM) , APPARENT DENSITY = 921. (KG/M3)
 LIQUID : ZNCL2 - WATER
 DENSITY = 1920.(KG/M3) , NOMINAL VISCOSITY = .0340 (NS/M2)
 SURFACE TENSION = .0809 (N/M) , CONTACT ANGLE = 97.9 (DEG.)

RUN NO.	TOTAL HOLD-UP (PCT.)	LIQUID VELOCITY (MM/S)	GAS VELOCITY (M/S)	PRESSURE DROP (N/M3)	RELATIVE LIQUID FLUX		
					INNER (-)	MIDDLE (-)	OUTER (-)
*** RUN420 ***							
*** GAS PRESSURE DROP THROUGH DRY BED *** HB = .437 , EPS = .4282							
4200001	0	0	.477	217.7	0	0	0
4200002	0	0	.674	408.1	0	0	0
4200003	0	0	.939	738.3	0	0	0
4200004	0	0	1.199	1159.5	0	0	0
4200005	0	0	1.531	1728.0	0	0	0
4200006	0	0	1.831	2428.1	0	0	0
*** RUN 421 *** . DIST = 19 , HB = .430 , EPS = .4282 , VIS = .04340							
4218101	2.691	.3228	0	0	1.753	.830	.856
4217101	2.441	.1632	0	0	1.553	.808	.935
4217102	2.489	.1659	.472	298.8	1.478	.700	1.031
4217103	2.517	.1698	.707	645.4	1.499	.744	1.002
4217104	2.850	.1703	1.002	1388.9	1.279	.359	1.309
4217105	3.818	.1773	1.282	2994.5	.290	.111	1.795
4217105	5.204	.2013	1.485	4691.3	.003	.040	1.935
4217107	6.361	.1952	1.659	5719.8	.019	.065	1.914
4217108	6.471	.2031	1.720	6052.8	.292	.746	1.401
4217109	6.344	.2022	1.828	5985.6	.330	1.102	1.167
*** RUN 422 *** . DIST = 19 , HB = .435 , EPS = .4180 , VIS = .04610							
4225102	2.548	.0321	.822	1224.1	.361	.849	1.315
4225103	3.172	.0315	1.262	2694.0	.500	.159	1.698
4225104	4.051	.0348	1.557	4513.3	.014	.049	1.929
4225105	4.323	.0326	1.732	5345.2	0	.042	1.934
*** RUN 423 *** . DIST = 19 , HB = .435 , EPS = .4180 , VIS = .03820							
4235101	2.560	.0364	0	0	1.225	.494	1.246
4234101	2.488	.0148	0	0	1.189	.595	1.204
4235101	2.845	.1000	0	0	.687	1.006	1.108
4237101	3.116	.2210	0	0	1.754	.740	.914
4239101	3.433	.4405	0	0	1.506	.565	1.105
4239101	4.153	.4541	0	0	1.490	.568	1.109
4239102	4.103	.8637	.584	236.7	1.190	.695	1.131
4239103	4.253	.8680	.627	728.2	1.282	.571	1.177
4239104	4.777	.8927	.954	2035.7	.589	.085	1.700
4239105	5.021	.8563	1.082	3600.3	.168	.180	1.793
4239106	6.434	.8712	1.084	3794.2	.159	.246	1.755
4239107	7.511	.8724	1.146	4546.3	.299	.348	1.645
4239108	8.480	.8556	1.175	5451.2	.387	.487	1.529
4239109	9.235	.8893	1.237	6001.2	.140	.651	1.511
4239110	10.405	.8997	1.353	6544.6	.427	.747	1.355

EXPERIMENTAL RESULTS FOR **W11/ZNCL** **SYSTEM**

NO. 1

PACKING : WAX-COATED COKE
 AVERAGE SIZE = 11.0 (MM) , APPARENT DENSITY = 1210. (KG/M3)
 LIQUID : ZNCL2 - WATER
 DENSITY = 1920.(KG/M3) , NOMINAL VISCOSITY = .0340 (NS/M2)
 SURFACE TENSION = .0809 (N/M) , CONTACT ANGLE = 97.9 (DEG.)

RUN NO.	TOTAL HOLD-UP (PCT.)	LIQUID VELOCITY (MM/S)	GAS VELOCITY (M/S)	PRESSURE DROP (N/M3)	RELATIVE LIQUID FLUX		
					INNER (-)	MIDDLE (-)	OUTER (-)
*** RUN440 ***							
*** GAS PRESSURE DROP THROUGH DRY BED *** HB = .416 , EPS = .5316							
4400001	0	0	.384	202.7	0	0	0
4400002	0	0	.662	545.9	0	0	0
4400003	0	0	.933	1018.4	0	0	0
4400004	0	0	1.244	1725.6	0	0	0
4400005	0	0	1.558	2512.0	0	0	0
4400006	0	0	1.822	3493.6	0	0	0
*** RUN 441 *** . DIST = 19 , HB = .416 , EPS = .5316 , VIS = .02830							
4417101	3.679	.2616	0	0	1.359	.524	1.181
4417102	3.757	.2649	.462	440.8	1.748	.570	1.021
4417103	3.941	.2713	.692	943.0	.140	1.262	1.133
4417104	4.209	.2745	.902	1704.4	1.209	.528	1.228
4417105	5.171	.2808	1.104	3088.2	1.037	.347	1.398
4417106	6.132	.2882	1.228	4163.1	1.190	.521	1.239
4417107	7.212	.3012	1.313	5077.8	.347	.484	1.544
4417108	8.470	.3094	1.373	5990.1	.229	.408	1.631
4417201	3.919	.3060	0	0	.885	.696	1.233
4414201	3.278	.0335	0	0	.242	1.121	1.184
4415201	3.400	.0694	0	0	.141	.979	1.309
4416201	3.612	.1409	0	0	.435	.616	1.433
4418201	4.352	.5637	0	0	.832	.530	1.353
4419201	5.185	1.0997	0	0	1.105	.679	1.170
*** RUN 442 *** . DIST = 19 , HB = .416 , EPS = .5316 , VIS = .02790							
4425101	3.442	.0541	0	0	.671	.970	1.136
4425102	3.487	.0606	.472	445.5	.462	.903	1.249
4425103	3.460	.0434	.708	968.9	.059	1.047	1.294
4425104	3.593	.0657	.699	973.6	.073	.845	1.413
4425105	3.974	.0685	1.029	2114.6	.231	.508	1.568
4425106	4.402	.0588	1.224	3253.2	.546	.584	1.384
4425107	5.671	.0667	1.422	4851.5	1.497	.379	1.225
4425108	7.475	.0690	1.557	6459.2	.126	.155	1.623

EXPERIMENTAL RESULTS FOR ■■ PL13/CACL ■■ SYSTEM

NO. 1

PACKING : PLASTIC SPHERES

AVERAGE SIZE = 13.2 (MM) . APPARENT DENSITY = 921. (KG/M3)

LIQUID : CACL2 - WATER

DENSITY = 1350.(KG/M3) . NOMINAL VISCOSITY = .0059 (NS/M2)

SURFACE TENSION = .0888 (N/M) . CONTACT ANGLE = 108.9 (DEG.)

RUN NO.	TOTAL	LIQUID	GAS	PRESSURE	RELATIVE LIQUID FLUX		
	HOLD-UP (PCT.)	VELOCITY (MM/S)	VELOCITY (M/S)	DROP (N/M3)	INNER (-)	MIDDLE (-)	OUTER (-)
*** RUN400 ***							
*** GAS PRESSURE DROP THROUGH DRY BED ■■ HB = .423 . EPS = .4076							
4000001	0	0	.465	248.1	0	0	0
4000002	0	0	.684	496.1	0	0	0
4000003	0	0	.982	955.2	0	0	0
4000004	0	0	1.254	1523.2	0	0	0
4000005	0	0	1.555	2176.9	0	0	0
4000006	0	0	1.822	2949.0	0	0	0
*** RUN 401 *** . DIST = 19 . HB = .423 . EPS = .4076 . VIS = .00592							
4017101	2.645	.1442	0	0	1.047	.809	1.108
4017102	2.788	.1468	.469	389.5	.821	.849	1.159
4017103	2.902	.1463	.685	820.7	1.151	.981	.969
4017104	3.216	.1469	.937	1757.3	.395	.264	1.666
4017105	4.160	.1477	1.210	3326.9	.006	.579	1.600
4017106	5.504	.1445	1.307	4379.4	.023	.646	1.553
4017107	6.142	.1406	1.374	4914.9	.056	.846	1.419
4017108	6.987	.1423	1.449	5647.5	.256	.631	1.484
*** RUN 402 *** . DIST = 19 . HB = .423 . EPS = .4076 . VIS = .00609							
4029101	3.221	.2712	0	0	1.089	.772	1.118
4029101	3.579	.5337	0	0	.841	.744	1.218
4027101	3.062	.1411	0	0	1.028	.714	1.174
4026101	2.931	.0682	0	0	1.364	.590	1.133
4024101	2.763	.0148	0	0	1.178	.633	1.169
4025101	2.790	.0341	0	0	.873	.564	1.316
*** RUN 403 *** . DIST = 19 . HB = .423 . EPS = .4076 . VIS = .00602							
4035101	2.917	.0775	0	0	1.210	.597	1.185
4036101	3.055	.1640	0	0	1.076	.556	1.257
4037101	3.280	.3292	0	0	.839	.966	1.081
4038101	3.574	.6440	0	0	1.054	.975	1.003
4039101	4.021	1.1800	0	0	1.067	1.130	.903
4039102	4.192	1.1434	.373	252.7	1.191	1.146	.852
4039103	4.203	1.1677	.624	730.3	1.046	.573	1.255
4039104	4.637	1.1561	.864	1766.6	.115	.440	1.649
4039105	5.225	1.1353	.981	2689.3	.152	.514	1.591
4039106	8.211	1.1172	1.063	4801.3	.489	.689	1.370
*** RUN 404 *** . DIST = 19 . HB = .423 . EPS = .4076 . VIS = .00614							
4045101	2.855	.0323	0	0	.833	.542	1.347
4045102	2.973	.0330	.460	350.1	.500	.698	1.365
4045103	2.981	.0336	.693	746.5	.528	.789	1.297
4045104	3.052	.0326	.921	1381.7	.500	.770	1.317
4045105	3.411	.0329	1.205	2751.9	.218	.151	1.791
4045106	4.238	.0321	1.489	4513.9	.010	.182	1.641
4045107	4.592	.0352	1.632	5086.5	.581	.052	1.737
4045108	5.465	.0304	1.793	5867.8	.257	.874	1.340

EXPERIMENTAL RESULTS FOR W13/GLY SYSTEM

NO. 1

PACKING : WAX-COATED SPHERES
 AVERAGE SIZE = 13.3 (MM) . APPARENT DENSITY = 921. (KG/M3)
 LIQUID : GLYCEROL - WATER
 DENSITY = 1210. (KG/M3) . NOMINAL VISCOSITY = .0640 (NS/M2)
 SURFACE TENSION = .0652 (N/M) . CONTACT ANGLE = 96.6 (DEG.)

RUN NO.	TOTAL HOLD-UP (PCT.)	LIQUID VELOCITY (MM/S)	GAS VELOCITY (M/S)	PRESSURE DROP (IN/M3)	RELATIVE LIQUID FLUX		
					INNER (-)	MIDDLE (-)	OUTER (-)
*** RUN 300 ***							
*** GAS PRESSURE DROP THROUGH DRY BED *** HB = .430 . EPS = .4180							
3000001	0	0	.462	225.8	0	0	0
3000002	0	0	.650	417.4	0	0	0
3000003	0	0	.861	702.4	0	0	0
3000004	0	0	1.115	1117.5	0	0	0
3000005	0	0	1.397	1683.1	0	0	0
3000006	0	0	1.621	2225.9	0	0	0
3000007	0	0	1.830	2784.6	0	0	0
*** RUN 301 *** . DIST = 71 . HB = .430 . EPS = .4180 . VIS = .06430							
3018101	2.794	.1794	0	0	2.297	1.283	.396
3019101	3.345	.3769	0	0	1.919	1.372	.468
3017101	2.496	.0833	0	0	2.170	1.752	.149
3016101	2.374	.0334	0	0	.697	1.979	.504
3017201	2.482	.0721	0	0	1.419	1.689	.439
3017202	2.528	.0721	.457	305.6	1.228	1.443	.657
3017203	2.539	.0729	.624	561.0	.392	2.099	.529
3017204	2.686	.0699	.865	1154.0	.112	.773	1.444
3017205	4.159	.0670	1.117	2700.3	.051	.055	1.913
3017206	4.905	.0656	1.238	3425.5	.011	.018	1.945
3017207	6.028	.0614	1.366	4285.3	.492	.505	1.483
3017208	9.440	.0511	1.410	5560.2	1.025	.771	1.140
*** RUN 302 *** . DIST = 71 . HB = .430 . EPS = .4180 . VIS = .07280							
3028101	3.255	.1674	0	0	2.429	1.027	.510
3025101	2.648	.0163	0	0	1.570	1.629	.430
3026101	2.737	.0383	0	0	2.326	1.311	.372
3027101	2.838	.0777	0	0	2.449	1.237	.373
3028201	3.125	.1785	0	0	1.957	1.655	.290
3029101	3.554	.3726	0	0	2.362	1.474	.255
3029102	3.573	.3852	.452	314.7	2.549	1.359	.264
3029103	3.657	.3830	.620	595.2	3.302	.890	.303
3029104	4.614	.3863	.821	1594.2	.583	.375	1.532
3029105	5.187	.3753	.920	2159.8	.328	.546	1.512
3029106	9.071	.3567	1.006	3920.4	.504	.583	1.431
*** RUN 303 *** . DIST = 71 . HB = .430 . EPS = .4180 . VIS = .06290							
3039101	2.357	.1441	0	0	4.190	.670	1.142
3035101	2.490	.0105	0	0	3.378	.764	.362
3038101	2.767	.0834	0	0	3.104	1.373	.070
3037101	2.534	.0442	0	0	3.763	.890	1.149
3036101	2.553	.0215	0	0	2.587	1.575	.119
3036102	2.591	.0220	.458	301.0	2.605	1.250	.315
3036103	2.547	.0231	.551	599.8	2.235	1.350	.381
3036104	2.648	.0212	.867	1133.5	.601	.649	1.360
3036105	3.546	.0240	1.131	2469.9	.060	.100	1.979
3036106	4.891	.0258	1.336	3763.0	.177	.132	1.833

EXPERIMENTAL RESULTS FOR W13/GLY SYSTEM

NO. 2

RUN NO.	TOTAL HOLD-UP (PCT.)	LIQUID VELOCITY (MM/S)	GAS VELOCITY (M/S)	PRESSURE DROP (IN/M3)	RELATIVE LIQUID FLUX		
					INNER (-)	MIDDLE (-)	OUTER (-)
3036107	5.859	.0236	1.424	4547.6	1.682	.687	.972
3036108	8.225	.0185	1.515	5414.2	1.556	.500	1.134
*** RUN 304 *** . DIST = 19 . HB = .430 . EPS = .4180 . VIS = .05570							
3047101	3.149	.0635	0	0	1.007	1.483	.707
3045101	2.764	.0149	0	0	.982	1.338	.804
3048101	3.383	.1322	0	0	1.293	1.303	.721
3046101	2.932	.0349	0	0	1.023	1.421	.738
3049101	3.746	.2538	0	0	.318	1.513	.917
3046201	3.136	.0709	0	0	.775	1.411	.826
3044101	2.707	.0086	0	0	.853	1.297	.877
3049201	3.681	.2594	0	0	1.540	1.419	.565
3046301	3.117	.1439	0	0	1.341	1.318	.696
*** RUN 305 *** . DIST = 13 . HB = .430 . EPS = .4180 . VIS = .06570							
3057101	2.965	.0640	0	0	.905	1.734	.585
3059101	3.364	.2278	0	0	1.545	1.792	.333
3058101	3.133	.1388	0	0	.414	2.041	.558
3055101	2.669	.0166	0	0	2.001	1.363	.453
3056101	2.775	.0297	0	0	2.291	1.354	.359
*** RUN 306 *** . DIST = 13 . HB = .430 . EPS = .4180 . VIS = .06570							
3068101	2.941	.0941	0	0	2.961	1.054	.317
3057101	2.781	.0514	0	0	3.149	1.262	.123
3066101	3.106	.1662	0	0	3.161	1.359	.059
3069101	2.661	.0188	0	0	2.869	.983	.392
*** RUN 320 ***							
*** GAS PRESSURE DROP THROUGH DRY BED *** HB = .425 . EPS = .4106							
3200001	0	0	.469	246.9	0	0	0
3200002	0	0	.624	417.7	0	0	0
3200003	0	0	.826	687.6	0	0	0
3200004	0	0	1.053	1068.4	0	0	0
3200005	0	0	1.306	1578.3	0	0	0
3200006	0	0	1.526	2097.5	0	0	0
3200007	0	0	1.814	2886.6	0	0	0
*** RUN 321 *** . DIST = 19 . HB = .425 . EPS = .4106 . VIS = .06070							
3218101	3.165	.1571	0	0	1.146	1.234	.775
3217101	2.819	.0612	0	0	1.277	1.220	.900
3217102	2.920	.0539	.453	346.1	1.451	1.223	.718
3217103	3.053	.0507	.535	692.2	1.415	1.027	.853
3217104	3.354	.0618	.806	1227.6	.859	.642	1.277
3217105	4.669	.0591	.999	2515.1	.098	.146	1.836
3217106	5.972	.0594	1.186	3655.0	.006	.351	1.745
3217108	8.201	.0505	1.296	4790.3	.069	1.773	.842
3217109	11.412	.0479	1.322	5997.1	1.386	1.850	.349
*** RUN 322 *** . DIST = 19 . HB = .425 . EPS = .4106 . VIS = .06310							
3229101	4.144	.3904	0	0	.970	1.187	.901
3229102	4.229	.3967	.380	263.1	.865	1.134	.969
3229103	4.334	.4182	.464	394.6	.980	1.095	.953
3229104	4.573	.4196	.595	673.8	.438	.382	1.205
3229105	4.825	.4175	.676	955.3	.934	.651	1.244
3229106	5.703	.4114	.766	1746.7	.180	.346	1.686
3229107	6.818	.4214	.863	2679.0	.165	.407	1.653
3229108	9.392	.4256	.923	3895.0	.447	1.218	1.057

EXPERIMENTAL RESULTS FOR W13/GLY SYSTEM

NO. 3

EXPERIMENTAL RESULTS FOR W13/GLY SYSTEM

NO. 4

RUN NO.	TOTAL HOLD-UP (PCT.)	LIQUID VELOCITY (MM/S)	GAS VELOCITY (M/S)	PRESSURE DROP (N/M3)	RELATIVE LIQUID FLUX		
					INNER (-)	MIDDLE (-)	OUTER (-)
3229109	13.339	.3743	.937	5254.1	.508	1.243	1.021
3225102	4.158	.0218	.940	1968.3	0	.523	1.642
3225103	5.868	.0244	1.339	4111.9	.906	1.395	.790
3225104	9.845	.0163	1.476	5826.3	2.602	.758	.629
*** RUN 323 *** . DIST = 71 . HB = .425 . EPS = .4106 . VIS = .06820							
3237101	3.134	.0990	0	0	2.957	1.268	.185
3237102	3.241	.1025	.458	327.7	.994	1.991	.394
3237103	3.357	.0950	.626	623.0	1.753	1.715	.313
3237104	3.894	.0992	.862	1416.8	.738	1.042	1.069
3237105	5.325	.0901	1.071	2773.5	.079	.763	1.462
3237106	6.411	.0871	1.158	3578.9	.680	1.293	.932
3237107	7.858	.0880	1.192	4259.6	1.574	1.364	.590
3237108	12.041	.0773	1.259	5957.9	1.509	1.317	.640
*** RUN 324 *** . DIST = 71 . HB = .425 . EPS = .4106 . VIS = .07730							
3247101	3.214	.0734	0	0	2.500	1.193	.383
3249101	3.815	.2697	0	0	2.050	1.307	.465
3248101	3.510	.1536	0	0	2.238	1.201	.467
3246101	3.036	.0384	0	0	2.211	1.038	.580
3245101	2.887	.0184	0	0	2.912	.840	.455
*** RUN 325 *** . DIST = 19 . HB = .425 . EPS = .4106 . VIS = .06780							
3259101	4.153	.3596	0	0	1.425	1.301	.677
3258101	3.744	.2242	0	0	.605	1.491	.835
3257101	3.453	.1103	0	0	.718	1.561	.753
3256101	3.211	.0532	0	0	1.625	1.297	.613
3255101	3.011	.0262	0	0	1.980	1.132	.594
*** RUN 380 ***							
*** GAS PRESSURE DROP THROUGH DRY BED *** HB = .430 . EPS = .4180							
3800001	0	0	.455	225.8	0	0	0
3800002	0	0	.679	465.2	0	0	0
3800003	0	0	.957	897.2	0	0	0
3800004	0	0	1.243	1399.0	0	0	0
3800005	0	0	1.501	1979.6	0	0	0
3800006	0	0	1.798	2764.1	0	0	0
*** RUN 381 *** . DIST = 19 . HB = .430 . EPS = .4180 . VIS = .07330							
3815101	2.250	.0142	0	0	.537	1.513	.848
3815102	2.387	.0153	.453	291.9	.598	1.488	.844
3815103	2.417	.0164	.682	561.4	1.096	1.302	.856
3815104	2.696	.0164	.915	1363.8	.850	.708	1.209
3815105	4.376	.0194	1.197	2987.6	.029	.494	1.645
3815106	5.976	.0182	1.347	4036.7	.877	.529	1.276
3815107	7.170	.0198	1.421	4647.3	.750	.784	1.222
3815108	7.589	.0202	1.453	4733.9	.595	.875	1.220
3815109	8.296	.0176	1.527	5277.4	.829	1.218	.927
*** RUN 382 *** . DIST = 19 . HB = .430 . EPS = .4180 . VIS = .06460							
3827101	2.821	.0933	0	0	1.127	1.337	.618
3827201	3.839	.0905	0	0	1.025	1.345	.847
3825101	3.325	.0220	0	0	.393	1.422	.753
3824101	2.189	.0131	0	0	.736	1.405	.840
3826101	3.433	.0509	0	0	.953	1.423	.760
3828101	4.288	.0262	0	0	1.139	1.079	.834
3823101	3.538	.4771	0	0	.547	1.805	.625

RUN NO.	TOTAL HOLD-UP (PCT.)	LIQUID VELOCITY (MM/S)	GAS VELOCITY (M/S)	PRESSURE DROP (N/M3)	RELATIVE LIQUID FLUX		
					INNER (-)	MIDDLE (-)	OUTER (-)
3829102	3.933	.5009	.367	228.1	.909	1.618	.554
3829103	3.988	.5002	.513	456.1	1.454	1.132	.772
3829104	4.490	.4874	.675	1040.0	.777	.775	1.220
3829105	4.552	.4828	.763	1434.5	.420	.519	1.437
3829106	5.347	.4632	.886	2253.3	.197	.868	1.357
3829107	7.631	.4738	.955	3329.7	.376	1.159	1.111
3829108	12.826	.4843	.987	5277.4	.377	.974	.231
*** RUN 383 *** . DIST = 19 . HB = .430 . EPS = .4180 . VIS = .05870							
3838101	3.025	.1345	0	0	1.229	1.280	.750
3838102	3.171	.1380	.448	314.7	.923	1.282	.856
3838103	3.244	.1423	.671	736.6	.908	.965	1.093
3838104	3.866	.1472	.924	1799.4	.195	.269	1.729
3838105	6.578	.1532	1.127	3587.4	.578	.591	1.407
3838106	8.797	.1504	1.266	4734.6	.588	.492	1.432
3839107	10.517	.1428	1.333	5252.3	.340	.442	1.573
3835102	7.734	.0171	1.533	5129.1	.477	1.553	.838
3835103	9.568	.0220	1.595	5993.5	1.157	1.272	.792
3835104	8.537	.0176	1.632	5758.6	1.073	1.552	.053
3835105	6.056	.0166	1.305	3975.1	.835	.778	.283

EXPERIMENTAL RESULTS FOR ■■ H13/GLY ■■ SYSTEM

NO. 3

EXPERIMENTAL RESULTS FOR ■■ H13/GLY ■■ SYSTEM

NO. 4

RUN NO.	TOTAL HOLD-UP (PCT.)	LIQUID VELOCITY (MM/S)	GAS VELOCITY (M/S)	PRESSURE DROP (N/M3)	RELATIVE LIQUID FLUX		
					INNER (-)	MIDDLE (-)	OUTER (-)
3229109	13.339	.3743	.937	5254.1	.508	1.243	1.021
3225102	4.158	.0218	.940	1968.3	0	.523	1.642
3225103	5.868	.0244	1.339	4111.9	.906	1.395	.790
3225104	9.845	.0163	1.476	5826.3	2.602	.758	.629
*** RUN 323 *** . DIST = 71 . H8 = .425 . EPS = .4106 . VIS = .06820							
3237101	3.134	.0990	0	0	2.957	1.268	.185
3237102	3.241	.1025	.459	327.7	.994	1.991	.394
3237103	3.357	.0950	.626	623.0	1.753	1.715	.313
3237104	3.884	.0892	.862	1416.8	.738	1.042	1.069
3237105	5.325	.0901	1.071	2773.6	.079	.763	1.462
3237106	6.411	.0871	1.158	3578.9	.680	1.293	.932
3237107	7.858	.0880	1.192	4259.6	1.574	1.364	.590
3237108	12.041	.0773	1.259	5957.9	1.509	1.317	.640
*** RUN 324 *** . DIST = 71 . H8 = .425 . EPS = .4106 . VIS = .07730							
3247101	3.214	.0734	0	0	2.500	1.193	.383
3249101	3.815	.2697	0	0	2.050	1.307	.465
3248101	3.510	.1536	0	0	2.238	1.201	.467
3245101	3.036	.0384	0	0	2.211	1.038	.580
3245101	2.887	.0184	0	0	2.912	.840	.465
*** RUN 325 *** . DIST = 19 . H8 = .425 . EPS = .4106 . VIS = .06780							
3259101	4.153	.3596	0	0	1.425	1.301	.677
3258101	3.744	.2242	0	0	.605	1.491	.835
3257101	3.453	.1103	0	0	.718	1.561	.753
3256101	3.211	.0532	0	0	1.625	1.297	.613
3255101	3.011	.0262	0	0	1.980	1.132	.594
*** RUN 380 ***							
*** GAS PRESSURE DROP THROUGH DRY BED *** H8 = .430 . EPS = .4180							
3800001	0	0	.456	225.8	0	0	0
3800002	0	0	.679	465.2	0	0	0
3800003	0	0	.967	887.2	0	0	0
3800004	0	0	1.243	1398.0	0	0	0
3800005	0	0	1.501	1979.6	0	0	0
3800006	0	0	1.798	2764.1	0	0	0
*** RUN 381 *** . DIST = 19 . H8 = .430 . EPS = .4180 . VIS = .07330							
3815101	2.260	.0142	0	0	.537	1.513	.848
3815102	2.387	.0153	.453	291.9	.598	1.489	.944
3815103	2.417	.0164	.682	661.4	1.086	1.202	.856
3815104	2.696	.0164	.915	1363.8	.850	.729	1.229
3815105	4.376	.0194	1.197	2987.6	.028	.494	1.545
3815106	5.976	.0182	1.347	4036.7	.877	.629	1.276
3815107	7.170	.0199	1.421	4647.9	.750	.784	1.222
3815109	7.539	.0202	1.463	4793.9	.595	.873	1.220
3815109	8.295	.0176	1.527	5277.4	.829	1.218	.927
*** RUN 382 *** . DIST = 19 . H8 = .430 . EPS = .4180 . VIS = .06460							
3827101	2.821	.0933	0	0	1.127	1.237	.818
3827201	2.838	.0905	0	0	1.025	1.246	.847
3825101	2.325	.0220	0	0	.993	1.422	.753
3824101	2.189	.0131	0	0	.735	1.408	.840
3826101	2.493	.0509	0	0	.353	1.423	.762
3828101	3.288	.2262	0	0	1.190	1.079	.894
3829101	3.638	.4771	0	0	.647	1.806	.625

RUN NO.	TOTAL HOLD-UP (PCT.)	LIQUID VELOCITY (MM/S)	GAS VELOCITY (M/S)	PRESSURE DROP (N/M3)	RELATIVE LIQUID FLUX		
					INNER (-)	MIDDLE (-)	OUTER (-)
3829102	3.933	.5009	.367	228.1	.609	1.618	.654
3829103	3.988	.5002	.513	456.1	1.454	1.132	.772
3829104	4.490	.4874	.675	1040.0	.777	.775	1.220
3829105	4.552	.4828	.763	1434.5	.420	.619	1.437
3829106	5.347	.4632	.886	2253.3	.197	.868	1.357
3829107	7.631	.4738	.965	3329.7	.376	1.169	1.111
3829108	12.826	.4843	.987	5277.4	.377	.974	1.231
*** RUN 383 *** . DIST = 19 . H8 = .430 . EPS = .4180 . VIS = .06870							
3838101	3.025	.1345	0	0	1.229	1.289	.750
3838102	3.771	.1380	.448	314.7	.929	1.282	.856
3838103	3.244	.1423	.671	736.6	.908	.965	1.093
3838104	3.866	.1472	.924	1799.4	.195	.269	1.729
3838105	6.578	.1532	1.127	3587.4	.378	.691	1.407
3838106	8.797	.1504	1.266	4734.6	.668	.492	1.432
3838107	10.517	.1428	1.333	5252.3	.340	.442	1.573
3835102	7.734	.0171	1.333	5129.1	.477	1.553	.838
3835103	9.568	.0220	1.695	5993.5	1.157	1.272	.792
3835104	8.537	.0176	1.632	5758.6	1.073	1.552	.653
3835105	6.066	.0166	1.305	3975.1	.836	.778	1.208

EXPERIMENTAL RESULTS FOR ■■ W13/GLY ■■ SYSTEM

NO. 1

PACKING : WAX-COATED SPHERES
 AVERAGE SIZE = 13.3 (MM) . APPARENT DENSITY = 921. (KG/M3)
 LIQUID : GLYCEROL - WATER
 DENSITY = 1210. (KG/M3) . NOMINAL VISCOSITY = .0640 (NS/M2)
 SURFACE TENSION = .0652 (N/M) . CONTACT ANGLE = 96.6 (DEG.)

EXPERIMENTAL RESULTS FOR ■■ W13/GLY ■■ SYSTEM

NO. 2

RUN NO.	TOTAL HOLD-UP (PCT.)	LIQUID VELOCITY (MM/S)	GAS VELOCITY (M/S)	PRESSURE DROP (N/M3)	RELATIVE LIQUID FLUX		
					INNER (-)	MIDDLE (-)	OUTER (-)
3036107	5.859	.0236	1.424	4547.6	1.682	.687	.972
3036108	8.225	.0185	1.515	5414.2	1.556	.500	1.134
*** RUN 304 *** . DIST = 19 . HB = .430 . EPS = .4180 . VIS = .06570							
3047101	3.149	.0635	0	0	1.007	1.483	.707
3045101	2.764	.0149	0	0	.982	1.338	.804
3048101	3.383	.1322	0	0	1.293	1.303	.721
3046101	2.932	.0349	0	0	1.023	1.421	.738
3049101	3.746	.2538	0	0	.318	1.513	.917
3046201	3.136	.0709	0	0	.775	1.411	.826
3044101	2.707	.0086	0	0	.853	1.297	.877
3049201	3.681	.2594	0	0	1.540	1.419	.565
3046301	3.117	.1439	0	0	1.341	1.318	.596
*** RUN 305 *** . DIST = 19 . HB = .430 . EPS = .4180 . VIS = .06570							
3057101	2.965	.0640	0	0	.905	1.734	.585
3059101	3.364	.2278	0	0	1.545	1.792	.333
3058101	3.133	.1388	0	0	.414	2.041	.558
3055101	2.669	.0166	0	0	2.001	1.363	.453
3056101	2.775	.0297	0	0	2.291	1.354	.359
*** RUN 306 *** . DIST = 19 . HB = .430 . EPS = .4180 . VIS = .06570							
3068101	2.941	.0941	0	0	2.961	1.054	.317
3067101	2.781	.0514	0	0	3.149	1.262	.123
3066101	3.106	.1662	0	0	3.161	1.359	.059
3069101	2.661	.0188	0	0	2.869	.983	.292
*** RUN 320 ***							
*** GAS PRESSURE DROP THROUGH DRY BED *** HB = .425 . EPS = .4106							
3200001	0	0	.469	246.9	0	0	0
3200002	0	0	.624	417.7	0	0	0
3200003	0	0	.826	687.6	0	0	0
3200004	0	0	1.053	1069.4	0	0	0
3200005	0	0	1.306	1578.3	0	0	0
3200006	0	0	1.526	2097.5	0	0	0
3200007	0	0	1.814	2896.6	0	0	0
*** RUN 321 *** . DIST = 19 . HB = .425 . EPS = .4106 . VIS = .06570							
3218101	3.165	.1571	0	0	1.146	1.294	.776
3217101	2.819	.0612	0	0	1.277	1.020	.900
3217102	2.920	.0639	.453	346.1	1.451	1.223	.718
3217103	3.063	.0607	.635	692.2	1.415	1.027	.853
3217104	3.354	.0618	.806	1227.6	.859	.642	.277
3217105	4.669	.0591	.999	2515.1	.098	1.146	.336
3217106	5.972	.0594	1.186	3655.0	.006	.351	1.745
3217108	8.201	.0505	1.236	4790.3	.069	1.773	.842
3217109	11.412	.0479	1.522	5997.1	1.386	1.850	.349
*** RUN 322 *** . DIST = 19 . HB = .425 . EPS = .4106 . VIS = .06910							
3229101	4.144	.3804	0	0	.970	1.187	.901
3229102	4.229	.3957	.380	263.1	.865	1.134	.369
3229103	4.334	.4182	.464	394.6	.980	1.095	.353
3229104	4.573	.4196	.586	673.8	.438	.982	1.205
3229105	4.825	.4175	.676	955.3	.934	.651	1.244
3229106	5.703	.4114	.766	1746.7	.180	.346	1.665
3229107	6.818	.4214	.863	2679.0	.165	.407	1.653
3229108	9.392	.4256	.923	3895.0	.447	1.218	1.057

RUN NO.	TOTAL HOLD-UP (PCT.)	LIQUID VELOCITY (MM/S)	GAS VELOCITY (M/S)	PRESSURE DROP (N/M3)	RELATIVE LIQUID FLUX		
					INNER (-)	MIDDLE (-)	OUTER (-)
*** RUN 300 ***							
*** GAS PRESSURE DROP THROUGH DRY BED *** HB = .430 . EPS = .4180							
3000001	0	0	.462	225.8	0	0	0
3000002	0	0	.650	417.4	0	0	0
3000003	0	0	.861	702.4	0	0	0
3000004	0	0	1.115	1117.5	0	0	0
3000005	0	0	1.397	1683.1	0	0	0
3000006	0	0	1.621	2225.9	0	0	0
3000007	0	0	1.830	2784.6	0	0	0
*** RUN 301 *** . DIST = 71 . HB = .430 . EPS = .4180 . VIS = .06430							
3018101	2.794	.1794	0	0	2.297	1.283	.396
3019101	3.345	.3768	0	0	1.919	1.372	.468
3017101	2.496	.0833	0	0	2.170	1.752	.149
3016101	2.374	.0334	0	0	.697	1.979	.504
3017201	2.482	.0721	0	0	1.419	1.689	.438
3017202	2.528	.0721	.457	305.6	1.228	1.443	.657
3017203	2.539	.0729	.624	561.0	.392	2.099	.529
3017204	2.686	.0699	.865	1154.0	.112	.773	1.444
3017205	4.169	.0670	1.117	2700.3	.051	.055	1.913
3017206	4.905	.0656	1.238	3425.5	.011	.018	1.945
3017207	6.028	.0614	1.356	4285.3	.492	.505	1.483
3017208	9.440	.0511	1.410	5560.2	1.025	.771	1.140
*** RUN 302 *** . DIST = 71 . HB = .430 . EPS = .4180 . VIS = .07230							
3028101	3.255	.1674	0	0	2.429	1.027	.510
3025101	2.648	.0163	0	0	1.570	1.629	.430
3026101	2.737	.0383	0	0	2.326	1.311	.372
3027101	2.838	.0777	0	0	2.449	1.237	.373
3028201	3.125	.1785	0	0	1.957	1.655	.280
3029101	3.554	.3726	0	0	2.362	1.474	.255
3029102	3.573	.3852	.452	314.7	2.849	1.359	.254
3029103	3.657	.3830	.620	595.2	3.302	.890	.303
3029104	4.614	.3863	.821	1594.2	.583	.375	1.532
3029105	7.187	.3753	.920	2159.8	.328	.546	1.612
3029106	9.071	.3567	1.006	3920.4	.504	.583	1.431
*** RUN 303 *** . DIST = 71 . HB = .430 . EPS = .4180 . VIS = .06290							
3035101	2.987	.1441	0	0	4.190	.670	.142
3035102	2.490	.0105	0	0	3.378	.764	.362
3034101	2.767	.0834	0	0	3.104	1.373	.070
3037101	2.634	.0442	0	0	3.763	.890	.149
3036101	2.553	.0215	0	0	2.587	1.575	.118
3035102	2.591	.0220	.458	331.0	2.605	1.250	.315
3036104	2.547	.0231	.651	699.8	2.235	1.350	.391
3036104	2.648	.0212	.867	1133.5	.601	.649	1.360
3036105	3.546	.0240	1.131	2463.9	.060	1.879	1.679
3036106	4.991	.0258	1.336	3763.0	.177	.132	1.833

ACKNOWLEDGEMENTS

The author wishes to express his most sincere gratitude and appreciation to Dr. V. Rajakumar for his supervision, encouragement and generous support during the course of this work.

Thanks are due to all the members of the John Percy Research Group for their help on many occasions and in particular, to Mr. A.L. Neve for his advice on technical matters. Mrs. G. Hopkins is also thanked for her excellent typing of the thesis.

Grateful acknowledgement is due to the Kawasaki Steel Corporation for their financial support during the course of this work.

Finally, the author wishes to express his sincere gratitude to Professor F.D. Richardson for his generous encouragement during the course of the work.

LIST OF SYMBOLS

<u>Symbol</u>	<u>Explanation</u>	<u>Units*</u>
<u>Roman</u>		
a, b, c, d, e	constants used in Equations (6.1), (6.5), (6.9), (6.12)	
a_t	total surface area of particles per unit volume of bed	(m^2/m^3)
C_p	capillary number defined by Equation (3.10)	(-)
C_{ph}, C_{ps}	capillary number defined by Equations (6.7) and (6.6)	(-)
C_{pm}	modified capillary number defined by Equation (6.10)	(-)
D	characteristic length of the system	(m)
d_g	diameter of spheres in the grid	(m)
d_h	hydraulic diameter of packing ($=4\epsilon/a_t$)	(m)
d_h'	characteristic length of packing based on hydraulic diameter (Equation 6.4).	(m)
d_i	hydraulic diameter of the smallest inner area of a ring	(m)
d_p	nominal diameter of packing	(m)
d_{pe}	diameter of a sphere having the same volume as a piece of packing	(m)
d_s	characteristic length of packing based on specific surface area Equation (6.3)	(m)
F	ratio of pressure drop of gas through an irrigated bed to that through dry bed at the same gas velocity	(-)
Fl_i	relative liquid flux to i-th annulus	(-)

<u>Symbol</u>	<u>Explanation</u>	<u>Units*</u>
Fr	Froude number ($=u^2/gD$)	(-)
f	force	(N)
f_g	gravitational force, Equation (3.1)	(N)
f_i	inertial force, Equation (3.2)	(N)
f_k	friction factor, Equation (2.6)	(-)
f_p	the force exerted on liquid by the gas flowing through the bed, Equation (3.6)	(N)
f_s	surface force, Equation (3.4)	(N)
f_{si}	interfacial force, Equation (3.5)	(N)
f_v	viscous force, Equation (3.3)	(N)
Ga	Galileo number, Equation (3.9)	(-)
Ga_m	modified Galileo number, Equation (6.15)	(-)
g	gravitational accerelation	(m/s ²)
H_b	effective column height	(m)
H_{bt}	total column height	(m)
H_g	height of the grid	(m)
h_d	dynamic hold-up	(-)
h_f	contribution to hold-up by slow liquid flow	(-)
h_o	operational hold-up	(-)
h_o^*	operational hold-up defined by Gelbe ⁽⁴⁷⁾	(-)
h_s	static hold-up	(-)
h_s^*	static part of the hold-up (Equation 6.1)	(-)
h_t	total hold-up	(-)
k	constant in Equation (2.12)	(-)

<u>Symbol</u>	<u>Explanation</u>	<u>Units*</u>
L	length of bed for which pressure drop ΔP is measured	(m)
N	number of particles per unit volume of bed	(1/m ³)
N _c	dimensionless interfacial force Equation (3.11)	(-)
N _{cap}	capillary number defined by Equation (2.3) or (2.4)	(-)
N' _{cap}	capillary number defined by Equation (6.8)	(-)
n	constant in formula 5 in Table 2.3	(-)
ΔP	gas pressure drop	(N/m ²)
ΔP^*	dimensionless pressure drop, Equation (3.12)	(-)
ΔP_d	gas pressure drop through a dry column	(N/m ²)
ΔP_w	gas pressure drop through an irrigated column	(N/m ²)
ΔP_w^*	dimensionless pressure drop through an irrigated column Equation (6.25)	(-)
Q	liquid flow rate through a column	(ml/s)
Q _i	liquid flow rate through the i-th annulus	(ml/s)
Re	Reynolds number, Equation (3.8)	(-)
Re _g	Reynolds number for gas flow, Equation (2.7)	(-)
Re _m	modified Reynolds number, Equation (6.14)	(-)
S	cross-sectional area of the column	(m ²)
S _i	cross-sectional area of the i-th annulus	(m ²)
S _r	residual saturation, Equation (2.5)	(-)
S _r [*]	residual saturation based on h _s [*]	(-)

<u>Symbol</u>	<u>Explanation</u>	<u>Units*</u>
u	superficial velocity of liquid based on empty column	(m/s)
V	superficial velocity of gas based on empty column	(m/s)
Wa	reversible energy of adhesion of liquid to solid	(J/m ²)
We	Weber number ($=\rho_l u^2 D / \sigma$)	(-)
<u>Greek</u>		
ϵ	fractional voidage of packing	(-)
ϵ_w	fractional voidage of irrigated bed	(-)
η	viscosity of liquid in centipoise	(cP)
θ	contact angle of liquid on solid	(-)
μ	viscosity	(Ns/m ²)
ρ	density	(kg/m ³)
ρ_w	density of water	(kg/m ³)
σ	surface tension of liquid	(N/m)
σ_w	surface tension of water	(N/m)
ϕ	shape factor of packing	(-)

Subscript

l	for liquid
g	for gas

* Those which are indicated by (-) show that the variables are dimensionless

REFERENCES

- 1) The Australian Institute of Mining and Metallurgy, Blast Furnace Aerodynamics Symposium, Wollongong, Australia, 1975.
- 2) Ergun, S., Ind. Eng. Chem., 1953, 45, 477.
- 3) Philbrook, N.O., J. Metals, 1954, 6, 1396.
- 4) Elliott, J.F., Buchanan, R.A., Wagstaff, J.B., J. Metals, 1952, 4, 709
- 5) Beer, H., Heynert, G., Stahl u. Eisen, 1964, 84, 1353.
- 6) Segawa, K., Ishikawa, H., Trans. I.S.I. Japan, 1968, 8, 172
- 7) Bates, M.P., J.I.S.I., 1973, 211, 677.
- 8) Jeschar, R., Pötke, W., Peterson, V., Polthier, K., "Blast Furnace Aerodynamics", ed. Standish, N., 1975, Australian Inst. Min. Met.
- 9) Koup, V., Tien, R.H., Olsson, R.G., Perzak, T.F., "Process Simulation and Control in Iron and Steelmaking", Metallurgical Soc. Conferences, Vol 32, AIME, 1964, 125.
- 10) Muchi, I., Trans. ISI Japan, 1967, 7, 223.
- 11) Yagi, J., Muchi, I., ibid, 1970, 10, 392.
- 12) Flierman, G.A., Oderkirk, H., "Mathematical Models in Iron- and Steel-making", 1975, The Metals Soc., London.
- 13) Kuwabara, M., Muchi, I., "Blast Furnace Aerodynamics", 1975, Australian Inst. Mining. Met., 61.
- 14) Kodama, K., Hagiwara, T., Shigemi, A., Kondo, S., Kanayama, Y., Wakabayashi, K., Hiramoto, N., Tetsu-to-Hagané, 1976, 62, 535.
- 15) Sasaki, M., Ono, K., Suzuki, A., Okuno, Y., Yoshizawa, K., Nakamura, T., ibid, 559.
- 16) Sasaki, K., Hatano, M., Watanabe, M., Shimoda, T., Yokotani, K., Ito, T., Yokoi, T., ibid, 580.
- 17) Radestock, J., "Theoretische Untersuchung der Stationären inkompressiblen und kompressiblen Strömung in ruhenden, geschichteten, und isotropen Schüttungen, Dr. Diss. Tech. Univ. Clausthal, West Germany, 1969.
- 18) Radestock, J., Jeschar, J., Stahl u. Eisen, 1970, 90, 1249.
- 19) Tate, M., Suzuki, K., Ree, H., Kuwano, Y., Chang, T., Go, H., Matsuzaki, M., Nakamura, S., Tetsu-to-Hagané, 1976, 62, 535

- 20) Tate, M., Kuwano, Y., Suzuki, K., Chang, T., Go, H., Matsuzaki, M., Tetsu-to-Hagané, 1976, 62, 495
- 21) Beer, H., Heynert, G., Stahl u. Eisen, 1964, 84, 1353.
- 22) Zimmermann, K-A., Heynert, G., Peters, K.H., ibid, 1974, 94 1283.
- 23) Humenik, M., Hall, D.W., Van Alsten, R.L., Metal Progress, 1962, 81.
- 24) Keverian, J., Taylor, H.F., Trans. Amr. Foundrymen's Soc., 1957, 65, 212.
- 25) Towers, H., Trans. Brit. Ceram. Soc., 1954, 53, 180
- 26) Turkdogran, E.T., "Physical Chemistry of Oxygen Steelmaking. Thermochemistry and Thermodynamics" Monograph series on BOF, Steelmaking vol II, Theory and Fundamentals, U.S. Steel.
- 27) Shulman, H.L., Ullrich, C.F., Walls, N., AIChE J., 1955, 1, 247.
- 28) Gardner, G.C., Chem. Eng. Sci., 1956, 5, 101.
- 29) Elgin, J.C., Weiss, F.B., Ind. Eng. Chem. 1931, 31, 435.
- 30) Uchida, S., Fujita, S., Kogyo-Kagaku-Zasshi, J. Soc. Chem. Ind. Japan, 1936, 39, 876.
- 31) Uchida, S., Fujita, S., ibid, 1937, 40, 538.
- 32) Piret, E.L., Mann, C.A., Wall, T., Jr., Ind. Eng. Chem., 1940, 32, 861.
- 33) Jesser, B.W., Elgin, J.C., Trans. Amr. Inst. Chem. Engr., 1943, 39, 277.
- 34) Shulman, H.L., Ullrich, C.F., Wells, N., Proulir, A.Z., AIChE J., 1955, 1, 259.
- 35) Larkins, R.P., White, R.R., Jeffrey, DW., AIChE J., 1961, 7, 231
- 36) Ross, L.D., Chem. Eng. Progr., 1965, 61, 77.
- 37) Mohunta, I.M., Laddha, G.S., Chem. Eng. Sci., 1965, 20, 1069.
- 38) Brož, Z., Kolář, V., Coll. Czech. Chem. Comm., 1968, 33, 2722.
- 39) Tichy, J., Chem. Eng. Sci., 1973, 28, 655.
- 40) Warner, N.A., Chem. Eng. Sci., 1959, 11, 149.
- 41) Standish, N. Chem. Eng. Sci., 1968, 23, 51.

- 42) Standish, N., Chem. Eng. Sci., 1968, 23, 945.
- 43) Andrieu, J., Chem. Eng. Sci., 1975, 30, 217.
- 44) Davidson, J.F., Trans. Instn. Chem. Engrs., 1959, 37, 131
- 45) Otake, T., Okada, K., Soc. Chem. Eng. Japan, 1953, 17, 176.
- 46) Buchanan, J.E., I and EC Fundamentals, 1967, 6, 400
- 47) Gelbe, J., Chem. Eng. Sci., 1968, 23, 1401
- 48) Davidson, J.F., Cullen, E.J., Hanson, D., Roberts, D.,
Trans. Instn. Chem. Engrs. 1959, 37, 122.
- 49) Dombrowski, H.S., Brownell, L.E., I and EC, 1954, 46, 1207
- 50) Turner, G.A., Hewitt, G.F., Trans. Instn. Chem. Engrs.,
1959, 37, 329.
- 51) Uchida, S., Fujita, S., Kogyo-Kagaku-Zasshi (J. Soc. Chem.
Ind. Japan), 1938, 41, 563.
- 52) Mersmann, A., Chemie Ing. Techn., 1965, 37, 218
- 53) Ergun, S., Chem. Eng. Progress, 1952, 48, 89
- 54) Carman, P.C., Trans. Instn. Chem. Engrs., 1937, 15, 150
- 55) Leva, M., Chem. Engng. Prog. Symp. Ser., 1958, 10, 51
- 56) Brawer, H., Chem. Ing. Techn., 1960, 32, 585.
- 57) Morton, F., King, P.J., Atkinson, B., Trans Instn. Chem. Engrs, 1964
42, 35.
- 58) Buchanan, J.E., I and EC Fundamentals, 1969, 8, 502.
- 59) Dutkai, E., and Ruchenstein, E., Chem. Eng. Sci., 1970,
25, 483.
- 60) Sherwood, T.K., Shipley, G.H., Holloway, F.A.L., Ind. Eng.
Chem., 1938, 30, 765.
- 61) Lobo, W.E., Friend, L., Hashmall, F., Zenz, F., Trans.
Amer. Inst. Chem. Enger., 1945, 41, 693.
- 62) Newton, W.M., Mason, J.W., Metcalfe, T.B., Summers, C.O.,
Petroleum Refiner, 1952, 31, No. 10, 141.
- 63) Standish, N., Drinkwater, J.B., J. Metals, 1972, 24, 43.
- 64) Szekely, J., Mendrykowski, J., Chem. Eng. Sci., 1972, 27, 959.
- 65) Shavrin, S.V., Zakharov, I.M., Ipatov, B.V., Izv., V.U.Z.,
Chern. Metall., 1962, No.9, 54.

- 66) Rikhter, R.G., Potevnya, Yu. M., Izv, V.U.Z., Chern. Met., 1974, No. 4, 37.
- 67) Nakane, C., Kuwano, Y., Suzuki, K., Otani, K., Honda, K., Chan. T.S., Matsuzaki, M., Kim, C.W., Tate, M., Trans. ISI Japan, 1973, 13, 247.
- 68) Standish, N., Colquhoun, L., "Blast Furnace Aerodynamics" 1975, Australian Inst. Min. Met., 20.
- 69) Warner, R.E., *ibid*, 23
- 70) Zisman, W.A., "Contact Angle, Wettability, Adhesion", Advances in Chemistry Series 43, Am. Chem. Soc., 1964, 1.
- 71) Fox, H.W., Zisman, W.A., J. Colloid Sci., 1952, 7, 428.
- 72) Inst. of Petroleum, "IP Standards for Petroleum and Its Products", 19th ed., 1960, 637.
- 73) Porter, K.E., Trans. Instn. Chem. Engrs., 1968, 6, T74.
- 74) Hosaka, M., "Jyoho-syori" (Data Processing), 1969, 10 121.
- 75) Wylie, C.R., "Advanced Engineering Mathematics", 3rd ed. 1966, McGraw-Hill Inc., New York, p 126-141.